Regulation and reproductive functions of membrane-bound vesicles secreted by the *Drosophila* male accessory gland

Laura Corrigan

Exeter College

Trinity Term 2014

Wellcome Trust D.Phil. in Chromosome and Developmental Biology

Supervisor: Dr Clive Wilson

Department of Physiology, Anatomy and Genetics

University of Oxford

i. Acknowledgements

I would like to express enormous thanks to my supervisor, Clive Wilson. There is no doubt that any achievement I have enjoyed during my D.Phil. is owed significantly to Clive's qualities as a supervisor. The ability to immediately share the excitement of your findings with a supervisor who truly cares about your professional growth and success is something few graduate students get to experience, and has made my D.Phil. immeasurably fulfilling and rewarding. His relentless enthusiasm gave me a real belief in the work I was doing and simply put, I would like thank him whole-heartedly for being the best supervisor I could possibly have asked for.

The members of the Wilson lab have contributed immensely to creating such a relaxed and enjoyable atmosphere in which to work. I would like to express sincere gratitude to Aaron Leiblich, whose initial fascinating work establishing the secondary cell system attracted me to the Wilson lab in the first place. I owe special thanks to both Siamak Redhai and Sumeth Perera, whose experimental contributions were indispensable to the acceptance of my first author paper for publication. I am also particularly grateful to Carina Gandy, the almighty gate-keeper of the flies, for enduring the pain of stocks and keeping them safe and organised, as well as providing the lab with a seemingly unlimited supply of pink lab equipment; Shih-Jung Fan, for his patient help with molecular protocols; and Prof. John Morris, for offering his world-class electron microscopy expertise. I would like to thank the many undergraduate students that have worked with me on aspects of this thesis, in particular Rachel Patel, for patiently observing copious fly matings; as well as Katie Windsor, for her relentless perseverance optimising the EM protocol. I would also like to thank Mark Wainwright and Ben Kroeger, whose respective irrefutable fly expertise and ambitious, fresh eyes, offer peace of mind that the projects I have left behind are in excellent hands.

I am sincerely grateful to Jo Begbie for her distinctively approachable nature and willingness to offer supportive, yet always honest, advice on experimental, professional and personal issues.

Of the many graduate students with whom I have shared numerous pub trips and nights out, I would particularly like to express my thanks to Ellie Grant and Rozzy Roberts, who were always available for emergency coffee breaks and provided the strongest corridor-based support system I could have ever asked for.

Last but by no means least, I would like to express my gratitude to my partner, Arnie Francis, whose boundless positivity and unwavering support got me through my rollercoaster of a PhD; and of course my parents for their life-long support and encouragement to pursue my passion for biology, even when they had no idea what I was coming home rambling on about!

ii. Abstract: Regulation and reproductive functions of membrane-bound vesicles secreted by the *Drosophila* male accessory gland

Laura Corrigan, Exeter College

D.Phil. in Chromosome and Developmental Biology, Trinity Term, 2014

Membrane-bound vesicle secretion provides a novel intercellular communication mechanism, whose roles and regulation remain poorly characterised, particularly *in vivo*. I have identified two classes of lipid-containing, vesicle-like structures secreted into seminal fluid by epithelial cells of the *Drosophila* male accessory gland (AG). Exosomes, one class of membrane-bound vesicle formed inside late endosomal multivesicular bodies, are specifically secreted by secondary cells (SCs). The unusual cell biology of SCs allowed me to develop a powerful new high resolution *in vivo* system to characterise the mechanisms underlying intracellular membrane trafficking events underlying exosome biogenesis using real-time live imaging. I characterise how specific ESCRTs (endosomal sorting complexes required for transport) control SC exosome biogenesis, and identify a novel role for BMP signalling in regulating endolysosomal trafficking events necessary for exosome secretion. I also identify roles for epidermal growth factor receptor (EGFR) and phosphatidylinositide 3-kinase (PI3K) signalling in exosome biogenesis. Importantly, SC exosomes are transferred to females during mating. Here, they fuse with sperm, mirroring *in vitro* interactions between human prostate exosomes and sperm, and interact with the female reproductive tract epithelium. Blocking SC exosome production specifically suppresses post-mating effects on female receptivity to remating, demonstrating that exosomes have an important reproductive signalling function *in vivo,* directly or indirectly reprogramming female cells. Finally, I show that main cells, the major epithelial AG cell type, shed lipid-containing microvesicle-like structures from their apical surface. Remarkably, these vesicles carry the seminal peptide, sex peptide, into females during mating and also contribute to the anterior mating plug. In summary, my data reveal previously unsuspected roles for exosomes and microvesicles in *Drosophila* reproduction that may be evolutionarily conserved. Since these vesicles mediate physiological processes previously thought to involve soluble peptides, my work suggests that current models explaining male reprogramming of female behaviours in flies and higher organisms need substantial revision.

iii. List of Abbreviations

Abbreviation	Description
Acp	**A**ccessory gland **p**roteins
AG	**A**ccessory **g**land
ALiX	**A**poptosis **li**nked factor **X** or **AL**G-2 **i**nteracting protein **X**
ANCE	**An**giotensin-**c**onverting **e**nzyme
ATPase	**A**denosine **t**riphos**p**hat**ase**
BMP	**B**one **m**orphogenic **p**rotein
Btl	**B**rea**th**l**e**ss (FGFR)
Dad	**D**aughters **a**gainst **D**pp
CA	**C**onstitutively **a**ctive
DN	**D**ominant **n**egative
Dsx	**D**ouble**sex**
ED	**E**jaculatory **d**uct
EGFR	**E**pidermal **g**rowth **f**actor **r**eceptor
Esg	**Es**car**g**ot
ESCRT	**E**ndosomal **s**orting **c**omplexes **r**equired for **t**ransport
EV	**E**xtracellular **v**esicles (exosomes and microvesicles)
FGFR	**F**ibroblast **g**rowth **f**actor **r**eceptor
Gbb	**G**lass **b**ottom **b**oat
GPI	**G**lycosyl-**p**hosphatidyl **i**nositol
GTPase	**G**uanosine **t**ri**p**hosphat**ase**
HG	**H**ind**g**ut
Hrs	**H**epatocyte **r**eceptor tyrosine kinase **s**ubstrate
iLE	**i**mmature **l**ate **e**ndosome
ILV	**I**ntra-**l**uminal **v**esicle
MAPK	**M**itogen-**a**ctivated **p**rotein **k**inase
MC	**M**ain **c**ell
mMVBL	**m**aturing **m**ultivesicular **b**ody/lysosome
MV	shed **m**icro**v**esicle
MVB	**M**ulti**v**esicular **b**ody
mTOR(C1)	**m**echanistic **t**arget **o**f **r**apamycin (complex 1)
Ovi	**Ovi**duct
PI3K	**P**hospho**I**nositide 3-**K**inase
PtdIns()P	**P**hospho**t**i**d**yl**in**o**s**itol-()**p**hosphate
Pten	**P**hosphatase and **ten**sin homologue
RTK	**R**eceptor **t**yrosine **k**inase
RNAi	**RNA i**nterference
SC	**S**econdary **c**ell
SP	**S**ex **P**eptide
spi	**S**pitz
Spt	**Sp**erma**t**hecae
SR	**S**eminal **r**eceptacle
SV	**S**ecretory **v**acuole

(m)TORC	**m**echanistic **t**arget **o**f **r**apamycin **c**omplex
Abbreviation	**Description**
Tkv	**T**hic**kv**eins
TGF-β	**T**ransforming **g**rowth **f**actor-**beta**
Tsg101	**T**umour **s**usceptibility **g**ene **101**
UAS	**U**pstream-**a**ctivating **s**equence
Ut	**Ut**erus
VDRC	**V**ienna ***D****rosophila* **R**NAi **C**entre
Vps	**V**acuolar **s**orting **p**rotein
Wt	**w**ild **t**ype

iv. Contents

i. Acknowledgements 2
ii. Abstract: 3
iii. List of Abbreviations 4
v. List of Tables 10
vi. List of Figures 10

1. Introduction 13
1.1 Intercellular signalling 13
1.2 Cellular membrane and protein trafficking 13
1.2.1 Membrane trafficking: the endocytic pathway 14
1.2.2 Membrane trafficking regulation: the role of the Rabs/SNAREs 17
1.3 The role of the endolysosomal system in signalling 19
1.3.1 Membrane-bound vesicles: novel signalling mediators 20
1.3.2 EVs and cancer 22
1.3.3 Studying the roles of EVs 22
1.3.4 EV Markers 23
1.3.5 Vesicle biogenesis 24
1.3.5.1 Exosome biogenesis 27
1.3.5.2 ESCRT-mediated exosome biogenesis 27
1.3.5.3 The role of ALiX in ESCRT-dependent biogenesis 29
1.3.5.4 ESCRT-independent exosome biogenesis 29
1.3.5.5 Interaction of ESCRT-dependent and -independent mechanisms 30
1.3.5.6 Trafficking regulation of exosome secretion 31
1.3.6 Limitations of studying exosome biogenesis 32
1.3.7 EV interactions with recipient cells 34
1.4 Reproductive signalling 36
1.4.1 The *Drosophila* male accessory gland 37
1.4.2 The *Drosophila* female post-mating response 40
1.4.3 SP targets 44
1.4.4 Roles of SCs in PMR 45
1.5 Aims and objectives 47

2. Materials and methods 49
2.1. Buffers/media table 49
2.2 Fly strains 50
2.2.1 Fly strains table 50
2.2.2 SC-Gal4 driver lines 53
2.2.3 Fly husbandry 55
2.2.4 UAS/Gal4/Gal80^{ts} transgene expression system 55
2.3. AG Staining 58
2.3.1 Antibody table 58
2.3.2 AG Immuno-staining 58
2.3.3 Lysotracker staining 59
2.4 Imaging 59
2.4.1 Confocal microscopy 59
2.4.2 Image analysis 59
2.5. Secretion quantification experiments 61
2.5.1 Mating protocol 61
2.5.2 Image acquisition 61
2.5.3 Particle analysis 61

2.6 Statistical analysis....62
2.7 Electron microscopy....62
2.7.1 Structural EM....62
2.7.2 Immuno-EM....63

3. Characterisation of exosomes secretion by SCs....64
3.1 Introduction....64
3.1.1 Exosome secretion in *Drosophila*....64
3.1.2 Aims and objectives....66
3.2 Methods....66
3.2.1 Pulse chase experiments....66
3.2.2 Secreted ANCE staining quantification....67
3.2.3 Western blots....67
3.2.3.1 Protein extraction....67
3.2.3.2 Blotting....68
3.2.4 Electron Microscopy....68
3.2.5 CD63-GFP puncta quantification experiments....69
3.3 Results....69
3.3.1 SC-specific secretion of CD63-GFP....69
3.3.2 CD63-GFP localises to late endosomal, lysosomal and secretory compartments....70
3.3.3 Age-dependent changes in endolysosomes....78
3.3.4 Secretory and endolysosomal compartments possess distinct Rab GTPase signatures....82
3.3.5 Ultra-structural analysis of SCs and AG lumen....86
3.3.6 CD63-GFP traffics via the secretory pathway to reach late endosomes....90
3.3.7 Live cell imaging reveals dynamic interactions between and within compartments....92
3.3.8 Regulation of late endosomal trafficking by mating....94
3.3.9 SCs secrete exosomes in an ESCRT-dependent manner....94
3.3.9.1 Effects of ESCRT knockdown on SC biology....94
3.3.9.2 ESCRT-dependent exosome secretion....100
3.4 Discussion....107
3.4.1 SCs secrete CD63-GFP-postive exosomes into the seminal fluid....108
3.4.2 The SC as a novel *in vivo* model to study exosome biogenesis in live cells....110
3.4.3 SCs produce CD63-GFP exosomes in a ESCRT-dependent manner....111
3.4.4 Mechanism of exosome secretion....113
3.4.5 SC compartment dynamics....114

4. Investigating the reproductive functions of SC exosomes....115
4.1 Introduction....115
4.1.1 Exosomes in mammalian reproduction....115
4.1.2 Aims and objectives....117
4.2 Materials and Methods....117
4.2.1 Reproductive physiology experiments....117
4.2.2 Single-pair CD63-GFP transfer experiments....118
4.2.3 Immuno-staining of female reproductive tract....119
4.3 Results....119
4.3.1 CD63-GFP is transferred to neighbouring MCs....119
4.3.2 Exosomes fuse with sperm in the female....122
4.3.3 Exosomes interact with the epithelial surface of the female reproductive tract....125
4.3.4 'Exosomeless' males fail to induce the full post-mating response....126
4.4 Discussion....130
4.4.1 SC exosomes mediate inter-organism signalling....130

4.4.2 A role for exosomes in sperm competition 131
4.4.3 Exosome-sperm fusion and the PMR 132
4.4.4 Exosome-female cell interactions 134
4.4.5 Concluding remarks 135

5. The role of BMP signalling in the regulation of SC exosome secretion 136
5.1. Introduction 136
5.1.1 Roles of BMP signalling 136
5.1.2 BMP signal transduction pathway 137
5.1.3 BMP signalling and endocytic trafficking 140
5.1.4 BMP signalling: cancer and exosomes 140
5.1.5. Aims and objectives 140
5.2 Methods 142
5.2.1 Nuclear size experiments 142
5.3 Results 143
5.3.1 BMP signalling in SCs is required for exosome secretion. 143
5.3.2 BMP signalling regulates endolysosomal trafficking 143
5.3.3 *ALiX,* but not *Hrs,* function is required for SC growth 144
5.4 Discussion 151
5.4.1 BMP-dependent regulation of endolysosomal trafficking as a novel mechanism for controlling exosome secretion 151
5.4.2 Exosome secretion is not required for cell growth 153
5.4.3 Regulation of cell growth by endolysosomes 154
5.4.4 Reciprocal functions for BMP and Hrs in the regulation of late endosomal size 155

6. The role of RTK signalling in the regulation of exosome secretion. 156
6.1 Introduction 156
6.1.1 EGFR signalling 156
6.1.1.1 EGFR signal transduction 156
6.1.1.2 EGFR trafficking 159
6.1.1.3 EGFR signalling regulates trafficking 160
6.1.1.4 EGFR and exosomes 160
6.1.2 PI3K signalling 161
6.1.2.1 Class I PI3K in RTK signalling and cell growth 164
6.1.2.2 Class I PI3K signalling and endocytic trafficking 165
6.1.2.3 PI3K, PTEN, cancer and exosomes 165
6.1.3 Aims and objectives 166
6.2 Methods 166
6.3 Results 167
6.3.1 SCs secrete EGFR-GFP and FGFR-GFP into the accessory gland lumen 167
6.3.2 Autocrine EGFR signalling regulates endocytic and secretory trafficking events 167
6.3.4 Class I PI3K signalling regulates endocytic and secretory trafficking events in SCs 173
6.4 Discussion 182
6.4.1 The EGFR and FGFR are potential exosome cargos 182
6.4.1.1 Autocrine EGFR signalling by SCs 184
6.4.2 Regulation of exosome secretion by EGFR and PI3K signalling 184
6.4.3 Regulation of endocytic trafficking by EGFR and PI3K signalling 186
6.4.3.1 EGFR signalling regulates endocytic trafficking in SCs 187
6.4.3.2 PI3K activity regulates endocytic trafficking in SCs 188

7. MCs of the AG shed sex peptide-carrying microvesicles into the gland lumen 190

7.1 Introduction 190
7.1.1 MV biogenesis 190
7.1.2 Regulation of MV biogenesis 193
7.1.3 Roles of MVs 194
7.1.4 MVs and *Drosophila* 195
7.2 Methods 196
7.2.1 Electron microscopy 196
7.2.2 Single-pair GFP transfer experiments 196
7.3 Results 197
7.3.1 SCs secrete GPI-anchored GFP into the AG lumen. 197
7.3.2 MCs shed MVs into the AG lumen 197
7.3.3 MVs are transferred to the female reproductive tract during mating 198
7.3.4 Sex peptide is carried by MVs into the female 199
7.4 Discussion 207
7.4.1 Lipid raft-enriched MVs are predominantly shed by MCs 207
7.4.2 GFP^{GPI} vesicles in the AG lumen are unlikely to be lipoprotein particles 209
7.4.3 SCs may also secrete a distinct EV marked by GFP^{GPI} 210
7.4.4 A role of AG MVs in reproductive signalling 211
7.4.4.1 MVs carry SP into the female during mating 211
7.4.4.2 MVs in the *Drosophila* seminal fluid contribute to the mating plug 212
7.4.5 A conserved role for MVs in coagulation 213

8. Concluding remarks 214
8.1 Summary of findings 214
8.2 Implications for past, present and future exosome studies 215
8.3 Implications for cell biology 216
8.4 Implications for reproductive biology 216
8.5 Implications for cancer cell biology 218

9. Bibliography 222

v. List of Tables

1.1 Endocytic compartment identities..... 15
1.2 Factors with identified roles in the PMR..... 43
2.1. Standard buffers and media..... 49
2.2. Gal4 driver lines..... 50
2.3. Misc. stocks..... 50
2.4. Fluorescent tagged transgenic constructs..... 51
2.5. Non-RNAi transgenics..... 52
2.6. RNAi lines..... 53
2.7. Primary and secondary antibodies..... 58
5.1. *Drosophila* BMP receptors..... 138
5.2. *Drosophila* BMP receptor ligands and examples of characterised (developmental) roles. 138

vi. List of Figures

1.1 Secretory and endocytic trafficking..... 16
1.2 Rab GTPase cycling..... 18
1.3 Asymmetric lipid raft domain organisation..... 26
1.4 Schematic structure of GPI-anchored proteins..... 26
1.5 ESCRT-dependent ILV formation..... 28
1.6 Schematic of ALiX domain structure. 28
1.7 MV and exosome secretion and uptake. 35
1.8 Male reproductive tract schematic 38
1.9 Confocal imaging of the male reproductive tract. 39
1.10 Female reproductive tract schematic..... 40

2.1. Cell-type-specific reporter construct expression in the male reproductive tract by Gal4 driver lines..... 54
2.2. Genetic approach to the generation of transgene-expressing males..... 56
2.3. Genetic approach to the generation of combinatorial *UAS/Gal4/Gal80^{ts}* stocks..... 57
2.4. Schematic representation of AGs with surface and transverse optical confocal sectioning..... 60

3.1. The *Drosophila* accessory gland. 72
3.2. Not all CD63-GFP-positive large vacuoles contain a dense ANCE core..... 73
3.3. Secondary cells (SCs), and not main cells (MC), secrete CD63-GFP-positive puncta into the lumen of the accessory gland..... 74
3.4. CD8-RFP is not incorporated into exosomes..... 75
3.5. Cytoplasmic GFP is occasionally seen inside large vacuolar compartments..... 75
3.6. CD63-GFP colocalises with anti-CD63 and anti-GFP antibody stains but SCs can also contain a compartment filled with CD63-GFP that exhibits only limited GFP fluorescence..... 76
3.7. CD63-GFP fluorescent puncta secreted into the AG lumen by SCs co-localise with anti-CD63 and anti-GFP antibody..... 77

3.9. Age-dependent mMVBL maturation. …… 81
3.10. Live imaging of SCs reveals dynamic fusion between mMVBLs…… 81
3.11. Rab GTPase signatures define different SC subcellular compartments…….. 84
3.12. PI4KII localises to the limiting membrane of mMVBLs…… 85
3.13. SC endosomal and secretory compartments possess a stereotypical Rab GTPase signature…… 85
3.14. Electron microscopy reveals the presence of exosome-like vesicles in the AG lumen and large SC compartments…… 87
3.15. Ultra-structural electron microscopic analysis of SC SVs…… 88
3.16 Immuno-EM analysis of SC mMVBLs confirms the presence of CD63-GFP on putative ILVs…… 89
3.17. CD63-GFP trafficking and exosome biogenesis in SCs…… 91
3.18. Real-time live imaging reveals dynamic trafficking events inside acidic late endosomal compartments…… 93
3.19. The effect of mating on late endocytic and secretory SC compartments…… 97
3.20. Knockdown of ESCRT components effects morphology of SC compartments…… 98
3.21. Knockdown of ESCRT components effects number and size of SC compartments…… 99
3.22. Depletion of ESCRT components reduces the secretion of CD63-GFP puncta…… 103
3.23. Knockdown of ESCRT components significantly reduces the number of CD63-GFP-positive puncta quantified, even when glands were imaged under two confocal gain settings…… 104
3.24. Western blot analysis of AGs and mated females following ESCRT knockdown…… 105
3.25. Blocking exosome biogenesis does not affect the localisation or secretion of ANCE…… 106

4.1. CD63-GFP exosomes are transferred to neighbouring MCs…… 120
4.2. CD63-GFP exosomes are transferred into the female reproductive tract during mating.. 121
4.3. AG exosomes interact with sperm in females …… 123
4.4. Exosomes may interact with sperm tails in the female reproductive tract…… 124
4.5. Transferred exosomes interact with epithelial cells of the female uterus…… 127
4.6. Exosomeless males fail to induce specific aspects of the female post-mating response.. 128
4.7. ‘Exosomeless’ males induce equal levels of egg laying and sire equal numbers of progeny compared to control males. …… 129

5.1.1. Schematic of the *Drosophila* BMP signalling pathway components…… 139
5.1. BMP signalling in SCs is required for exosome secretion. …… 146
5.2. Modulating BMP signalling affects morphology of SC compartments…… 147
5.3. BMP signalling regulates intracellular trafficking events inside SCs…… 148
5.4. Effect of ESCRT knockdown on SC growth…… 149
5.5. Effect of ESCRT knockdown on SC growth; exosome secretion is not required for normal post-developmental SC growth…… 150

6.1.1 The core PI3K and EGFR signalling pathways and their interaction via EGFR-mediated PI3K recruitment …… 157
6.1.2. Schematic representation of EGFR…… 163
6.1.3. Isoform-specific lipid kinase activity of PI3K…… 163
6.1. SCs secrete EGFR-GFP into the accessory gland lumen…… 169
6.2. FGFR-GFP is secreted by SCs into the accessory gland lumen…… 170

6.3. Modulating EGFR signalling in virgin males alters the morphology of SC endocytic and secretory compartments…… 171
6.4. Modulating EGFR signalling alters the number and size of SC endocytic and secretory compartments.…….. 176
6.5. Modulating EGFR signalling alters CD63-GFP exosome secretion in a non-reproducible manner. ……. 177
6.6. Modulating Class I PI3K (*Dp110*) signalling alters the morphology of endocytic and secretory compartments. …… 178
6.7. Modulating PTEN signalling alters the morphology of endocytic and secretory compartments. …… 179
6.8. Modulating PI3K signalling alters the number and size of endocytic and secretory compartments…….. …….. 180
6.9. Modulating PI3K signalling alters CD63-GFP exosome secretion in a non-reproducible manner…….. 181

7.1. SCs secrete GPI-anchored GFP into the accessory gland lumen…… 201
7.2. MCs shed GFP^{GPI}–containing MVs into the accessory gland lumen…… 202
7.3. The AG lumen contains many large, cigar-shaped particles of various sizes, which appear to be shed by MCs…… 203
7.4. GPI-anchored GFP-labelled MVs are transferred to the female reproductive tract during mating. …….. 204
7.5. SP-GFP localises to MVs shed into the lumen of the gland by MCs…….. 205
7.6. SP-GFP transferred to females is associated with MVs and is released to permit sperm binding …….. 206

Approximate word count: 41,000

1. Introduction

1.1 Intercellular signalling

Cell-cell communication is fundamental to multicellular life; intercellular signalling permits the coordination of a plethora of developmental or physiological processes. Intercellular signalling can be mediated by: direct cell-cell contact and the physical forces exerted by neighbouring cells; the secretion of simple ligands, which are able to diffuse to target cells and either diffuse across the lipid bilayer into the cell cytoplasm or activate specific receptors situated on the plasma membrane; or the secretion of membrane-bound vesicles (Raposo et al. 2013). Membrane-bound secreted vesicles mediate intercellular signalling by assisting the transport of ligands, receptors, intracellular proteins and even nucleic acids between cells. The majority of vesicle cargos reflect the function of the cell type of origin (Christianson et al. 2014). Membrane-bound vesicles have been implicated in several well-characterised signalling pathways, including Wnt (Korkut et al. 2009; Koles et al. 2012; Beckett et al. 2013) and EGFR (Al-Nedawi et al. 2008; Higginbotham et al. 2011), many of whose components are integral membrane or membrane-associated proteins, as well as many physiological and disease processes ranging from reproduction to tumourigenesis (Raposo et al. 2013; Aalberts et al. 2014).

1.2 Cellular membrane and protein trafficking

Lipid bilayers are utilised by the majority of multi- and uni-cellular organisms as barriers separating the inside of a cell from the extracellular space. Further membrane-mediated compartmentalisation of individual cells generates organelles, which function to segregate specific molecules, forming internal microenvironments that are also functionally distinct. Consequently, organelles possess unique protein and lipid compositions. In order to maintain the identity and function of these various compartments, the trafficking of protein and lipid components between them occurs in a heavily regulated manner. Specific peptide sequences

target proteins to specific compartments. For example, proteins destined for import into mitochondria or secretion into the extracellular space or possess specific signal peptide sequences that are cleaved off during transport (Paschen et al. 2001; Hegde et al. 2008). In contrast to proteins, the regulation of lipid transport between cellular compartments is less well characterised. However, several compartments utilise membrane-bound vesicles to exchange material. This vesicle-mediated protein transport inevitably results in large amounts of lipid flux between specific organelles and therefore mechanisms must exist to maintain lipid homeostasis (Flis et al. 2013). There are two major vesicle-mediated trafficking pathways that function in all eukaryotic cell types: the secretory and endocytic pathways. The secretory pathway defines the route of newly synthesised protein/lipids from the endoplasmic reticulum (ER) to Golgi and then into the extracellular space, whilst the endocytic pathway describes the route of proteins and lipids internalised into a cell.

1.2.1 Membrane trafficking: the endocytic pathway

Endosomal compartments can be subdivided based on their morphology, density, the rate and kinetics of cargo delivery, and also their protein or lipid content, into early endosomes (EEs), late endosomes (LEs), multivesicular bodies (MVBs) and lysosomes (**Table 1.1**). Nevertheless, an 'endocytic spectrum' exists arising from both the gradual maturation of endocytic compartments, as well as the formation of hybrid compartments as a result of dynamic trafficking and fusion events between them. Classically characterised in budding yeast, early endosomes are typically smaller, sometimes tubular, mildly acidic and located towards the cell periphery. In contrast, LEs are larger, more centrally located and acidic due to the action of the V_0 H^+ATPase situated at the limiting membrane (Beyenbach et al. 2006). LEs containing vesicles, so-called intra-luminal vesicles (ILVs), are known as MVBs. MVB biogenesis was classically thought to be completely dependent upon the activities of the Endosomal Sorting Complex Required for Transport (ESCRT) complex, a large multi-subunit group of proteins involved in a number of late endosomal

trafficking events (Schmidt et al. 2012). However, recent studies also suggest that ESCRT-independent ILV biogenesis mechanisms exist (see Chapter 1.3.5.4) (Trajkovic et al. 2008; Stuffers et al. 2009; Markus 2011).

Several models have been proposed for the transfer of proteins, destined for degradation, from late endosomes to lysosomes (reviewed in (Scott et al. 2014)). The first involves gradual maturation of late endosomes into lysosomes, involving further acidification and the delivery of lysosomal enzymes directly from the Golgi or through release from internal stores. Alternatively, proteins can be transported on vesicles, as has been demonstrated in a cell-free yeast reconstitution experiment (Vida et al. 1999). Direct transfer via a 'kiss-and-run' mechanism, which may involve transient tubules connecting these compartments, has been observed in live cells in real time (Bright et al. 2005). Finally, complete fusion between late endosomes and lysosomes has been observed, resulting in the formation of a temporary hybrid compartment that reverts to a lysosome following maturation (Van Deurs 1995; Pryor et al. 2000; Bright et al. 2005). Within the same system, both kiss-and-run and direct fusion mechanisms have been observed (Bright et al. 2005), as have maturation and direct fusion (Futter et al. 1996), suggesting combinations of these mechanisms contribute in a single cell.

	Compartment	pH	Rab signature	Additional markers
EE	Early endosome	6.8-6.1	Rab5 (Sönnichsen et al. 2000; Hirota et al. 2007)	Clathrin (Raiborg et al. 2002), Hrs (Raiborg et al. 2002)
LE	Late endosome	6.0-4.8	Rab7 (Yousefian et al. 2013)	Hrs (Raiborg et al. 2002)
RE	Recycling endosome	6.8-6.1	Rab11 (Sönnichsen et al. 2000)	
MVB	Multivesicular body	6.0-4.8	Rab7 (Bucci et al. 2000)	ALiX (Sadoul 2006) Hrs (Katzmann et al. 2003) ESCRTs 1-3 (Katzmann et al. 2003) LBPA (Matsuo et al. 2004) CD63 (Pols et al. 2009)
	Lysosome	4.5	Rab7,9 (Bucci et al. 2000)	LAMP1(Rosenfeld et al. 2001) CD63 (Pols et al. 2009)

Table 1.1. Endocytic compartment identities.

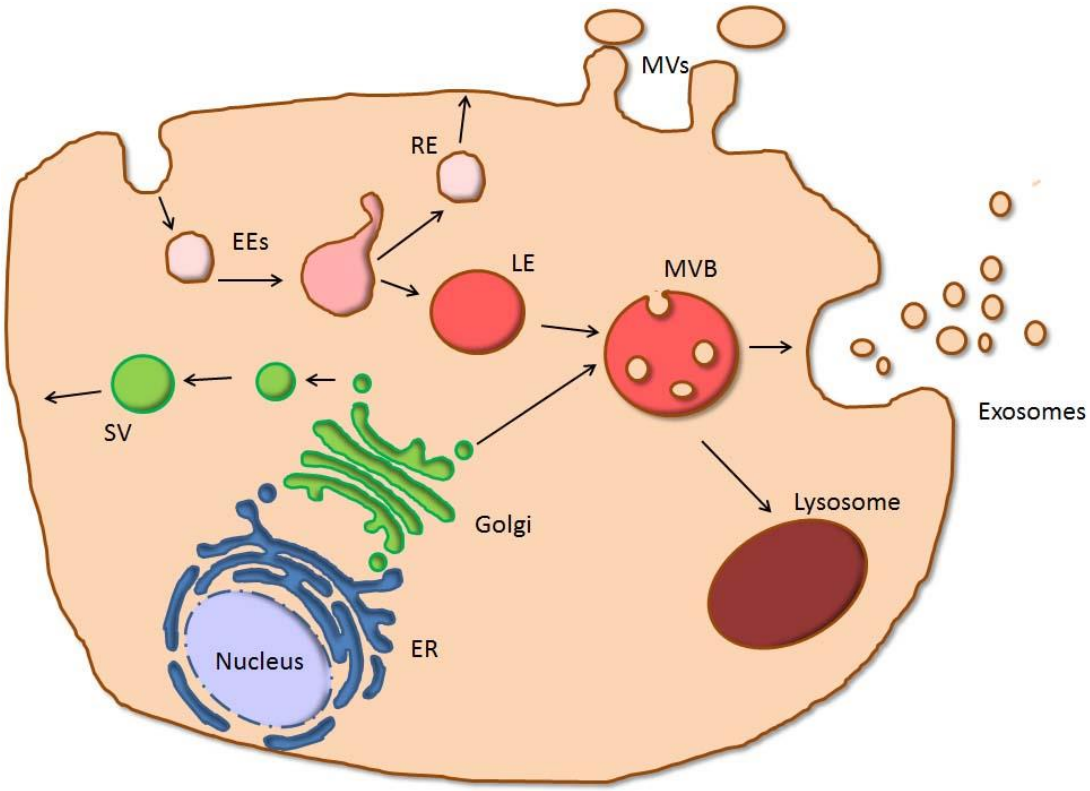


Figure 1.1. Secretory and endocytic trafficking. Newly synthesised material is transported via the secretory pathway (green) following biosynthesis in the ER. Following vesicular transport through the Golgi apparatus, transport vesicles fuse with the plasma membrane to release soluble material into the extracellular space or transfer transmembrane proteins and lipids to the plasma membrane. Proteins and lipids can also be internalised by cells via the endocytic pathway (red). Endocytosed vesicles, EEs, are either recycled back to the plasma membrane or mature into late endosomes. Vesiculation of LEs, whereby the limiting membrane invaginates and pinches off small vesicles (ILVs) of 40-150nm diameter, results in the formation of MVBs. Material can also be transferred to MVBs or lysosomes directly from the Golgi apparatus. MVBs can either fuse with the lysosome or the plasma membrane, the latter resulting in the release of the internal vesicles into the extracellular space as exosomes (Scott et al. 2014). The outward budding and pinching off of a cell's limiting membrane can also release membrane-bound MVs, containing cytoplasmic components as well as lipids, into the extracellular space.

1.2.2 Membrane trafficking regulation: the role of the Rabs/SNAREs

In order to maintain the identity and function of secretory and endolysosomal compartments, inter-compartmental trafficking of protein or lipid components occurs in a heavily regulated manner. Rab GTPases (Rabs) regulate many aspects of membrane trafficking. Each Rab occupies specific, yet partially overlapping, intracellular membrane domains (Sönnichsen et al. 2000) (**Table 1.1**). Rabs reversibly associate directly with membranes through their prenylated C terminal motifs (**Fig.1.2**). Rabs also interact with a wide range of effector proteins via adaptors. Examples include SNAREs (SNAP (Soluble NSF Attachment Protein) Receptor) and motor proteins, which mediate specific membrane fusion and trafficking events, respectively (Pryor et al. 2004). Rab function is dependent upon its GTPase activity that hydrolyses GTP to GDP, which is regulated through the activity of regulatory proteins (**Fig. 1.2**).

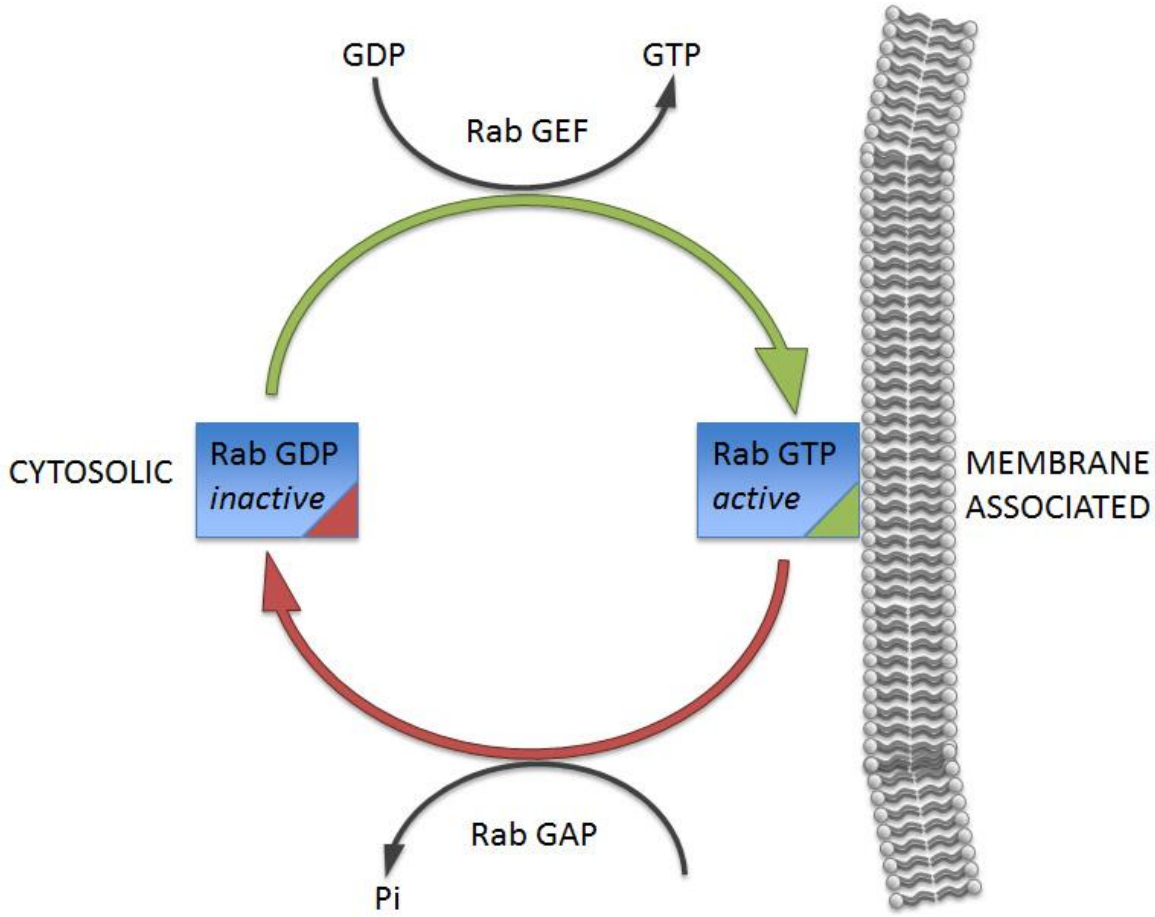


Figure 1.2. Rab GTPase cycling. GTP-bound 'active' Rab associates with specific membrane compartments as well as effector proteins (not shown); GDP-bound 'inactive' Rab dissociates from the membrane and forms a cytosolic pool. The cycling of Rab GTPases from active to inactive states is mediated by Rab GTPase Activating Proteins (Rab GAPs), whilst the conversion of Rab-GDP to Rab-GTP is catalysed by Rab Guanine Exchange Factors (Rab GEFs) (Delprato et al. 2004).

1.3 The role of the endolysosomal system in signalling

The endocytic pathway has classically been considered to function solely as a protein degradation and nutrient recycling pathway (Scott et al. 2014). Proteins, frequently flagged for degradation by ubiquitination, traffic via the endocytic pathway to the lysosome where they are degraded at low pH by acid-activated proteolytic enzymes. This well-established role plays a crucial part in receptor tyrosine kinase (RTK) signal down-regulation through receptor degradation (Jékely et al. 2003). Following autophosphorylation (of the epidermal growth factor receptor {EGFR}, for example) and recruitment of the adaptor, Grb2, the active-EGFR-ligand complex is internalised and traffics to the lysosome for degradation (Opresko et al. 1995) (Section 6.1.1.2).

Nevertheless, the physiologically relevant step in signal down-regulation is not receptor degradation, but signal attenuation by either the dissociation of the ligand from the ligand-receptor complex, the physical separation of RTKs from their downstream effectors, as well as receptor dephosphorylation (Eden 2009). The former two may result either from the removal of the activated RTKs from the plasma membrane, where effectors reside, by endocytosis, or by their sequestration inside MVBs on ILVs (Sorkin 2008). Many studies have indicated that blocking ILV formation by knockdown of ESCRT components such as *Hrs* (mammalian Hepatocyte Receptor tyrosine kinase Substrate) (Robertis 2011) results in ectopic RTK signal activation (Lloyd et al. 2002). However, other studies do not support this finding (Yousefian et al. 2013). This discrepancy may be explained by the positive role of endocytic membranes in RTK signalling, which have been suggested to function in the maintenance of some signalling by acting as platforms for the recruitment of downstream effectors (Robertis 2011). For example, endocytic trafficking has been demonstrated to be necessary for the induction and amplification of BMP signalling, whereby the endocytic membranes act as signal transduction platforms for the recruitment of downstream effectors (Hayes et al. 2002). Furthermore, due to the cyclic nature of endocytic membrane trafficking, it is likely that blocking one specific step in the trafficking pathway has widespread effects on the entire pathway. This may result in abnormal maturation and trafficking

of compartments upstream or downstream of the blockade, and subsequently affect the levels and dynamics of RTK signalling.

Recent studies have also demonstrated a central role of late endosomes and lysosomes in the regulation of cellular growth (Ögmundsdóttir et al. 2012; Betz et al. 2013). Mechanistic (formerly mammalian) target of rapamycin complex (mTOR) is recruited to the surface of LELs following amino acid stimulation to form mTOR Complex 1 (mTORC1) (D Ci Goberdhan 2010; Ögmundsdóttir et al. 2012). Here, it activates downstream effectors ultimately responsible for cell growth by inhibiting the translation initiation factor repressor, 4E-binding protein, and activating S6-kinase, the kinase for the ribosomal protein, S6 (Betz et al. 2013).

The endocytic pathway also plays a central role in intercellular signalling through the generation of membrane-bound vesicles that can be secreted as exosomes (Section 1.3.1) (Raposo et al. 2013).

Despite the wealth of experiments characterising the effect of endocytosis on signal transduction, limited studies have attempted to characterise the role of specific intercellular signalling cascades on endocytic trafficking events.

1.3.1 Membrane-bound vesicles: novel signalling mediators

In addition to cell-cell signalling via direct cell-cell contact or secretion of soluble ligands, membrane-bound vesicle secretion is a more recently appreciated means of intercellular communication, whereby cells secrete nano-sized particles into the extracellular space, which act as vessels to carry a wealth of cargos between distant cells (reviewed in (Ludwig et al. 2012; Raposo et al. 2013)). In addition to protein ligands, membrane-bound vesicles have been shown to also transport integral membrane (Adamczyk et al. 2011), intracellular proteins (Korkut et al. 2009; Beckler et al. 2013; Di Noto et al. 2013; Gabriel et al. 2013), specific lipids such as ceramides and phosphosphingolipids (Trajkovic et al. 2008), as well as nucleic acids including mRNAs,

miRNAs and DNA (Gusachenko et al. 2013). Secreted microvesicles are classified by their subcellular origin: exosomes are formed inside specific multivesicular endosomes (MVBs), whilst microvesicles (MVs) are shed from a cell's plasma membrane (**Fig. 1.1**). Exosomes and MVs are morphologically and biochemically distinct. Due to the differing mechanisms of biogenesis (Sections 1.3.5 and 7.1.1), the two types of vesicles have distinct size profiles: exosomes range from 40-150nm, whilst MVs are typically larger, ranging from 100mn-1000nm (Raposo et al. 2013). Furthermore, although exosomes and MVs share many lipid and protein cargos, several molecules have been demonstrated to associate with specific EVs (Section 1.3.4 (Cocucci et al. 2009)). However, confusion in the nomenclature, failures to distinguish the origin of secreted vesicles as well as their overlapping size profiles have hindered progression of our understanding of the roles and regulation of these two types of vesicle. In this thesis mixed populations of exosomes and MVs will be referred to as extracellular vesicles (EVs).

It has been hypothesised that the majority of cell types secrete EVs. EVs have been isolated from a wide range of body fluids, including blood (Caby et al. 2005), seminal fluid (Ronquist et al. 1985; Park et al. 2011; Aalberts et al. 2013), breast milk (Admyre et al. 2007) and amniotic fluid (Asea et al. 2008).The function of EVs reflect the cargos they carry, which, to some extent, reflects the cell type of origin (Section 1.3.4). EVs have been implicated in an equally wide range of physiological processes, ranging from immunosuppression (Admyre et al. 2007) to sperm capacitation (Park et al. 2011). EVs have more recently been shown to carry bioactive molecules and mediate their horizontal transfer between cells (Gross et al. 2012; Ronquist et al. 2013). EVs secreted into the extracellular milieu are able to interact with target cells to initiate a signalling response (Gross et al. 2012; Beckler et al. 2013). Indeed, EVs have been demonstrated a carry components of several signalling pathways including EGF (Al-Nedawi et al. 2008; Adamczyk et al. 2011), Wnt (Gross et al. 2012; Beckett et al. 2013), Notch (Sheldon 2010) and Hh (Liégeois et al. 2006) signalling pathways, several of which have been demonstrated to be competent signalling entities (Gross et al. 2012).

However, whether EVs play physiologically relevant signalling roles *in vivo* remains under debate (Gross et al. 2012; Beckett et al. 2013).

1.3.2 EVs and cancer

A large number of studies have implicated EV secretion in the progression of cancer (Cocucci et al. 2009; Muralidharan-Chari et al. 2010; Kharaziha et al. 2012). Exosomes are produced by a plethora of cancer cell types in culture, and in the case of prostate cancer the circulating level of tumour-derived exosomes has been shown to correlate with disease prognosis (Lance et al. 2011). Consequently, there is great clinical interest in cancer-derived EVs as biomarkers for disease that can be sampled non-invasively. Furthermore, there is some evidence in the field that cancer cells utilise EVs to manipulate the tumour microenvironment. For example, tumour-derived exosomes have been demonstrated to promote angiogenesis (Mineo et al. 2012) and tumour cell invasion (Higginbotham et al. 2011), potentially through their ability to prime pre-metastatic sites by reprogramming distant cells.

1.3.3 Studying the roles of EVs

As the cargos carried by EVs are critical for their signalling function, there has been intense focus in the EV field on the development of methods to isolate and purify EVs from body fluids or cell culture medium, in order to study their composition and thus infer function. Once isolated, several studies have probed EV function by adding these isolated populations either onto cells in culture (Park et al. 2011; Mineo et al. 2012; J. P. Webber et al. 2014) or *in vivo* administration (Alvarez-Erviti et al. 2011; Beckler et al. 2013; J. P. Webber et al. 2014). As the majority of cells are likely to produce both exosomes and MVs, as has been directly shown for platelets (Heijnen et al. 1999), there has been particular emphasis on the ability to separate exosomes from MVs. Current methods employed to isolate exosomes from a heterogeneous EV population include: a complex 100,000g ultracentrifugation protocol, ultrafiltration using filters of varying size, as well

as sucrose density gradient separation (Momen-Heravi et al. 2013). However, such isolation methods come with inherent limitations including artefactual size and shape alterations (Momen-Heravi et al. 2013). Furthermore, the potential size overlap between the two types of particle creates obvious limitations when employing these methods. Importantly, a study by Muralidharan-Chari et al. 2009 demonstrated that the pellet sedimented using a 100,000g ultracentrifugation protocol, heavily utilised to specifically isolate exosomes from mixed EV populations, does, however, also contain MVs (Muralidharan-Chari et al. 2009). Therefore, conclusions regarding EV function drawn from the numerous studies utilising this protocol referring specifically to one type of vesicle should be interpreted with caution.

A more direct method of investigating function is to block EV production *in vivo* and assay the effects. Although advances have been made in understanding the mechanisms of EV biogenesis, whether many of the identified regulators function *in vivo* is yet to be investigated (Sections 1.3.5 and 7.1.1). Furthermore, a recent review emphasized the requirement of a model system in which factors required for specific vesicle biogenesis can be modulated to definitively determine vesicle origin and subsequently study the particular vesicle's *in vivo* function (Raposo et al. 2013).

1.3.4 EV Markers

The inherent biochemical similarities between EVs results in a large degree of overlap in the cargos they carry. Recent efforts have been made to identify *specific* markers to distinguish the two types of vesicle. To date, many of the markers identified reflect the differences in their mechanisms of biogenesis (Sections 1.3.5 and 7.1.1).

Exosomes typically contain several endosome-associated proteins, including specific Rab GTPases, and factors involved in ILV biogenesis e.g. specific ESCRTs and ALiX (Duijvesz et al. 2013; Ghossoub et al. 2014). Exosomes are also enriched in tetraspanins, transmembrane proteins which cluster into specific membrane microdomains (distinct from lipid rafts) (Hemler 2003), including CD81, CD82, CD9 and CD63. Of these, CD63 is considered by some to be solely found on

exosomes (and not MVs) and is consequently heavily relied upon as a specific exosome marker (Heijnen et al. 1999; Pols et al. 2009; Raposo et al. 2013). The exact general intracellular function of CD63 remains unclear; although it does possess cell-type specific functions (Pols et al. 2009). Recent studies have also identified a role for CD63 in exosome biogenesis (Van Niel et al. 2011; Edgar et al. 2014). In contrast to exosomes, a MV-specific protein marker is yet to be identified (Raposo et al. 2013).

In addition to shared protein content, exosomes and MVs both share similar lipid compositions. For example, both have been shown to be enriched in lipid raft components (De Gassart et al. 2003; Del Conde et al. 2005). These are self-assembling sphingolipids- and cholesterol- enriched microdomains within membranes that act as sorting platforms for specific transmembrane proteins as well as caveolin and Src-tyrosine kinases (Simons et al. 1997; De Gassart et al. 2003), indicative of their functional roles in signal transduction (**Fig. 1.3**) (Simons et al. 2000). Lipid rafts mediate protein sorting in various subcellular compartments within cells, including the multivesicular body and plasma membrane (Helms et al. 2004). For example, at the plasma membrane, GPI-anchored proteins (**Fig. 1.4**) sort into lipid raft domains and are internalised via a clathrin-independent mechanism dependent on protein clustering and the formation of caveolae, caveolin-enriched membrane invaginations, although caveolin-independent mechanisms have also been reported (Fujimoto 1996; Simons et al. 1997; Sabharanjak et al. 2002; Nichols 2003). It has been proposed that the formation of lipid-raft enriched domains function in (ESCRT-independent) exosomes biogenesis (De Gassart et al. 2003; Trajkovic et al. 2008).

1.3.5 Vesicle biogenesis

Exosomes are formed as a result of the maturation of late endosomal compartments. The inward budding and pinching off of the late endosomal limiting membrane results in the formation of intraluminal vesicles (ILVs) (**Fig. 1.5**), which are released as exosomes into the extracellular milieu following the trafficking to, and fusion of, MVBs with the plasma membrane (**Fig. 1.1**). Both

trafficking and fusion are highly regulated processes that rely on a wide range of specific factors (Section 1.3.4.6).

MV formation involves the extracellular protrusion and pinching off of the limiting plasma membrane, also known as apical membrane shedding. The wide range of MV sizes suggests either that several mechanisms may operate to produce vesicles, or alternatively that the process of biogenesis is not as heavily regulated as exosome biogenesis. Original models for the biogenesis of MVs involved the passive shedding of a cell's limiting membrane incurred from extracellular forces. However, recent studies have suggested that MV shedding may also be an active process (Section 7.1.2).

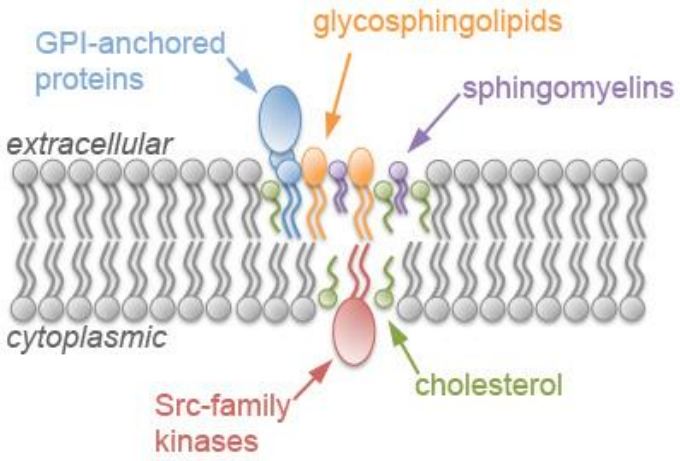


Figure 1.3. Asymmetric lipid raft domain organisation. Self-assembling lipid raft segregate from other regions of lipid bilayers (grey) can be enriched with GPI-anchored proteins (blue), glycosphingolipids (orange), sphingomyelin (purple) and cholesterol (green) in the outer extracellular leaflet of lipid bilayers, whilst the cytoplasmic leaflet can contain cholesterol and acylated proteins such as Src-family kinases (red).

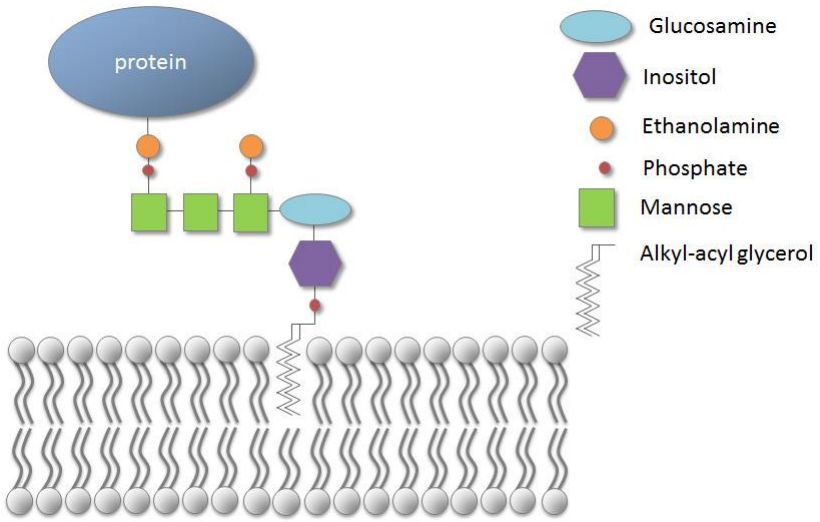


Figure 1.4. Schematic structure of GPI-anchored proteins. Proteins are covalently attached via their C-terminus to a GPI-anchor, comprising: an alkyl-acyl glycerol lipid moiety that is inserted into the outer leaflet of the membrane, an inositol ring, glucosamine and sugar residues such as mannose. The core structure can possess a range of side-chain modifications including phosphoethanosamines (Orlean et al. 2007).

1.3.5.1 Exosome biogenesis

Several models have been proposed to describe the mechanism of ILV formation inside MVBs, from which exosomes are derived. Despite the long-held belief that the ESCRT-complex mediates maturation of LEs to MVBs, and thus exosome biogenesis, by facilitating both ILV formation and cargo sorting at the surface of LEs, recent studies in both yeast (Katzmann et al. 2001; Babst et al. 2002; Babst et al. 2002) and mammalian cells (Stuffers et al. 2009; Van Niel et al. 2011), involving the inhibition or depletion of components of the ESCRT complex, have alluded to the possibility of both ESCRT-dependent and -independent mechanisms of exosome biogenesis.

1.3.5.2 ESCRT-mediated exosome biogenesis

The sequential recruitment of members of the ESCRT complex (ESCRTs 0 -III) (**Fig. 1.5**) to the surface of LEs is initiated by Hrs, a subunit of ESCRT-0 (Katzmann et al. 2003). Hrs is essential for ILV formation in several cells types, a function which is conserved in *Drosophila* (Lloyd et al. 2002). Hrs possess a FYVE (Fab1, YGL023, Vps27, and EEA1) domain that allows it to directly interact with the phosphatidyl-inositol 3 phosphate(PtdIns(3)P)-enriched cytoplasmic leaflet of the endosomal membrane (Misra et al. 1999), created by the activity of the Class III PI3-Kinase (PI3K), Vps34. Inhibition of Class III PI3K activity prevents the formation of multivesicular endosomes (Fernandez-Borja et al. 1999; Futter et al. 2001), presumably due to the loss of Hrs and thus downstream ESCRT component recruitment. Consistent with this, several studies have demonstrated a requirement for Hrs for CD63-positive exosome secretion (Tamai et al. 2010; Tamai et al. 2012; Colombo et al. 2013). The ESCRT complex subunits, as well as the accessory factors ALiX (Section 1.3.5.3) and Vps4, act sequentially to mediate sorting and ILV formation (**Fig. 1.5**).

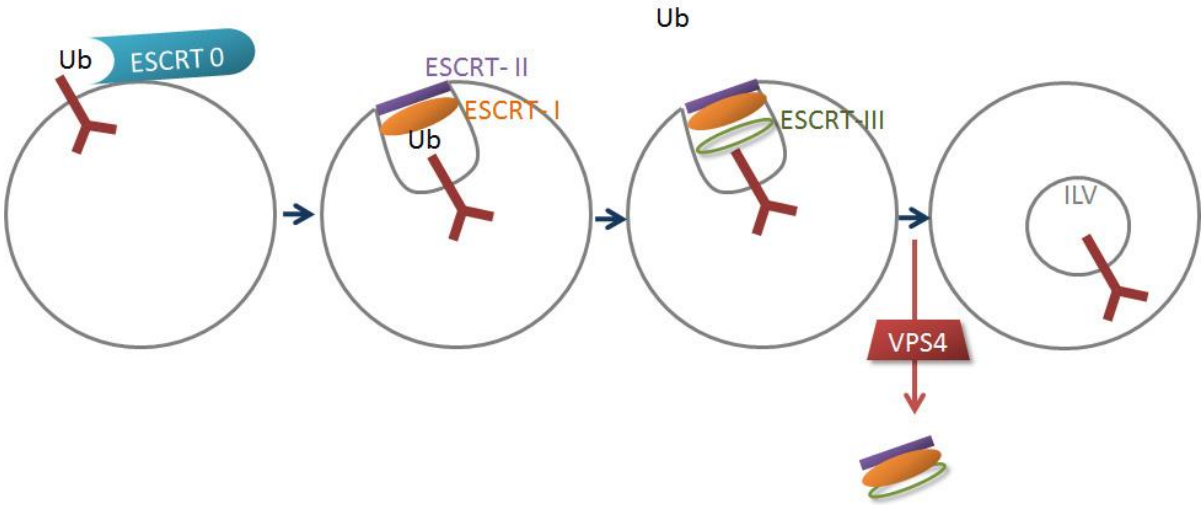


Figure 1.5. ESCRT-dependent ILV formation. ESCRTs 0 (blue) and I (orange) recognise ubiquitinated proteins such as RTKs (flagged for degradation) (Katzmann et al. 2001). ESCRT II (purple) is subsequently recruited (Babst et al. 2002) whose Y-shaped structure may function, together with ESCRT I to initiate membrane invagination (Wollert et al. 2010). ESCRT II subsequently recruits ESCRT III (green), whose polymerisation into a helical filament (Ghazi-Tabatabai et al. 2008) is hypothesised to provide the driving force for the inward budding of the limiting membrane (Hanson et al. 2008) as well as driving membrane scission (Wollert et al. 2009), as well as potentially the AAA-ATPase, Vps4, whose contribution to this process remains controversial (Wollert et al. 2009; Adell et al. 2011), but may mediate disassembly of the ESCRT complex for repeated ILV biogenesis (Babst et al. 2002; Wollert et al. 2009).

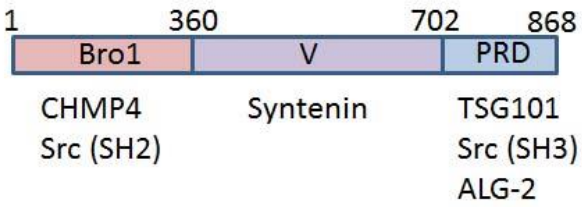


Fig. 1.6 Schematic of ALiX domain structure. ALiX contains Bro1, Variable (V) and Proline-rich (PRD) domains. Numbers above indicate amino acid residues. Known interaction partners are listed underneath their identified binding domains, adapted from (Baietti et al. 2012).

1.3.5.3 The role of ALiX in ESCRT-dependent biogenesis

Bro1 (BCK1-like resistance to osmotic shock 1) was identified in the yeast screen for vacuolar sorting proteins (Raymond et al. 1992) and is required for MVB maturation in yeast (Odorizzi et al. 2003).

Bro1's mammalian homolog *ALiX* (apoptosis-linked gene 2-interacting protein X) has been shown to be involved in selective sorting at the surface of MVBs both directly through ubiquitin-binding activities (Pashkova et al. 2013) as well as indirectly through its interactions with members of the ESCRT complex (Wemmer et al. 2011). Recent studies have demonstrated its important role in exosome biogenesis (Matsuo et al. 2004; Baietti et al. 2012): knockdown of *ALiX* by siRNA reduces ILV formation inside late endosomes of HeLa cells (Matsuo et al. 2004), and *ALiX* RNAi in hematopoietic stem cells reduces the secretion of CD63-GFP exosomes (Baietti et al. 2012). However, as these studies relied upon western blot analysis of isolated exosomes it remains possible that ALiX is simply required for protein sorting into ILVs rather than ILV biogenesis itself.

Importantly, as *Bro1* and mammalian *ALiX* exhibit only 22% sequence homology, it is likely that the yeast/mammalian homologues harbour specific cellular functions (Sadoul 2006). In addition to the Bro1 domain, mammalian ALiX contains a V domain and PRD domain, which have been shown to be required for interactions with syntenin and TSG101, respectively, both of which have been implicated in exosome biogenesis (Baietti et al. 2012; Edgar et al. 2013). Importantly, *Drosophila ALiX* homolog possesses the proline-rich C terminal region shown to be responsible for interactions with syntenin and TSG101 (Tsudaa et al. 2006).

1.3.5.4 ESCRT-independent exosome biogenesis

As previously mentioned, several recent studies have demonstrated that in the absence of ESCRTs ILVs are still able to form (Trajkovic et al. 2008; Stuffers et al. 2009), suggesting that alternative mechanisms exist to allow ILV formation. The majority of ESCRT-independent models proposed

involve the utilisation of distinct lipid microdomains to generate membrane curvature (Contreras et al. 2003; Markvoort et al. 2007; Staneva et al. 2009) and mediate cargo sorting. These models build upon the observation that the exosomal membrane is enriched in lipid raft components (Wubbolts et al. 2003), and that cholesterol-enriched microdomains are specifically internalised on ILVs from the surface of MVBs (Möbius et al. 2003). Studies in various cell lines have implicated ceramides (derivative of sphingolipids; (Trajkovic et al. 2008)), as well as lysobisphosphatidic acid (LBPA), a phospholipid selectively enriched on endosomal membranes (Matsuo et al. 2004), in formation of a distinct ESCRT-independent lipid-raft-enriched ILV populations.

A recent study has also demonstrated a role for an inhibitory G protein (Gi)-coupled sphingosine 1-phosphate receptor (S1P) in ESCRT-independent ILV formation and cargo sorting (Kajimoto et al. 2013). G_i S1P receptor activity has been shown to be required to permit ILV formation and thus exosome release in an autocrine fashion.

1.3.5.5 Interaction of ESCRT-dependent and -independent mechanisms

Distinct ILVs formed by ESCRT-dependent and ESCRT-independent mechanisms have been identified in the same MVB, suggesting that the two mechanisms sort distinct cargos into distinct vesicles, forming a mixed population of ILVs in one compartment (Stuffers et al. 2009). Nevertheless, several studies have indicated complex antagonistic interaction between these two mechanisms.

LBPA has been shown to interact with ALiX, which in turn interacts both directly with the ESCRT machinery and indirectly via CHMP4A (Katoh et al. 2003; Odorizzi et al. 2003). Interestingly, LBPA-dependent multivesicular liposome formation is inhibited by *ALiX* (Matsuo et al. 2004), suggesting that ALiX antagonises ESCRT-independent ILV biogenesis. Whether this occurs *in vivo* has not yet been clearly demonstrated due to addition effects of *ALiX* knockdown on protein expression in

the cell types studied (Matsuo et al. 2004). Furthermore, recent studies in HeLa cells have demonstrated that knockdown of the ESCRT-0 component *Hrs*, resulted in the up-regulation of ESCRT-independent ILV biogenesis (Edgar et al. 2014). Together, these data suggest that ESCRT-dependent and -independent mechanisms may act antagonistically. Although these two mechanisms give rise to distinct types of vesicles, they appear to act in a 'redundant' manner to ensure the maturation of LEs into MVBs (Edgar et al. 2014).

The mechanism of ILV formation has been shown to be dependent on the cell's microenvironment; the decision between the utilisation of ESCRT-dependent or independent mechanisms is influenced by extracellular signals. A study in HEp-2 cells has demonstrated EGF-induced ILV formation occurring in an ESCRT-dependent manner; yet, in the absence of EGF, ILVs form in an ESCRT-independent manner (Stuffers et al. 2009). This study has provided the first indication that the choice between the predominant ILV formation mechanism utilised may be regulated by growth factor signalling.

1.3.5.6 Trafficking regulation of exosome secretion

In order to identify Rab GTPases that specifically regulate the trafficking of MVBs to the plasma membrane several studies have carried out candidate screens. A screen utilising mammalian cells identified a role for Rab11 in the delivery of MVBs to the plasma membrane and thus a novel role in exosome secretion (Savina et al. 2002; Fader et al. 2005; Savina et al. 2005). Interestingly, Rab11 is classically described to associate with recycling endosomes (Sönnichsen et al. 2000) and is thought to regulate the delivery of endocytosed material back to the plasma membrane. Nevertheless, Rab11 has also been implicated in the classical secretory pathway (Chen et al. 1998), although this function may be cell-type-specific.

In addition to Rab11, further studies in mammalian cell lines have identified roles for Rab7, Rab27 and Rab35 in exosome secretion: knockdown of Rab7 by RNAi prevents the release of 'syndecan'

exosomes (Baietti et al. 2012); Rab27 was identified in studies utilising HeLa cells (Ostrowski et al. 2010), despite Rab27 originally being described as a regulator of secretory vesicle and granule secretion; and Rab35 has also been identified in a screen for regulators of exosome secretion in oligodendrocytes (Hsu et al. 2010), despite its well-characterised role in regulating recycling endosome trafficking. Rab11, Rab27 and Rab35 have all been proposed to function in the docking or tethering of MVBs at the plasma membrane for secretion. The role of Rab7 in exosome biogenesis and/or secretion is yet to be directly addressed. Interestingly, studies in *Drosophila* have failed to identify a conserved role for Rab35 and 27 in vesicle secretion (see below).

Despite the interest in identifying Rab GTPases or Rab effectors that specifically regulate exosome secretion, the majority of studies to date fail to assess whether the Rabs identified also regulate secretion of proteins produced in the classical secretory pathway.

1.3.6 Limitations of studying exosome biogenesis

Recent studies have revealed surprising degrees of complexity, antagonism and redundancy in the exosome biogenesis mechanisms (Section 1.3.5.5), and many studies have reported apparently conflicting results. This wealth of conflicting literature could be explained by cell type specificity of the choice of exosome biogenesis mechanism employed. Furthermore, there may be multiple ESCRT-dependent or –independent mechanisms functioning in a particular cell simultaneously. The choice of markers employed by researchers largely governs the population(s) studied and thus conclusions drawn. The lack of a 'gold-standard' marker for distinct populations may have therefore hindered studies to date (Section 1.3.4).

Alternatively, differences in experimental approaches employed, many of which are associated with inherent limitations, may also explain the apparent conflicting roles of many factors in exosome biogenesis. *in vitro* experiments utilising Giant Unilaminar Vesicles (GUVs) and liposomes have been extremely helpful in characterising the sequential recruitment of ESCRTs

during ESCRT-dependent ILV formation (Matsuo et al. 2004; Falguières et al. 2008); however the simplicity of the system is likely to produce artefactual results. Whether the mechanisms described occur *in vivo* has not yet been explored with comparable detail.

Cell culture systems have been heavily utilised to study exosome biogenesis. Advantages of cell culture include the large volume of culture medium from which huge numbers of exosomes can be isolated. Such large volumes allow the quantitative study of vesicles by methods such as NanoTracking Analysis (NTA) (Van Der Pol et al. 2014). However, this method fails to discriminate between distinct exosome populations that may carry unique cargos and may be made by distinct mechanisms. Ongoing advances in e.g. exosome pull down as well as flow cytometry will be critical in studying the regulation of distinct exosome population secreted by cells in culture.

Many cell culture experiments are reliant upon manipulation of cells from the wild type situation in order to study the late endosomal compartments, which are normally only several hundred nanometers in diameter. These include addition of the ionophore Monensin (Savina et al. 2005) as well as the expression of a constitutively activated Rab5 in order to enlarge late endosomal compartments for imaging purposes (Stenmark 1994; Trajkovic et al. 2008; Baietti et al. 2012; Kajimoto et al. 2013). Such manipulations are likely to cause widespread disruption to the endolysosomal trafficking system, and consequently produce artefactual results. Furthermore, cell culture experiments often utilise immortalised and/or cancer cell lines exhibiting excessive growth factor signalling and cultured in non-physiological conditions e.g. in 2D cultures lacking exhibiting abnormal cell polarity, all of which may also produce artefactual results not reflective of *in vivo* physiology.

In summary, the exosome field is limited by a distinct lack of a good *in vivo* genetic model system in which to study exosome biogenesis; *in vitro* and cell culture methods for isolating exosomes (1.3.3) and studying the mechanisms of ILV biogenesis are associated with a range of inherent

limitations that have hindered the current understanding of the physiological roles of exosomes *in vivo*.

1.3.7 EV interactions with recipient cells

Several models have been proposed for the interaction between EVs and target cells (**Fig. 1.7**). Firstly, EVs can fuse with cells, delivering their soluble contents into the recipient cell cytoplasm and their lipid-associated components directly to the cell membrane (Parolini et al. 2009). Secondly, EVs can dock at the plasma membrane (Denzer et al. 2000), inducing signalling via the interactions with surface cargos or components of the limiting membrane such as receptors. Finally, EVs can be endocytosed by recipient cells (Morelli et al. 2004; Tian et al. 2012) and then either fuse with the endosomal limiting membrane or be transported intact through the endosomal system until they are degraded inside the lysosome.

EVs have been shown to demonstrate target cell specificity, which was initially demonstrated by the selective binding of B cell exosomes to follicular dendritic cells within lymphoid follicles (Denzer et al. 2000). This finding demonstrated that their interaction with recipient cells is a high regulated process, which is likely to be governed by the specific surface expression of adhesion molecules and receptors. Indeed, cell-type-specific gene knockdown utilising EVs harbouring siRNAs has been achieved *in vivo* by systemic injection of EVs expressing specific surface peptides, targeting them to specific cellular subtypes within the brain (Alvarez-Erviti et al. 2011).

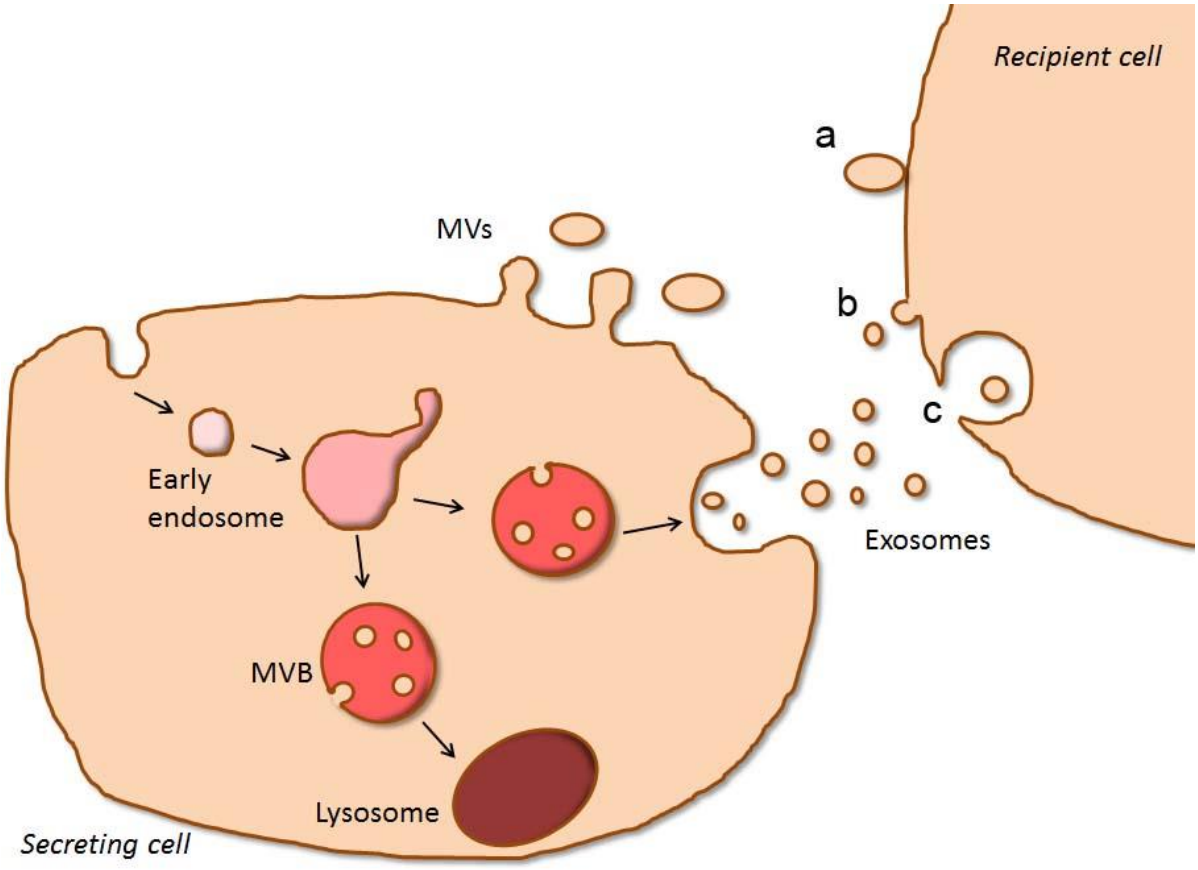


Figure 1.7. MV and exosome secretion and uptake. Following transport to target cells, EVs can either: (a) dock onto target cells, (b) fuse directly with the plasma membrane or (c) be endocytosed intact. Adapted figure from (Cocucci et al. 2009).

1.4 Reproductive signalling

Intercellular signalling during reproduction can also effectively be inter-organismal signalling: male-derived signals can influence female physiology and behaviour. In sexually reproducing species, sexual conflict describes the conflicting reproductive strategies employed by males and females, and their physiological and behavioural manifestations. Consequently, mating induces a wide range of physiological, and in many species, behavioural effects, known as post-mating responses (PMR) (reviewed in (Wolfner 1997)). In addition to these, there are additional costs of mating to females of reduced longevity as well as effects on total lifetime reproductive success (Wigby et al. 2005).

As both egg production and laying are energetically costly, females alter their investment in these physiological processes depending on their reproductive state. In *Drosophila*, the rate of egg laying rapidly increases shortly after mating when sperm are available to fertilise the eggs made (Herndon et al. 1995). A similar mechanism has also been reported in Llamas, whereby β- Nerve Growth Factor (β-NGF) transferred in seminal fluid induces ovulation (Kershaw-Young et al. 2012), suggesting that seminal fluid may also influence mammalian female physiology. Furthermore, in many species including insects, the occurrence of multiple matings, whereby females are able to mate with multiple males within a single period of fertility, leads to the possibility of the presence of sperm from multiple males in the reproductive tract at one time. This permits the possibility of males competing with each other to fertilise a female's eggs, known as 'sperm competition' (Parker 1970). In *Drosophila,* the second male sires the majority of the offspring (Smith 1984). One behavioural mechanism, utilised by many insect species including *Drosophila,* is for mated females to reject courting males, known as 'reduced receptivity to remating', which is induced by the first male mate (Manning 1962). An additional sperm competition strategy employed by males is to induce the formation of a mating plug, which provides a physical barrier to subsequent matings and sperm entry (Lung et al. 2001). These diverse processes are all dependent on factors present in the seminal fluid that are secreted by male reproductive organs and transferred to the

female reproductive tract during mating. To date, the small number of factors identified to have important signalling roles in *Drosophila* reproduction have all been proteins or peptides (Kubli 2003; Kershaw-Young et al. 2012; Kubli et al. 2012), which undergo complex processing by proteolytic enzymes produced by both the male and female during mating (Heifetz et al. 2005; Ravi Ram et al. 2007; Laflamme et al. 2012; Sitnik et al. 2014).

The identification of membrane-bound vesicles in seminal fluid led to the hypothesis that membrane-bound vesicles may play a central role in reproductive signalling, by mediating the delivery of proteins, lipids or nucleic acids to sperm or between male and female cells (Ronquist et al. 1985; Sullivan et al. 2005; Sullivan et al. 2013) (see Section 4.1.1). Two mammalian reproductive glands: the prostate and epididymis, secrete membrane-bound vesicles that could act as delivery vehicles (Sullivan et al. 2005; Kim J 2014). Indeed, *in vitro* experiments incubating sperm with isolated and marked exosomes has demonstrated that they are capable of fusing with sperm under physiological conditions, and can transfer signalling molecules including the progesterone receptor and calcium signalling tools (Park et al. 2011).

Importantly, whether these interactions occur *in vivo* and whether membrane-bound vesicles have a role in sperm signalling or even inter-organism signalling has not yet been answered due to a lack of a genetic model system in which to address these questions. Furthermore, whether EVs are secreted into reproductive fluids in invertebrates has not yet been investigated.

1.4.1 The *Drosophila* male accessory gland

The *Drosophila* Accessory Gland (AG) shares functional similarities with the mammalian prostate and seminal vesicles, secreting many components of the seminal fluid that is transferred to females during mating. *Drosophila* males possess two accessory glands comprising a monolayered epithelium forming a blind-ended sac encased by a muscular sheath, which contracts during mating to expel the stored lumenal contents into a single ejaculatory duct (**Fig 1.8**) (Bairatia

1968). The epithelium contains two binucleate cells types: main cells (MCs) and secondary cells (SCs) that are morphologically (Bairatia 1968) and biochemically distinct (Bertram et al. 1992). There are approximately 40 SCs, which are dispersed between the predominant (approximately 1000) main cells in the distal third of each gland (Bertram et al. 1992). In contrast to the flat, hexagonal MCs, SCs are larger, spherical cells that bulge into the lumen of the gland (Bertram et al. 1992) (**Fig. 1.9**). Together with sperm, the stored contents of the AG are transferred into the female reproductive tract during mating (**Fig. 10**). Males lacking AGs are sterile (Xue et al. 2000), demonstrating the importance of AG secretions in *Drosophila* reproduction. AG secretions have important roles inducing a range of physiological and behavioural post-mating responses (PMRs) in females following mating (Walker et al. 2006; Ravi Ram et al. 2007) (Section 1.4.2).

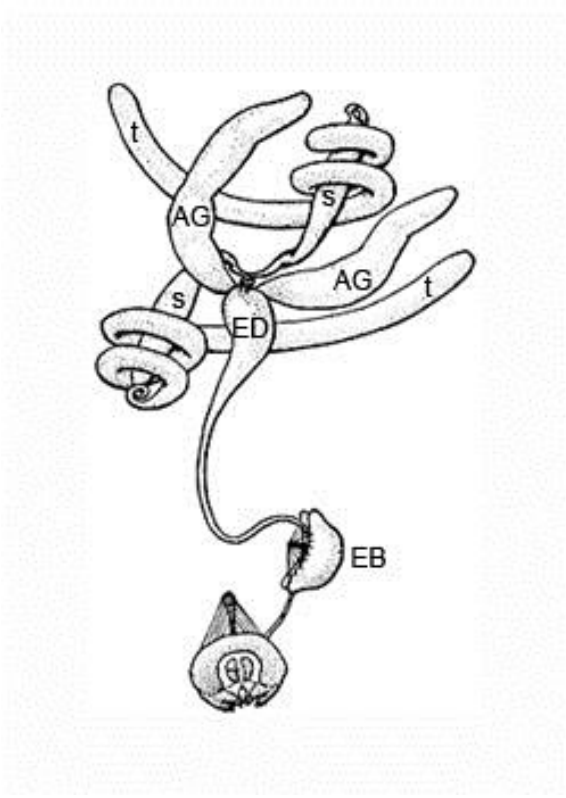


Figure 1.8. Male reproductive tract schematic (Miller 1950). Sperm are made in the testes (T). Mature sperm are stored in the seminal vesicles (s). Both sperm and the seminal fluid products made by the accessory glands (AGs) exit the male via the ejaculatory duct (ED) through the ejaculatory bulb (EB).

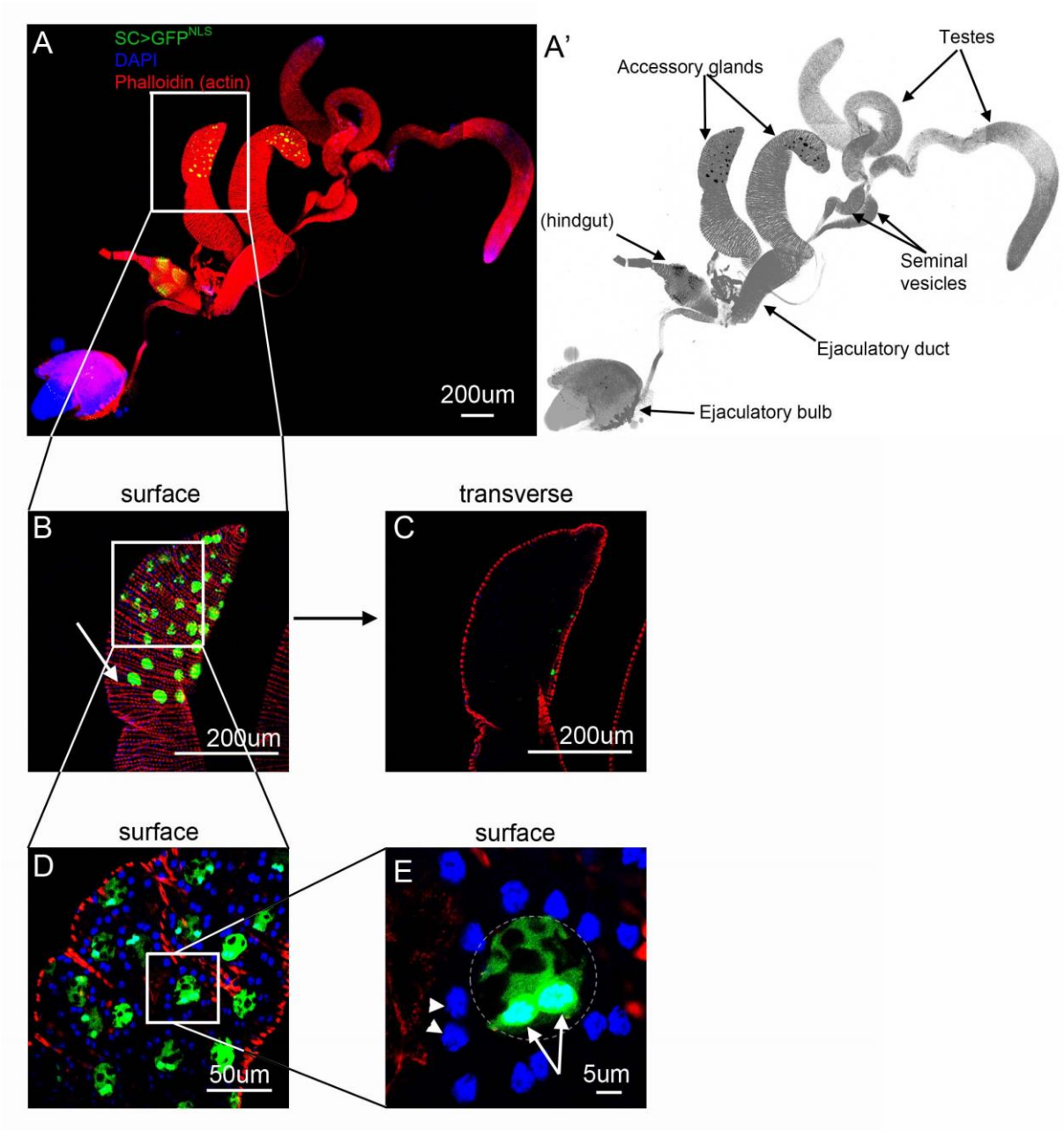


Figure 1.9. Confocal imaging of the male reproductive tract. (**A-E**) 3-day-old *spi-Gal4; UAS-GFP^{NLS}* virgin male reproductive tract, stained with Phalloidin (red) to show encasing muscular sheath (arrows in **B**) and DAPI (blue) to shown cell nuclei. GFP containing a nuclear-localisation sequence (NLS) is expressed specifically in SCs under UAS-GAL4 control utilising a SC-specific promoter (*spitz-Gal4*) (see Fig 2.1). (**E**) Shows a single outlined GFP-positive SC; arrow heads indicate a pair of MC nuclei, arrows indicate a pair of SC nucleic which are GFP-positive. **A'** shows a schematic representation of tract in **A**. **B, D** and **E** show higher magnification images of the regions outlined in **A, B** and **D**, respectively. **C** shows a transverse confocal section through the lumen of the gland shown in **B**. Scale bars marked on images.

The accessory gland secretes a complex concoction of proteases and antiproteases (Laflamme et al. 2013)(Accessory gland proteins [Acps]), many of which are likely to function not only in the coagulation of the mating plug but also in the processing of prohormone-like factors and signalling molecules. The secretion of Acps is responsive to external cues. Both RNA and protein synthesis in the accessory gland is responsive to mating (Schmidt et al. 1985; DiBenedetto et al. 1990), which has been hypothesised to function to replenish the gland's secretory contents following its expulsion during mating (Bertram et al. 1992). If flies are maintained in virgin state, the rate of protein synthesis within the gland decreases from 3-day-old (DiBenedetto et al. 1990); synthesis is only stimulated upon copulation. Furthermore, the composition of the ejaculate passed to females has been shown to be modulated by males depending on external cues such as the partnering female's mating status (Sirot et al. 2011).

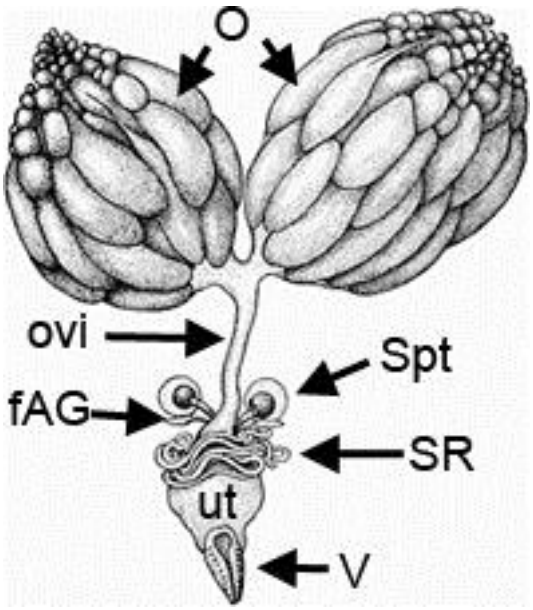


Figure 1.10. Female reproductive tract schematic (Patterson 1943). Sperm and secretions of the AG enter the uterus (Ut) through the vagina (V). Within 15 minutes, sperm reach the two storage organs, the seminal receptacle (SR) and the spermathecae (Spt), where they are stored. Gradual release of sperm from storage is dependent on SP (Avila et al. 2010). The female accessory glands (fAGs) attach posterior to the spermathecae. Matured eggs exit from the ovaries (O) and travel down the oviduct (ovi) to be fertilised in the uterus.

1.4.2 The *Drosophila* female post-mating response

The PMR includes increased egg laying, resulting from both increased oogenesis (Soller et al. 1999) and ovulation (Heifetz et al. 2005); increased immunosuppression through reduced release of antimicrobial peptides (Peng et al. 2005); and reduced receptivity to remating, which

comprises behavioural responses to courting males including kicking and ovipositor extrusion (Manning 1962). The PMR can be divided into the short- (STR) and long- (LTR) term responses, which differ both in their molecular regulation as well as their physiological and behavioural manifestations. The STR describes female physiological and behavioural changes that occur over the first 24 hours following copulation (Kalb et al. 1993); the LTR describes subsequent changes and lasts for approximately 10 days (Manning 1962). Specific aspects of these responses are induced by specific factors, some of which act redundantly (**Table 1.2**).

Use of *prd*Res (*prd* mutants rescued until adulthood) males, which possess 'severely reduced' AGs or lack them altogether, demonstrated that AG-derived signals are responsible for induction of most of the PMR (Xue et al. 2000). One Acp is considered to be the major mediator of the PMR: the main cell product Sex Peptide (SP) (Chen et al. 1988; Xue et al. 2002; Kubli et al. 2012). Ten years subsequent to its discovery, a gene which shared a large degree of sequence homology was identified, encoding the ejaculatory duct product DUP99B (Saudan et al. 2002; Rexhepaj et al. 2003). Despite their high sequence homology, in contrast to *SP*-null males SP_0, which elicit a very limited PMR (Liu et al. 2003), *DUP99B*-null males are capable of inducing nearly the full range of PMRs, suggesting that SP is the major PMR signalling mediator and the contribution of DUP99B is minimal (Kubli 2003).

The AG products ovulin (Herndon et al. 1995) and CG33943 (Ram et al. 2007) also play minor roles in the STR. The combinatorial activity of all these factors is required for the full stimulation of ovulation and egg-laying during the first 24 hours after mating (Herndon et al. 1995; Heifetz et al. 2005; Ram et al. 2007).

Importantly, many seminal fluid proteins responsible for inducing the PMR require complex processing by proteases produced by both the male and female during and after transfer to the female reproductive tract (Ravi Ram et al. 2006; Laflamme et al. 2012; Laflamme et al. 2013; Sitnik et al. 2014). For example the serine protease Seminase (CG10586) and the astacin-like

protease (CG11864) are required for the processing of PMR regulators including ovulin and SP (Peng et al. 2005; Ravi Ram et al. 2006; Laflamme et al. 2012).

Injection of synthetic membrane-bound-SP or isolated SP into virgin females induces only a 'short-term' mating response lasting approximately 1 day (Chen et al. 1988; Kubli 2003). Furthermore, spermless (*tudor*) males are incapable of inducing the LTR despite producing normal and functional SP and other Acps (Manning 1962; Boswell et al. 1985; Kalb et al. 1993; Bertram 1996; Liu et al. 2003). The *storage* of transferred sperm has been shown to be crucial for the LTR, the so-called 'sperm effect' (Kalb et al. 1993). SP is the mediator of this 'sperm effect' (Chapman et al. 2003; Liu et al. 2003), as a proportion of the SP transferred to females interacts with sperm via its N-terminal domain and 'hitchhikes' its way to the sperm storage organs (Peng et al. 2005). Gradual cleavage of SP releasing a C terminal fragment, mediated by an unknown trypsin protease (Peng et al. 2005), allows the long term maintenance of the PMR (Peng et al. 2005). The gradual release of sperm from the storage organs is in turn dependent on SP (Avila et al. 2010). Additional Acps involved in the LTR are thought to be required for binding of SP to sperm. These include the serine protease CG19997, the lectins CG1656 and CG1652 as well as CRISP (CG17575; a cysteine rich secretory protein) (Ram et al. 2007; Ram et al. 2009). It has been hypothesised that the long sperm tails of *Drosophila* species may have evolved to facilitate this sperm-dependent function of SP (Peng et al. 2005).

Signal	Response	Effects
Sex Peptide (SP; Acp70A)	STR and LTR	• Increased egg laying (Liu et al. 2003) • Increased oogenesis (via JH) (Fan et al. 1999) • Reduced receptivity to remating (Liu et al. 2003; Peng et al. 2005) • Sperm release from storage (Avila et al. 2010)
DUP99B	STR	• Increased egg laying (STR) • Reduced receptivity to remating (Saudan et al. 2002)
Ovulin (Acp26Aa)	STR	• Increased egg laying (Herndon et al. 1995)
Acp36De	LTR (indirect)	• Conformational change of uterus, sperm storage (Avila et al. 2009) • Sperm competition (Chapman et al. 2000)
CG33943	STR	• Increase egg laying (Ram et al. 2007)
Sperm	LTR (indirect)	Carrier of SP into storage organs (Liu et al. 2003; Peng et al. 2005)
CG11864 (astacin protease)	STR	• Processing of Ovulin and Acp36De required for STR functions (Laflamme et al. 2012)
Seminase	STR and LTR	• Processing of multiple factors including CG11864 and LTR machinery(Laflamme et al. 2012)
CG9997 (serine protease)	LTR	• Required for CG1652 and CG1656 transfer to females and thus SP binding to bind sperm (Ram et al. 2007; Ram et al. 2009)
CRISP (CG17575)	LTR	• Required for CG1652, CG1656 and SP to bind sperm (Ram et al. 2007; Ram et al. 2009)
Lectins (CG1652 and CG1656)	LTR	• Binds sperm • May recruit SP to sperm (Ram et al. 2007; Ram et al. 2009)

Table 1.2. Factors with identified roles in the PMR.

Following its transfer to the female reproductive tract SP undergoes several processing events (Laflamme et al. 2012; Laflamme et al. 2013). Injection of synthetic SP fragments of the peptide into the abdomen of virgin females demonstrated that the C-terminal domain is required to induce the PMR (Schmidt et al. 1993). Whilst the N-terminal is required for sperm binding, the C-terminal domain binds to and activates the SP receptor (SPR) (Yapici et al. 2008). As previously mentioned, gradual cleavage of SP, releasing the C-terminal domain is responsible for maintaining the PMR over several days (Peng et al. 2005). The N-terminal domain of SP is also necessary to elicit sustained oogenesis via the stimulation of juvenile hormone (JH) synthesis (Moshitzky 1996; Fan et al. 1999), although the molecular mechanism of this activity is not yet known. DUP99B has also been demonstrated to activate the SPR (Yapici et al. 2008), although does not stimulate JH synthesis (Fan et al. 1999), nor maintain reduced receptivity to remating. Thus SP and DUP99B can only be said to be partially functionally redundant.

In summary, AG-derived signals including SP, DUP99B and ovulin govern the STR, whilst the LTR is mediated by the gradual cleavage and release of sperm-bound SP from storage organs.

1.4.3 SP targets

After mating, SP can be detected not only in the female reproductive tract but also in the fly hemolymph (Pilpel et al. 2008). Furthermore, the SP-mediated PMR can be induced in virgin females by ectopic SP transgenic expression in female cells (Aigaki et al. 1991; Nakayama S 1997) or injection of synthetic SP into the hemolymph (Chen et al. 1988). The neural circuitry involved in the PMR is well-characterised, and SP-responsive neurons terminate both inside the female reproductive tract, as well as within the central and peripheral nervous system (E. Kubli 2003; Rezával et al. 2012). Furthermore, the SP receptor, SPR, is expressed both within the reproductive tract as well as in specific cells of the nervous system (Yapici et al. 2008), in neurons that express both fruitless (*fru*) and pickpocket (*ppk*) (Yang et al. 2009). However, only a subpopulation of these *fru/ppk* neurons are necessary and sufficient to induce the SP-dependent PMR (Yang et al.

2009; Häsemeyer et al. 2009). Importantly, *fru/ppk* neurons that also express the sex determination factor doublesex (*dsx*) are necessary to initiate the PMR (Rezával et al. 2012).

1.4.4 Roles of SCs in PMR

The role of SCs in reproduction is relatively poorly characterised, largely due to both their low incidence in the AG as well as a lack of tools to specifically modulate their gene expression. SCs have been shown to contribute to the production of several factors also secreted by MCs, including male-specific proteins (msPs) 355a and 355b (Monsma 1990); however, their role in producing these proteins is likely to be negligible given that they represent only 4% of secretory cells in the AG. Secondary cells have been shown to secrete Angiotensin Converting Enzyme (ANCE) (Rylett et al. 2007), which has also been identified as a component of human seminal fluid (Pilch et al. 2006) and has been proposed to contribute to seminal fluid protein processing (Rylett et al. 2007), although this has not yet been addressed. ANCE is localised to the dense secretory core of large secretory vacuoles of SCs (Rylett et al. 2007), which is surrounded by filamentous material of unknown identity that is also secreted into the gland lumen (Bairatia 1968; Tandler et al. 1968).

Importantly, recent studies indicate that in addition to MCs, which produce key PMR regulators such as SP and ovulin, SCs also have a specific role in the LTR; however, the nature of this contribution is yet to be fully established. Certain MC secretory products implicated in the PMR, such as ovulin, have been shown to require SCs in order to be processed to produced mature signalling protein (Gligorov et al. 2013), suggesting that SCs either secrete the processing enzymes responsible into the seminal fluid, or endocytose MC-derived factors in order to carry out processing.

Previous work in the host lab revealed that BMP signalling in adult SCs is required for males to induce the full PMR in females (Leiblich et al. 2012). BMP signalling is required specifically in SCs

to prevent females from remating for at least 3 days following copulation. Importantly, under the conditions of this study, BMP signalling does not modulate other aspects of the PMR i.e. egg laying or fecundity, in the short (<1 day) or long term (>1-3 days), indicating that this SC-mediated function either acts independently of SP, or modulates only specific aspects of the SP-dependent LTR. In addition, BMP signalling in SCs promotes growth, delamination and sporadic migration of these cells, which occurs only in multiply-mated aged (11-day-old) wild-type males. Delaminated SCs can be transferred to females via the seminal fluid. Importantly, all mating experiments performed in this publication, as well as this present study (Section 4.3.3), were carried out with 4-day-old males and therefore we conclude that SC transfer is not critical for the BMP-dependent role of SCs in modulating the PMR (Leiblich et al. 2012).

Secondary cells contain approximately 15 giant secretory vacuoles. It has been suggested that these 'secretory' vacuoles are not all equivalent (Rylett et al. 2007), however the identities of all large compartments within the SC has not previously been characterised. Importantly, the mechanisms underlying the regulation of SC secretion have also not been characterised. Interestingly, a recent study has identified a transcriptional network driven by the Hox gene *Abdominal B* (*Abd-B*) in the regulation of SC secretory function (Gligorov et al. 2013). Loss of *Abd-B* leads to the loss of SC vacuoles as well as defects in the many aspects of the PMR, including reduced egg laying, as well as reduced receptivity to remating. *Abd-B* expression in SCs is required for processing events of secreted factors involved in the short and long term mating responses: ovulin (Herndon et al. 1995), and the lectins CG1656 and CG1652 (Ram et al. 2007), respectively. These data suggest that SCs may produce proteases that are responsible for the processing of many AG products, including MC products, and thus modulate the PMR induced by these factors.

In summary, the BMP-dependent modulatory role of SCs functions in only specific aspects of the LTR (receptivity to remating), whereas the *Abd-B*-dependent activities of SCs influence a broader

range of aspects of the LTR, presumably because it plays a fundamental role in programming the fate of these cells.

1.5 Aims and objectives

Despite the rapidly increasing interest in membrane-bound vesicles over the recent years, there are many key outstanding questions that have yet to be answered, including which key signalling pathways(s) regulate EV biogenesis and/or secretion (Chapters 5 and 6). With regard to reproduction, whether EVs present in the seminal fluid have an important signalling function is yet to be addressed *in vivo* (Chapters 4 and 7). Indeed, although previous studies have illustrated that EVs are secreted into mammalian seminal fluid, whether this event is conserved in insects has not yet been investigated (Chapters 3 and 7).

My work presented in this thesis addresses these outstanding questions by establishing a novel genetic system in which to study EV biogenesis and secretion, as well as investigate the roles of seminal fluid EVs in fly reproduction, using the *Drosophila* accessory gland.

The aims of this thesis include:

1. Identify the **nature** and **origin of membrane-bound vesicles** (EVs) secreted by cells of the accessory gland.
2. Identify **regulators** of EV secretion, and analyse the subcellular function of these regulators.
3. Characterise **roles of** AG-derived EVs in reproduction.

The majority of work presented focuses on the regulation and role of exosomes secreted by the secondary cell of the accessory gland (Chapters 3-6). Although initial work characterising MVs

secreted by main cells is also presented (Chapter 7), further work will be required to fully characterise their regulation and roles in *Drosophila* reproduction.

Much of the material presented in Chapters 3, 4 and 5 has now been accepted for publication in the *Journal of Cell Biology* (Corrigan et al. 2014).

2. Materials and methods

2.1. Buffers/media table

Buffer/media	Description
PBS (Phosphate buffered saline)	One tablet dissolved in 200ml of ddH20, yielding: 0.01M Phosphate buffer 0.0027M KCl 0.137 M NaCl pH 7.4
PBST	PBS with 0.3% (v/v) Triton X-100
PBSTG	PBST with 10% (v/v) Goat serum
PBSTG-fem	PBS with: 0.5% Triton X-100 3% Goat Serum 0.1% BSA
TBST	Tris-buffered saline Tween 20
TBST/BSA	TBST 5% BSA
PFA	4% Paraformaldehyde in PBS
Fly food (25L)	241g agar 17.5g calcium 1875g cornmeal 300ml ethanol 2325g glucose 62.5g Nipagen 215g KNa tartrate 787g yeast
Chitinase solution	6U of chitinase (Sigma No. C6137; (*Streptomyces Griseus*) per ml in PBST-0.3%

Table 2.1. Standard buffers and media. All chemicals are from Sigma unless otherwise stated.

2.2 Fly strains

2.2.1 Fly strains table

Table 2.2. GAL4 driver lines. See Fig. 2.1 for Gal4 driver line expression patterns.

stock no.	Genotype	Source/Ref	Description
A13005	*w; esg-GAL4 tub-GAL80ts UAS-GFPnls/CyO; UAS-flp act>CD2>GAL4/TM6*	Edgar (Jiang et al. 2009)	"*esg^{ts} F/O*" SC driver
A13006	*w; spi-GAL4 on II (NP0261)*	Kyoto112-114 (Hayashi et al. 2002)	SC driver
A13008	*w; dsx-GAL4/TM6B*	Goodwin (Rideout et al. 2010)	SC (and ejaculatory duct) driver
A13059	*w, Acp26Aa-GAL4*	Goodwin (Chapman et al. 2003)	MC driver
A4441	y^1 w^*; P{w^{+mc}=Act5C-GAL4} 17bFO1/TM6B, Tb^1	Bl-3954	
A15068	*w; spi-GAL4, tubGAL80ts/CyO*	Corrigan	Temperature sensitive SC driver
A4441	*y^1 w^*; P{w^{+mc}=Act5C-GAL4} 17bFO1/TM6B, Tb^1*	Bl-3954	Actin-Gal4 (ubiq. driver)
	w; UAS-CD63-GFP, tubulin-GAL80^{ts} ; dsx-GAL4/SM5.TM6	Corrigan	SC CD63-GFP driver line

Table 2.3. Misc. stocks

stock no.	Genotype	Source/Ref	Description
A217	w; $dpten^1$ (F9.2)/CyO Roi	Goberdhan (Goberdhan et al. 1999)	2nd Chr balancer
B989	*w; Df(2L)170B FRT 40A/SM5^TM6*	C Wilson (Goberdhan et al. 1999)	2nd and 3rd Chr balancer
A13015	*w[*]; noc[Sco]/CyO; P{w[+mC]=tubP-GAL80[ts]}7*	Bl 7016	temperature sensitive repressor
A13016	*w[*]; P{w[+mC]=tubP-GAL80[ts]}10; TM2/TM6B, Tb[1]*	Bl 7108	temperature sensitive repressor
A4054	*w; P[w+; tub-hpten HD9.4]/TM3 Ser*	Goberdhan (Goberdhan et al. 1999)	3rd chromosome balancer

Table 2.4. Fluorescent tagged transgenic constructs.

stock no.	Genotype	Source/Ref	Description
A15013	*w[*]; P{w[+mC]=UAS-mCD8.ChRFP}3 on III*	Bl 27392	CD8-RFP
A4429	*$W^{[1118]}$;P{$w^{[+mc]}$=UAS-GFP.nls}14* on II	Bl 4775	nuclear GFP
A15050	*UAS-GFPgpi2.1/CyO*	Eaton (Panakova et al. 2005)	GPI-anchored GFP (MV marker)
A15051	*UAS-CD63-GFP/CyO; Dr/TM3 Sb*	Eaton (Panakova et al. 2005)	Exosome marker
A15052	*UAS-GFPgpi3.1 (533-17)*	Eaton (Panakova et al. 2005)	GPI-anchored GFP (MV marker)
A15749	y[1] w[*]; P{w[+mC]=UAS-btl::GFP-S65T}3	Bl 41802 (Sato et al. 2002)	FGFR-GFP
A15164	*UAS-Egfr-GFP on II*	Kornberg (Alvarado et al. 2004)	EGFR-GFP
A15177	*protB-RFP-160 (2)*	Belote/Pinick (Köttgen et al. 2011)	Sperm head marker
A15183	*w; SP:GFP (II)*	Goodwin (Villella et al. 2006)	Sex peptide-GFP driven by SP promoter
A15191	*UAS-memb-Spi-GFP*	Shilo (858) (Tsruya et al. 2002)	membrane-bound Spitz
A15296	*w; tub-YFP-Rab7 on III*	JP Vincent (Marois et al. 2006)	Ubiquitious Rab7-YFP
A15298	*w; tub-YFP-Rab11 on III*	JP Vincent (Marois et al. 2006)	Ubiquitious Rab11-YFP
A15299	*w; tub-YFP-Rab5 on III*	JP Vincent (Marois et al. 2006)	Ubiquitious Rab5-YFP
	tub-PI4KII-YFP on II	Julie Brill (Burgess et al. 2012)	Ubiquitous PI4KII-YFP

Table 2.5. Non-RNAi transgenics.

stock no.	Genotype	Source/Ref	Description
A15081	*y[1] w[*]; P{w[+mC]=UAS-Egfr.DN.B}29-77-1; P{w[+mC]=UAS-Egfr.DN.B}29-8-1*	Bl 5364 (Freeman 1996)	EGFR DN
A15096	*w[*]; P{w[+mC]=Egfr.1.A887T.UAS}12-7 – EGFR-act*	Bl 9536 (Freeman 1996)	EGFR CA
A4626	*w; P[w+ UAS-Dad]*	D. Bennett (Tsuneizumi et al. 1997)	Dad overexpression
A15154	*w[*]; P{w[+mC]=UAS-tkv.Q253D.Nb}3/TM3, Sb[1] Ser[1]*	Bl 36536(Adachi-Yamada et al. 1999)	*tkv* CA
A6023	*Yw hsFLP; TM3 UAS-shiK44A/TM6B*	Neufeld (Hennig et al. 2006)	*shibire* DN
A472	*SJ9-UAS-Dp110* on II	Hafen (Leevers et al. 1996)	*PI3K* over-expression
A470	*SJ4-UAS-Dp110-CAAX* on II	Hafen (Leevers et al. 1996)	*PI3K* CA
A471	*SJ16-UAS-Dp110^{D974A}* on III	Hafen (Leevers et al. 1996)	*PI3K* DN
A4041	W; P[w+; UAS-dpten FF20.2]/CyO	Goberdhan (Goberdhan et al. 1999)	*pten* over-expression
A5261	W; UAS-pten2-PDZ on II	Xu/Pichaud (Pinal et al. 2006)	*pten*-PDZ (membrane-targeted pten)
A15104	*y[1] w[*]; P{w[+mC]=UASp-YFP.Rab11.S25N}35 – Rab11-dn*	Bl 9792 (Zhang et al. 2007)	*Rab11* DN

Table 2.6. RNAi lines.

stock no.	Genotype	Source/Ref	Description
A9040	*Alix* (CG12876)	VDRC 32047 (Dietzl et al. 2007)	*ALiX* RNAi 1
A15370	*y[1] sc[*] v[1]; P{y[+t7.7] v[+t1.8]=TRiP.HMS00298}attP 2 – ALiX* (CG12876)	Bl 17675 (Ni et al. 2008)	*ALiX* RNAi 2
A15060	*y[1] sc[*] v[1]; P{y[+t7.7] v[+t1.8]=TRiP.GLV21075}attP 2 – Tsg101* (CG9712)	Bl 35710 (Ni et al. 2008)	*Tsg101* RNAi 1
A9036	*Tsg101(*CG9712)	VDRC 23944 (Dietzl et al. 2007)	*Tsg101* RNAi 2
A9042	*Vps4 (*CG6842)	VDRC 35125 (Dietzl et al. 2007)	*Vps4* RNAi 1
A15281	*y[1] sc[*] v[1]; P{y[+t7.7] v[+t1.8]=TRiP.HMS00841}attP 2 - Hrs(*CG2903)	Bl 33900 (Ni et al. 2008)	*Hrs* RNAi 1
A15282	*y[1] sc[*] v[1]; P{y[+t7.7] v[+t1.8]=TRiP.HMS00840}attP 2 - Hrs(*CG2903)	Bl 34086 (Ni et al. 2008)	*Hrs* RNAi 2
A15343	*Pten*	VDRC101475 (Dietzl et al. 2007)	*pten* RNAi
A15126	*y[1] v[1]; P{y[+t7.7] v[+t1.8]=TRiP.JF01083}attP2 – Egfr (*CG10079)	Bl 31525 (Ni et al. 2008)	*Egfr* RNAi
A12251	*y[1] v[1]; P{y[+t7.7] v[+t1.8]=TRiP.JF03322}attP2 – spi(*CG10334)	Bl 28387 (Ni et al. 2008)	*spitz* RNAi

2.2.2 SC-Gal4 driver lines

See **Fig. 2.1** for *Gal4* driver line expression patterns in the AG, and table 2.2 for full *Gal4* line genotypes. *spi-GAL4* and *dsx-Gal4* are expressed only in SCs within the AG. *esg-Gal4* (*esgF/O*^{ts}) gives highly specific SC expression in the male reproductive system (Leiblich et al. 2012). It is important to note that the expression of these driver lines is, however, not exclusive to the reproductive system in adult flies i.e. they are also expressed in specific cells within other organs.

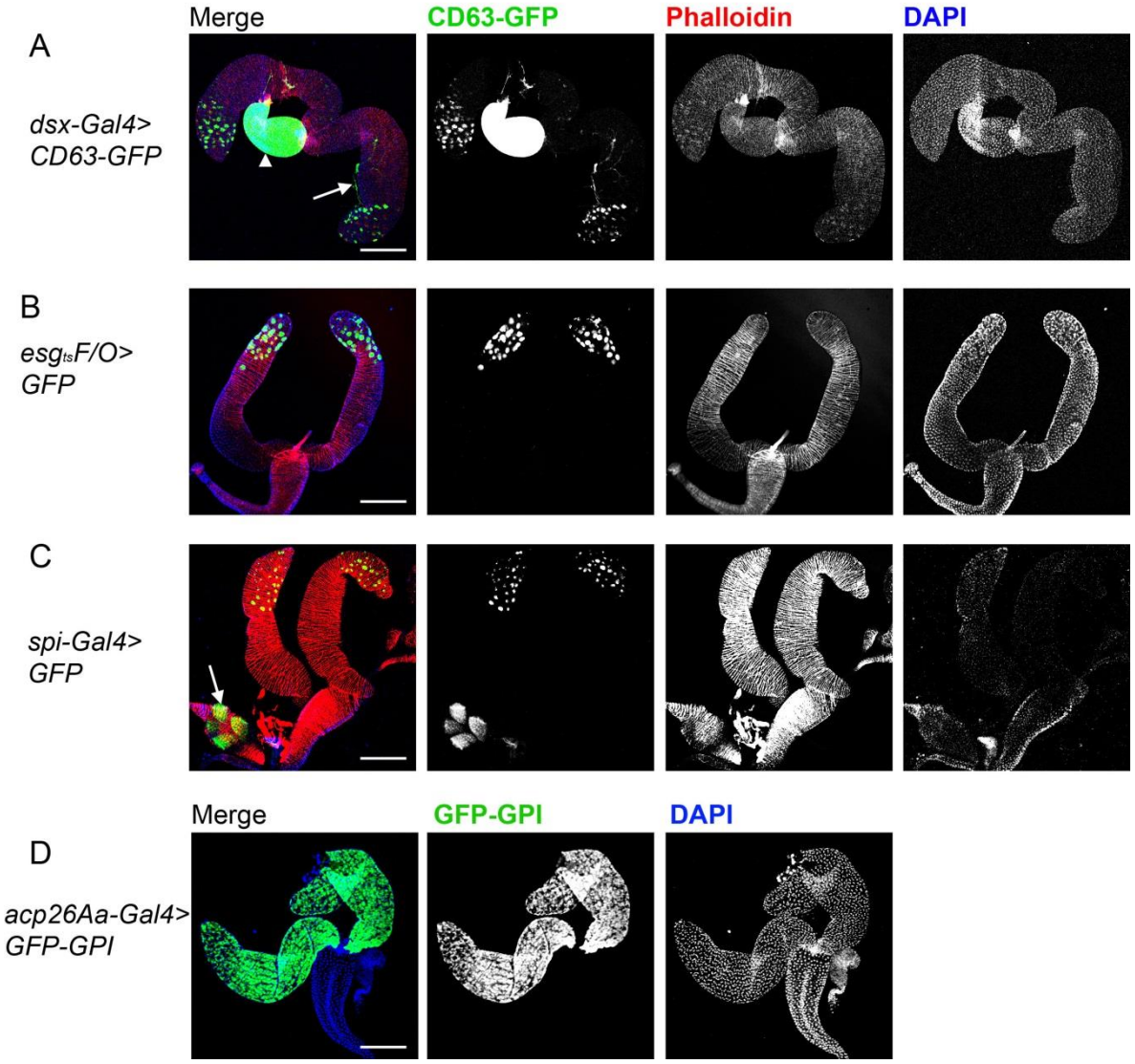


Figure 2.1. Cell-type-specific reporter construct expression in the male reproductive tract by Gal4 driver lines. Representative AGs stained with phalloidin (muscular sheath, red; **A-C**) and DAPI (cell nuclei, blue; **A-D**). (**A**) SC expression of *UAS-CD63-* driven by *dsx-Gal4*. *dsx-Gal4* is also expressed in neurons that terminate on the AG (arrow) as well as the epithelial cells of the ejaculatory duct (arrow head). (**B**) SC-specific expression of *UAS-GFP^{NLS}* driven by *esg^{ts}F/O* (*esg-Gal4; actin-FRT>CD2>FRT–Gal4, UAS-GFP^{NLS}, Tub-Gal80^{ts}, UAS-FLP*). *esg-Gal4* is specifically expressed only in SCs within the male reproductive tract when flies are incubated at 18˚C until eclosion and shifted to 28.5˚C at eclosion to induce transgene expression. (**C**) *UAS-GFP^{NLS}* driven by *spitz-Gal4* is specifically expressed in SCs within the male reproductive tract. *spi-Gal4* is also expressed in the hindgut (arrow). (**D**) MC-specific expression of *UAS-GFP^{GPI}* by *Acp26Aa-Gal4*. Scale bars, 200µm.

2.2.3 Fly husbandry

Flies were reared on cornmeal/yeast-based food (**Table 2.1**) at 18˚C during development and 28.5˚C after eclosion, unless otherwise stated. Genetic crosses (e.g. to make new combination lines) were maintained at 25˚C.

2.2.4 UAS/Gal4/Gal80^{ts} transgene expression system

The UAS-Gal4 transcriptional regulatory system is employed by yeast to drive endogenous gene expression in response to nutritional status. The UAS-Gal4 system can be utilised in *Drosophila* to induce cell-type-specific transgene expression (Brand et al. 1993) (Section 3.3.1) and can be used in combination with a ubiquitously expressed temperature-sensitive transcriptional repressor, *Gal80^{ts}* driven by the *tubulin* promoter, to permit temporal control of transgene expression (Suster et al. 2004). The temperature sensitive repressor inhibits Gal4-driven gene expression at 18˚C, but is inactivated at 28.5˚C to allow transgene expression. This additional level of regulation allows reversible expression of a gene of interest (e.g. UAS-CD63-GFP) (e.g. Section 3.3.6) as well as the ability to induce transgene expression post-developmentally (all experiments using transgenes to modulate gene expression e.g. RNAi lines and over-expression constructs), bypassing potential embryonic/developmental lethality issues.

To induce SC- or MC-specific gene expression of transgenes, SC or MC driver lines (SC-Gal4/MC-Gal4) were crossed to (UAS-transgene) at 18˚C using standard genetic techniques (**Fig. 2.1**). Fly strains containing multiple transgenes (combination lines) were created and balanced using standard genetic techniques (see **Fig. 2.2**).

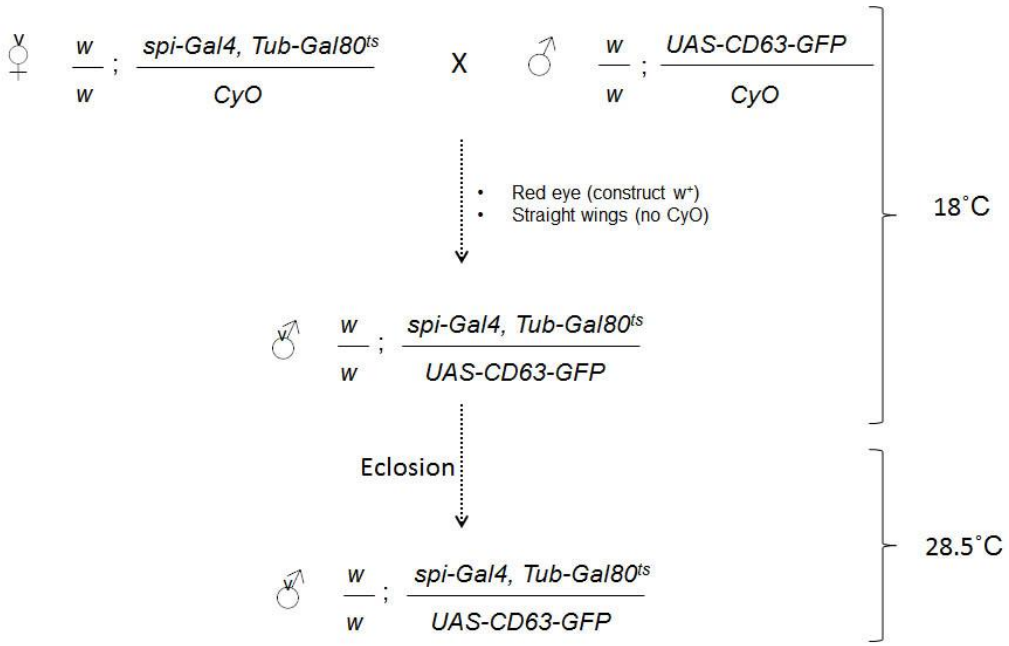


Figure 2.2. Genetic approach to the generation of transgene-expressing males. Virgin female *Gal4/Gal80^{ts}* driver lines were crossed to *UAS-transgene* males at 18˚C. There was therefore no transgene expression during development, because at 18˚C, the activity of the transcriptional repressor, Gal80^{ts}, blocks Gal4 activity. Newly eclosed (virgin) male flies were sorted, and those of desired genotype were selected based on genetic markers e.g. eye colour, lack of balancer chromosome markers (e.g. Cy, curly wings). These males were incubated and aged in a separate vial at 28.5˚C to induce transgene expression.

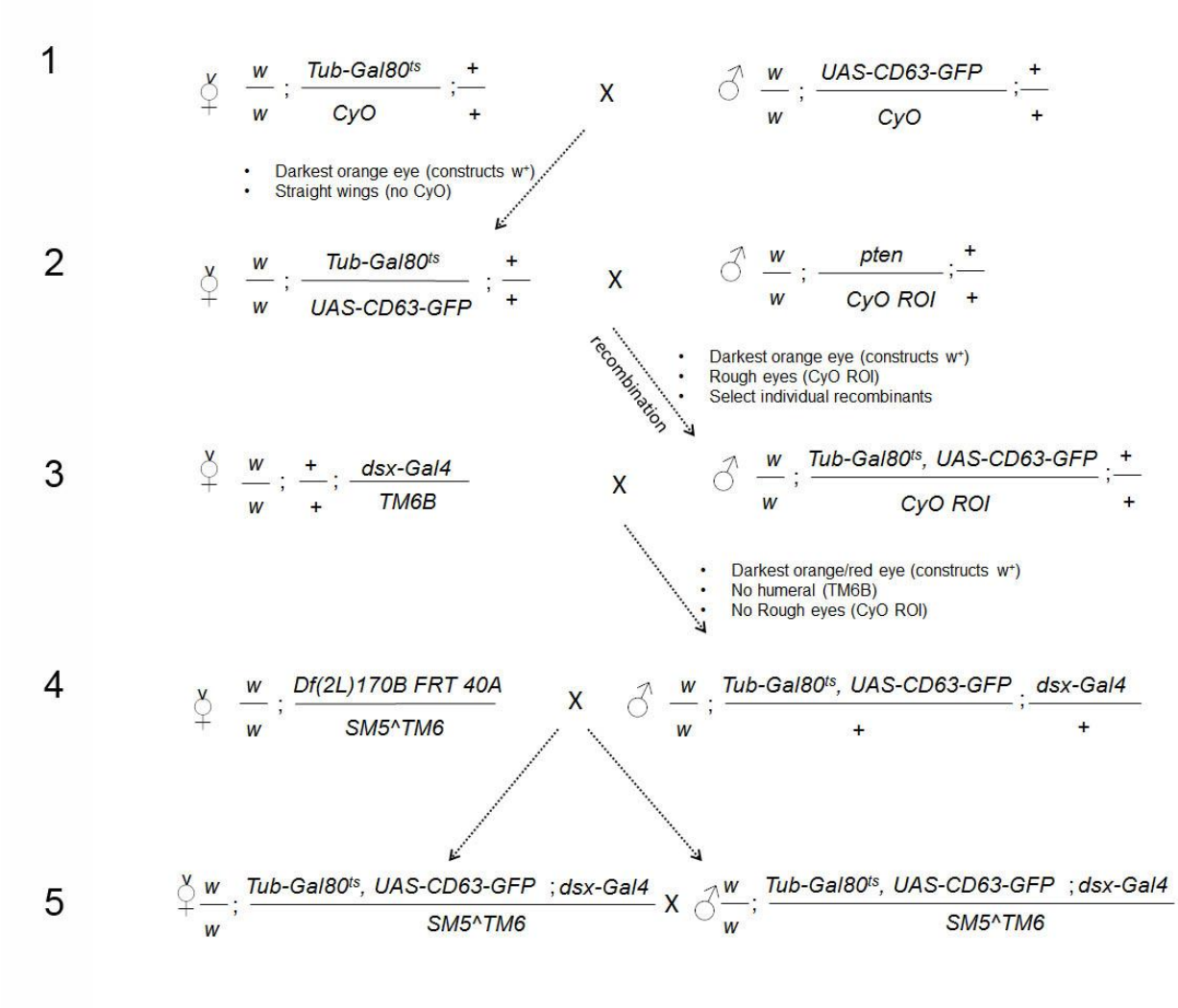


Figure 2.3. Genetic approach to the generation of combinatorial *UAS/Gal4/Gal80^{ts}* stocks. Balanced stocks containing multiple transgenes were created by exploiting naturally occurring recombination events in the female germ line, recombining transgenes onto a single chromosome (1-3). Additional transgenes could also be incorporated subsequently using standard genetic techniques: utilising eye colour markers to track transgene inheritance (3-4) and balanced using attached chromosome balancers (4-5; **Table 2.3**). Stable fly stocks were created by crossing male and female progeny of the final balanced combination (5).

2.3. AG Staining

2.3.1 Antibody table

Protocol	Antibody	Antigen	Species	Source	Dilution
IF	Primary	Fasciclin3	Mouse	DSHB #7G10 (Narasimha et al. 2008)	1:10
		ANCE	Rabbit	E Isaac (Rylett et al. 2007)	1:2000
		GFP	Rabbit	ABCAM #ab6556 (Wang et al. 2005) (Koles et al. 2012)	1:2000
		CD63	Mouse	DSHB #H5C6 (Bampton et al. 2005)	1:10
	Secondary	Alexa 649-conjug. Anti-Mouse	Donkey	Jackson lab. #715-607-003-JIR	1:400
		Cy3-conjug. anti-Rabbit	Donkey	Jackson lab. #711-167-003-JIR	1:400
Western	Primary	ANCE	Rabbit	E Isaac (Rylett et al. 2007)	1:1000
		Actin	Rabbit	Millipore #04-1040	1:10000
		GFP	Rabbit	ABCAM #ab6556 (Krüttner et al. 2012)	1:500
	Secondary	HRP-conjug. anti-rabbit		Promega #W4018	1:20000
EM	Primary	GFP	Rabbit	ABCAM #ab6556	1:2000
	Secondary	Protein A 20nm colloidal gold	n/a	Sigma Aldrich #P6855	1:5000

Table 2.7. Primary and secondary antibodies.

2.3.2 AG Immuno-staining

The age of dissected flies is given as days after eclosion. Immunostaining of the AG was performed as previously reported (Leiblich et al. 2012). Dissections were carried out in 4% paraformaldehyde in PBS with a minimum total fixation period of 15 minutes, followed by a 20 minute wash in PBST (PBS, 0.3% Triton X-100) and then a 30 minute wash in PBSTG (PBST, 10% goat serum). All washes were carried out at room temperature (22˚C). Samples were incubated with primary antibodies overnight at 4˚C, before washing in PBST (6x 10 min at 22˚C). Samples

were then incubated for 2 hours at 22˚C with fluorescent-conjugated donkey secondary antibodies (1:400 dilution; Jackson Laboratories; Alexa 649- and Cy3- labelled) before 6 further 10 minute washes in PBST. Stained glands were mounted in Vectashield with DAPI (Vector Laboratories).

For phalloidin staining of actin, AGs were incubated in TRITC-phalloidin in PBS (diluted 1:400 of 1mg/ml stock solution; or PBSTG if also immuno-staining) for a minimum of 30 minutes at 22˚C.

2.3.3 Lysotracker staining

Glands were dissected in ice-cold PBS medium and left in ice-cold 5μM Lysotracker-Red DND-99 (Invitrogen) in PBS for 5 minutes. They were then washed in PBS for 5 minutes and mounted in PBS using a coverslip bridge for imaging. Specimens were imaged within 1 hour, although longer incubation periods demonstrated no signs of cell death for several hours.

2.4 Imaging

2.4.1 Confocal microscopy

Live and fixed samples were imaged on a Zeiss Axioplan 2 (LSM 510Meta) scanning confocal microscope. 'Low' magnification images were obtained using a Zeiss Plan-Apochromat 10x/0.45 objective, 'High' magnification images were obtained using a Zeiss Plan-Apochromat 63x/1.4Oil DIC objection. See **Fig. 2.4** for schematic of AG image acquisition.

2.4.2 Image analysis

Images were processed in LSM Image Browser (Zeiss), Image J (for time series, processing of maximum projection images, quantitative particle analysis, nuclear size analysis, western blot band intensity analysis) and/or Adobe Photoshop CS5 (antibody intensity analysis). Photoshop CS5 was used for all figure processing. See methods for specific experiments for more details.

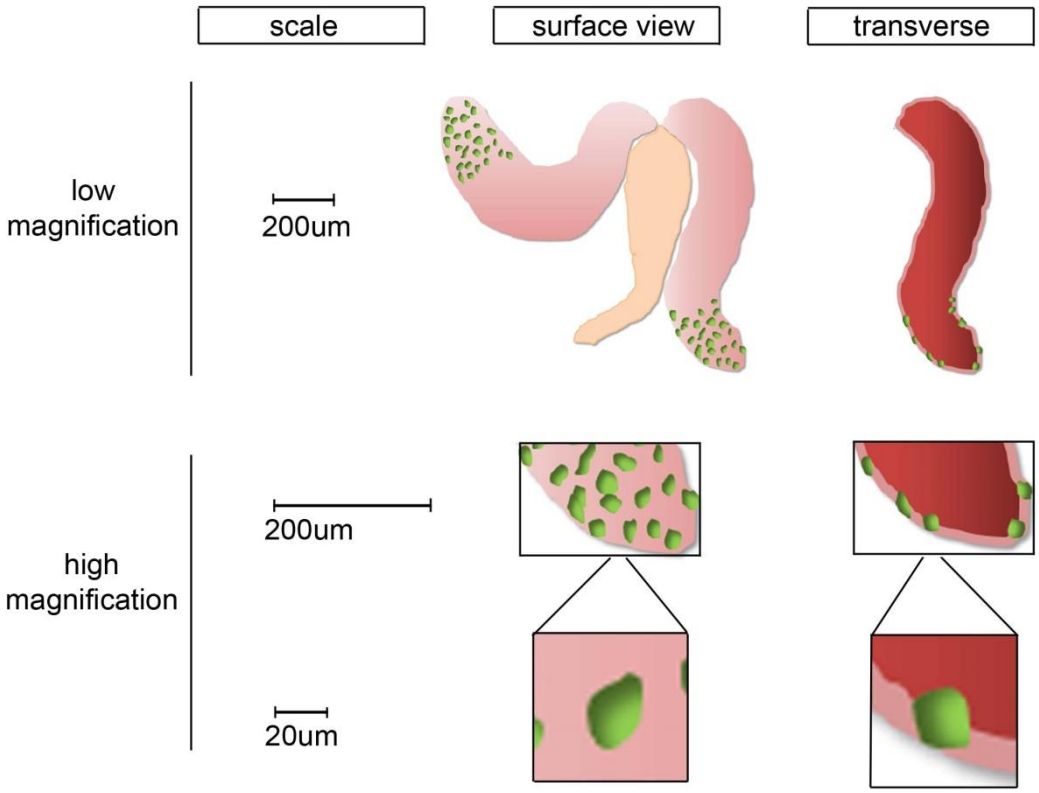


Figure 2.4. Schematic representation of AGs with surface and transverse optical confocal sectioning. The AG is effectively a blind-ended sack composed of a monolayered epithelium comprising 2 binucleate cell types: MCs and SCs (cells shown at tip, green). Surface images show a confocal section across the plane of the epithelium; transverse image shows confocal sections through the plane of the epithelium. The apical cell surface refers to the lumenal surface of the epithelium; the basal surface refers to the outer surface of the epithelium next to the encasing muscle layer (not shown on schematic). Low magnification images obtained using a 10x objection; high magnification images obtained using a 63x oil objective.

2.5. Secretion quantification experiments

2.5.1 Mating protocol

For *in vivo* exosome quantification (CD63-GFP puncta present in the AG lumen) or secreted ANCE quantification, newly eclosed males were incubated at 28.5°C to induce transgene expression. After 2 days, each male was mated to 3 w^{1118} virgin females overnight, after which the females were removed and males left for a further day before dissection and fixation at 4 days post-eclosion. This procedure allowed stored contents of the AG lumen to be partly expelled and replenished at least 2-3 times during the period of transgene expression. Each test experiment was carried out simultaneously with a control for direct comparison and relative secretion calculated.

2.5.2 Image acquisition

Three stacked confocal images of the lumen were obtained at 5µm intervals within the central third of each gland at x1.7 zoom, using x63 objective. A minimum of 8 individual glands were imaged, one AG 'arm' per individual. For each experimental data set, the image acquisition settings were kept constant i.e. laser intensity, gain and offset.

2.5.3 Particle analysis

The number of particles (CD63-GFP) were analysed using ImageJ. Background noise was removed using the 'noise>despeckle' function, and the image converted to 'binary'. The number of particles was quantified using 'particle analysis' function, ('size: 0-infinity'; circularity: 0.00-1.00). The number of particles was quantified for each Z section for each gland, and then averaged for each gland, providing average number of particles per 7400µm^2 (the area of one confocal scan Z section at magnification x1.7). For multiple experiment comparisons the average lumen count values were normalised against the control of that experiment to produce a percentage of control.

2.6 Statistical analysis

Data were analysed using Excel or SPSS. Normality of the data was assessed using a Shapiro-Wilk test (SPSS). Based on the results of this test, data were analysed using either a two-tailed unpaired Student's t test for single pair comparisons (parametric data sets; excel) or the Mann Whitney U Test (non-parametric data; SPSS). Fisher's Exact Test of independence was used to test the significance of association between categories for categorical data.

2.7 Electron microscopy

Rapid processing protocols were devised to ensure maximum tissue and membrane preservation, and carried out in collaboration with Katie Windsor (FHS student) and Prof. John Morris (DPAG).

2.7.1 Structural EM

3-day-old w^{1118} male reproductive tracts were dissected and incubated overnight in 2.5% gluteraldehyde and 4% formaldehyde in PBS (pH 7.2). Glands were then washed with PBS, re-fixed in 1% osmium tetroxide for 20 minutes, washed 3 times in distilled water and dehydrated in graded ethanol, starting with 70%, then 80% and 90% (5 minutes each) and 100% absolute ethanol (2x5 minutes, 1 x 10 minute). For embedding, the glands were incubated in ethanol and Spurr's epoxy resin (1:1), followed by embedding in 100% Spurr's epoxy resin between two sheets of polythene and polymerised overnight at 60°C. Ultrathin sections were prepared with a Reichert ultratome, mounted on formvar-coated slot grids. Sections were stained with 2% uranyl acetate and lead citrate, and imaged using a JEOL 1010 electron microscope (80kV). Although several methodologies for fixation were tested in order to improve the protocol and optimize membrane preservation, membranes in AG preparations were typically poorly preserved.

2.7.2 Immuno-EM

AGs were fixed and dehydrated as above. They were then incubated in methanol and LRGOLD (1:1; London Resin Company) for 15 minutes, followed by 30 minute incubation in pure LRGOLD and finally LRGOLD and benzoin (25mg in 10ml) for a final 30 minutes. AGs were placed between two sheets of polythene in a drop of LRGOLD and benzoin, and left to polymerise under UV light at -20◦C overnight. AGs were sectioned as above. For immuno-staining, sections were blocked using 10% EA in PBS, incubated with the primary antibody (anti-GFP ABCAM ab6556, 1:2000) for 1 hour and washed in 10% EA in PBS (x3). Sections were then labelled with protein A-gold particles (15nm, 1:5000) and washed in 10% EA in PBS (x3) three washes in distilled water. Sections were imaged as above. For more details of genotypes employed, see Sections 3.2.4 and 7.2.1.

3. Characterisation of exosomes secretion by SCs

3.1 Introduction

3.1.1 Exosome secretion in *Drosophila*

Despite the amenability of *Drosophila* to *in vivo* genetic screening and analysis, limited studies have utilised this model system to gain a better understanding of the roles and regulation of exosome secretion. The initial identification of exosomes secreted by *Drosophila* epithelial cells utilised a GFP-tagged human CD63, the classical exosome marker utilised in mammalian cell line studies of exosomes, e.g. (Baietti et al. 2012; Hoshino et al. 2013), to mark exosomes secreted *in vivo* (Panakova et al. 2005). Utilising the UAS-Gal4 system (Brand et al. 1993) to express UAS-CD63-GFP in specific compartments of the developing imaginal wing disc, Panakova et al. identified CD63-GFP-positive vesicles that were secreted into the extracellular space and diffused across the epithelial plane (Panakova et al. 2005). CD63-GFP staining originated inside acidic late endosomes (presumed MVBs), therefore characterising the vesicles as exosomes. Further studies utilising CD63-GFP in both *Drosophila* S2 cell lines (isolating exosomes using ultracentrifugation techniques and sucrose density gradients) and in the imaginal wing disc demonstrated a role for Rab11 in the regulation of CD63-GFP-exosome secretion (Beckett et al. 2013). The v-SNARE, Ykt6, has also been identified as a regulator of CD63-GFP exosome secretion both in cell culture and *in vivo* (Gross et al. 2012), although this remains controversial, because of its very general roles in membrane trafficking (JP Vincent, personal communication).

Several studies have identified components of the Wnt signalling pathway, including Wingless (Wg; the *Drosophila* Wnt*)* and the transmembrane Wg-binding protein, Evi/Wntless (*Evenness interrupted*), as cargos of exosomes secreted by both the wing disc and S2 cells (Beckett et al. 2013). Despite exosomal Wg being capable of inducing a signalling response in recipient cells,

only a small proportion (8%) of extracellular Wg is carried on CD63-GFP vesicles suggesting that the majority of Wg signalling is induced by soluble Wg ligand (Gross et al. 2012). Interestingly, the transmembrane protein Evi was also identified on exosomes secreted both by S2 cells and in the wing disc. However Evi-GFP has been observed on distinct particles (by confocal colocalisation analysis) to Wg, suggesting these Wnt components are sorted into distinct exosomal populations (Gross et al. 2012). Importantly, whether exosomal Wg plays a significant role in patterning the wing disc remains under debate (Gross et al. 2012; Beckett et al. 2013; Alexandre et al. 2014).

Subsequent studies in *Drosophila* have focused on exosomes secreted at synaptic boutons at the neuromuscular junction, complemented with studies in cultured S2 cells, and the role of exosomes in the trans-synaptic trafficking of Evi (Korkut et al. 2009; Koles et al. 2012). A candidate screen for regulators of Evi vesicle release by cultured cells using a dsRNA assay identified Rab11 and Syntaxin1A (as well as several subunits of the V_0 ATPase and Arf79F), whose roles regulating secretion were also confirmed *in vivo* (Koles et al. 2012). This study concluded that these particles were exosomes based on three lines of evidence: 1) S2 cell exosomes sediment in a 100,000g pellet following ultracentrifugation, which is classically considered to contain the 'exosome fraction' (Momen-Heravi et al. 2013); 2) immuno-electron microscopy confirmed the presence of Evi-GFP inside multivesicular compartments at synaptic boutons; 3) knockdown of components of the V_0 ATPases, known to be required for acidification and maturation of late endosomal compartments (Nishi et al. 2002), significantly reduced Wg/Evi vesicle release by S2 cells (Koles et al. 2012). Previous studies in mammalian cell culture have identified Rab11, Rab35 and Rab27 as regulators of CD63-positive exosome secretion (Savina et al. 2002; Hsu et al. 2010; Ostrowski et al. 2010). However, *Drosophila* Wg/Evi-exosome secretion does not require Rab35 (Gross et al. 2012; Koles et al. 2012; Beckett et al. 2013) or Rab27 (Gross et al. 2012), despite a requirement for Rab11 (Koles et al. 2012; Beckett et al. 2013), suggesting that either their role in the regulation of exosome secretion is not conserved in flies or that Wg/

Evi-exosome secretion is regulated by a distinct mechanism to the CD63-containing exosomes, which have typically been analysed in mammalian studies.

In summary, to date, *Drosophila* exosomes have been identified that are marked by CD63-GFP or Evi/Wg, and secreted by the epithelial cells of the wing disc as well as S2 cells and at synaptic boutons. Rab11 has been shown to regulate Evi/Wg and CD63-GFP exosomes secretion, being hypothesised to mediate intracellular trafficking events critical for secretion.

3.1.2 Aims and objectives

I have discovered that exosomes are secreted by specific cells of the AG and are stored in its lumen. I set out to investigate whether the AG might provide a more powerful system to study exosome biogenesis and secretion *in vivo* by addressing the following:

1. Investigate whether the AG secrete exosomes and identify the cell-type of origin.
2. Identify specific AG exosome marker(s).
3. Characterise their mechanism of biogenesis.

3.2 Methods

3.2.1 Pulse chase experiments

spi-Gal4, Tub-Gal80^{ts}; UAS-CD63-GFP virgin males were collected at eclosion and maintained at 18˚C for 24 hours. Virgin males were then shifted to 29˚C for 8 hours to inactivate Gal80^{ts}, thus inducing transgene expression. Males were then shifted back to 18˚C to reactivate Gal80^{ts}, turning transgene transcription off to provide the 'chase'. Males were dissected, stained with Lysotracker–Red (Section 2.3.3) and imaged live. The presence of one or more iLEs (<2µm, stained with Lysotracker) or mMVBLs (>2µm, stained with Lysotracker), which were GFP-positive, within a given SC was scored as a GFP-positive iLE/mMVBL-containing cell.

3.2.2 Secreted ANCE staining quantification

See Section 2.5 for mating, staining and imaging protocol for lumen secretion quantification.

The luminal ANCE staining intensity was quantified using Photoshop CS5. Each Z section image was converted to grey scale and the average pixel intensity across each Z section was analysed (record measurements>grey value (mean)), and then averaged for each gland. *n*= total number of glands imaged.

3.2.3 Western blots

3.2.3.1 Protein extraction

For male AG samples, 3-day-old virgin *tub-Gal80^{ts}; UAS-CD63-GFP; dsx-Gal4* males (incubated at 28.5˚C from eclosion onwards) expressing *UAS-ALiX-RNAi, UAS-Hrs-RNAi,* or *UAS-Rab11DN* constructs, or crossed to *w^{1118}*, were dissected in ice-cold PBS. *w^{1118}* virgin males were used as a negative control.

For female samples, these males were introduced to single *w^{1118}* virgin females and matings were observed. The female reproductive tracts with the ovaries removed were dissected in ice-cold PBS immediately after the end of mating. *w^{1118}* virgin females and *w^{1118}* females mated to *w^{1118}* males were used as a negative controls.

AG proteins were extracted by homogenizing the glands using a polycarbonate pestle on ice in 100µl lysis buffer (RIPA buffer, Sigma Cat no, R0278) supplemented with anti-protease and -phosphatase cocktails (Sigma, P8340, P0044). The crude lysates were centrifuged (13000xg; 10 min) and the protein-containing supernatant extracted. Proteins were quantified using a BCA assay kit (Thermo Scientific Pierce, 10741395).

3.2.3.2 Blotting

Blotting of AG proteins was carried out as previously described (Rylett et al. 2007) with minor alterations. Samples containing 2.5µg of homogenized protein (made up to 15 µl) were added to 5 µl of 4X sampling buffer (0.2M Tris-HCl pH 6.8, 12%SDS, 40% Glycerol, 20% β-mercaptoethanol, 0.008% bromophenol blue) and heated to 95˚C for 5 minutes. Proteins were separated using 10% mini-Protean TGX precast gels (Bio-Rad) for 30 min along with a pre-stained ladder (Precision Plus Protein Dual Colour Standards #161-0374). Separated proteins were transferred to a PVDF membrane (Millipore Immobilon-P #IPVH00010) at 100V for 1 hour. The PVDF membrane was then blocked for 1 hour in 5% skimmed milk in Tris-buffered saline with Tween-20 (TBST) and then incubated with anti-ANCE antibody (Rylett at al. 2007) at a 1:1000 dilution, anti-GFP 1:500 (Rabbit, ABCAM ab6556) or anti-actin 1:10000 antibody (Millipore, Rabbit Cat #04-1040) in 5% milk in TBST overnight at 4˚C. The membrane was washed in TBST 3 x 5 min and incubated at room temperature for 1 hour with a horseradish peroxidase-conjugated anti-rabbit secondary antibody (Promega #W4018) at 1:20000 in 5% milk in TBST, and then washed in TBST 3 x 5 min. Bound anti-ANCE, anti-GFP or anti-actin antibody was detected using a SuperSignal West Pico Chemiluminescent Substrate kit (#34080, Thermo Scientific) as described in the manufacturer's instructions. Photographic films were exposed to the membrane for 30 sec - 1 min prior to film development. Band intensities were calculated using ImageJ.

3.2.4 Electron Microscopy

For structural EM, 3-day-old virgin w^{1118} males were dissected. AGs were fixed, processed and sectioned as in Section 2.7.1. For immuno-EM, 3-day-old *spi-Gal4; UAS-CD63-GFP* virgin males were dissected. AGs were fixed, processed, sectioned and stained (rabbit anti-GFP 1:2000) as in Section 2.7.2.

3.2.5 CD63-GFP puncta quantification experiments

All lumen counts were repeated at least once, and significantly reduced in 2/2 (*ALiX*-RNAi1), 2/2 (*ALiX*-RNAi2), 1/2 (*Hrs*-RNAi), 2/2 (*Hrs*-RNAi2), 1/2 (*Tsg101*-RNAi2), 2/2 (*Tsg101*-RNAi1), 1/4 (Vps4-RNAi). *Vps4*-RNAi also resulted in significant increases in exosome secretion (1/4).

3.3 Results

3.3.1 SC-specific secretion of CD63-GFP

To investigate whether cells of the AG secrete exosomes, we expressed a form of human CD63, an integral-membrane tetraspanin frequently associated with exosomes that is fluorescently tagged at it's C-terminus with GFP (Panakova et al. 2005), using the UAS-Gal4 system (Brand et al. 1993) specifically in the two AG epithelial cells types: the SCs and MCs. To do this we utilised the Gal4 drivers *spitz-Gal4* and *Acp26Aa-Gal4*, which have been previously identified in the lab to drive gene expression specifically in the SCs and MCs, respectively (**Fig. 2.1**). In SCs, CD63-GFP localised to the limiting membrane of the numerous large vacuoles, often containing Angiotensin Converting Enzyme (ANCE) (**Fig. 3.1**). Previous work has characterised the secretion of ANCE into the AG lumen following its synthesis in SCs, where it localises to the dense secretory granular cores found in SC secretory vacuoles (SVs) (**Fig. 3.1, Fig. 3.16**) (Rylett et al. 2007). CD63-GFP was also seen at the apical plasma membrane (**Fig. 3.2B; 3.3C-D and F**), perhaps because of transfer of membrane from SVs to the plasma membrane during secretion. CD63-GFP puncta could also be observed in the lumen of the gland (**Fig. 3.2B, 3.3C-D and F**). Importantly, another fluorescently-tagged mammalian transmembrane protein CD8-RFP, which localises to the plasma membrane of *Drosophila* epithelial cells (Olguín et al. 2011), was not secreted into the gland lumen when expressed specifically in SCs, despite localising to the limiting membrane of large SC vacuoles and the apical plasma membrane. This suggests that the secreted CD63-GFP puncta are not an artefact of fluorescently-tagged transmembrane protein expression (**Fig 3.4**). Interestingly, we did

not observe these CD63-GFP puncta in the lumen when CD63-GFP was expressed in MCs (**Fig. 3.3E**). These data are consistent with a model in which membrane-bound vesicles that carry the four-transmembrane fusion protein CD63-GFP are specifically secreted by SCs into the AG lumen. This conclusion is contingent on the CD63-GFP fusion remaining intact, but subsequent immunoblots confirmed that this is the case (Section 13.24).

3.3.2 CD63-GFP localises to late endosomal, lysosomal and secretory compartments

Exosomes are defined by their endocytic origin inside late endosomal MVBs (Raposo et al. 2013). We hypothesised that the large compartments of SCs that do not contain a dense ANCE core may be MVBs, as CD63-GFP could often be seen inside (**Fig. 3.2A**).

When GFP containing a nuclear localisation sequence was expressed at high levels using the *esg^{ts}F/O* system (Jiang et al. 2009), such that the GFP leaks out into the cytoplasm (Leiblich et al. 2012), we occasionally observed GFP in discrete puncta inside the large SC compartments (**Figure 3.5**), further suggesting the presence of membranous structures in these compartments that contain cytoplasmic contents.

To confirm the presence of CD63-GFP inside these compartments, we stained AGs with antibodies against CD63 and GFP. SCs contained approximately 1 or 2 compartments filled with (fluorescent) CD63-GFP and the majority of CD63-GFP in SCs colocalised with antibody stains for both CD63 and GFP (**Fig. 3.6A-B**). Interestingly, we also observed antibody staining in approximately 1 or 2 additional large compartments per SC that did not exhibit GFP fluorescence (**Fig. 3.6C-D**) and did not contain a dense ANCE core (**Fig. 3.6D**). We hypothesise that the environment of this particular compartment inhibits GFP fluorescence and may represent a mature multivesicular late endosome. Consistent with this, CD63-GFP puncta secreted into the seminal fluid stored in the gland lumen often colocalised anti-CD63 staining (**Fig. 3.7**), suggesting that CD63-GFP remains intact and the fluorophore is still capable of fluorescence after it is secreted. This was further

confirmed by western blot analysis of AGs and females mated to SC>CD63-GFP males, which produced a strong signal at 52kDa, corresponding the full length fusion protein, and no obvious smaller products when probed with an anti-GFP antibody, indicating that CD63-GFP inside SCs as well as secreted into the gland lumen remains intact (**Fig. 3.24**).

To identify late endosomal compartments within SCs, we established a live imaging protocol in which we could stain AGs with the vital dye Lysotracker-Red, which specifically stains acidic compartments including late endosomes and lysosomes. Under live imaging conditions the morphology of SCs was much clearer than that observed in fixed tissue, allowing us to quantify the numbers and size of the internal compartments that were lined with CD63-GFP. SCs contained non-acidic SVs lined with CD63-GFP ranging between approximately 2-5µm in diameter (**Fig. 3.8B**). In addition, SCs of glands from 3-day-old adult males contained an average of 2.9 +/- 0.16 large (>2µm) acidic compartments that were also lined with CD63-GFP (**Figure 3.8B and 3.13**), but often contained CD63-GFP puncta (**Figure 3.8B**), suggesting that they were MVBs containing CD63-GFP-positive ILVs. We observed at least one large acidic compartment with CD63-GFP puncta in every SC.

Given the presence of internal CD63-GFP-marked membrane, their acidity as well as their ultra-structural morphology, Rab signature and membrane trafficking dynamics (see below and **Figs. 3.13**), we named these acidic late endosomal compartments mMVBLs (maturing MultiVesicular Bodies/Lysosomes, as we were unable to distinguish whether there compartments were late endosomes or lysosomes). They are defined as CD63-GFP- and Lysotracker-positive compartments greater than 2µm in diameter. SCs also contained several smaller CD63-GFP-positive acidic compartments (<2µm), the lumen of which were not easily distinguishable given the resolution limitations of confocal microscopy. We named these iLEs (immature Late Endosomes) (given their Rab signature and trafficking dynamics, **see Fig. 3.13**), and defined them as CD63-GFP- and Lysotracker-positive compartments less than 2µm in diameter.

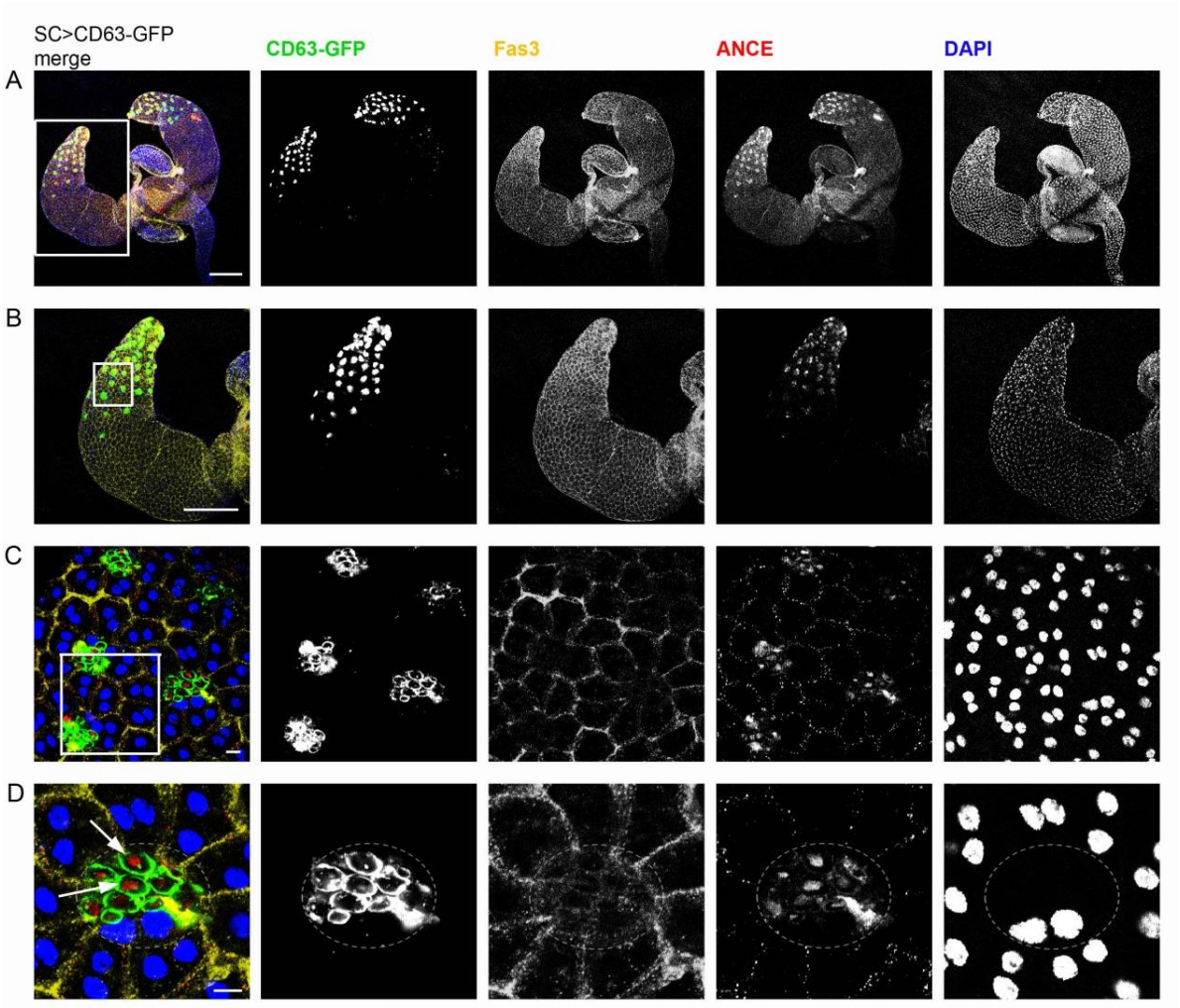


Figure 3.1. The *Drosophila* accessory gland. 3-day-old *spi-Gal4; UAS-CD63-GFP* virgin male, stained for ANCE (red), which localises to the dense core of SC secretory vacuoles (**D**, arrows), Fasciclin3 (Fas3, yellow) antibody marks septate junctions between cells and DAPI (blue) marks cell nuclei. The AG is effectively a blind-ended sack composed of a monolayered epithelium comprising 2 binucleate cell types: main cells and SCs (here, expressing CD63-GFP). 'Surface' images capture a confocal plane skimming across the gland epithelium. Scale bars: **A-B** 200µm; **C-D** 5µm. SC outlines marked by dashed grey line in **D**. Images in **B**, **C** and **D** are higher magnifications images of the regions outlines in **A**, **B** and **C**, respectively.

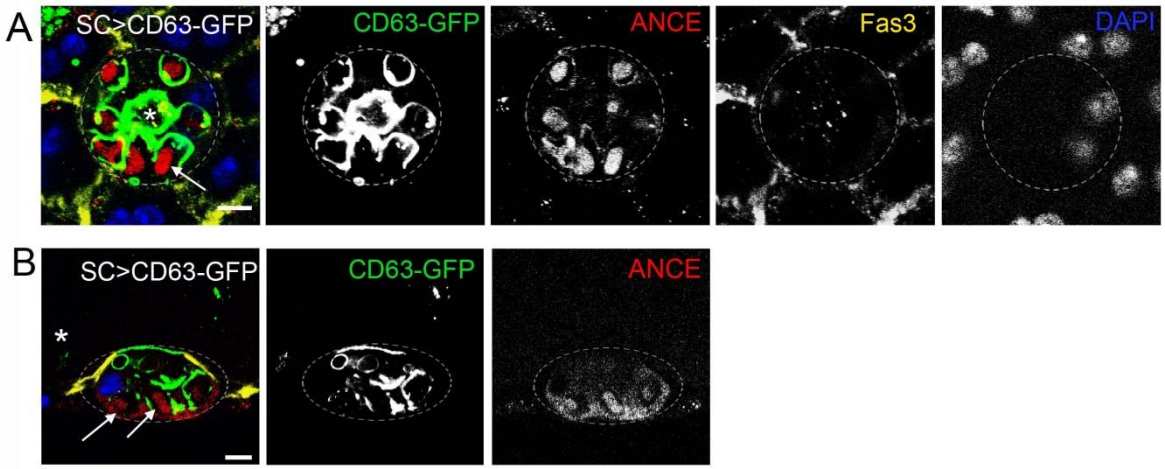


Figure 3.2. Not all CD63-GFP-positive large vacuoles contain a dense ANCE core. (**A** and **B**) 3-day-old *spi-Gal4; UAS-CD63-GFP* virgin male, stained for ANCE (red), which localises to the dense core of SC secretory vacuoles (arrows), Fasciclin3 (Fas3, yellow) marks apicolateral septate junctions between cells and DAPI (blue) marks cell nuclei. (**A**) is a high magnification surface images of a SC. (**B**) is a transverse confocal secretion through the AG epithelium, CD63-GFP can been seen at the apical plasma membrane between the SJs. SVs lined by CD63-GFP often contain a dense ANCE core (**A**, **B**, arrows), however some large CD63-GFP-postive vacuoles do not contain a dense core (**A**, *). Scale bars, 5µm.

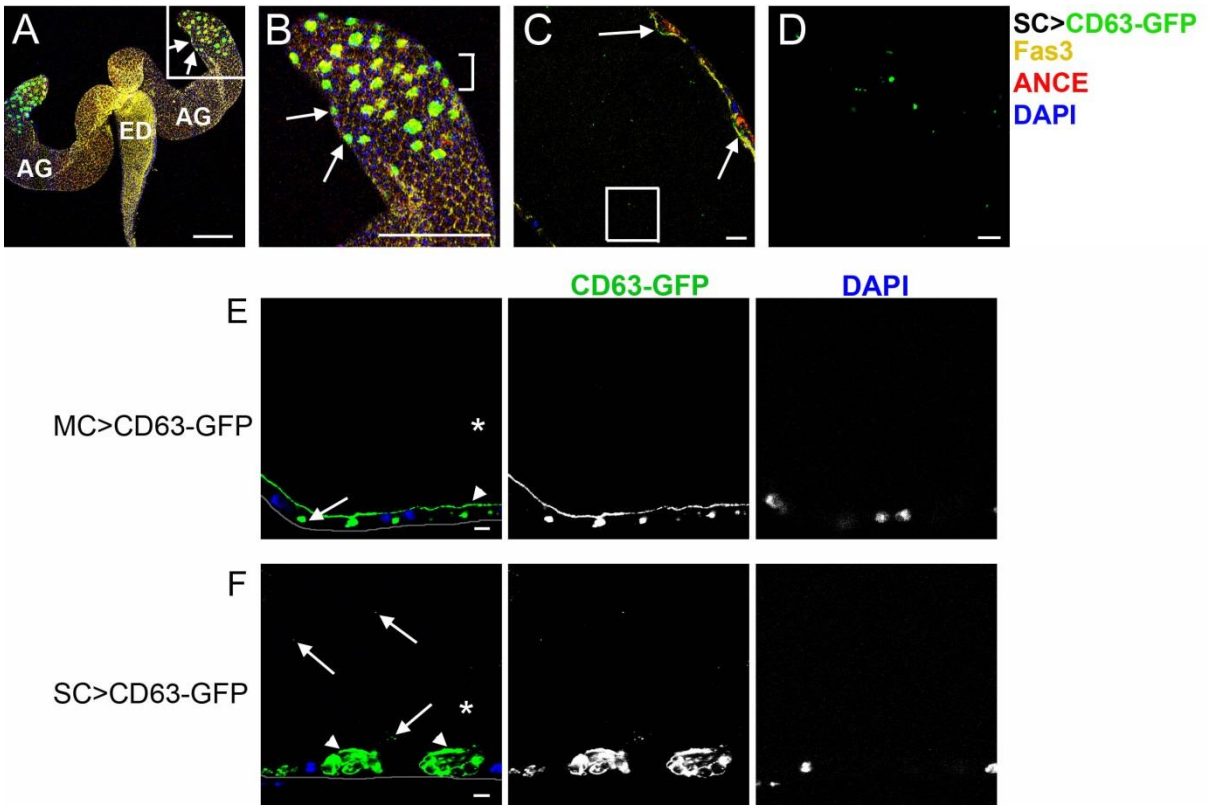


Figure 3.3. Secondary cells (SCs), and not main cells (MC), secrete CD63-GFP-positive puncta into the lumen of the accessory gland. (**A-D**) Paired AGs (AG; **A**) expressing CD63-GFP in SCs pass their contents into the ejaculatory duct (ED; **A**). Images of different magnification show surface sections of SCs within the AG epithelium (**B**; from square in **A**, two SCs marked with arrows); a transverse section through the lumen (**C**; bracketed region in **B**, two SCs marked with arrows), inside which epithelial secretions are stored until mating, including CD63-GFP-positive puncta (**D**; square in **C**). (**E-F**) Transverse images through the epithelium and gland lumen of 3-day-old *Acp26Aa-Gal4; UAS-CD63-GFP* (**E**) and *spi-Gal4; UAS-CD63-GFP* virgin males. When expressed in SCs, CD63-GFP puncta (**F**, arrows) are secreted into the gland lumen (**F**, *). When expressed specifically in MCs, CD63-GFP fills intracellular compartments (**E**, arrow), but is not secreted into the gland lumen (**E**, *). When expressed in either MCs or SCs, CD63-GFP also localises to the apical plasma membranes (**E, F**; arrow heads). Grey outline indicates basal (external) epithelial surface. Scale bars, (**A** and **B**) 200µm; (**C**) 20µm; (**D-F**) 5µm.

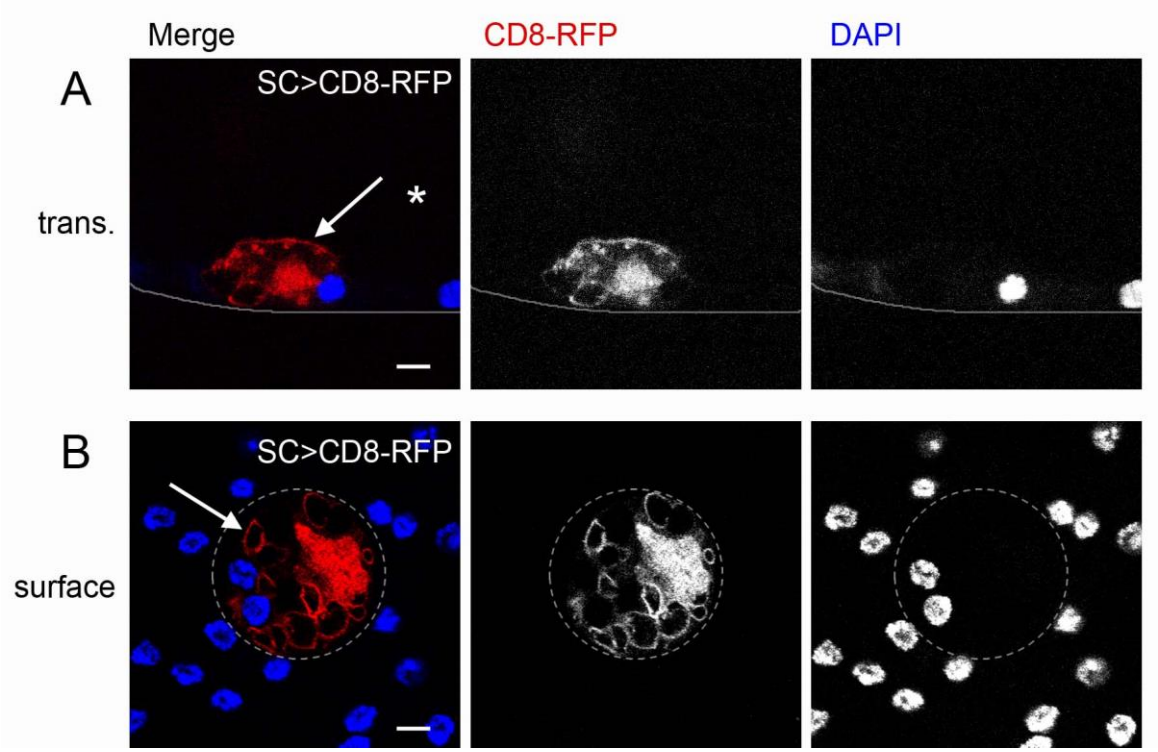


Figure 3.4. CD8-RFP is not incorporated into exosomes. Transverse (**A**) and surface (**B**) views of SCs of *spi-Gal4; CD8-RFP* 3-day-old virgin males stained with DAPI (blue). CD8-RFP is not secreted into the gland lumen (**A**, *), but localises to the apical plasma membrane (**A**, arrow) and the limiting membrane of secretory vacuoles (**B**, arrow). Scale bars, 5µm. Cell outline in **B** marked by dashed circle; basal (external) epithelial surface in **A** marked by grey line.

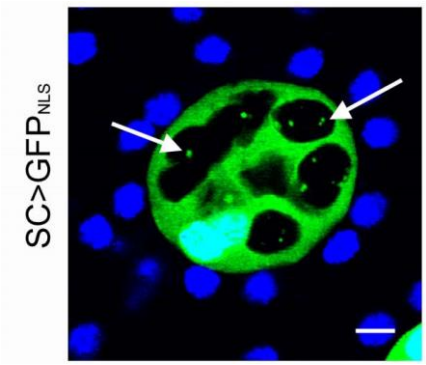


Figure 3.5. Cytoplasmic GFP is occasionally seen inside large vacuolar compartments. Fixed gland of a *esg^{ts}F/O; UAS-GFP^{NLS}* 5-day-old virgin male stained with DAPI (blue). GFP possessing a nuclear localisation sequence (NLS) leaks into the cytoplasm, and is occasionally incorporated into puncta within large SC compartments (arrows). Scale bar 5µm.

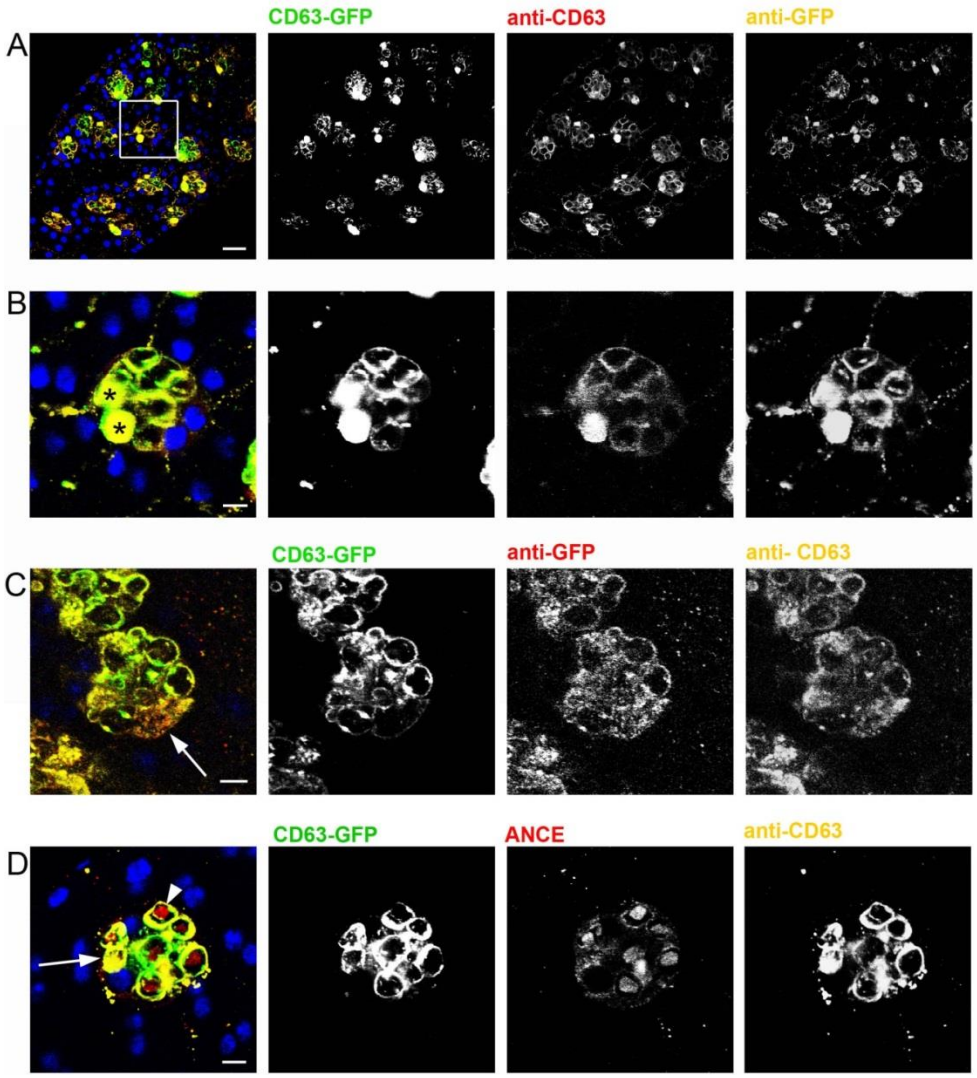


Figure 3.6. CD63-GFP colocalises with anti-CD63 and anti-GFP antibody stains but SCs can also contain a compartment filled with CD63-GFP that exhibits only limited GFP fluorescence. 3-day-old virgin *spi-Gal4;UAS-CD63-GFP* male stained for CD63 (**A** and **B**, red; **C** and **D**, yellow), anti-GFP (**A** and **B**, yellow; **C**, yellow) and ANCE (**D**, red) and DAPI (blue). Upper panels in **A** show lower magnification, lower panels in **B** show a high magnification of the region outlined in **A**. GFP, anti-GFP and anti-CD63 colocalise at the limiting membrane of SC compartments and also filling a presumptive mMVBL (**B**, *), although the upper compartment exhibits weak anti-CD63 staining. However, SCs also contained compartments that stained strongly with anti-CD63 or anti-GFP yet exhibited weak GFP fluorescence (**C-D**, arrows), these do not contain an ANCE core (e.g. **D**, arrowhead). Scale bars, (**A**) 20µm; (**B-D**) 5µm**.**

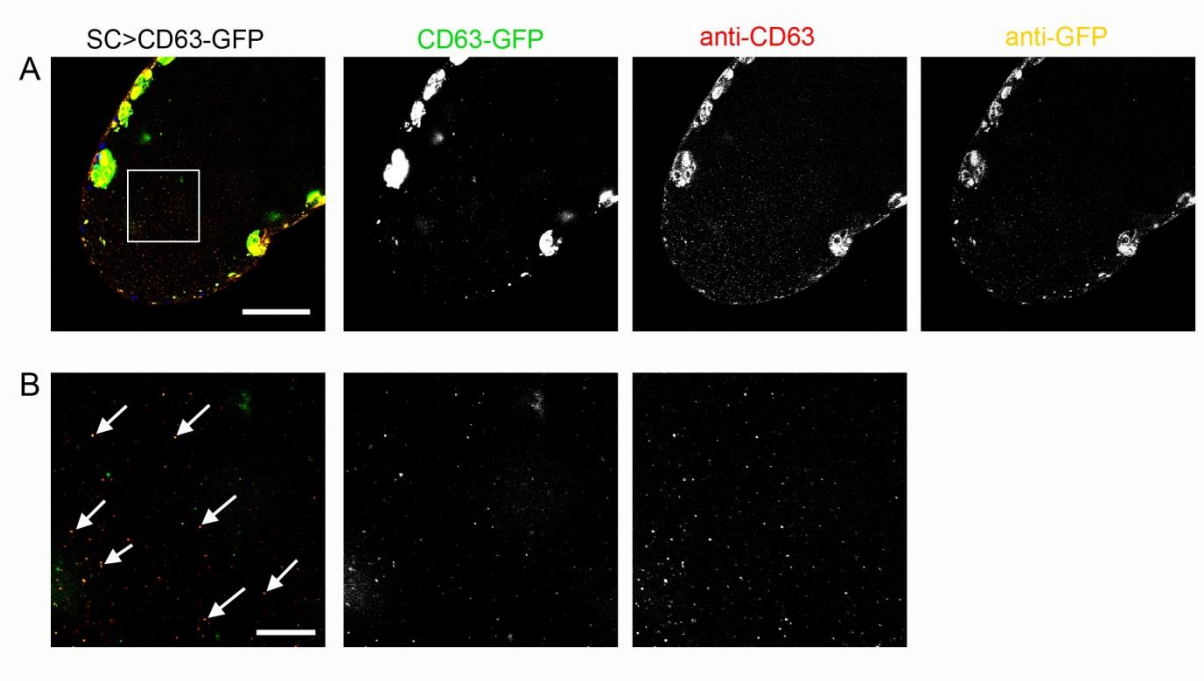


Figure 3.7. CD63-GFP fluorescent puncta secreted into the AG lumen by SCs co-localise with anti-CD63 and anti-GFP antibody. Representative transverse confocal images through the AG lumen of a 3-day-old virgin *spi-Gal4; UAS-CD63-GFP* male stained for CD63 (red) and anti-GFP (yellow). Upper panels show lower magnification, lower panel shows a high magnification of the region outlined in **A** (x2.7 zoom). GFP and anti-CD63 puncta often co-localise in the lumen (**B**, arrows). Scale bars, 50µm in **A**; 10µm in **B**.

Importantly, we observed large (>2µm) acidic regions inside control SCs from wild-type w^{1118} glands (**Fig. 3.11D**), however we were unable to quantify their number and size as it was not possible to distinguish their limiting edge without a membrane marker. These data suggest that the formation of the unusually large mMVBLs found in SCs does not result from expression of the CD63-GFP transgene.

3.3.3 Age-dependent changes in endolysosomes

Given the age-dependent changes on SC biology previously characterised by the host lab, such as growth (Leiblich et al. 2012), we conducted a time course by imaging glands dissected from 1-, 3-, 6- and 9-day-old flies (incubated at 28.5˚C from eclosion) to investigate whether endolysosomal compartments also exhibited age-dependent changes (**Figs. 3.8** and **3.9**). We noted a significant reduction in the number mMVBLs stained strongly with Lysotracker with age (**Figure 3.9**). 1-day-old SCs contained 3.7 +/- 0.14 mMVBLs, this number reduced to only 1.6+/- 0.09 per SC at 9-days-old (**Fig. 3.9A**). Furthermore, the size of mMVBLs, measured by the widest diameter of the largest acidic compartment lined with CD63-GFP, increased with age from 6.2+/- 0.17µm in 1-day-old SCs to 14.1 +/- 0.6µm in 9-day-old SCs (**Fig. 3.9B**). Given this negative correlation between mMVBL number and size, it is tempting to speculate that as SC age, mMVBLs fuse with each other to form larger acidic compartments; indeed, during live imaging of SCs, we infrequently observed such events (**Figure 3.10**).

mMVBLs of 1-day-old SCs contained less internalised CD63-GFP than SCs of older glands (**Fig. 3.8**). mMVBLs within an individual SC of 3- and 6-day-old contained variable amounts of internal CD63-GFP. However, at least one compartment per SC, which was usually the largest, contained many CD63-GFP puncta (**Fig. 3.8B-C**). The single mMVBL of 9-day-old SCs contained a variable amount of internal CD63-GFP (**Fig. 3.8D**). It was not possible to obtain an accurate quantification of the amount of internal CD63-GFP within individual mMVBLs. This was due to our previous finding that

GFP fluorescence is often masked by the internal mMVBL environment, making this statistic a significant under-representation of CD63-GFP ILVs in at least half of all SCs imaged.

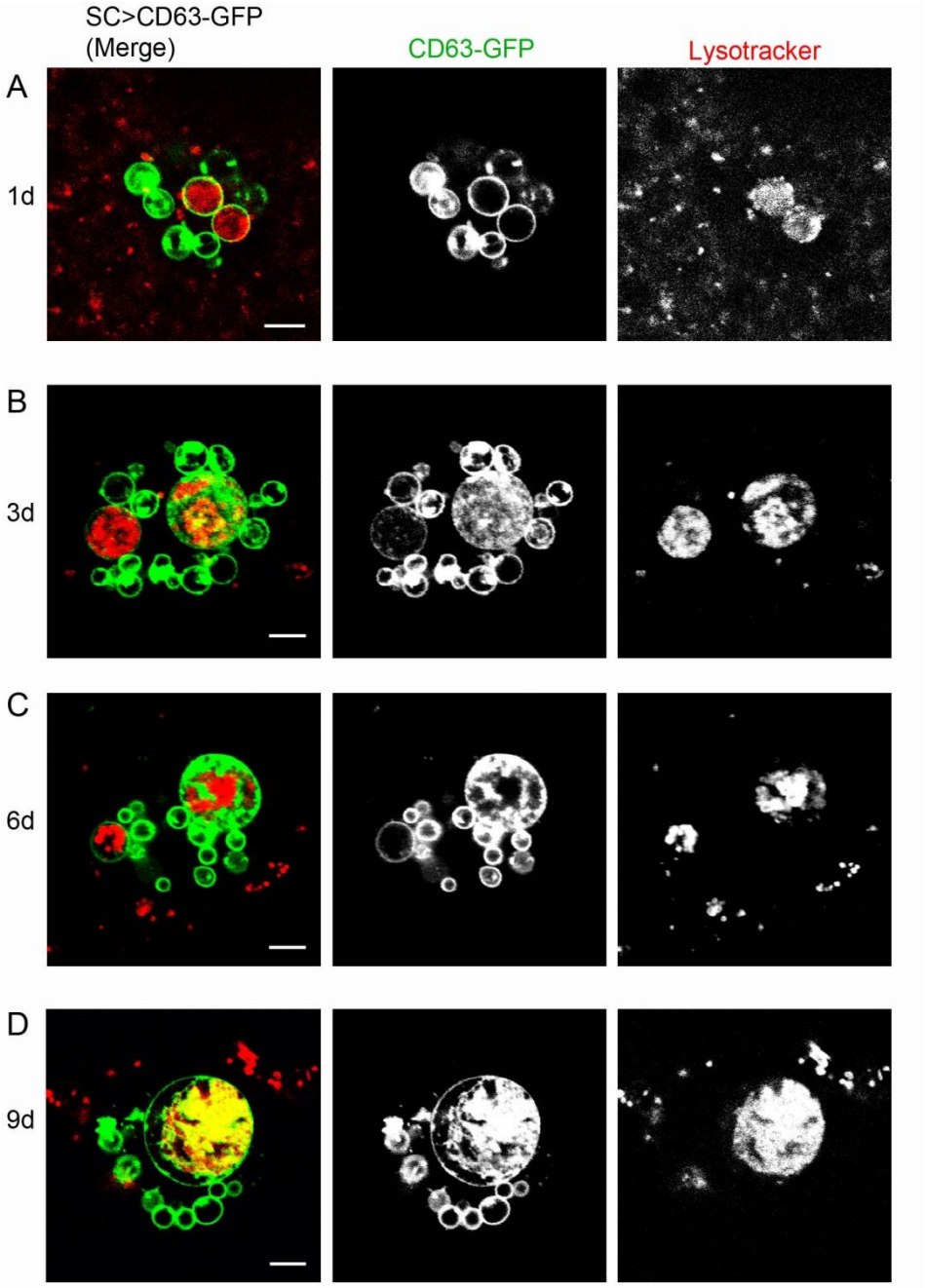


Figure 3.8. Age-dependent changes in SC late endocytic compartments. (A-D) SCs from *spi-Gal4; UAS-CD63-GFP* virgin males at 1, 3, 5 and 9 days after eclosion, stained with Lysotracker (red). Age of gland is indicated to the left of panels, d=days after eclosion (at 28.5˚C). The glandular epithelium is initially columnar and becomes more squamous with age. Therefore, mMVBLs of young SCs, in particular of 1-day-old glands (**A**), sit at various planes within individual SCs. Consequently, we were unable to obtain an image depicting all mMVBLs in an individual cell in the same confocal plane. Scale bars, 5µm.

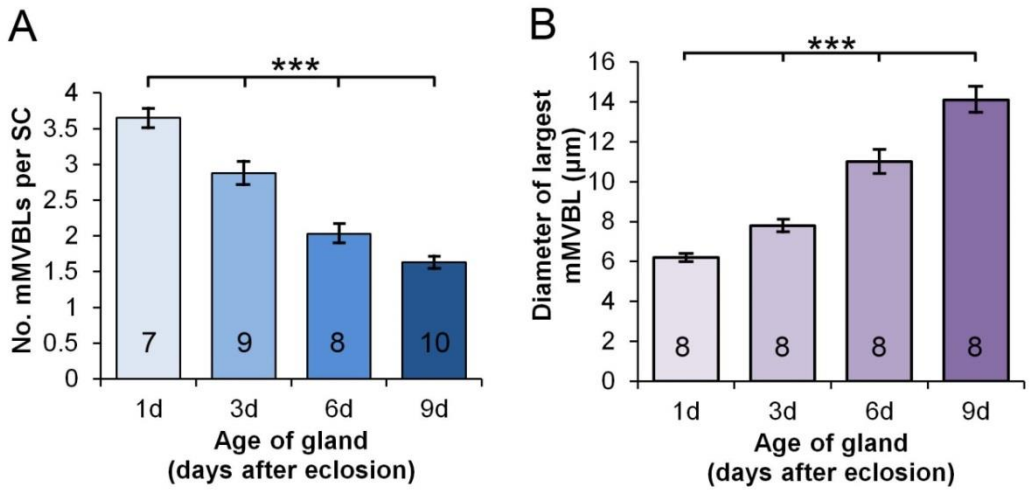


Fig. 3.9. Age-dependent mMVBL maturation. mMVBLs were counted in *spi-Gal4; UAS-CD63-GFP* virgin males at 1, 3, 6 and 9 days after eclosion (at 28.5˚C). mMVBLs were defined as compartments lined with CD63-GFP, stained with Lysotracker and greater than 2µm in diameter. 3 SCs per gland were measured and averaged across 'n' glands (numbers in bars). ***p<0.001: (**A**) One-way ANOVA; (**B**) Kruskal-Wallis test, following Shapiro-Wilk test for normality. Error bars indicate ±SE.

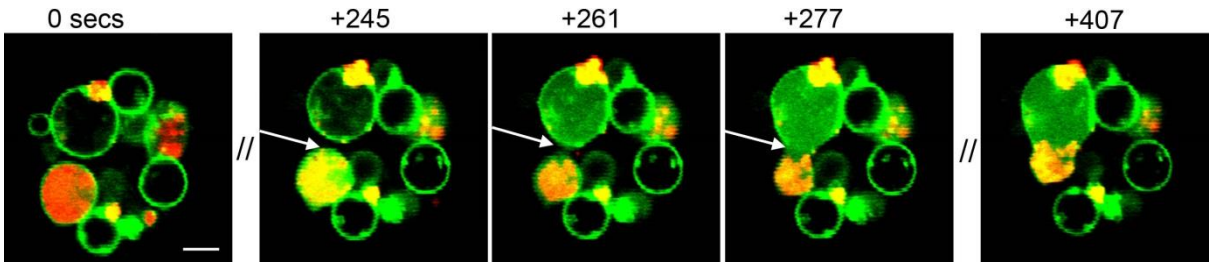


Figure 3.10. Live imaging of SCs reveals dynamic fusion between mMVBLs. Image sequence of 3-day-old *spi>CD63-GFP* AG stained with lysotracker and imaged live showing fusion (arrow) of two mMVBLs (0 secs; *) and a small degree of mixing of their contents. Numbers above images indicate time point relative to start (0) in seconds; // indicate missing frames. Scale bar, 5µm.

3.3.4 Secretory and endolysosomal compartments possess distinct Rab GTPase signatures

The unusually large size of acidic and non-acidic compartments in SCs led us to perform more detailed experiments to confirm their identity. We analysed the subcellular localisation of specific ubiquitously expressed YFP-tagged Rab GTPases (Marois et al. 2006) previously implicated in the regulation of endocytic trafficking and exosome secretion (Fader et al. 2005; Savina et al. 2005; Stenmark 2009; Koles et al. 2012; Beckett et al. 2013). Rab7 associates with late endosomes, MVBs and lysosomes and regulates aspects of late endosomal trafficking (Vitelli et al. 1997; Bucci et al. 2000; Vanlandingham et al. 2009). Importantly, all acidic compartments were Rab7-positive; SCs contained 2.4 +/-0.9 (n=11) large vacuoles (>2µm) lined with Rab7-YFP, 85% of which were acidic, confirming our assignment of these compartments as mMVBLs (**Fig. 3.11A; see Fig. 3.13**). Rab11-YFP, a marker for exocytic and recycling endocytic secretion as well as a regulator of exosome secretion in mammalian cell lines, *Drosophila* cells lines and *in vivo* (Chen et al. 1998; Koles et al. 2012; Beckett et al. 2013), localised to the limiting membrane of non-acidic vacuoles (**Fig. 13.11B**), suggesting Rab11 may regulate the secretion of SVs. However, expression of this marker driven by the tubulin promoter resulted in the loss of mMVBLs in most SCs (10/13 cells), a phenotype that may result from altered trafficking to mMVBLs following 'wild type' Rab11 overexpression, as observed in other systems (Savina et al. 2002; Savina et al. 2005). Finally, Rab5-YFP, a marker for early endosomes, mainly localised to small (<2µm) non-acidic, centrally clustered compartments, often in close proximity to iLEs (**Fig. 13.11C**). We noted that both the Rab7-YFP-positive iLEs and Rab5-YFP we often found more apically in SCs, whilst Rab7-YFP-positive mMVBLs and Rab11-positive SVs were often found more basally within individual SCs.

It is important to note that Rab7 is believed to associate with both late endosomes and lysosomes. In addition to Rab7, a GFP-tagged form of the late endosome- and lysosome-associated factor Phosphatidylinositol-4-Kinase II (PI4KII), previously shown to localise to the

limiting membrane of late endosomes and lysosomes of *Drosophila* salivary gland secretory cells (Burgess et al. 2012), also localised to the limiting membrane of mMVBLs, as well as tubules extending between them (**Fig. 3.12**), further supporting our classification of these compartments (see **Fig. 3.13**). This suggests that in addition to direct homotypic fusion, these compartments also interact via projections, as previously reported in other tissues including the salivary gland (Burgess et al. 2012). We attempted to mark SC lysosomes by driving expression of *UAS-Lamp1-HRP*; however the high level expression of this construct under control of the UAS-Gal4 system had severe effects on SC endocytic and secretory compartments (data not shown). It is likely that mMVBLs possess characteristics of both late endosomes and lysosomes as continued trafficking between them during the maturation process results in the formation of hybrid compartments (Huotari et al. 2011; Cameron C. Scott et al. 2014). We also tried previously published antibodies against late endosomal or lysosomal factors, including anti-ALiX and anti-Lamp1, but we were unable to observe any staining in the AG.

We noticed the presence of an additional Rab7-YFP-positive compartment that was not acidic (**Fig. 13.11A**). This compartment was typically surrounded by acidic Rab7-YFP-positive iLEs. We hypothesise that these compartments form following the fusion of Rab11-positive SVs with iLEs and subsequently undergo a Rab11-to-Rab7 'switch'. Indeed, work by another D.Phil. student in the lab (Siamak Redhai) has shown that Rab7 co-localises with Rab11-YFP at the limiting membrane of a subpopulation of Rab11-YFP-lined secretory vacuoles. It remains possible that Rab11 also localises to mMVBLs as it appears to regulate mMVBL trafficking, although without an additional (fixable) marker for mMVBLs, we cannot assess this directly in wild-type SCs. In conclusion, SC secretory vacuoles, MVBs and lysosomes are unusually large, permitting the *in vivo* analysis of these compartments at an unprecedentedly high spatial resolution.

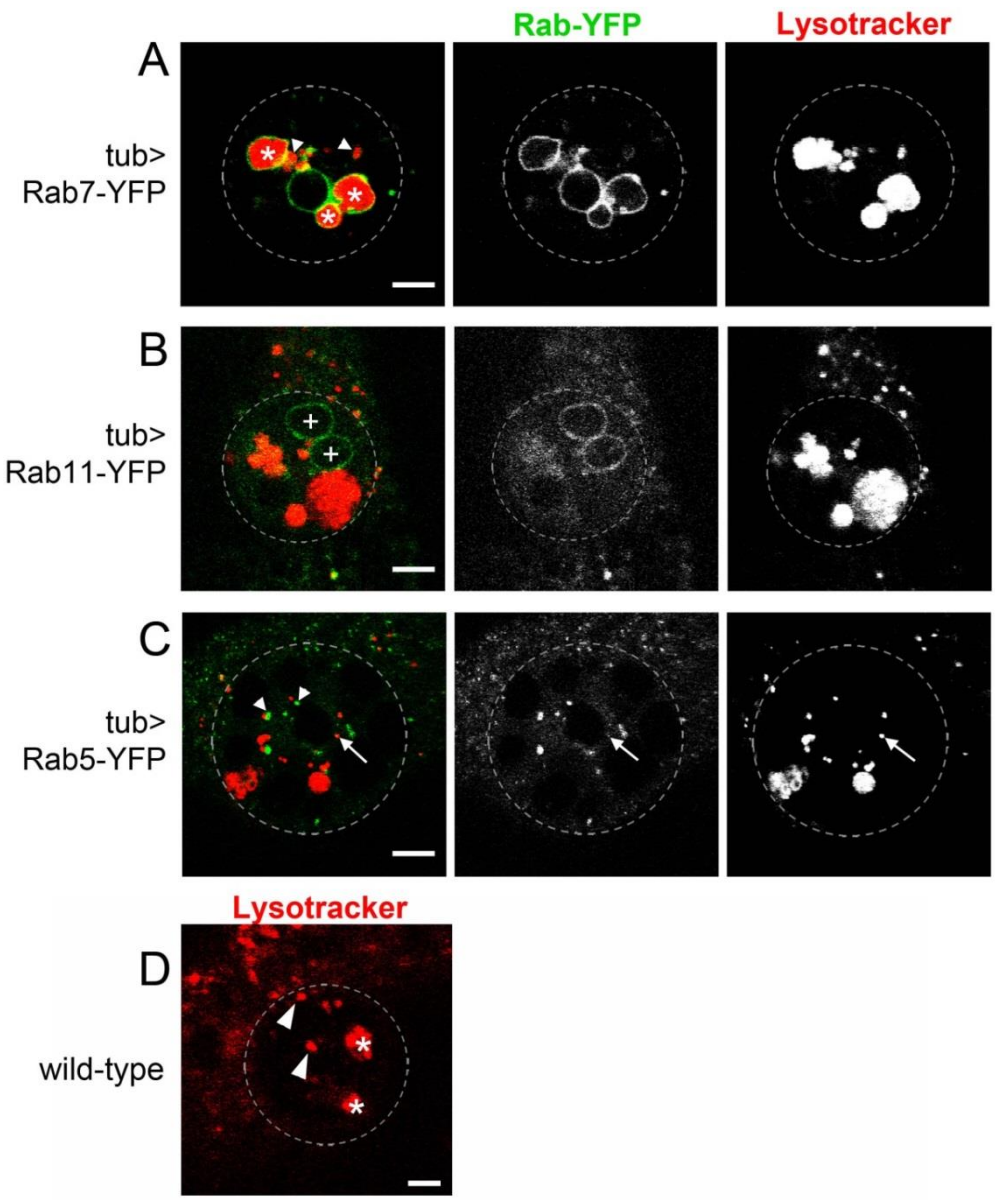


Figure 3.11. Rab GTPase signatures define different SC subcellular compartments. (**A-C**) YFP-Rab-expressing SCs stained with Lysotracker (red) have small acidic YFP-Rab7-positive iLEs (**A**, arrowheads; most of which are located more apically than this confocal section), large acidic YFP-Rab7-positive mMVBLs (**A**, *), YFP-Rab11-positive, non-acidic secretory vacuoles (**B**, '+'), YFP-Rab5-positive small non-acidic compartments (**C**, arrowheads), and more rarely (4/16 SCs) YFP-Rab5-positive small acidic compartments (**C**, arrow). (**D**) mMVBLs also form in 'wild-type' SCs, image shows a w^{1118} virgin male stained with Lysotracker (red). Presumptive iLEs (arrow heads; acidic compartments <2µm) and mMVBLs (*; acidic compartments >2µm) form inside wild-type SCs. Cell outline indicated by dotted circle. Scale bars, 5µm. Approximate outline of SCs is marked in all images. All SCs from 3-day-old virgin males incubated at 28.5˚C after eclosion.

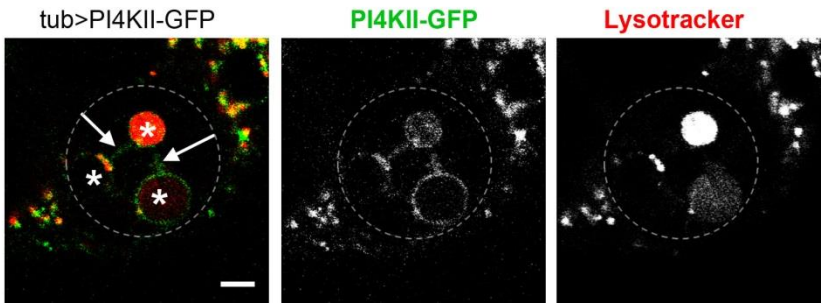
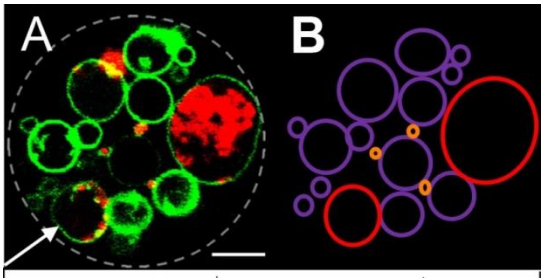


Figure 3.12. PI4KII localises to the limiting membrane of mMVBLs. Live image of an SC of a *Tub-PI4KII-GFP* (green) male stained with Lysotracker (red). The late endosome and lysosome marker PI4KII localises to the limiting membrane of large acidic compartments (*), as well as tubulations extending between them (arrow), which have been observed previously in *Drosophila* salivary gland cells (Burgess et al., 2012). Scale bar 5µm.



Compartment	No. per SC	Rabs
mMVBL	2.8 +/- 0.2 (22)	Rab7
iLEs	2.5 +/- 0.2 (22)	Rab7
SVs	12.6 +/- 1.1(22)	Rab11

Figure 3.13. SC endosomal and secretory compartments possess a stereotypical Rab GTPase signature. (**A**) Vital staining of SCs with Lysotracker-Red reveals CD63-GFP-positive puncta (putative ILVs) in large acidic compartments (arrow). Representative image of a 3-day-old virgin male (**A**) incubated at 28.5˚C post-eclosion, with accompanying schematic (**B**) indicating the identity of endosomal and secretory compartments. Values below indicate average total numbers of each compartment in 6-day-old control SCs counted from multiple sections along apical-basal axis; number of SCs analysed in brackets. mMVBLs were classified as acidic Rab7- and CD63-GFP-postive, acidic, >2µm in diameter; iLEs were classified as Rab7-positive, acidic, CD63-GFP-positive, <2µm in diameter; SVs were classified as non-acidic, Rab11-and CD63-GFP positive, >2µm in diameter. Scale bar 5µm.

3.3.5 Ultra-structural analysis of SCs and AG lumen

To confirm the presence of ILVs inside mMVBLs and exosomes in the AG lumen we analysed wild type AGs by electron microscopy. Unfortunately, preservation of membranes within the entire AG proved challenging. Nevertheless, electron micrographs demonstrated the presence of exosome-like vesicles of ≈40nm diameter (typical of exosomes, which can range from 40-150nm (Raposo et al. 2013)) in the gland lumen (**Fig. 13.14A-C**). SCs contained vesicles of similar size and morphology inside large compartments (**Fig. 13.14D-E**), void of the fibrillar material or dense cores characteristic of SV (**Fig. 13.15**) (Rylett et al. 2007). Interestingly, the AG lumen contains exosome-like vesicles of differing size and density, suggesting that more than one type of exosome may be secreted into the gland lumen. It is important to note the presence of large amount of amorphous and floccular material both inside SC mMVBLs as well as the lumen of the gland, which may interact with the surface of exosomes. Indeed, we hypothesise that some of this material may be extracellular matrix components, such as heparin sulphate proteoglycans which have been shown to function in exosome biogenesis (Baietti et al. 2012).

We also analysed SCs expressing CD63-GFP by immuno-EM. Their mMVBLs seemed to be filled with denser material than wild type (**Fig. 13.16**). mMVBLs of SC>CD63-GFP SCs also contained more putative ILVs, exhibiting a larger range of sizes (40nm-150nm). Importantly, a number of these small vesicles were recognised by an anti-GFP antibody stain, indicating that they carried CD63-GFP. Our analysis demonstrates that wild type SCs secrete exosome-like vesicles that originate inside large MVBLs; however, CD63-GFP expression alters the ultrastructure of mMVBLs, though not their total number or size, potentially increasing the number and/or type of ILVs formed.

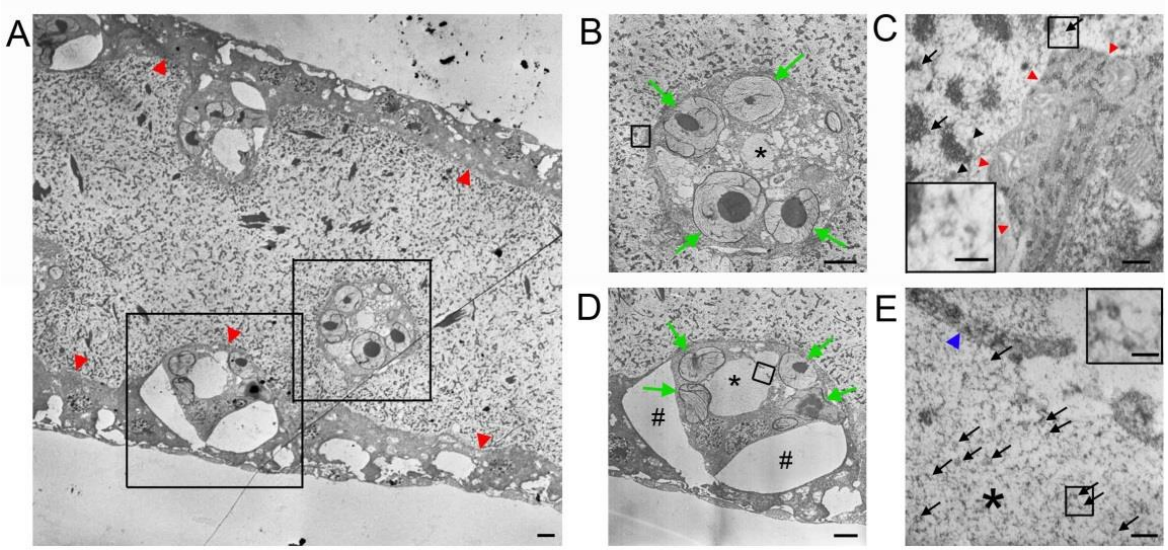


Figure 3.14. Electron microscopy reveals the presence of exosome-like vesicles in the AG lumen and large SC compartments. (**A-E**) Electron micrographs of 3-day-old virgin w^{1118} male AGs. MCs (apical membranes marked with red arrowheads in **A** and **C**) make up the majority of the monolayered epithelium; SCs (boxed in **A**) are dispersed between MCs, bulge into the lumen and can be seen in transverse (e.g. cell in **D**) or surface (e.g. cell protruding into lumen in **B**) section. SCs contain secretory vacuoles (SVs), comprising an electron dense core and fibrillar material (**B** and **D**, green arrows) and one or two large and less electron-dense, non-SV compartments (**B** and **D**, *, **E** shown at high magnification in **D**), which by a process of elimination, must represent the large acidic compartments seen in live confocal imaging. The AG lumen contains a range of secreted structures (**C**), including putative membrane-bound vesicles (**C**, black arrows and arrowheads; red arrowheads mark apical surface of epithelium), some of which (**C**, black arrows; enlarged in inset) resemble the ~40 nm vesicles observed inside the large multivesicular compartments in SCs (**E**, arrows; enlarged in inset). These compartments therefore appear to be the counterparts of much smaller mammalian MVBs. **B** and **D** are higher magnification images of the boxed regions in **A**; **C** and **E** show higher magnification images of the regions boxed in **B** and **D**, respectively. Note that despite attempting a number of fixation protocols, we were unable to prevent spaces forming at high frequency between SC and MC plasma membranes in the epithelium (# in **D**). Preservation of compartment membranes was also not optimal (e.g., blue arrowhead in **E**). Scale bars, (**A, B, D**) 2µm; (**C** and **E**) 200nm; (**C** and **E**, insets) 100nm. Electron micrographs were obtained in collaboration with Siamak Redhai and Prof. J Morris (DPAG).

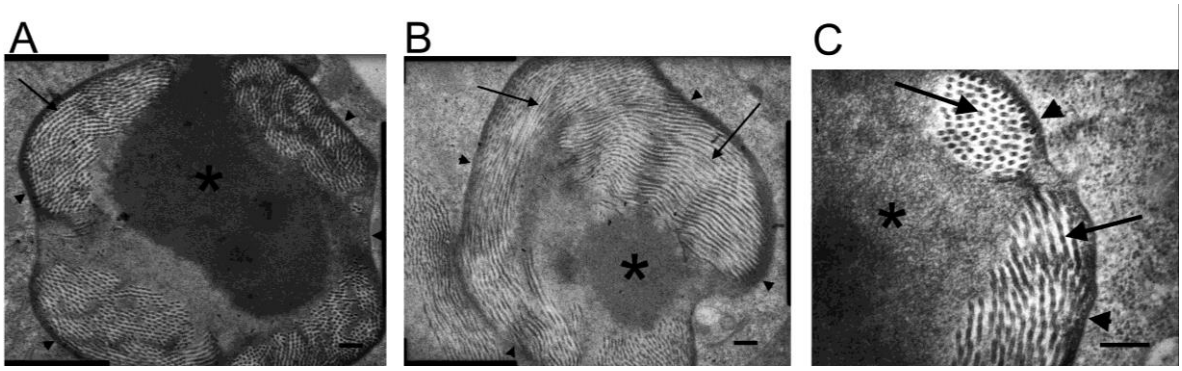


Figure 3.15. Ultra-structural electron microscopic analysis of SC SVs. SC secretory vacuoles contain fibrillar material (arrows) and a dense secretory core (*) as previously reported by Rylett et al., 2007, which can vary in size and density. **A** and **B** show variability of dense core between SVs of the same SC. (**C**) Fibrils may be composed of repeating units and can be arranged in any orientation within an individual SV. **C** shows a high magnification image of a SV showing transverse and longitudinal sections through SV fibres. The limiting membrane of SVs is marked by arrowheads. AG of a 3-day-old virgin w^{1118} male. Scale bars, 200nm. Electron micrographs were obtained in collaboration with Katie Windsor (FHS 2013) and Prof. J Morris (DPAG).

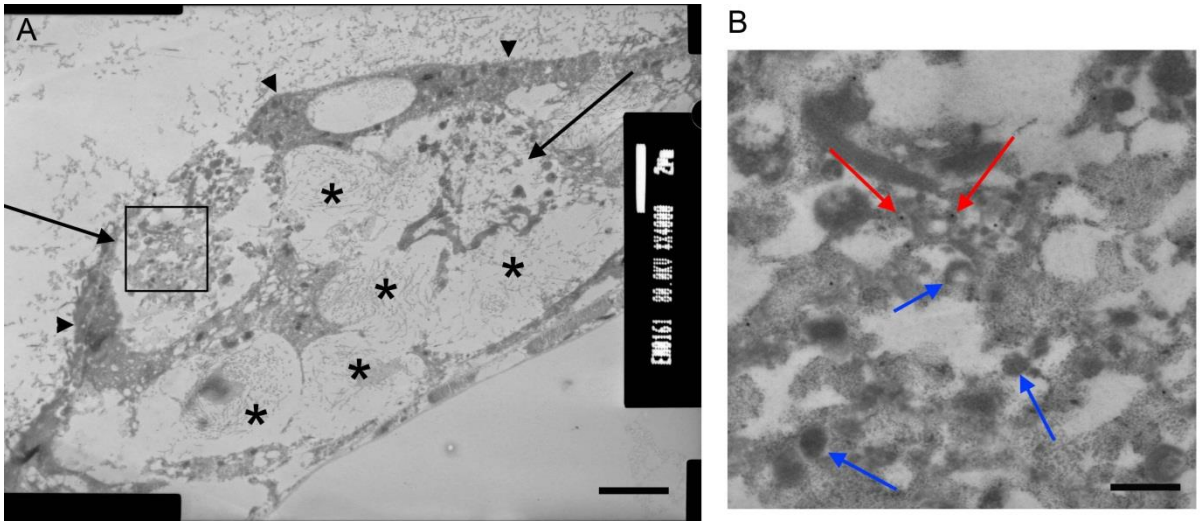


Figure 3.16 Immuno-EM analysis of SC mMVBLs confirms the presence of CD63-GFP on putative ILVs. (A and **B)** Electron micrograph of a 3-day-old *spi-Gal4; UAS-CD63-GFP* virgin male AG stained with anti-GFP (15nm gold-coupled secondary antibody). SCs expressing CD63-GFP contain SVs (* in **A**), large mMVBL compartments (A; arrows) containing many vesicles of various sizes (≈40-150nm, **B**). (**B**) Unlike those of w^{1118} glands (Fig. 13.14), the size and electron density of ILVs of SCs expressing CD63-GFP is variable. mMVBLs contained many small vesicles approximately 40nm in diameter that were recognised by anti-GFP (**B**, red arrows); these compartments also contained larger, approximately 100-150nm diameter, vesicles that were more electron dense and were not recognised by anti-GFP (**B**, blue arrows). The apical membrane is marked by arrowheads in **A**. **B** shows higher magnification image of boxed region in **A**. Scale bars: (**A**) 2µm, (**B**) 200µm. Electron micrographs were obtained in collaboration with Katie Windsor (FHS 2013) and Prof. J Morris (DPAG).

3.3.6 CD63-GFP traffics via the secretory pathway to reach late endosomes

The similar characteristics of the smaller and larger acidic compartments (pH and Rab signature) led us to preliminarily assign iLE and mMVBL identities to these compartments based on their differing size. To confirm that iLEs were indeed an immature precursor to mMVBLs we followed the trafficking of CD63-GFP through the secretory and endolysosomal systems utilising the temperature-sensitive Gal4 transcriptional repressor Gal80^{ts} by employing a pulse-chase approach.

A ubiquitously expressed temperature-sensitive transcriptional repressor, *Gal80^{ts}* driven by the *tubulin* promoter, can also be incorporated to permit temporal control of transgene expression (Suster et al. 2004). The temperature sensitive repressor inhibits Gal4-driven gene expression at 18˚C, but is inactivated at 28.5˚C thus allowing reversible transgene expression.

Induction of a short (8 hour) pulse of CD63-GFP expression, by inhibiting Gal80^{ts} at 28.5˚C, followed by a chase period at 18˚C of 0-60 hours, revealed rapid labelling of 1.9 +/- 0.2 (n=17) non-acidic large SVs, presumably receiving newly synthesised CD63-GFP from the Golgi apparatus (**Fig. 3.17A-B**). A small proportion of iLEs were also GFP-positive immediately after the pulse (0 hours chase), suggesting that CD63-GFP traffics to this endocytic compartment within the 8 hour pulse period (**Fig. 3.17G**), either via endocytosis from the plasma membrane or receiving newly synthesised protein directly from the Golgi. During the early part of the time course a greater proportion of SCs contained labelled iLEs than labelled mMVBLs (P=0.001, n>27) and this trend continued at later time points (**Fig. 3.17A-G**), supporting a model where CD63-GFP traffics first to the iLEs and subsequently to mMVBLs. This is consistent with our assignment of these two classes of acidic compartment.

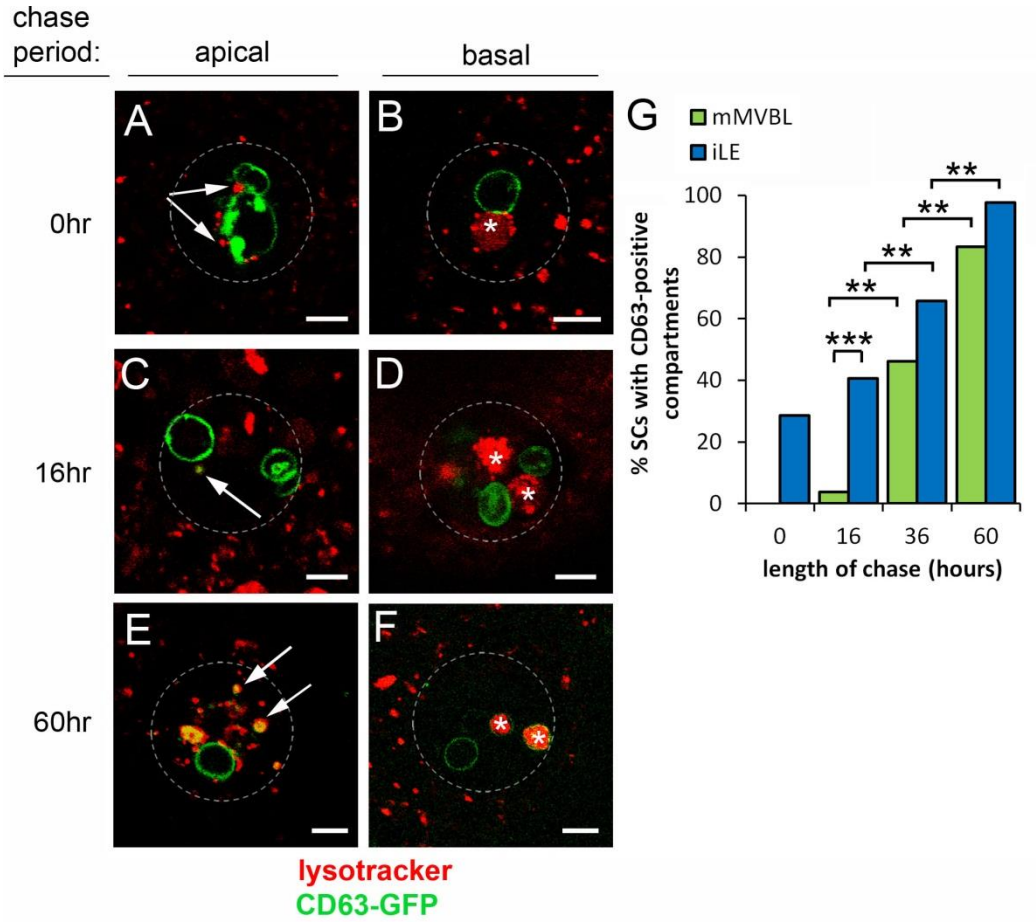


Figure 3.17. CD63-GFP trafficking and exosome biogenesis in SCs. An 8 hour pulse (at 28.5°C) of CD63-GFP expression was chased at 18˚C for 0-60 hours in virgin males and the proportions of cells with one or more Lysotracker-Red-positive iLEs (<2µm, arrows in **A**, **C**, **E**; apical views) and mMVBLs (>2µm; * in **B**, **D**, **F**; basal views) that were CD63-GFP-positive were scored (**G**). **p<0.01, ***p<0.001, n>24. Data analysed using Fisher's Exact Test (pairwise comparisons). Scale bars, 5µm.

3.3.7 Live cell imaging reveals dynamic interactions between and within compartments

As previously mentioned, real-time live-cell imaging of SCs revealed homotypic fusion events between mMVBLs, suggesting they mature by fusion (**Fig. 3.10**). Strikingly, we also observed non-acidic vacuoles fusing with mMVBLs (**Fig. 3.18A**). Although the internal contents of these compartments did not freely mix during the time period observed, these findings suggest a surprising level of exchange between secretory vacuoles and mMVBLs, and might explain how CD63-GFP-positive structures accumulate in secretory vacuoles (**Fig. 3.2A**). We were unable to obtain convincing real-time live image sequences of iLEs fusing with mMVBLs. It is possible that iLEs mature into, rather that fuse with, mMVBLs, with their growth being supported by either the trafficking of smaller vesicles to them or from direct iLE fusion. However, we frequently observed iLEs in close proximity to mMVBLs, as if they had docked onto mMVBLs prior for fusion. We believe it is likely we did not capture this event in real time due to the small size of iLEs making this difficult to image using confocal microscopy, which would only capture events in one optical plane, and so we cannot estimate their frequency.

Surprisingly, we were able to capture by time-lapse imaging a deformation of the mMVBL membrane that preceded the appearance of a fluorescent CD63-GFP puncta at the edge of this compartment (**Fig. 3.18B**). We speculated that this was the invagination and budding of a new ILV inside this compartment. This event was associated with a sudden increase in acidity in surrounding region within the mMVBL. We hypothesise that the vacuolar proton pump (V-ATPase) forms a proton gradient outside ILVs that cannot be dissipated locally by proton-mediated nutrient uptake because nutrients rapidly accumulate inside the ILVs (**Fig. 3.18C**). Indeed, in many SC observed the mMVBLs were filled with apparently discrete acidic puncta. As discussed previously, anti-CD63 staining indicates that many CD63-positive ILVs are not marked by GFP fluorescence (**Fig. 3.6**). We speculate that the ILVs are initially fluorescent but the gradual dissipation of the proton gradient or build of nutrients inside them precludes GFP fluorescence.

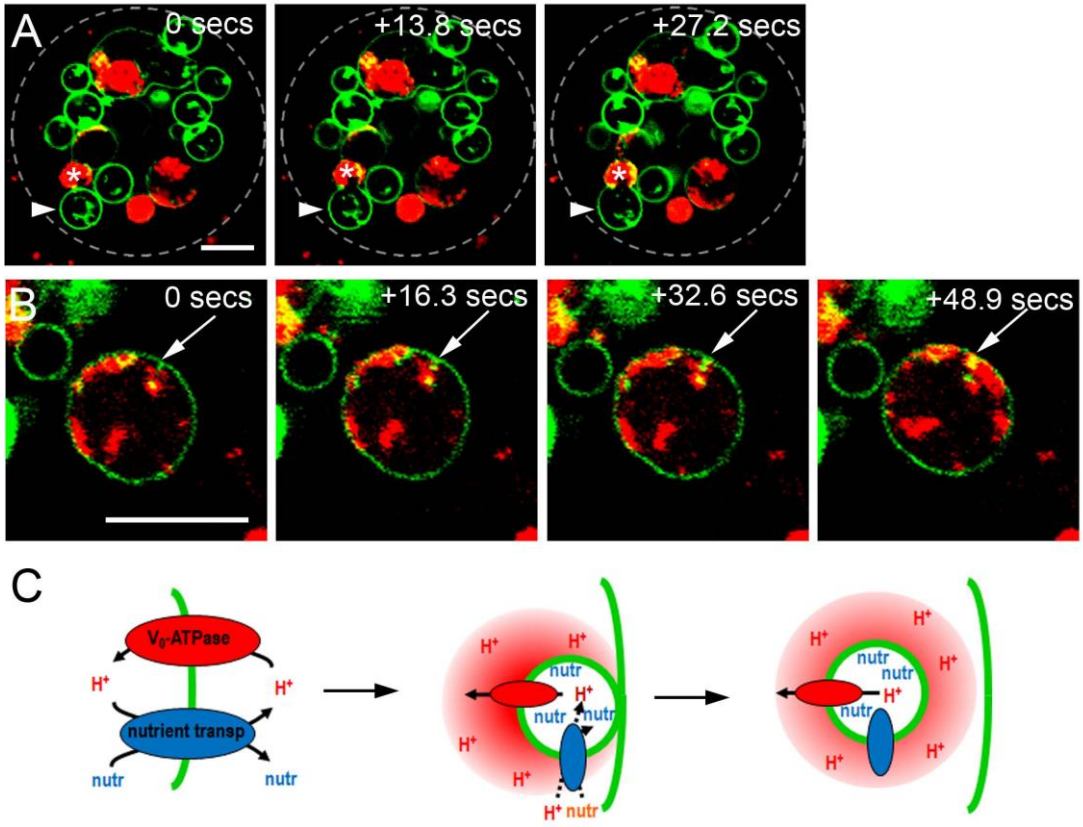


Figure 3.18. Real-time live imaging reveals dynamic trafficking events inside acidic late endosomal compartments. (**A, B**) Time-lapse live imaging of 3-day-old SC>CD63-GFP males, stained with Lysotracker-Red reveals fusion between endocytic and non-acidic compartments (**A**) and ILV biogenesis (**B**) in real time. (**A**) An mMVBL containing ILVs (*****) fuses with a large non-acidic secretory vacuole (arrowhead). (**B**) A CD63-GFP-marked protrusion invaginates from the mMVBL membrane (arrows; 0 sec), forming a CD63-GFP-positive acidic puncta. This precedes the appearance of a wave of peripheral acidic microdomains (48.9 sec), although we cannot exclude this results from a change in the focal plane of imaging. (**C**) Model to explain how a proton gradient might be set up outside newly formed ILVs within mMVBLs. Green lines depict late-endosomal limiting membranes whose invagination results in the formation of ILVs, around which a high concentration of protons builds up from the action of the V-ATPase residing in the limiting membrane. Nutrients accumulate inside the ILVs via proton-assisted transport. Scale bars, 5µm.

3.3.8 Regulation of late endosomal trafficking by mating

To gain further support that the CD63-GFP puncta observed in the gland lumen were derived from mMVBLs and were therefore exosomes, we analysed the effects of mating on mMVBLs under the assumption that mating would increase mMVBL turnover. We observed a significant reduction in the number of mMVBLs following mating, with the fewest mMVBLs being observed 1 hour after mating, reducing from 2.4+/-0.1 in 3-day-old virgin glands to 1.6+/- 0.2 (**Fig. 3.19A**). We also observed a trend towards a reduction of SVs after mating; reducing from 5.8+/-0.2 in live virgin glands to 4.8 +/-0.08 after 1 hour but this change was not significant (**Fig. 3.19B**). These data suggest that the content of some mMVBLs is secreted shortly after mating, presumably following their fusion with the apical plasma membrane.

Unfortunately, technical limitations presented us from obtaining live images and thus size quantifications of mMVBLs after mating, or indeed time image sequences of mMVBLs fusing with the plasma membrane, as mating increases the excitability of the surrounding muscular sheath.

In summary, SCs contain unusually large late endosomal and secretory compartments that exhibit age-dependent and mating-dependent changes and possess unique Rab GTPase signatures (**Fig. 3.13**). These compartments can be studied using both fixed and live imaging techniques, the latter of which can be employed to capture dynamic events occurring both within and between individual compartments. The large acidic MVBLs of SCs contain CD63-GFP-positive ILVs, which may be secreted into the fluid stored in the AG lumen as exosomes.

3.3.9 SCs secrete exosomes in an ESCRT-dependent manner

3.3.9.1 Effects of ESCRT knockdown on SC biology

To confirm the identity of internal GFP inside mMVBLs as ILVs, we attempted to block their production by knocking down previously identified regulators of exosome biogenesis. As

exosomes carrying CD63 have been previously characterised to be made in an ESCRT-dependent manner (Colombo et al. 2013), we knocked down several ESCRT subunits (*Hrs*, CG2903, ESCRT-0; *TSG101*, CG9712, ESCRT-I) or their accessory components (*ALiX*, CG12876; and *Vps4,* CG6842) by RNAi and analysed the effect on the morphology of mMVBLs in CD63-GFP-expressing SCs. For these experiments, we utilised a SC-specific driver line containing the genetic elements: *UAS-CD63-GFP*; the SC driver, *dsx-Gal4* (which is expressed specifically in SCs in the AG epithelium (**Fig. 2.1**)); and a ubiquitously expressed Gal80^{ts}, *Tub-Gal80^{ts}*. This allowed us to express the RNAi constructs under UAS control specifically in SCs in a post-developmental manner, by rearing flies at 18˚C and shifting flies to 28.5˚C at eclosion in order to induce transgene expression. Thus, both RNAi constructs and CD63-GFP were expressed simultaneously only in adult flies. We analysed the effect of ESCRT-knockdown in 6-day-old virgin flies in order to clearly distinguish SC compartments and image the internal contents of mMVBLs as 6-day-old SCs contain enlarged mMVBLs. 6-day-old control SCs (driver line crossed to *w^{1118}*) imaged live and stained with Lysotracker contain many GFP-fluorescent puncta (**Figure 3.20A**). In contrast, mMVBLs of SCs expressing *Hrs*-RNAi (**Fig. 3.20B**), *ALiX*-RNAi (**Fig. 3.20C**) or *TSG101*-RNAi (**Fig. 3.20D**) were almost completely void of CD63-GFP fluorescent puncta. We noted that of these, *Hrs*-RNAi produced the strongest, most reproducible block on ILV production (100% of all 36 SCs imaged; 3 SCs across 12 glands) although, again, we were unable to effectively quantify this phenotype for the previously discussed reasons, i.e., most vesicles may not be fluorescent. Unlike the other ESCRT components, mMVBLs of *Vps4*-RNAi SCs were filled with internal CD63-GFP (**Fig. 3.20E**). We speculate that these late endosomal compartments produce normal numbers of ILVs, and the reduction in their size (**Fig. 21D**) and the maintenance of internal GFP fluorescence results in an mMVBLs containing increased amounts of fluorescent ILVs that can be observed by live imaging.

To gain a better understanding of the effect of ESCRT knockdown on SC endocytic and secretory cell biology as a whole, we quantified the number of mMVBLs (**Fig. 3.21A**), iLEs (**Fig. 3.21B**) and SVs (**Fig. 3.21C**) as well as the size of the largest mMVBL (**Fig. 3.21D**), as measured by its widest

diameter. In contrast to control SCs, which contained 2+/-0.1 mMVBLs of 11+/-0.3µm diameter, SC>*Hrs*-RNAi SCs contained significantly fewer mMVBLs that were also significantly larger than control. We utilised two distinct RNAi constructs to knockdown *ALiX*; only one significantly reduced the number of mMVBLs per SC. However, unlike *Hrs*-RNAi, both significantly reduced the size of the largest mMVBL, suggesting that ESCRT-0 and ALiX have different effects on mMVBL biology. In contrast, knockdown of *TSG101* by RNAi had no effect on the number or size of mMVBLs; however, this transgene also has the weakest effect on ILV formation, suggesting that either *TSG101* plays a minor role in SC mMVBL maturation or that this construct achieves weaker knockdown.

We observed no significant effect on iLE number following knockdown of ESCRT components (*Hrs*, *TSG101* or *ALiX*) (**Fig. 3.21B**), suggesting that ESCRTs function downstream of iLE formation. These data support the role of ESCRTs in mMVBL formation and is consistent with our assignment of these compartments as immature and mature late endosomes. *Vps4*-RNAi was the only exception to this, suggesting that Vps4 may have additional roles in endocytic trafficking to Hrs, ALiX and TSG101.

Interestingly, knockdown of ESCRT components also affected the number of SVs formed (**Figure 3.21C**). Knockdown of ESCRTs required for ILV formation, *Hrs*, *AliX* and *TSG101*, resulted in significantly more SVs per SC, suggesting that mMVBL function/maturation is required to regulate SV turnover. Importantly, further experiments demonstrated that these cells secrete normal levels of ANCE (see Section 3.3.9.2; **Fig. 3.24B and 3.25F**). Interestingly, *Vps4*-RNAi reduced the number of SVs in SCs, further supporting a model in which *Vps4* regulates distinct or additional aspects of membrane trafficking to ESCRTs and *ALiX*.

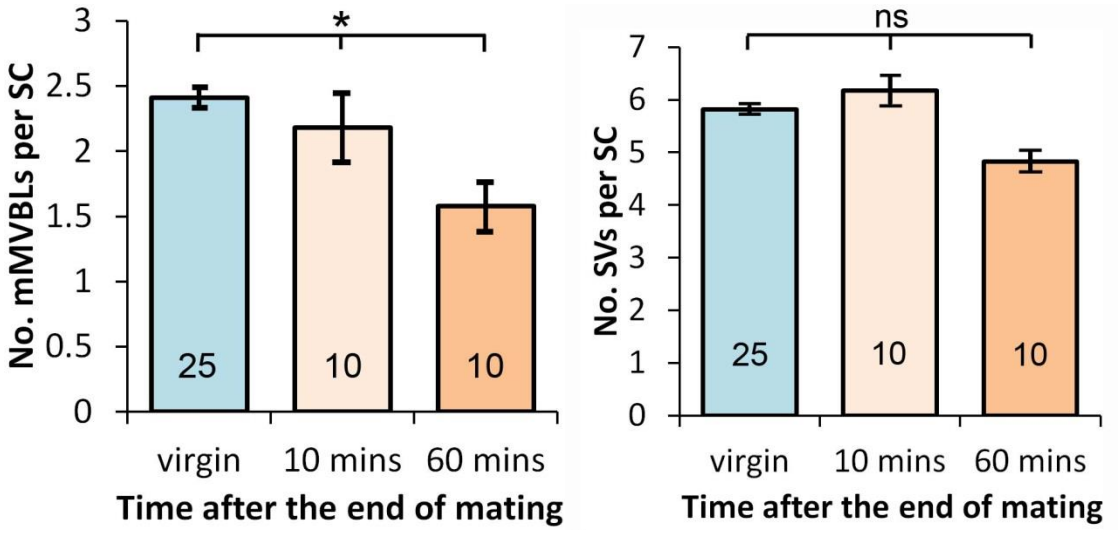


Fig. 3.19. The effect of mating on late endocytic and secretory SC compartments. 3-day-old *spi-Gal4; UAS-CD63-GFP* males were mated to w^{1118} virgin females, matings were observed and males were dissected at 10 minutes or 60 minutes after the end of mating, stained with Lysotracker (red) and imaged live. mMVBLs were defined as compartments lined with CD63-GFP, stained with Lysotracker and greater than 2µm in diameter; SVs were defined as compartments lined with CD63-GFP, not stained with Lysotracker and greater than 2µm in diameter. *p<0.05, One-way ANOVA (A); ns=not significant, Kruskal-Wallis test. Numbers in bars indicate number of SCs analysed across a minimum of 5 glands. Error bars indicate ±SE.

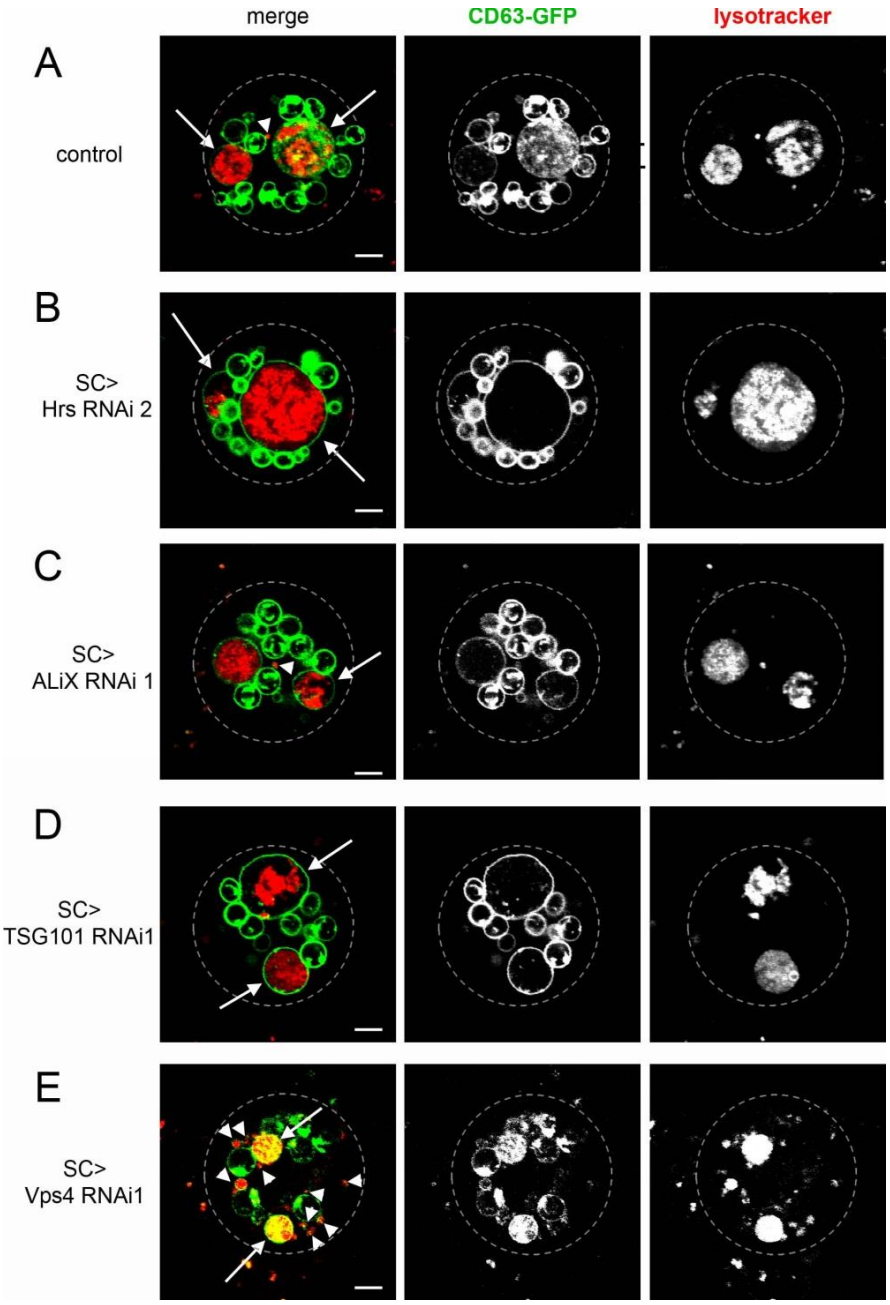


Figure 3.20. Knockdown of ESCRT components effects morphology of SC compartments. Representative images of 6-day-old virgin *UAS-CD63-GFP, tub-Gal80^{ts} ;dsx-Gal4* (driving transgene expression or crossed to *w^{1118}* for control) virgin males, stained with Lysotracker (red) and imaged live. Genetic manipulation of ESCRT components affects the morphology (and number, see Fig. 3.21) of both the iLEs (arrowheads) and mMVBLs (arrows). mMVBLs of control SCs often contain many CD63-GFP ILVs (**A**), whilst knocking down ESCRT components *Hrs* (ESCRT 0, **B**) or *TSG101* (ESCRT-I, **D**) or the ESCRT interactor *ALiX* (**C**), results in the formation of mMVBLs containing fewer CD63-GFP puncta (arrows). Knockdown of *Vps4* (E) formed small mMVBLs filled with CD63-GFP-positive ILVs. Scale bars, 5µm.

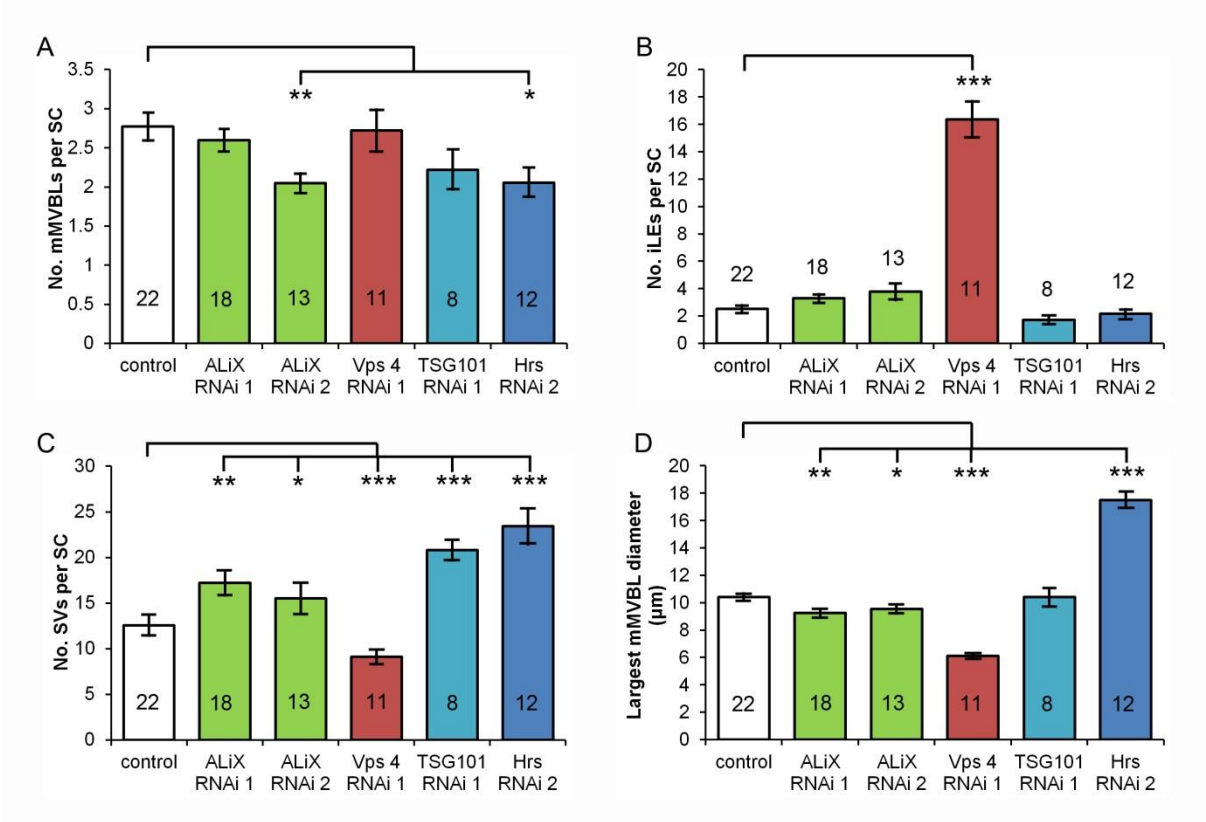


Figure 3.21. Knockdown of ESCRT components effects morphology of SC compartments. Quantifications of SC compartments of 6-day-old virgin *UAS-CD63-GFP, tub-Gal80^{ts};dsx-Gal4;* (driving transgene expression or crossed to *w^{1118}* for control) virgin males, stained with Lysotracker (red) and imaged live.*p<0.05, **p<0.01, ***p<0.001. Data were analysed using either unpaired two-tailed Student's t-test or Mann Whitney U (pairwise comparisons against control), following Shapiro-Wilk test for normality. Three SCs per gland were measured and averaged; numbers in bars indicate number of glands analysed. Error bars indicate ± SE.

3.3.9.2 ESCRT-dependent exosome secretion

Importantly, knockdown of *Hrs*, *ALiX* and *Tsg101* by RNAi, using two different RNAi transgenes for each, significantly reduced the number of CD63-GFP puncta secreted into the gland lumen, analysed by confocal images through the gland lumen (**Fig. 3.22 and 3.23C**), suggesting that these secreted particles are indeed exosomes produced in an ESCRT-dependent manner. Knockdown of Vps4 by RNAi also significantly reduced CD63-GFP puncta secretion in our initial experiments (**Fig. 3.23C**); however, we were unable to obtain consistent effects of *Vps4* knockdown on exosome secretion as repeat experiments also demonstrated an increase in exosome secretion (data not shown, Section 2.3.5). This may be explained by our previous findings that *Vps4*-RNAi has significant effects on multiple aspects of SC secretory and endocytic biology but does not appear to block ILV biogenesis itself.

When carrying out confocal image analysis of the AG lumen we optimised the confocal settings in order to obtain a clean image of maximal particles to background noise to control glands for each individual experiment. To exclude the possibility that confocal settings affected the results obtained, we imaged one experimental run under two confocal gain settings. Images obtained under these two settings captured differing numbers of CD63-GFP fluorescent particles in the gland lumen depending on their intensity (**Fig. 3.23A and B**). Importantly, we observed the same relative effects on exosome secretion by knockdown of ESCRTs when calculated relative to the control, irrespective of the gain setting utilised (**Fig. 3.23C**).

To eliminate the possibility that the observed reduction in CD63-GFP secretion following *ALiX* or *Hrs* knockdown resulted from effects on the level of CD63-GFP synthesis in SCs we analysed the protein content of dissected virgin AGs by western blot using an anti-GFP antibody. The full length fusion protein should have a molecular weight of approximately 52kDa (MW of CD63 is 26kDa; GFP is 26kDa). Importantly, we detected equivalent amounts of full length CD63-GFP protein in control, SC>*ALiX*-RNAi and SC>*Hrs*-RNAi (as well as SC>*Rab11-DN,* which has been shown to

reduce CD63-GFP puncta secreted into the gland lumen as analysed by confocal microscopy; Siamak Redhai, Wilson lab) (**Fig. 3.24A**), confirming that expression of these constructs does not affect total CD63-GFP expression levels. No obvious smaller products were recognised, supporting our previous hypothesis that CD63-GFP is not cleaved in the AG (or female reproductive tract; see **Fig. 24B**). Importantly, no protein was detected in wild-type AGs (**Fig. 3.24A)**, confirming specificity of antibody binding.

To confirm that both *ALiX-RNAi* and *Hrs-RNAi* do not affect production of other SC secretory products not carried on exosomes, we also probed the AG immunoblots for the SC secretory product ANCE. Importantly, we detected approximately equal amounts of ANCE in *SC>ALiX-RNAi*, *SC>Hrs-RNAi*, *SC>Rab11-DN* and control glands (Fig. **3.24A**), suggesting these genetic manipulations do not affect general protein synthesis in SCs. Furthermore, the ratio of CD63-GFP to ANCE detected in AGs did not differ following exosome biogenesis inhibition, suggesting that *ALiX-RNAi*, *Hrs-RNAi* and *Rab11-DN* expression do not specifically affect CD63-GFP synthesis.

We hypothesised that CD63-GFP exosomes are transferred into the female reproductive tract during mating via the seminal fluid. To test this, we mated SC>CD63-GFP males to wild-type w^{1118} females and analysed the protein content of the mated female reproductive tracts by western blot. As expected, we detected full length CD63-GFP in females mated to SC>CD63-GFP males with no evidence for degradation products. We did not detect CD63-GFP in the lysates of either virgin females or females mated to wild-type w^{1118} males, confirming the specificity of the antibody staining in the female reproductive tract.

Importantly, we detected significantly less CD63-GFP protein in female reproductive tracts mated to *SC>ALiX-RNAi*, *SC>Hrs-RNAi* and *SC>Rab11-DN* males, yet equal amounts of ANCE. Minimal ANCE protein was detected in virgin females, suggesting that almost all ANCE present after mating is derived from the male seminal fluid. Although we cannot absolutely exclude that mating induces ANCE synthesis in the female reproductive tract, the fact that these females were

dissected 20 minutes after the start of mating makes this is unlikely. Moreover, the localisation of ANCE to the dense core of SC SVs was not affected by *ALiX*-RNAi or *Hrs*-RNAi (**Fig. 3.25A-C**), or the intensity of ANCE staining in the gland lumen as analysed by confocal microscopy (**Fig. 3.25D-F**), suggesting that these manipulations do not affect or block the trafficking of ANCE through the classical secretory pathway. Interestingly, we detected approximately 25% less ANCE transferred into females in control AGs expressing *SC>CD63-GFP* than wild-type w^{1118} AGs as analysed by Western blots, suggesting that expression of *CD63-GFP* alone affects the amount of protein secreted by SCs (Fig. **3.24A**).

These western data provide further support that *ALiX*, *Hrs* and *Rab11-DN* knockdown reduced the number of CD63-GFP exosomes secreted into the seminal fluid. Furthermore, they suggest that these genetic manipulations specifically block exosome secretion and do not affect the classical secretory pathway in these cells.

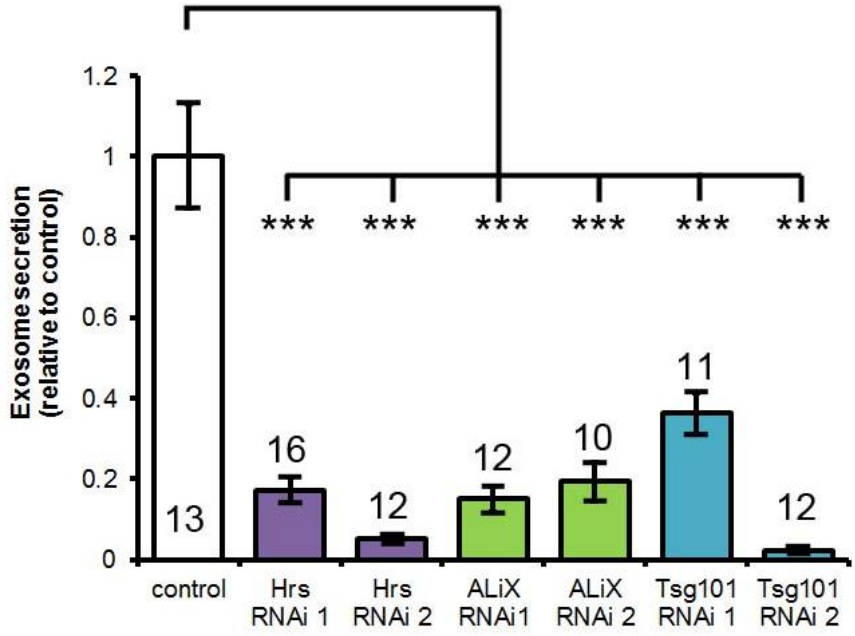


Figure 3.22. Depletion of ESCRT components reduces the secretion of CD63-GFP puncta. Figure shows a summary of results for different UAS-constructs assimilated from several experiments, where values are plotted relative to the control of the respective experiment. The values represent the average particles in a 7225 µm^2 luminal area, averaged over 3 confocal sections for each gland and then over 'n' glands (number above or in bars), and calculated as a percentage of the control value from an experiment carried out simultaneously. Virgin males (*UAS-CD63-GFP, tub-Gal80^{ts} ; dsx-Gal4* driving expression transgene expression or crossed to *w^{1118}* for control) were shifted to 28.5˚C at 0 days to induce transgene expression and mated to 3 females at 2 days to expel the stored luminal contents (in case RNAi-mediated knockdown and CD63-GFP transgene expression may differ in their kinetics), allowed to recover for 24 hours and then dissected at 4 days. ***P<0.001. Data were first analysed using the Shapiro Wilk test for normality; normal data were analysed using an unpaired Student's *t*-test, non-normal data analysed using the Mann Whitney U test. Error bars indicate ± SE.

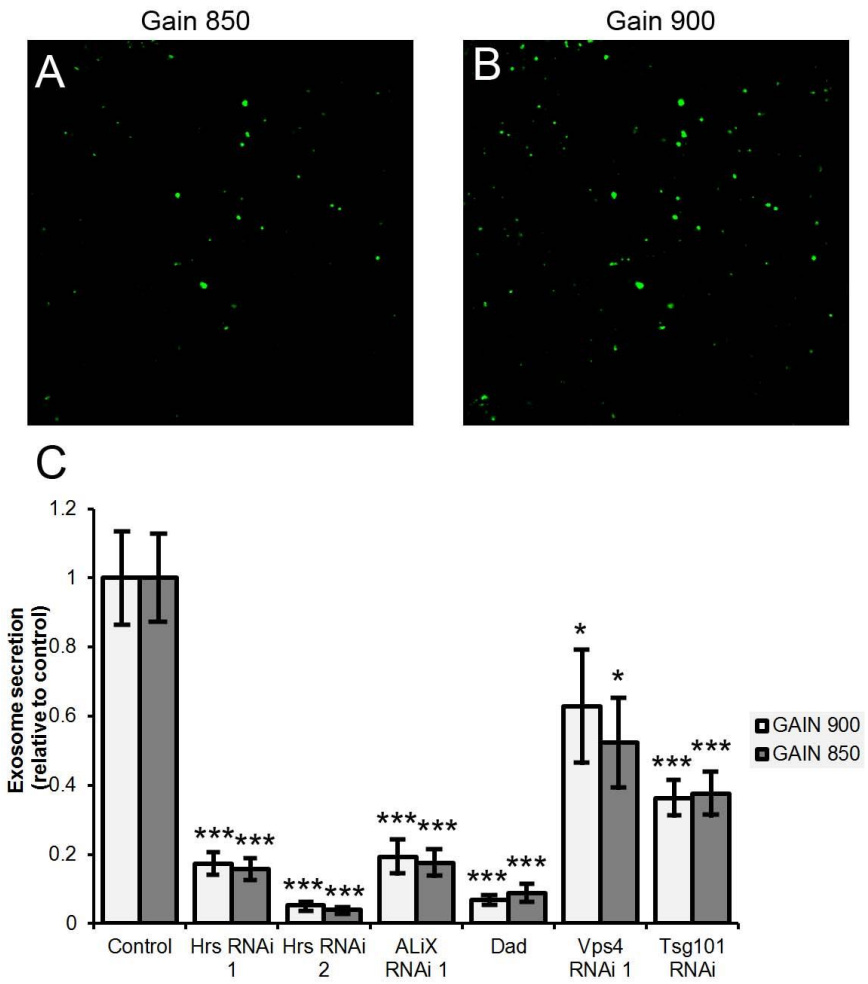


Figure 3.23. Knockdown of ESCRT components significantly reduces the number of CD63-GFP-positive puncta quantified, even when glands were imaged under two confocal gain settings. (**A** and **B**) confocal images of AG lumen of control *UAS-CD63-GFP, tub-Gal80^{ts}; dsx-Gal4* males, taken at two confocal settings: low gain (**A**) and high gain (**B**). Scale bars, 20µm. (**C**) *UAS-CD63-GFP, tub-Gal80^{ts}; dsx-Gal4* males were crossed to transgenes or *w^{1118}* for control. See **Fig. 3.22** for experimental and imaging protocol. Data were then obtained by imaging glands under two confocal 'gain' settings: 850 and 900. Data were then analysed using Image J particle analysis and calculated relative to control values for the two settings. Data were first analysed using the Shapiro Wilk test for normality; normal data were analysed using a Student's t-test, non-normal data analysed using Mann Whitney U test. * $p<0.05$, ***$P<0.001$; $n>10$. Data from one experiment with control and all 'test' glands carried out simultaneously. Error bars indicate ±SE.

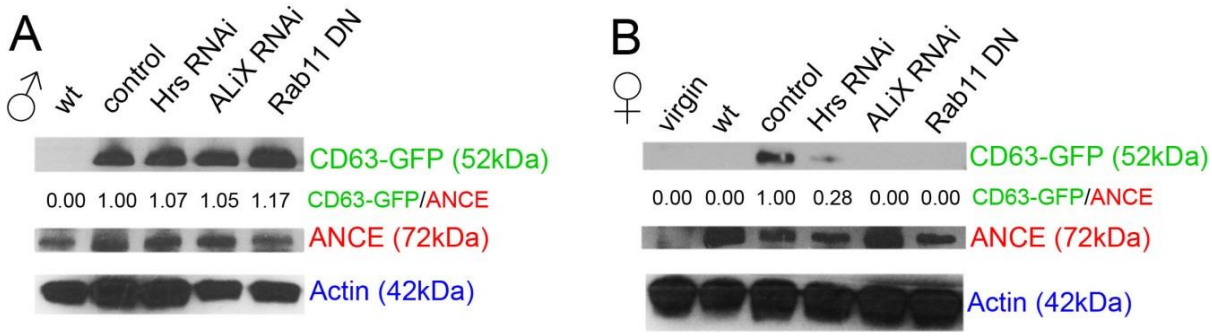


Figure 3.24. Western blot analysis of AGs and mated females following ESCRT knockdown. (**A**) Western analysis of AG protein extracts from 3-day-old w^{1118} (wild type) and flies expressing *tub-Gal80^{ts}, UAS-CD63-GFP; dsx-Gal4* without (control, crossed to w^{1118}) or with different transgenes. CD63-GFP fusion protein (expected Mw of 52kDa) recognised by an anti-GFP antibody. Blocking exosome secretion by *Hrs*-RNAi, *ALiX*-RNAi (or expression of Rab11-DN) does not reduce total CD63-GFP or ANCE produced in AGs and there is no change in the amount of CD63-GFP protein relative to the SC secretory product, ANCE (CD63-GFP/ANCE ratio). Importantly, no band is present at 52kDa for wild-type glands not expressing CD63-GFP, demonstrating specificity of the antibody. (**B**) Western analysis of protein extracts from reproductive tracts dissected from females immediately after mating to males of the same genotypes. Female tracts mated to Hrs-RNAi, ALiX-RNAi or Rab11-DN males contain less CD63-GFP, despite transferring normal amounts of ANCE. Note the reduced ANCE signal in females mated to control SC>CD63-GFP males compared to wild type males, indicating that CD63-GFP expression alone in SCs reduces the amount of ANCE secreted into the seminal fluid. Importantly, little ANCE is detected in virgin female tracts, indicating that seminal fluid is the major source of ANCE in mated tracts. Full-length CD63-GFP protein is observed in females. Western blots were obtained in collaboration with Sumeth Perera (Goberdhan lab, DPAG).

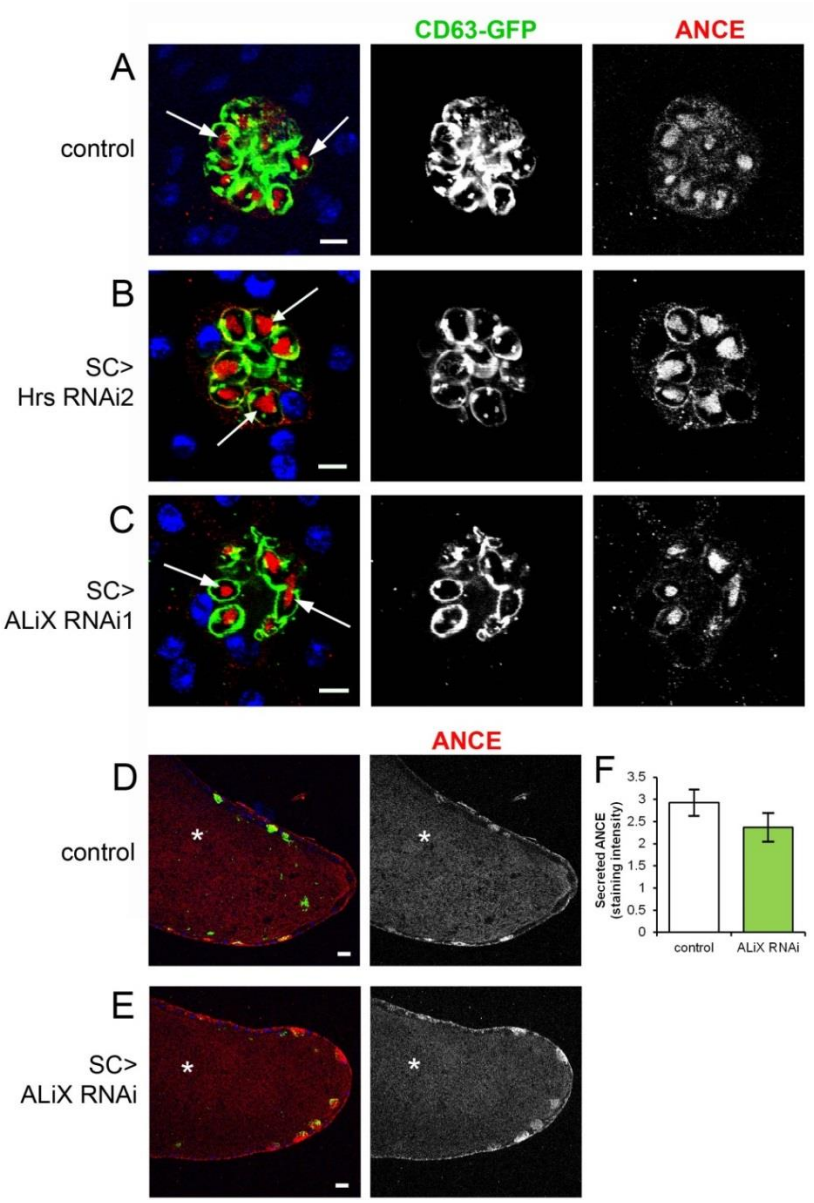


Figure 3.25. Blocking exosome biogenesis does not affect the localisation or secretion of ANCE. ANCE (immunostained in red) normally localises to the dense core of control SC secretory vacuoles (**A-C**, arrows) and is secreted into the gland lumen (**D**, *), but is not detectably expressed in main cells, does not show altered subcellular localisation in *ALiX*-RNAi- or *Hrs-RNAi*-expressing SCs (**B** and **C**, arrows). DAPI stains nuclei (blue). (**D-F**) There is no significant difference in the level of diffuse staining for ANCE in the AG lumen when *ALiX* is knocked down in SCs, as measured by the average signal intensities of 3 stacked confocal images from the lumen at 5µm intervals. Control and SC>*ALiX* RNAi males in **D-F** were as for lumen counts Fig. 3.22 and 3.23, while **A-C** were from virgin males. 'ns'=not significant; p=0.24, n>11 unpaired two-tailed Student's t-test, following the Shapiro-Wilk test. Error bars indicate ±SE; scale bars, 5µm (**A-C**), 20µm (**D** and **E**).

3.4 Discussion

In addition to the complex mixture of proteins, I have discovered that exosomes, secreted by SCs of the AG, are also present in the *Drosophila* seminal fluid. These exosomes can be specifically marked by CD63-GFP and require the ESCRT-0 component *Hrs*, the accessory factor *ALiX* and the ESCRT-I component *TSG101* to mediate their biogenesis inside the large multivesicular late endosomal compartments of SCs. CD63-GFP exosomes are transferred into the female reproductive tract during mating, suggesting that exosomes may play a role in reproductive signalling (see Chapter 4). Since exosomes can be loaded with a wide range of cellular components, our finding that they are secreted by SCs provides a potential explanation for the observation that accessory glands of several insects, including *Drosophila,* secrete intracellular proteins (Walker et al. 2006; Sirot et al. 2011).

In comparison to mammalian cells, *Drosophila* cell lines or epithelial tissues previously used to study exosome biology, the late endosomal and secretory compartments of SCs are huge, reaching 10-15µm in diameter. Preliminary EM analysis suggests that these unusually large compartments may also produce unusually large vesicles that have the potential to be resolved by light microscopy, allowing us to visualise exosome biogenesis for the first time *in vivo*. This makes the AG a powerful system to study the dynamics of exosome biogenesis and secretion in living tissue by confocal microscopy (see 3.4.2); however, it will be important to establish super-resolution live imaging techniques in order to image individual ILVs inside MVBLs with adequate resolution. Furthermore, the presence of large vacuoles containing the soluble secreted protease, ANCE permitted us to demonstrate the specificity of our genetic manipulations blocking exosome secretion, which in rarely tested in other systems.

3.4.1 SCs secrete CD63-GFP-postive exosomes into the seminal fluid

Most of our experiments were performed using the human CD63-GFP tetraspanin marker. Although *Drosophila* does not have a tetraspanin directly homologous to *CD63*, several studies have utilised this construct to mark fly exosomes as it is secreted extracellularly (Panakova et al. 2005; Gross et al. 2012), suggesting that it is loaded into exosomes. Despite several of the 40 + fly tetraspanins with significant homology with *CD63*, only Tsp42Ef and Tsp42Ee, and Tsp62F and Tsp42Ee have been identified on exosomes secreted by *Drosophila* S2 cells (Beckett et al. 2013) and Kc167 cells (Gross et al. 2012), respectively. Unfortunately, no tools were available for us to study the localisation of these two factors in the AG. It will be important to identify endogenous tetraspanins specifically loaded onto SC exosomes using GFP-fusion protein approaches.

In addition to the requirement of factors previously associated with exosome biogenesis and secretion, including ESCRT and ESCRT-associated proteins Hrs and ALiX as well as Rab11, for CD63-GFP secretion by SCs, there are several further lines of evidence supporting an exosomal identity of the CD63-positive puncta secreted from SCs and not shed from the plasma membrane. Firstly, we identified CD63-GFP puncta of a similar size to those secreted into the gland lumen inside large acidic compartments. Secondly, GFP-positive puncta were also observed in MVBLs of SCs expressing a cytoplasmic form of GFP. Thirdly, we found no evidence of a reduction in CD63-GFP at the plasma membrane following *Hrs* or *ALiX* knockdown, although we were unable to quantify this effectively.

Fourthly, we have used EM analysis of wild type AG and have identified particles of typical exosome morphology and size profile in both the AG lumen and mMVBLs of SCs. Furthermore, immuno-EM allowed us to demonstrate that several of these exosome-sized vesicles carry CD63-GFP. Interestingly, mMVBLS of CD63-GFP-expressing SCs contained an apparent increased number of ILVs, which were also more variable in size and morphology, suggesting that CD63-GFP expression itself may promote ILV biogenesis. This is consistent with previous reports

demonstrating a role for CD63 in exosome biogenesis; however, the molecular mechanism involved is still under debate as CD63 has been reported to regulate both ESCRT-dependent and –independent ILV biogenesis (Van Niel et al. 2011; Edgar et al. 2014). Our finding that CD63-GFP-positive ILVs are produced in an Hrs-dependent manner suggests that CD63-exosome biogenesis in SCs is ESCRT-dependent (see 3.4.3.1).

Lastly, inside the large acidic compartments we observed the invagination of the limiting membrane and apparent *de novo* formation of a CD63-GFP puncta by real-time live imaging. This seemed to be associated with a burst of acidity in this region of the compartment. We hypothesise this event represents the budding and scission of an ILV, with the associated increase in acidity around the newly formed vesicles from the action of the V_0 ATPase proton pump.

Importantly, as all acidic compartments marked by Lysotracker staining, in which we observed numerous CD63-GFP puncta (see Figs. 3.8 and 3.13), were also positive for late endosomal and lysosomal makers (see Figs. 3.11 and 3.12), this provides strong evidence for their origin inside multivesicular late endosomes.

Several of our localisation studies utilised the expression of fluorescently tagged proteins to mark specific compartments. It is possible that such over-expression could have phenotypic consequences on SC biology. We employed the UAS-Gal4 system to drive CD63-GFP expression. The strength of this genetic system at driving expression has been well documented (Mcguire et al. 2004). High level expression of an integral membrane protein such as CD63-GFP may have resulted in the artefactual growth of late endosomal compartments, which are being employed to degrade this exogenous factor. However, we still observed large (>2µm) acidic compartments inside wild-type SC not expression CD63-GFP, although we were unable to accurately quantify their number and size without a membrane marker and we also observed largest acidic compartments in both tub>Rab5-YFP and tub>Rab7-YFP SCs, suggesting that CD63-GFP

expression does not have a significant effect on SC endocytic trafficking, although we cannot exclude minor effects resulting in e.g. the growth of mMVBLs.

Exosomes typically fall between the size range of 40-150nm in diameter. Importantly, preliminary EM analysis of SCs suggested mMVBLs of wild type SCs contain ILVs approximately 40nm in diameter, whilst larger vesicles up to 200nm were observed inside MVBLs of SCs expressing CD63-GFP. Our ability to observe apparent membrane deformation leading to the budding and scission of an ILV suggests SC mMVBLs may give rise to CD63-GFP-positive ILVs of unusually large size. Several recent studies have demonstrated that the size profile of exosomes secreted is dependent upon the mechanisms utilised for their biogenesis and the availability of specific regulators; including: ESCRTs (Baietti et al. 2012; Colombo et al. 2013; Edgar et al. 2014); ALiX (Colombo et al. 2013); CD63 (Edgar et al. 2014); and Vps4 and Did2 (Nickerson et al. 2010). Therefore the size of vesicles formed is likely to depend upon the activity and availability of a range of factors, which may be cell-type specific as well as regulated by upstream signals.

3.4.2 The SC as a novel *in vivo* model to study exosome biogenesis in live cells

Exosome biogenesis, secretion and uptake have been previously reported in *Drosophila* (Section 3.1.1) as well as mammalian cell lines (Sections 1.3.3 – 1.3.7). However, the small size of exosomes and of MVBs, which usually fall within a range of a few hundred nanometres in diameter, have made these processes difficult to analyse, particularly *in vivo,* by light microscopy. Previous studies of ILV biogenesis have utilised *in vitro* reconstitution systems including liposomes and GUVs (Matsuo et al. 2004; Falguières et al. 2008), or EM analysis of late endosomal compartments of either yeast or mammalian cells lines (Baietti et al. 2012). Both of these systems carry inherent limitations: the former is likely to give rise to artefactual results due to the use of non-physiological conditions; the latter cannot provide information on the dynamic events. Furthermore, other studies have employed expression of an activated form of Rab5 (Stenmark 1994; Rink et al. 2005; Hirota et al. 2007; Wegener et al. 2010; Baietti et al. 2012; Dores et al.

2012; Schroeder et al. 2012; Ghossoub et al. 2014) in cell culture to enlarge the endolysosomal compartments. However, our data demonstrate that overexpressing even wild type Rab proteins can modulate normal trafficking events, as we observed when expressing Rab11-YFP at low levels in SCs.

SC late endosomal compartments reach 10-20µm in adult flies. This remarkably large size in SCs provides new opportunities to study exosome biogenesis and secretion in wild-type living cells in a manner unparalleled *in vivo;* to our knowledge, this is the first time ILV biogenesis has been visualised live *in vivo*. Therefore, our new SC model allows us to re-investigate previously reported regulators of exosome biogenesis and identify functional differences in trafficking phenotypes, as we have seen for *Hrs* and *ALiX* knockdown.

In conclusion, SCs provide a novel *in vivo* model to study the regulation of exosome secretion by live imaging that can be utilised to further unpick the regulation of exosome biogenesis.

3.4.3 SCs produce CD63-GFP exosomes in a ESCRT-dependent manner

SC exosome secretion requires the ESCRT-0 component Hrs; the ESCRT accessory factor, ALiX; and the ESCRT-I component, TSG101, strongly indicating SCs secrete CD63-GFP exosomes in an ESCRT-dependent manner. Several studies have begun to address whether previously identified regulators of exosome biogenesis in mammalian cell culture experiments have conserved roles in *Drosophila* (Gross et al. 2012). Although initial S2 cell culture work indicated TSG101 and Hrs are not required for Evi-exosome secretion (Beckett et al. 2013), our findings have demonstrated that Hrs, TSG101 and ALiX all have conserved roles in CD63-exosome biogenesis in *Drosophila in vivo*. However, we cannot exclude the possibility that SC exosomes marked by CD63-GFP are regulated by distinct mechanisms to Evi-exosomes.

There have been several conflicting reports regarding the regulation of exosome secretion by ALiX, TSG101, Vps4 and Hrs in mammalian systems and have already suggested multiple exosome

subtypes exist and may be regulated differently, e.g., different roles for ALiX (Baietti et al., 2012 *versus* Colombo et al., 2013), Hrs (Edgar et al., 2014) and Evi (Beckett et al., 2013). It is likely that additional populations of exosomes, not marked by CD63-GFP, are also secreted in SCs, perhaps made by ESCRT-independent manner. Analysing the localisation of candidate ESCRT-independent ILV markers, such as flotillin (Baietti et al. 2012), caveolin (Llorente et al. 2004), PMEL (Colombo et al. 2013) or LBPA (Matsuo et al. 2004) will be important in identifying novel exosome populations in the AG. If identified, the AG should offer an ideal system to study their differential regulation.

A role for ALiX in the positive regulation of (CD63) exosome biogenesis has only recently been demonstrated for the formation of exosomes that are also dependent upon the HSPG syndecan and its cytoplasmic adaptor syntenin (Baietti et al. 2012; Ghossoub et al. 2014). The authors speculate that the ability of HSPGs to bind extracellular signalling molecules including Wnts, BMPs and FGFs allows it to function in the sorting of these cargos onto exosomes, and ALiX links these factors to downstream biogenesis machinery. Our novel in vivo system lends itself to the exciting prospect of studying the role of extracellular matrix in the regulation of exosome biogenesis in living tissue.

We were unable to obtain reproducible effects on CD63-GFP exosome secretion by knockdown of Vps4, which may explain conflicting reports of its role in exosome secretion to date (Falguières et al. 2008; Colombo et al. 2013) versus (Baietti et al. 2012; Beckett et al. 2013). Moreover, the distinct cell phenotype *Vps4*-RNAi SCs suggests that unlike Hrs, ALiX and TSG101, Vps4 may function at several steps in the endocytic and/or secretory pathway.

Importantly, our ability to collect AG secretions in females and analyse their protein content has circumvented the issues associated with our methods quantifying secreted GFP-fluorescent puncta, which are theoretically smaller than the resolution of such microscopes, by confocal light microscopy. Our western blot analysis of male and mated female reproductive tracts demonstrated that although equal amounts of CD63-GFP were synthesised, significantly less

CD63-GFP was transferred into the female reproductive tract by *ALiX* and *Hrs* knockdown males than control males, despite equal amounts of soluble protein transfer (ANCE). This provides strong evidence that the observed reduction of lumenal CD63-GFP puncta does not result from e.g. changes in exosome size or propensity to aggregate, thus further supporting our conclusion that fewer particles are secreted in these genetic backgrounds.

3.4.4 Mechanism of exosome secretion

Previous studies in mammalian cells lines have demonstrated a role for Rab11, Rab35 and Rab27 in the regulation of exosome secretion (Savina et al. 2002; Savina et al. 2005; Hsu et al. 2010; Ostrowski et al. 2010). Previous publications, this study (Fig. 3.24), as well as work by another DPhil student (Siamak Redhai) in the lab have demonstrated these roles in the regulation of CD63-GFP exosome secretion are also conserved in *Drosophila* (Gross et al. 2012; Beckett et al. 2013). Rab GTPases are likely to regulate the trafficking events upstream and/or downstream of ILV biogenesis, feeding mMVBLs with membrane in order to make ILVs or regulating the trafficking of mMVBLs to the plasma membrane. Our finding that Rab11-YFP localises to SV membranes supports the former; however, we cannot exclude the latter possibility as we were unable to confirm whether Rab11 also localised to mMVBLs due to phenotypic effects of Rab11-YFP expression.

Interestingly, Evi-exosome secretion has been shown to be independent of Rab35 and Rab27 (Beckett et al. 2013), further supporting our previous conclusion that exosomes carrying CD63-GFP and Evi are regulated by distinct mechanisms in *Drosophila*. Consistent with previous reports in the wing disc (Gross et al. 2012), additional work in the lab has also demonstrated that Evi is not required for CD63-GFP exosome secretion by SCs (Siamak Redhai).

3.4.5 SC compartment dynamics

Our study has already revealed a surprisingly dynamic interaction between the secretory and endolysosomal systems in SCs. Communication between these compartments using vesicular transport and tubulation processes has been reported in other cell types in flies and mammals (Savina et al. 2005; Minogue et al. 2006; Burgess et al. 2012). The identification of PI4KII-GFP specifically at the limiting membrane of mMVBLs mirrors its localisation in secretory cells in the *Drosophila* larval salivary gland (Burgess et al. 2012). However, unlike salivary cells where PI4KII-GFP-positive late endosomal tubules connect with the Golgi apparatus, in SCs these tubules contact neighbouring mMVBLs, suggesting these protrusions may instead permit trafficking between late endosomal compartments. It will be interesting to investigate whether PI4K activity in SCs is required for mMVBL and/or SV maturation.

Our data suggests that fusion between mMVBLs and SVs may play a role in establishing distinct these compartments within SCs. These observations may help to explain why a molecule like Rab11, which is often associated with recycling secretory pathways, can play such an important role in exosome secretion (Koles et al. 2012; Beckett et al. 2013).

4. Investigating the reproductive functions of SC exosomes

4.1 Introduction

4.1.1 Exosomes in mammalian reproduction

During mammalian copulation sperm produced in the testes, matured in the epididymis and stored in the ampulla are mixed with secretions of additional organs of the male reproductive tract, including those of accessory glands such as the prostate. In addition to various proteins, the prostate also secretes membrane-bound vesicles, known as prostasomes (reviewed in (Aalberts et al. 2014)). The identification of MVB-like compartments, which contained vesicles of similar morphology to prostasomes isolated from semen, inside prostate epithelial cells led to the current identification of these vesicles as exosomes (Ronquist et al. 1985). Prostasomes are of typical exosome size and morphology and are also enriched in classical exosomal protein cargos, such as CD9 (Aalberts et al. 2012), as well as prostate-specific membrane proteins including membrane-associate prostate-specific antigen (PSMA) (Ronquist et al. 2012). Prostasomes also harbour a specific and unusual lipid composition. Prostasomal membranes are primarily composed of the modified glycophospholipids and sphingomyelin (as opposed to phosphatidyl-serine and –choline) and are also highly enriched in cholesterol and ceramide derivatives (Arvidson et al. 1989; Brouwers et al. 2013). Recent studies have identified two distinct prostasome populations of differing size (56nm vs. 100nm) and composition (+/- Annexin1) (Aalberts et al. 2012).

It is important to emphasize that, to date, it has not yet been definitely shown that the MVB-like compartments of prostate epithelial cells are indeed the only origin of secreted ‘prostasomes’, i.e. vesicles isolated from seminal fluid. It remains possible that the vesicles isolated in many published studies are a mixed population of EVs, originating from both the MVB as well as the

plasma membrane, or that the vesicles originate from other reproductive gland epithelial cells in addition to the prostate. For example, the epididymis has been shown to shed MVs into the seminal fluid, thus effectively 'contaminating' the semen from which prostasomes are isolated (Section 7.1.3). Importantly, several studies have begun to address this issue by isolating prostasomes from the semen of vasectomized men (Aalberts et al. 2012; Brouwers et al. 2013).

The interaction between prostasomes and sperm has been studied *in vitro* under a range of conditions (Section 1.4). This interaction has been shown to be pH-dependent; the initial binding/docking of prostasomes to sperm occurs at a moderately high pH, reflective of that inside the uterus (pH>7.5) (Aalberts et al. 2013). Conversely, fusion has been demonstrated to occur at a lower pH (pH<7) (Arienti et al. 1997; Palmerini et al. 1999). Such findings have led to the model whereby prostasomes first bind sperm in the uterus but sperm fusion is delayed until a permissive environment is reached immediately prior to oocyte fusion (Aalberts et al. 2013). Interestingly, prostasomes fuse specifically to the head/neck region of sperm (Park et al. 2011; Aalberts et al. 2013) in a regulated manner; specificity is lost when prostasomes fuse with dead sperm (Aalberts et al. 2013).

In vitro studies have implicated prostasomes in both the positive and negative regulation of several reproductive processes, including capacitation and the acrosome reaction. Capacitation broadly describes the process by which sperm gain the ability to fertilise an egg, prior to the acrosome reaction (Baker et al. 2012). Biochemically, capacitation involves the removal of cholesterol from the sperm membrane (Visconti et al. 1999), as well as the acquisition of hypermobility. Cholesterol enrichment in prostasomal membrane has led to a hypothesised inhibitory role for these structures in capacitation (Pons-Rejraji et al. 2011), through the transfer of cholesterol to the sperm plasma membrane. On the other hand, several studies have demonstrated a role for prostasomes in sperm motility (Fabiani et al. 1994; Park et al. 2011). Sperm motility is dependent upon Ca^{2+} influx, which is sustained by the activity of the ryanodine

receptor and CatSper channels (Qi et al. 2007), the opening of which is regulated by progesterone. Interestingly, prostasomes harbour both Ca^{2+} signalling tools including the ryanodine receptor, as well as the progesterone receptor (Park et al. 2011). Prostasome-dependent delivery of these factors has been suggested to be required for functional sperm motility (Park et al. 2011). As the acrosome reaction is also triggered by Ca^{2+} influx, prostasomes have also been implicated in its initiation (Palmerini et al. 1999; Aalberts et al. 2014).

4.1.2 Aims and objectives

As I have identified that SC secrete exosomes into the fluid stored in the AG (Chapter 3), I set out to investigate whether *Drosophila* reproductive exosomes share functional properties with prostasomes by addressing the following:

1. Identify cellular targets of exosomes transferred into the female reproductive tract during mating.
2. Characterise the consequence(s) of blocking SC exosomes secretion on reproductive physiology.

4.2 Materials and Methods

4.2.1 Reproductive physiology experiments

For analysis of the physiological role of exosomes in reproduction, multiple-mating experiments were carried out as previously reported (Leiblich et al. 2012). Newly eclosed virgin males (*esg^{ts}F/O> ALiX*-RNAi 1 or *esg^{ts}F/O* crossed to *w^{1118}*) were shifted to 28.5°C for 3 days to induce transgene expression. Individual males were then added to five 2- to 10-day-old virgin *w^{1118}* females (for a specific group of control and test flies, females were of identical age) overnight at

28.5°C. Previous work in the lab suggested that approximately 80-90% of females will mate with males during this period. The next morning, these females were replaced with three 2- to 5-day-old virgin w^{1118} females for 3 hours, and watched to score timing of mating events, after which the females were separated and incubated at 25°C. Females were transferred to separate, fresh vials on three consecutive days; egg counts and progeny counts were recorded for each vial, following their incubation at 25˚C. Each female was then introduced to a dominantly marked (*CyO Roi*) male and left for 3 hours and then separated. Males were then discarded and females were separated into individual vials. Remating events were scored by the presence of *CyO Roi* progeny following incubation of these vials at 25˚C. This protocol had been optimised such that a very small proportion of females previously mated to control males remated, whilst a significantly greater proportion of females mated to males with reduced BMP signalling in SCs remated.

4.2.2 Single-pair CD63-GFP transfer experiments

For single mating experiments to analyse exosome targets in the female reproductive tract, w^{1118} or w^{1118}; *actin-Gal4; UAS-CD8-RFP* virgin females (2- to 10-days-old) were incubated with individual *spi-Gal4; UAS-CD63-GFP, +/- protamine-RFP*, or control w^{1118} 3-day-old virgin males. Matings were observed and females were dissected at different time points after mating. Females were dissected in ice cold 4% paraformaldehyde in 1xPBS, fixed for a minimum of 15 minutes and then washed in PBS for 30 minutes at 22˚C. Dissected reproductive tracts were mounted in Vectashield with DAPI (Vector Laboratories). Females mated to control w^{1118} and SC>CD63-GFP males were imaged using identical confocal settings.

When dissected at 7 minutes after the start of mating, 2/8 female reproductive tracts did not contain CD63-GFP exosomes, suggesting that, despite sperm transfer from the testes, the contents of the AG had not yet been transferred in these individuals. This is consistent with previous reports (Lung et al. 2001; Ravi Ram et al. 2005).

4.2.3 Immuno-staining of female reproductive tract

Females were dissected 20 minutes after the start of mating in ice cold 1xPBS and then fixed in 4% paraformaldehyde in PBS at 22˚C. Tracts were washed for 6 x 5 minutes in PBST-0.3% (PBS, 0.3% Triton X-100) prior to incubation in 100µl of chitinase solution (Sigma No. C6137 (*Streptomyces Griseus*); 6U per ml in PBST-0.3%) for 2 hours at 22˚C (Lung et al. 1999). Tracts were washed in PBST-0.3% for 6 X 5 minutes and then refixed for 20 minutes at 22˚C. Samples were washed again in PBST-0.3% (3 x 5 minutes) and then blocked for 2 hours with gentle shaking at room temperature in 100µl of PBSTG-fem (PBST, 0.5% Triton X-100, 3% goat serum, 0.1% BSA). All washes were carried out at room temperature (22˚C). Female tracts were then stained as for AGs (Section 2.3.2), but with antibodies diluted in PBSTG-fem.

4.3 Results

4.3.1 CD63-GFP is transferred to neighbouring MCs

Previous work in flies has suggested a role for CD63-GFP exosomes in cell-cell signalling during epithelial tissue patterning (Section 3.1.1). In this developmental context, exosomes are secreted by epithelial cells of a tissue, such as the imaginal wing disc, diffuse across the epithelial plane and are endocytosed by target cells several cell diameters away (Panakova et al. 2005; Gross et al. 2012). A small number of CD63-GFP puncta were observed inside MCs adjacent to SCs when glands were imaged using settings typically utilised throughout this study (**Fig. 4.2A**). However, increasing the gain to saturate the GFP channel revealed many more CD63-GFP puncta inside MCs throughout the distal tip of the gland (**Fig. 4.2B**). Nevertheless, CD63-GFP puncta were only observed in a very small proportion of MCs (<1%) in the proximal end of the gland (furthest from SCs; **Fig. 4.2A'**), even at high gain settings (<10%; **Fig. 4.2B'**). Therefore, internalisation of CD63-GFP is almost exclusively limited to MCs in direct contact with SCs.

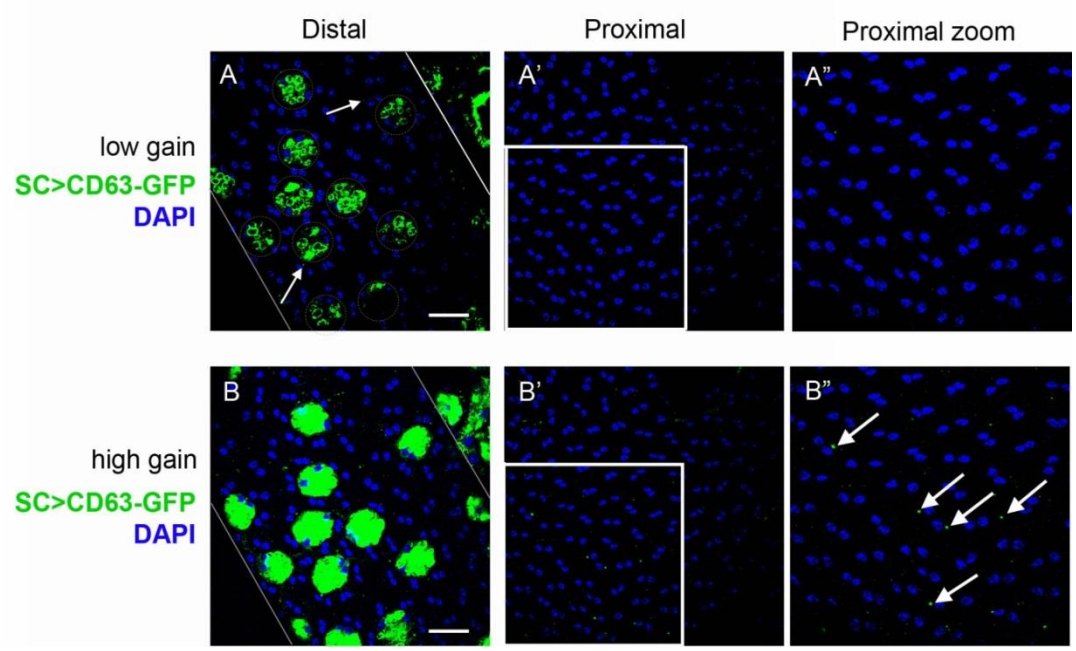


Figure 4.1. CD63-GFP exosomes are transferred to neighbouring MCs. Representative **s**urface confocal images, obtained under two confocal gain settings, of the distal (**A** and **B**) and proximal (**A'**, **A"**, **B'** and **B"**) (relative to the ejactulatory duct) AG epithelium of a 3-day-old *spi-Gal4; UAS-CD63-GFP* virgin male, stained with DAPI (nuclei; blue). **A"** and **B"** show enlargments of the regions outlined in **A'** and **B'**, respectively. At a low gain (**A**, **A'** and **A"**) a small proportion of main cells amongst SCs at the distal tip contain GFP fluorescence (**A**), but CD63-GFP rarely seen in MCs that are many cell diameters from the exosome-secreting SCs at the proximal end of the gland (**A'** and **A"**). At a higher gain setting, CD63-GFP is seen in the majority of MCs adjacent to SCs at the distal tip (**B**), whilst at the proximal end of the gland the minority of MCs contain CD63-GFP puncta (**B'** and **B"**, arrows). Scale bars, 20µm.

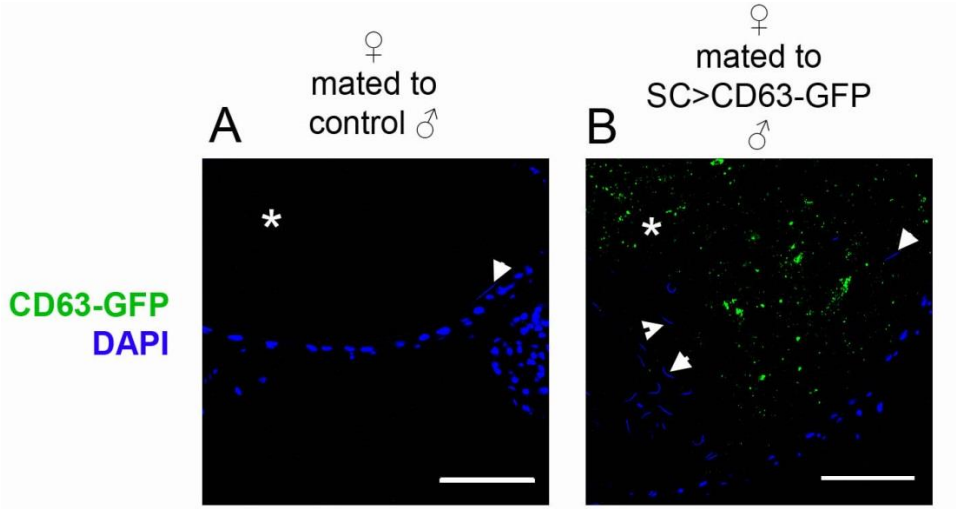


Figure 4.2. CD63-GFP exosomes are transferred into the female reproductive tract during mating. CD63-GFP exosomes accumulate in the uterus of females mated to *spi-Gal4; UAS-CD63-GFP* males (**B**), these are not visible in the tracts of females mated to control w^{1118} males (**A**). Images obtained under identical confocal image capture settings. Images show cross sections through the female uterus dissected immediately after mating, revealing the uterus lumen (*) containing sperm (heads marked with DAPI, arrowheads) and surrounding epithelium (bottom of images; nuclei stained with DAPI, blue). Scale bars 50µm. This work was carried out in collaboration with Rachel Patel (FHS project, 2013).

4.3.2 Exosomes fuse with sperm in the female

Given their secretion into the seminal fluid and transfer to the female reproductive tract during mating (**Fig. 3.28**), we hypothesised that seminal fluid exosomes may play an important role in reproductive signalling in *Drosophila*. To investigate whether AG exosomes interact with their target cells after transfer to the female reproductive tract, SC>CD63-GFP males were mated to females and the localisation of CD63-GFP within the female tract was analysed. Indeed, CD63-GFP exosomes transferred could be observed by confocal microscopy in the uterus or oviduct immediately after mating (**Fig. 4.2**) and for at least 1 hour after a mating event terminates (data not shown). The majority of CD63-GFP localised to the mating plug (7/7) and the uterus (7/7), and was also often observed in the oviduct (5/7) (Rachel Patel, FHS project 2013; **Fig. 4.7B**). CD63-GFP was not observed in either of the sperm storage organs (0/7) for at least an hour after the start of mating (Rachel Patel, FHS 2013).

Several seminal peptides target specific regions of the female reproductive tract and/or sperm after mating (Peng et al. 2005; Ravi Ram et al. 2005). Isolated human prostasomes fuse with the sperm midpiece *in vitro*, delivering Ca^{2+} signalling molecules implicated in sperm motility (Fabiani et al. 1994; Park et al. 2011). Consistent with this observation, we detected colocalisation of CD63-GFP and sperm heads, marked by protamine-RFP, in the female reproductive tract (**Fig. 4.3C-D**). Analysis of confocal Z series images revealed a narrow ring of GFP surrounding the sperm head (**Fig. 4.3D**), as might be expected after exosome-sperm fusion as the CD63-GFP diffuses laterally throughout the plasma membrane of spermatozoon. These events were most commonly observed at 20 minutes after the start of mating (Rachel Patel FHS project 2013; **Fig. 4.3E**; 88% {14/16} mated females) and were found in parts of the anterior portion of the female reproductive tract where sperm and exosomes accumulated, either in the anterior uterus (9/16) or the oviduct (5/16).

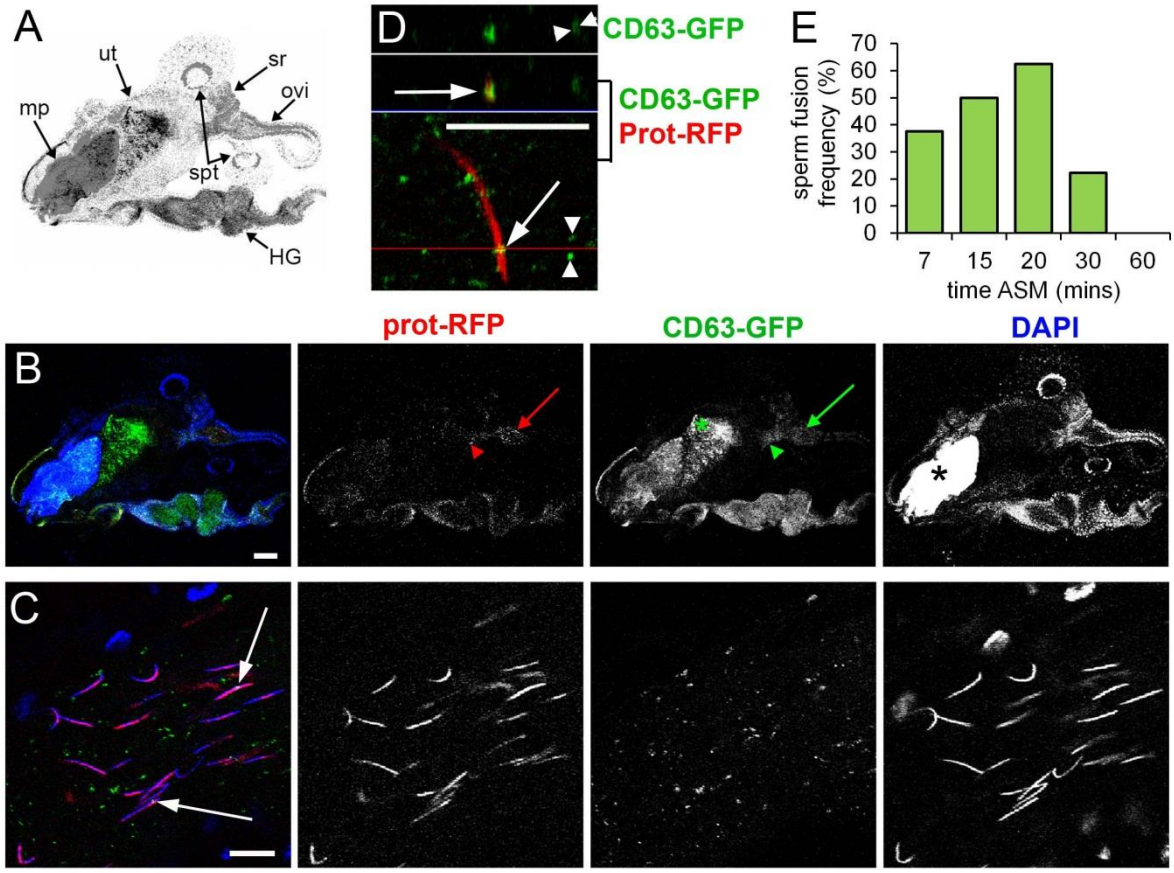


Figure 4.3. AG exosomes interact with sperm in females. (**A**) Schematic of female reproductive tract adapted from (**D**) showing the mating plug (mp), uterus (ut), oviduct (ovi), sperm storage organs spermathecae (spt) and seminal receptacle (sr), as well as the hindgut (HG). (**B-D**) Female reproductive tract 20 minutes after mating to a *protamine-RFP; spi-Gal4, UAS-CD63-GFP* male. (**B**) Protamine-RFP, which marks sperm heads (red), accumulates in the anterior uterus (red arrowhead) and oviduct (red arrow). The majority of CD63-GFP-positive exosomes localise to the posterior uterus (green star), but can also be seen in the anterior uterus (green arrowhead) and oviduct (green arrow). Autofluorescent mating plug (*). (**C**) CD63-GFP-positive exosomes co-localise with sperm heads marked by protamine-RFP and also stained with DAPI (red and blue, arrows). (**D**) Orthogonal view of a Z stack through CD63-GFP-positive membranes fused to protamine-RFP sperm head. CD63-GFP forms a near-complete ring around the sperm head (arrow). Note multiple pairs of parallel GFP-positive lines (arrowheads), presumably produced by sperm tail fusion. These are also seen in Fig. 4.4 (arrowheads), a maximum 3D projection image of a Z stack from female anterior uterus and oviduct where the epithelium is marked by *actin-Gal4; UAS-CD8-RFP*. (**E**) Female reproductive tracts were dissected and fixed at specific times after the start of mating to *spi-Gal4; UAS-CD63-GFP* males. The frequency of exosome-sperm interaction events (n=8 for each time point after the start of mating [ASM]) within the female reproductive

tract was analysed. These proportions are probably underestimates as they do not include frequent putative fusion events with the long sperm tail. Scale bars, (**B**) 200µm, (**C** and **D**) 5µm. This work was carried out in collaboration with Rachel Patel (FHS project, 2013).

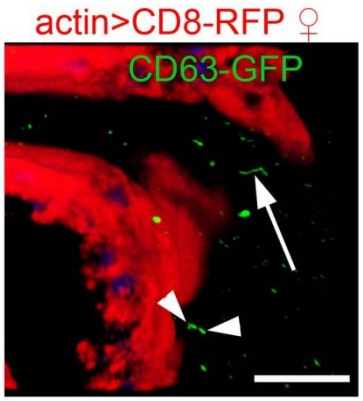


Figure 4.4. Exosomes may interact with sperm tails in the female reproductive tract. Reproductive tract of a*ctin-Gal4; UAS-CD8-RFP* female 20 minutes after mating to *spi-Gal4; UAS-CD63-GFP* male. Image shows region of female uterus (left) opening into the oviduct (right); CD8-RFP (red) localises to the apical plasma membrane as well as internal compartments in female epithelial cells. Strands of GFP (green, arrow) as well as parallel CD63-GFP puncta can be seen in the uterus/oviduct of mated females (arrowheads), potentially marking the sperm tail plasma membrane. DAPI marks sperm and cell nuclei. Scale bar 20µm.

Due to the huge number of sperm cells transferred to females we were unable to quantify the proportion of sperm that interact with CD63-GFP exosomes in an individual mating event. Furthermore, we believe detection of CD63-GFP fluorescence at the sperm membrane would only be a transient event as it is likely to rapidly diffuse and dissipate over the sperm surface after fusion, so the GFP fluorescence signal would quickly become undetectable; this may also explain our inability to detect CD63-GFP in the sperm storage organs. Therefore, the observed fusion frequency in each female is almost certainly an underestimate. In addition, it also seems likely that exosomes fuse with the long tails of *Drosophila*, which are many times longer than the length of the head marked by DAPI or Protamine-RFP. In support of this, GFP fluorescence was frequently observed as either two short parallel lines or an extended irregular line in the reproductive tract lumen (100%, n=8; **Fig. 4.3D and 4.4**), as would be expected following membrane fusion.

4.3.3 Exosomes interact with the epithelial surface of the female reproductive tract

Interestingly, CD63-GFP exosomes accumulated at the surface of the reproductive tract either in the uterus or oviduct in 40% of females (**Fig. 4.5**; n=34), suggesting that SC exosomes also interact with female epithelial cells. In some cases, aggregated exosomes made contact with the epithelium in concentrated patches (**Fig. 4.5C**), while in others, dispersed exosomes aligned along the epithelial surface (**Fig. 4.5D**). Aggregations of exosomes may reflect docking to a female target cell, either prior to internalisation via endocytosis, which has been reported in other systems (Morelli et al. 2004), or possibly as part of a cell surface signalling mechanism.

To confirm that the CD63-GFP observed along the epithelial surface was still in structures containing CD63 (there are numerous proteases present in the seminal fluid that might degrade exosomes), we stained female reproductive tracts with an anti-CD63 antibody. GFP fluorescence colocalised with this antibody stain (**Fig. 4.5D**), consistent with our previous western blot analysis of mated females suggesting CD63-GFP remains intact even after transfer to the female tract (**Fig.**

3.24). CD63-GFP was not observed inside female epithelial cells suggesting that exosomes are not endocytosed. In summary, almost all SC-derived exosomes remain within the AG lumen in virgin males, but fuse to sperm and interact with female epithelial cells after mating.

4.3.4 'Exosomeless' males fail to induce the full post-mating response

In contrast to virgin females, recently mated *Drosophila* females will reject a courting male by exhibiting a range of behavioural responses (Wolfner 1997) (Section 1.4.2). Previous work in the host lab demonstrated that BMP signalling in SCs is required for the full induction of this female PMR (Leiblich et al. 2012); these experiments indicated that BMP signalling in SCs is required for the long term maintenance of the PMR, as females, mated to males with reduced SC BMP signalling, remate sooner than controls. We hypothesised that SC-derived exosomes might be involved in this function. To test this we utilised the multiple mating protocol previously established to assay the effects of blocking exosome production (Leiblich et al. 2012) on egg laying, fecundity and post-mating behaviours using males exhibiting SC-specific knockdown of *ALiX* by RNAi. This assay involves multiply mating males to five females prior to mating them to an additional three, which are assayed for remating after three days (Section 4.2.1).

Importantly, blocking exosome production using SC-specific expression of *ALiX*-RNAi, as well as dominant negative *Rab11* (Siamak Redhai; Corrigan et al. 2014), reduced the ability of males to prevent females from remating (Fig. **4.6A**), suggesting that SC exosome secretion is required to maintain mating rejection behaviours in females.

Blocking BMP signalling in SCs did not have any significant effects on the male's mating behaviour, or egg laying and fecundity of the females (Leiblich et al. 2012). Similarly, *ALiX* knockdown had no effect on the total number of eggs laid or number of progeny that eclosed (Fig. **4.7**), and SC>*ALiX*-RNAi males themselves did not exhibit altered mating behaviours (**Fig. 4.6B-D**), suggesting the exosome secretion is not required for normal male fecundity.

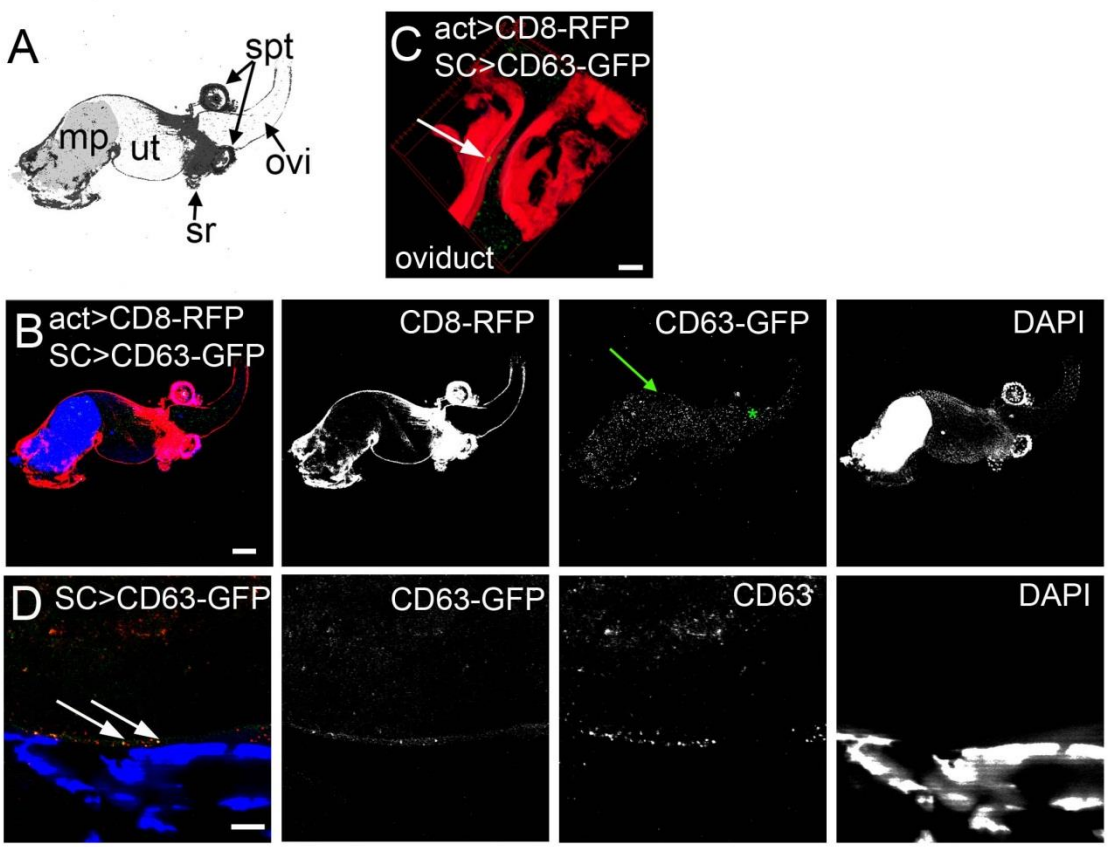


Figure 4.5. Transferred exosomes interact with epithelial cells of the female uterus. (**A**) Schematic of female reproductive tract shown in **B**: mp, posterior mating plug (autofluorescent); ut, uterus; sr, seminal receptacle; spt, spermathecae; ovi, oviduct. (**B** and **C**) *actin-Gal4; UAS-CD8-RFP* or (**D**) wild-type w^{1118} females mated to 3-day-old *spi-Gal4; UAS-CD63-GFP* males, dissected 20 minutes after mating. Ubiquitously expressed CD8-RFP localised to the apical surface as well as internal compartments of female epithelial cells lining the female reproductive tract. CD63-GFP exosomes in the uterus (**B**, green arrow) and oviduct (**B**, green star; **C**, arrow) accumulate at the apical cell surface of female reproductive tract epithelial cells, either marked with CD8-RFP (C, arrow) or unmarked (**D**, arrows). In **D**, reproductive tract is stained with an antibody against human CD63 (red) to confirm GFP fluorescence marks CD63 location. DAPI stains nuclei (blue). Image in (**B**) shows a confocal plane selected to show clear outline of reproductive tract marked with CD8-RFP. Specific spermathecal cells exhibit weak autofluorescence into the green channel. Scale bars, (**B**) 200µm and (**C**) 20µm, (**D**) 5µm.

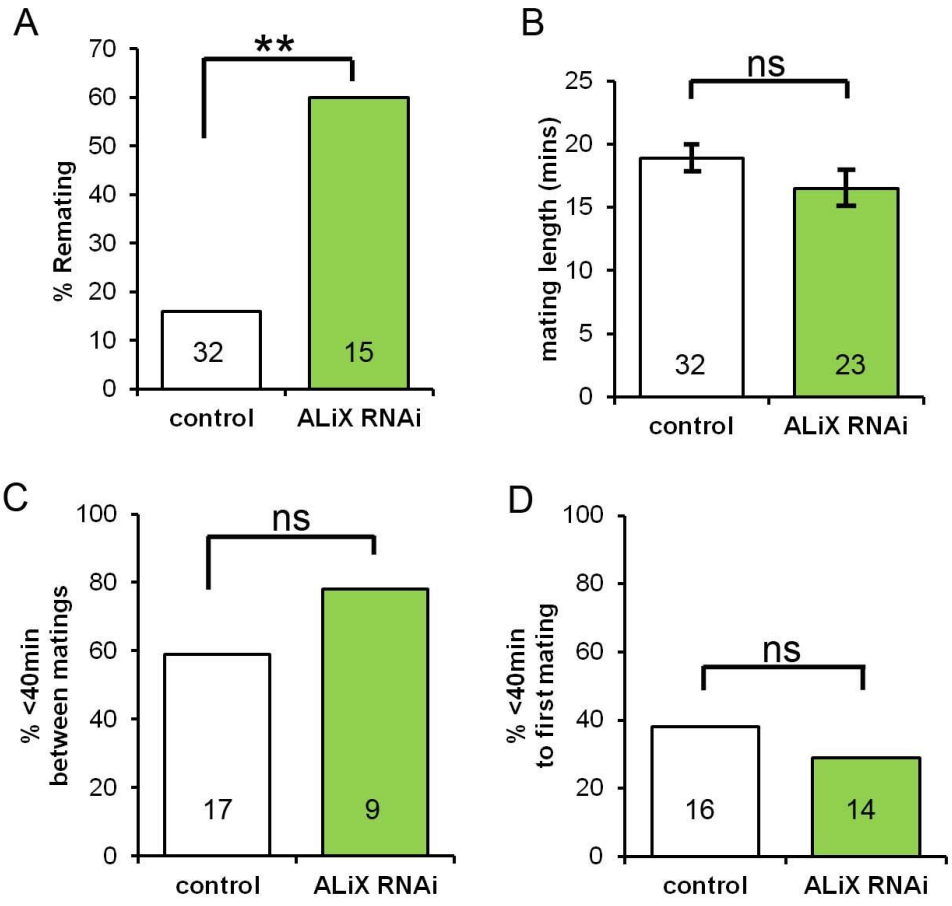


Figure 4.6. Exosomeless males fail to induce specific aspects of the female post-mating response. (**A**) A significantly greater proportion of w^{1118} females mated to $esg^{ts}F/O$>*ALiX-RNAi* males remated after three days than females originally mated to control $esg^{ts}F/O$ males. w^{1118} females were incubated with two dominantly marked (*PTEN/*CyO^{ROI}) males for three hours three days after mating to either the $esg^{ts}F/O$>*ALiX-RNAi* or $esg^{ts}F/O$ males. Their progeny were scored for successful remating events using the dominantly marked balancer, *CyO Roi*. (**B-D**) $esg^{ts}F/O$>*ALiX-RNAi* males exhibit no behavioural differences when mating to females. The length of copulation is not significantly different from control (**B**), neither is the delay between matings (**C**) or the time to start mating (**D**). Number in bars indicates total number of female flies assayed; each male was mated to three females over a three hour period. These females were then separated. Only females which successfully mated (bore progeny at any point over the three day period assayed) were included in quantifications. Error bars indicate ± SE; **P<0.01; 'ns' = no significant difference; data were analysed by Student's t-test following the Shapiro Wilk test for normality (**B**), or Fisher's Exact test (**A, C-D**).

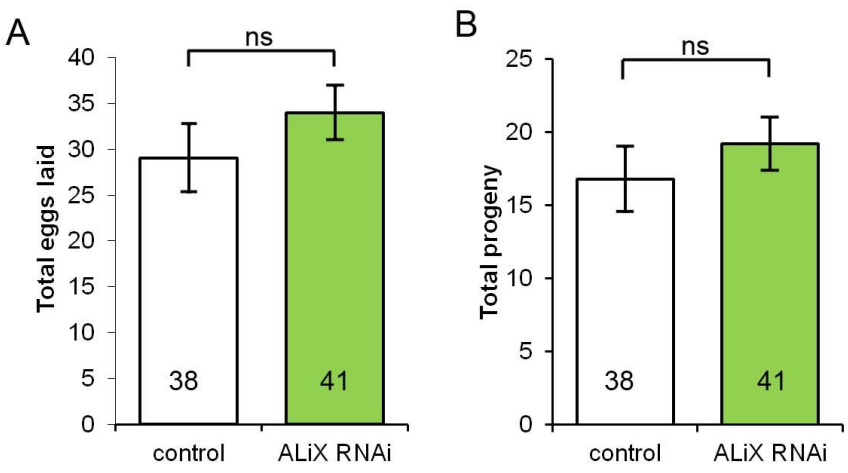


Figure 4.7. 'Exosomeless' males induce equal levels of egg laying and sire equal numbers of progeny compared to control males. Females mated to multiply-mated *esg^{ts}F/O>ALiX-RNAi* males lay the same total number of eggs (**A**) and produce the same number of total offspring (**B**) over the three day period observed as control *esg^{ts}F/O* males. Error bars indicate ± SE; number in bars indicates total number of female flies assayed. Each male was mated to three females, only females which successfully mated (bore progeny at any point over the three day period assayed) were included in quantifications. 'ns' = no significant difference; Student's t-test following Shapiro Wilk test for normality.

4.4 Discussion

I have demonstrated that SC-derived exosomes play an important role in reproductive signalling. Exosomes interact with specific target cells following transfer to the female reproductive tract, fusing with sperm and potentially docking at the surface of the female epithelium. Exosome secretion by SCs is be required for males to fully induce a specific behavioural aspect of the long-term post-mating response (LTR), suggesting that exosomes may carry important signalling molecules that reprogramme female behaviour after mating.

4.4.1 SC exosomes mediate inter-organism signalling

Although most studies of the fly AG have highlighted roles for MC products, such as SP (Chen et al. 1988; Chapman et al. 2003), in reprogramming female post-mating responses, several recent studies have suggested a central but poorly defined function for SCs in the modulation of these responses (Leiblich et al. 2012; Minami et al. 2012; Gligorov et al. 2013). Our findings now indicate that this function of SCs is at least partly mediated by exosomes, which may transport important signalling molecule(s) to the female.

We have shown that exosome secretion is required in SCs to induce a specific aspect of the PMR, namely maintaining reduced receptivity to remating. Exosome secretion is not required for any other aspect of the PMR we assayed, including induced egg laying and male fecundity, paralleling that previously characterised for BMP signalling in SCs, which is also not required for normal egg laying or fecundity (Leiblich et al. 2012). These previous studies in the host lab demonstrated that multiply-mated males of 11 days and older sporadically transfer SCs into the female reproductive tract and that increased BMP signalling promotes cell delamination and migration of SCs (Leiblich et al., 2012). Importantly, all mating experiments performed in this present study were carried out using 4-day-old males, and we never observed transfer of SCs in more than 50 females mated

to SC>CD63-GFP males that we imaged. Therefore we believe that the effect of *ALiX*-RNAi on female mating behaviours does not result from any effects on SC delamination or transfer.

A recent study has implicated an *Abdominal B(Abd-B)*-regulated transcriptional programme in the maintenance of the PMR (Gligorov et al. 2013). *Abd-B* mutant, *iab-6*^{cocu}, males fail to maintain reduced receptivity to remating as well as increased egg laying beyond 24 hours after mating. Gligorov et al. proposed that the *iab-6*^{cocu} phenotypes result from a SP storage deficiency, whereby less SP is stored to mediate both aspects of the PMR after 1 day. Interestingly, *iab-6* SCs lack all secretory vacuoles, suggesting an *Abd-B*-dependent transcriptional program is required for SC secretion. Our findings that a proportion of these secretory compartments are mMVBLs and that exosomes are required for the maintenance of male rejection behaviours, we hypothesise that this aspect of *Abd-B's* role may be mediated by exosomes. The additional egg-laying role of SCs reported by Gligorov et al. may be mediated by the factors secreted non-mMVBL compartments (SVs) of SCs. Importantly, we did not observe altered secretion of the soluble SV product ANCE in *ALiX*-RNAi or *Hrs*-RNAi SCs, suggesting that any additional function of SCs mediated by their soluble secretory products would have been unaffected by our genetic manipulations.

It is important to note that, given the apparent mutual antagonism described by several studies between ESCRT-dependent and -independent exosome biogenesis (see Chapter 3.4.3), without a marker of ESCRT-independent exosomes produced by SCs to assay the effects of ESCRT knockdown, we cannot be sure that the effect observed on female remating behaviours following *ALiX* knockdown does not result from additional effects in an alternative population.

4.4.2 A role for exosomes in sperm competition

As with many polygamous species that store sperm, in *Drosophila* a male's sperm storage abilities have knock-on effects on their ability to compete with other males. Preliminary results from

collaborative work with Stu Wigby (Zoology, Oxford) have suggested that both males with reduced BMP signalling in SCs as well as 'exosomeless' (SC>*ALiX*-RNAi) males are also better at sperm defence than control males (Stu Wigby, personal communication). SC>*ALiX*-RNAi males sire more progeny than controls when they are the first to mate to a female, prior to a wild-type male mating to the female (it is believed that the second male provides the factor(s) critical for the release of the first male's stored sperm). As this phenotype is indicative of a deficit in the storage and /or release of SP, it will be important to assay both sperm and SP storage in females mated to 'exosomeless' males in future work, to address whether exosomes have a role in SP storage.

Extremely low levels of both egg laying and hatchability resulting in low fecundity were observed for even our control *esg*^{ts}*F/O* males mated to *w*^{1118} females in all mating experiments, compared to those reported in other studies e.g. (Peng et al. 2005). We believe the poor quality of the food utilised in our experiments is likely to be responsible, given the well-characterised effects of dietary restriction on female fecundity (Mair et al. 2004). Although this may have led to our inability to detect subtle effects on fecundity, additional mating experiments with 'exosomeless' males fed on a more nutrient rich food (Stu Wigby, Zoology, Oxford) have indicated that 'exosomeless' males exhibit normal fecundity.

4.4.3 Exosome-sperm fusion and the PMR

We have identified specific target cells of SC exosomes within the female, namely sperm and epithelial cells in the uterus and oviduct. The specificity of these interactions suggests they occur in a regulated manner and therefore may be of physiological importance. However, we can only speculate as to whether these interactions are critical for the role of exosomes in the PMR.

Given the altered distribution of CD63-GFP colocalising with sperm i.e. no longer in distinct puncta, we believe exosomes fuse with sperm and would therefore be capable of transferring both cytoplasmic and membrane-associated cellular components. It is likely that these events can

only be transiently visualized if the CD63-GFP delivered rapidly diffuses laterally throughout the sperm membrane, and this may also explain why CD63-GFP was not observed inside sperm storage organs. We believe this also limited our ability to accurately estimate the frequency of SC exosome:sperm fusion events in each female fly. Therefore, it is possible that the majority of sperm fuse with exosome(s) prior to their migration into the seminal receptacle and spermathecae. As our data indicates that exosomes may also interact with sperm tails, the use of additional fluorescently tagged sperm and exosome markers may provide further insights into the proportion of sperm targeted by seminal fluid exosomes.

SP is loaded onto both the heads and tails of sperm (Peng et al. 2005). Importantly, only tail-associated SP is gradually cleaved to release the C terminal fragment that is responsible for the maintenance of the PMR (Peng et al. 2005). My findings have demonstrated that exosomes fuse with the sperm head and may also fuse with the sperm tail. Analysis of SP processing from 'exosomeless' males in the female tract will be important in addressing whether exosomes are implicated in SP processing. Interestingly, *Drosophila* sperm possess unusually long tails. It has been proposed that these long tails may increase the reproductive fitness of males as they allow maximal storage of SP to maintain the PMR. Our results suggest that in addition to SP, exosome-sperm fusion may have also contributed to the selection of long sperm tails in males.

Prostasomes have also been shown to fuse to sperm *in vitro;* however the role of prostasome fusion in sperm capacitation remains under debate (Section 4.1.1). This study has demonstrated that *Drosophila* exosomes also interact with sperm and may deliver cellular cargos, which may be required for the acquisition of fertilisation competence. Further studies should investigate whether SC exosomes carry analogous calcium signalling molecules to those delivered to sperm by prostasomes (Park et al. 2011),as well as whether exosomes are required for sperm storage in *Drosophila*, which is dependent upon functional sperm motility (Köttgen et al. 2011). However, as

total fecundity was not reduced in 'exosomeless' males, it is unlikely that exosomes play a significant role in sperm capacitation in *Drosophila.*

The interactions of exosomes with their target cells has been reported to require adhesion molecule such as integrins and specific tetraspanins, and such molecules govern target cells selection (Clayton et al. 2004; Rana et al. 2012; Hazawa et al. 2014). Therefore, it is possible the observed exosome-target cell interactions we observed are an artefact of the incorporation in CD63-GFP into SC exosomes. The identification and tagging of an endogenous SC exosome marker will permit further studies of exosome targets under physiological conditions.

4.4.4 Exosome-female cell interactions

We did not find any evidence of CD63-GFP internalisation into these cells, suggesting that exosomes may simply dock onto female epithelial cells and induce a signalling response via molecules present on their surface.

Following cleavage from sperm, SP C-terminal fragments activate a G-protein coupled receptor, SPR, expressed in *dsx/fru/ppk* neurons within the female reproductive tract (Yang et al. 2009; Häsemeyer et al. 2009; Rezával et al. 2012), which are critical for the male rejection behaviours elicited by mated females (Rezával et al. 2012). It will be interesting to investigate whether these neurons are also targeted by exosomes e.g. by marking *ppk/fru* neurons.

Many Acps, including SP, ovulin and the SC products Msp355a and Msp355b, are found in the female hemolymph after mating (Monsma 1990; Lung et al. 1999). Western blot analysis of mated female hemolymph would begin to address the interesting possibility that exosomes may also target cells outside the female reproductive tract, such as those in the CNS where they could directly influence female behaviour, particularly as circulating exosomes in mammals have been shown to be able to cross the blood brain barrier (Alvarez-Erviti et al. 2011).

4.4.5 Concluding remarks

Whatever the target tissue(s), our data clearly demonstrate a role for SC exosomes in female reprogramming and, like human prostasomes (Arienti et al. 1997; Park et al. 2011), SC exosomes can fuse with sperm, highlighting possible conserved roles for exosomes in male reproductive biology. Our data suggest that exosomes may modulate specific aspects of SP function in the LTR, potentially by regulating processing events at the sperm membrane. An alternative hypothesise is that exosomes play a more direct role in the modulation of female post-mating behaviours, potentially via interaction with female cells. The presented characterisation of the cellular targets of exosomes in the female tract is insufficient to be able to distinguish between these two possibilities.

Prostasomes have been shown to interact with lymphocytes and are capable of modulating their activity in cell culture (Kelly 1991; Skibinski G 1992). *Drosophila* seminal fluid also possesses immunosuppressive activity attributed to Acps (Peng et al. 2005; K. Ravi Ram et al. 2007). It will be interesting to investigate whether this activity requires exosomal delivery, thus providing an insight into whether the immunosuppressive activity of prostasomes has a physiologically significant role *in vivo*.

5. The role of BMP signalling in the regulation of SC exosome secretion

5.1. Introduction

5.1.1 Roles of BMP signalling

BMP signalling mediates a wide range of cellular events, including the regulation of cell growth and proliferation (Kirilly et al. 2005; Ballard et al. 2010), cell fate decisions (Raftery et al. 1999) and cell migration (Ninov et al. 2010). BMPs are members of the TGF-β superfamily of intercellular signalling factors, which mediate long- and short-range signalling events through the secretion of soluble BMP ligands into the extracellular space. BMPs have well-characterised roles in directing complex tissue patterning through the generation of long-range diffusible morphogen gradients, for example in the *Drosophila* imaginal disc (O' Connor et al. 2006), as well as short-range signalling between signal-sending and -receiving cells, such as in the *Drosophila* germ line stem cell niche (Michel et al. 2011). BMP gradient formation is a complex process, involving ligand endocytosis and binding to extracellular matrix components such a heparan sulphate proteoglycans (HSPGs) (Kruse et al. 2004; Affolter et al. 2007; Bornemann et al. 2008).

BMP signalling regulates migratory cell behaviours during *Drosophila* development (Ninov et al. 2010). Previous studies have shown a role for BMP signalling in the regulation of post-developmental growth, delamination and migration of SCs in the AG: BMP signalling is both necessary and sufficient for these SC behaviours (Leiblich et al. 2012) (Section 1.4.7).

The cell migratory function of BMP signalling is conserved in mammalian systems, regulating epithelial-to-mesenchymal transition in many mammalian developmental contexts (Xu et al. 2009; Miura et al. 2010; Garside et al. 2013). The mis-regulation of BMP signalling is associated with many forms of cancer, including prostate and colon cancers (Bailey et al. 2007; Assinder et al. 2009) (Section 5.1.4).

5.1.2 BMP signal transduction pathway

Across vertebrates and invertebrates, BMP signalling involves a conserved Smad-mediated signal transduction pathway, which transduces the extracellular signal to a transcriptional cellular response (reviewed in (Raftery et al. 1999)). Broadly speaking, BMP ligands activate a receptor complex, composed of two types of transmembrane serine-threonine kinases, at the plasma membrane. The Type I receptor is activated following phosphorylation by the Type II receptor (Raftery et al. 1999; Mueller et al. 2012). The active receptor complex is comprised of two Type I and two Type II receptors (Massagué et al. 1994). The Type I receptor transduces the extracellular signal to downstream effectors through the phosphorylation of the Receptor-Smad (R-Smad). R-Smads interact with Co-Smads to form a heterodimeric complex. The R-Smad/Co-Smad complex translocates into the nucleus, binding DNA and additional DNA-binding proteins, to modulate transcription of target genes. One such class of transcriptional target genes are the anti-Smads. Anti-Smads act antagonistically to down-regulate BMP signalling, through binding to R-Smads and Co-Smads, preventing formation and nuclear translocation of the active heterodimeric complex (Hata et al. 1998). Consequently, anti-Smads act as negative feedback mediator to down-regulate BMP signalling following activation of the pathway by an external stimulus.

Drosophila possesses two Type I receptors and two Type II receptors that respond specifically to BMPs (and not activins) (**Table 5.1**). There are three fly BMPs (**Table 5.2**). Depending on the cellular and developmental context, different BMP ligands activate different receptor complexes, however the BMP ligands appear to share redundant, synergistic or antagonist roles depending on the biological context (Khalsa et al. 1998). *Drosophila* also possesses two R-Smads, Mad (O' Connor et al. 2006) and Smox (Henderson et al. 1998), and one Co-Smad, Medea (Hudson et al. 1998). *Daughters of Dpp* (Dad) is a *Drosophila* anti-Smad (I-Smad), Dad binds the type I receptors Sax and Tkv and prevents downstream homodimerisation and activation of Mad (Inoue et al. 1998; Kamiya et al. 2008) (**Fig. 5.1.1**). As *Dad* is a transcriptional target of Dpp signalling, it functions in a negative feedback loop to moderate the level of signalling following ligand

activation, which is particularly important during tissue patterning steps in development (Tsuneizumi et al. 1997).

Type I	Type II
Thickveins (Tkv) (Brummel et al. 1994)	Wishful Thinking (Wit) (Aberle et al. 2002)
Saxophone (Sax) (Brummel et al. 1994)	Punt (Pnt) (Letsou et al. 1995)

Table 5.1. *Drosophila* BMP receptors. Multimeric active BMP receptor complexes are comprised of two Type I and two Type II receptors. Many combinations of Type I and Type 2 receptors have been described and the type employed depends on developmental context.

Ligand	Characterised development roles
Glass bottom boat (Gbb)	Growth control • NMJ (Mccabe et al. 2003) • Stem cell self-renewal (Kawase et al. 2004)
Decapentaplegic (Dpp)	Tissue patterning (morphogen) e.g. • Embryonic DV axis (Araujo et al. 2000) • Wing disc (Zecca et al. 1995)
Screw (Scw)	Embryonic tissue patterning • Embryonic DV axis (Neul et al. 1998)

Table 5.2. *Drosophila* BMP receptor ligands and examples of characterised (developmental) roles. Interestingly, the BMP ligand Gbb appears to function in SC growth, delamination and migration, through activation of Tkv (A. Leiblich, unpublished).

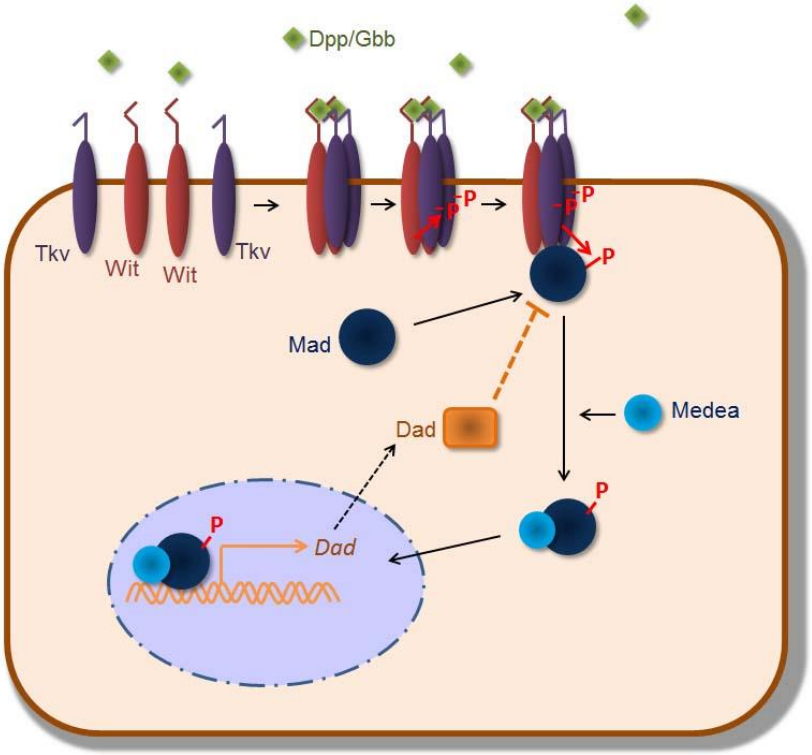


Figure 5.1.1. Schematic of the *Drosophila* BMP signalling pathway components. A receptor complex including Tkv and Wit receptors function together during oogenesis and is activated by Dpp (Marmion et al. 2013). The signalling events involved in activation are discussed in the text. The transcriptional target of BMP signalling, Dad, forms a negative feedback loop by inhibiting Mad homodimerisation and activation by the activated Type II receptor (Raftery et al. 1999; Kamiya et al. 2008).

5.1.3 BMP signalling and endocytic trafficking

Intracellular trafficking events play a crucial role in BMP signal transduction. Endocytic trafficking has been demonstrated to be necessary for the induction and amplification of BMP signalling, whereby the endocytic membranes act as signal transduction platforms for the recruitment of downstream R-Smad and Co-Smad effectors (Hayes et al. 2002). Blocking endocytosis by expression of dominant-negative Dynamin in HeLa cells not only prevents receptor-ligand complex internalisation and accumulation in early endosomes, but also R-Smad/Co-Smad complex nuclear translocation and BMP-dependent reporter expression (Hayes et al. 2002).

5.1.4 BMP signalling: cancer and exosomes

Cancer cells often secrete high levels of TGF-β family molecules, and prostate cancer cells secrete high levels of various BMP ligands (Bobinac 2005). Humans have over 20 BMP ligands, seven Type I receptors and five Type II receptors (Ye 2007). In early tumor biology, BMP signalling initially possesses tumour suppressor qualities by inhibiting cancer cell growth (Principe et al. 2014). However, in later stages of tumour progression, BMP signalling has a positive oncogenic role promoting metastasis, attributed to its roles in promoting epithelial-mesenchymal transition, angiogenesis and bone remodelling (Juárez et al. 2011; Morrison et al. 2013; Principe et al. 2014).

The majority of secreted TGF-β is soluble; however, TGF-βs have been identified on exosomes isolated from several cell types, including prostate cancer cell lines (PC3, LNCaP (Ramteke et al. 2013); and DU145 (Webber et al. 2010)). The functional role(s) of exosomal TGF-β has only just begun to be investigated in cell line models. Whether BMP signalling regulates exosome biogenesis or secretion, or indeed any aspect of endolysosomal trafficking, has not yet been addressed.

5.1.5. Aims and objectives

1. Investigate whether BMP signalling regulates exosome secretion in SCs

2. Characterise the role of BMP signalling in the regulation of SC endocytic and secretory trafficking.
3. Investigate links between exosome secretion and SC growth.

5.2 Methods

See Sections 2.3.3- 2.6 for live imaging of SCs and quantification of exosome secretion assays. Expression of *Dad* significantly reduced exosome secretion in 2/2 independent experiments as well as in an additional repeat in the host lab (Jeeun Song, FHS 2013).

5.2.1 Nuclear size experiments

Nuclear size quantification experiments were carried out as previously reported (Leiblich et al. 2012). Flies were reared at 18˚C, virgin males were collected at eclosion and shifted to 28.5˚C to induce transgene expression. Males were dissected, fixed and stained for Fasciclin3 (to mark septate junctions) and DAPI (to stain nuclei) at 6-days-old (Section 2.3.2).

Confocal images were acquired using x63 objective with x1.7 zoom (Section 2.4.1). Images were obtained at two different Z positions in order to capture the maximal optical cross-section for either the SC or MC nuclei, for each of the three SC/MCs per gland (as they are positioned at slightly different planes within the gland epithelium). Images for test and control glands were captured under identical confocal settings.

Three SCs per gland and a minimum of 10 glands per genotype were analysed. For each SC, 3 neighbouring MCs were also analysed. Images were analysed using ImageJ by drawing around both nuclei of each cell and calculating the area in μm^2 (Analyse>Measure). Data were analysed using Excel, by calculating the average nuclear size for the surrounding MCs, and using this value to calculate the nuclear size ratio of SC:MC for each SC. This ratio was then averaged across the gland to obtain a gland average, and then averaged

5.3 Results

5.3.1 BMP signalling in SCs is required for exosome secretion.

As our data and previous work in the host lab demonstrate a key role for ESCRT function and BMP signalling in SCs in order for males to fully induce specific aspects of the PMR (Leiblich et al. 2012), we investigated whether this function of BMP signalling is dependent upon exosome secretion. To test this, we assayed the effect of modulating BMP signalling in SCs on exosome secretion. Strikingly, antagonising BMP signalling in SCs by expression of the negative regulator *Dad* significantly reduced exosome secretion (lumenal exosome numbers were reduced to approximately 10% of control; **Fig. 5.1**). Unfortunately, we were unable to assay the effect of up-regulating BMP signalling by expression of a constitutively-activated Type I BMP receptor (Tkv^{ACT} containing a Q199D substitution (Hoodless et al. 1996)) as this caused large clumps of CD63-GFP-positive material to form in the gland lumen, even in virgin glands (data not shown). This is consistent with previous reports of this genetic manipulation inducing the shedding of large amounts of cellular debris into the gland lumen (Leiblich et al. 2012). Nevertheless, this data suggest BMP signalling is required for secretion of CD63-GFP exosomes in SCs.

5.3.2 BMP signalling regulates endolysosomal trafficking

To investigate the role of BMP signalling in exosome secretion, we analysed the effect of modulating BMP signalling on the number, size and morphology of SC endocytic and secretory compartments by live imaging of CD63-GFP expressing cells. *Dad*-expressing SCs contained normal numbers of mMVBLs but these were smaller than control SCs (**Fig. 5.2C**). Surprisingly, in contrast to knockdown of *Hrs*, *ALiX* or *Tsg101* (**Fig. 3.20**), mMVBLs of *Dad*-expressing SCs still contained many CD63-GFP ILVs (**Fig. 5.3B**), suggesting that BMP signalling is not required for ILV biogenesis in SCs. Conversely, SC>Tkv^{ACT} cells contained significantly fewer mMVBLs (**Fig. 5.2A**) but these were significantly larger than those of controls (largest mMVBL diameter increased by

approximately 100%; **Fig. 5.2C**). Furthermore, *Tkv*^{ACT}-expressing SCs contained significantly more iLEs (**Fig. 5.2B**). In contrast to Dad-expressing SCs, mMVBLs of SCs>*Tkv*^{ACT} were completely void of CD63-GFP (**Fig. 5.3C**), suggesting that BMP signalling may regulate ILV formation, secretion or degradation. Interestingly, SVs of SC>*Tkv*^{ACT} cells were observed clustering around the enlarged mMVBL (17/19; **Fig. 5.3C**) in a larger proportion of cases than in controls (16/31; p=0.003, Fisher's Exact Test), supporting a model whereby increased BMP signalling increases trafficking into this large acidic compartment from the secretory pathway. *Dad*-expressing SCs contained significantly fewer SVs, although *Tkv*^{ACT}-expressing SC SV numbers were not significantly different to control (**Fig. 5.2D**). Our data suggest that BMP signalling regulates one or more aspects of endolysosomal and/or secretory trafficking that are required for exosome secretion.

5.3.3 *ALiX,* but not *Hrs,* function is required for SC growth

As previous work in the host lab demonstrated that BMP signalling is required for post-developmental SC growth (Leiblich et al. 2012), we wondered whether exosome secretion was involved in this process. To test this, we utilised a previously established SC growth assay in which SC growth is measured by total nuclear cross-sectional area and is assessed relative to surrounding MC nuclei. At eclosion, the total binuclear area of SCs is less than that of the surrounding individual MCs (approximately 80%). However, the post-developmental growth rate of SCs exceeds that of MCs, such that at 6-day-old SCs nuclei are approximately 1.2(+/-0.2 SE)-times greater than MC nuclei (**Fig. 5.4 and 5.5A**). We analysed the growth of SCs in which we genetically blocked exosome secretion by expression of *ALiX*-RNAi or *Hrs*-RNAi, and calculated this relative to control values obtained during parallel experiments. Interestingly, whilst SCs expressing *ALiX*-RNAi had significantly smaller nuclei relative to MCs than controls (**Fig. 5.4A and 5.5C**), SCs expressing *Hrs*-RNAi had significantly larger nuclei relative to MCs (**Fig. 5.4A and 5.5B**); although these effects were less severe than that following genetic manipulation of BMP signalling (**Fig. 5.4**). Interestingly, although the *absolute* nuclear size of MCs surrounding *ALiX*-

RNAi SCs was not significantly different to controls, MCs cells surrounding *Hrs*-RNAi SCs were significantly smaller than controls (**Fig. 4.5C**). Nevertheless, the *absolute* nuclear size of *Hrs*-RNAi SCs was still significantly greater than control, whilst the absolute nuclear size of *ALiX*-RNAi SCs was significantly smaller than control (**Fig. 4.5B**). These data suggest that whilst *ALiX* function is required for post-developmental SC growth, *Hrs* function has a negative impact on growth. Given the opposing effects on SC growth following inhibition of exosome secretion, our data do not support a role for exosome secretion or biogenesis, in SC growth.

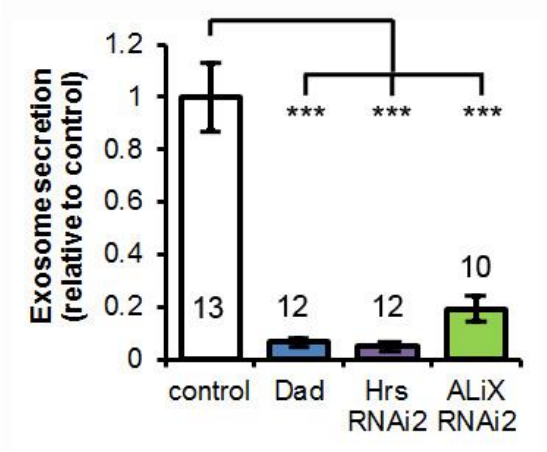


Figure 5.1. BMP signalling in SCs is required for exosome secretion. Reducing BMP signalling by overexpression of the negative regulator *Dad* blocks exosome secretion, phenocopying the effect of *Hrs* and *ALiX* knockdown. The numbers of CD63-GFP-positive puncta secreted into the AG lumen were significantly reduced in SC>*Dad*, SC>*Hrs-RNAi2* and SC>*ALiX*-RNAi2 males compared to control. The values represent the average particles in a 7225 μm^2 luminal area, averaged over 3 confocal sections for each gland and then over 'n' glands (number above or in bars), and calculated as a percentage of the control value carried out simultaneously. Virgin males (*UAS-CD63-GFP, Tub-Gal80^{ts}; dsx-Gal4* crossed to respective RNAi lines, or *w^{1118}* for control) were shifted to 28.5˚C at 0 days to induce transgene expression and mated to 3 females at 2 days to reduce the stored lumenal contents, allowed to recover and then dissected at 4 days. Graph shows data from one experiment with all genotypes carried out and imaged simultaneously, all genotypes repeated at least once in independent experiments. Data were analysed using an unpaired Student's t test, following the Shapiro Wilk test for normality. **P<0.01, ***P<0.001. Errors bars indicate SE.

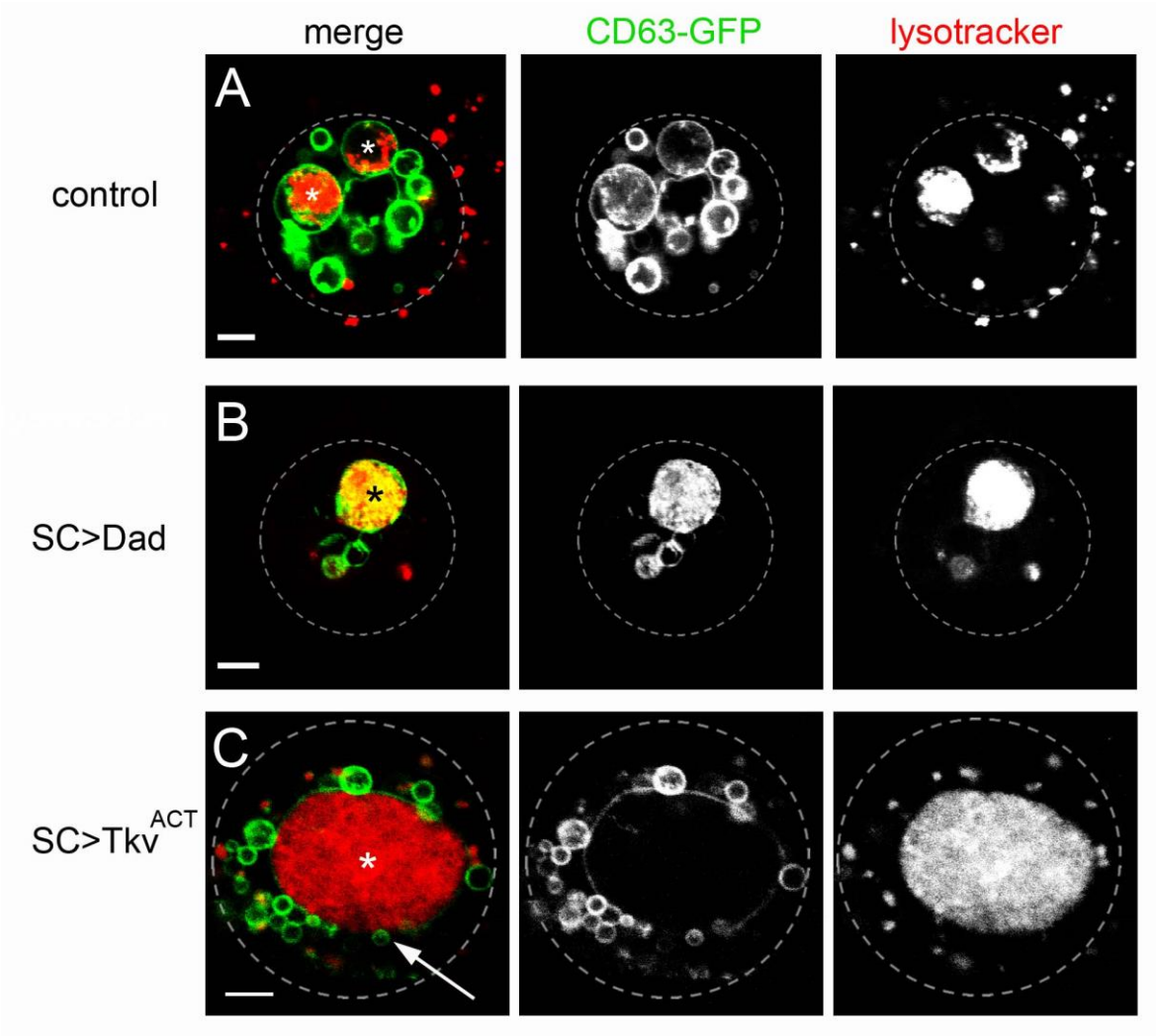


Figure 5.2. Modulating BMP signalling affects morphology of SC compartments. Representative images of 6-day-old *UAS-CD63-GFP, tub-Gal80^{ts}*; *dsx-Gal4* control (**A;** crossed to *w^{1118}*), *UAS-Dad* (**B**) or *UAS-Tkv^{ACT}* (**C**) virgin males stained with Lysotracker (red) and imaged live. (**B**) Reducing levels of BMP signalling by overexpression of the negative regulator, *Dad*, results in small mMVBLs (*, **B**) typically containing a higher density of CD63-GFP ILVs than controls (*, **A**). (**C**) SCs expressing an activated form of the BMP receptor, *Tkv^{ACT}*, contained a single enlarged mMVBL, void of internal CD63-GFP fluorescence. Image in (**C**) shows a representative *Tkv^{ACT}*-expressing SC, containing one enlarged mMVBL, surrounded by multiple SVs in close proximity (arrow). For quantification of cell phenotypes see **Fig. 5.3**. Scale bars= 5µm. Approximate cell outlines indicated with dashed line.

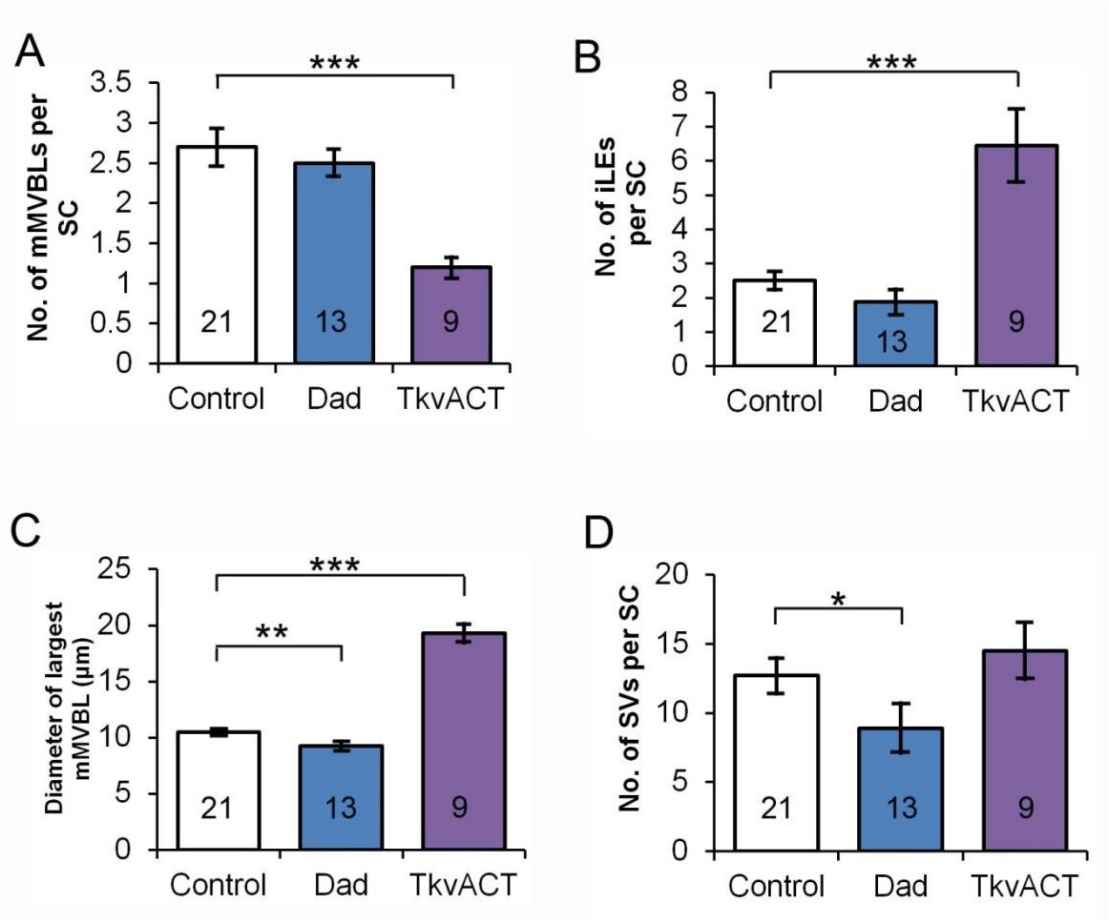


Figure 5.3. BMP signalling regulates intracellular trafficking events inside SCs. AGs dissected from 6-day-old virgin males of genotype *dsx-Gal4; UAS-CD63-GFP, Tub-Gal80^{ts}*; with no other transgenes (control), or with *UAS-Dad* or *UAS-Tkv^{ACT}* and stained with Lysotracker-Red (red) and the CD63-GFP-positive intracellular compartments were subsequently quantified and measured: (**A**) average number of mMVBLs per SC; (**B**) average number of iLEs per SC; (**C**) average size of the largest mMVBL in each SC, measured by the widest diameter in a confocal Z series; (**D**) average number of SVs per SC. Reducing levels of BMP signalling by overexpression of the negative regulator, *Dad*, results in significantly smaller mMVBLs (**C**); conversely increasing levels of BMP signalling by expression of the constitutively activated receptor, *Tkv^{ACT}*, resulted in the formation of one (**A**), enlarged mMVBL (**C**), with an associated increase in the number of iLEs (**B**). Reducing BMP signalling resulted in modest, yet significant reduction in the number of SVs per SC (**D**). 3 SCs per gland were measured and averaged over 'n' glands (number in bars). Error bars indicate ±SE. Data were analysed using either an unpaired two-tailed Student's T test or Mann-Whitney U test, for normally and non-normally distributed data sets respectively (as assessed by the Shapiro-Wilk test); *p<0.05, **p<0.01, ***p<0.001.

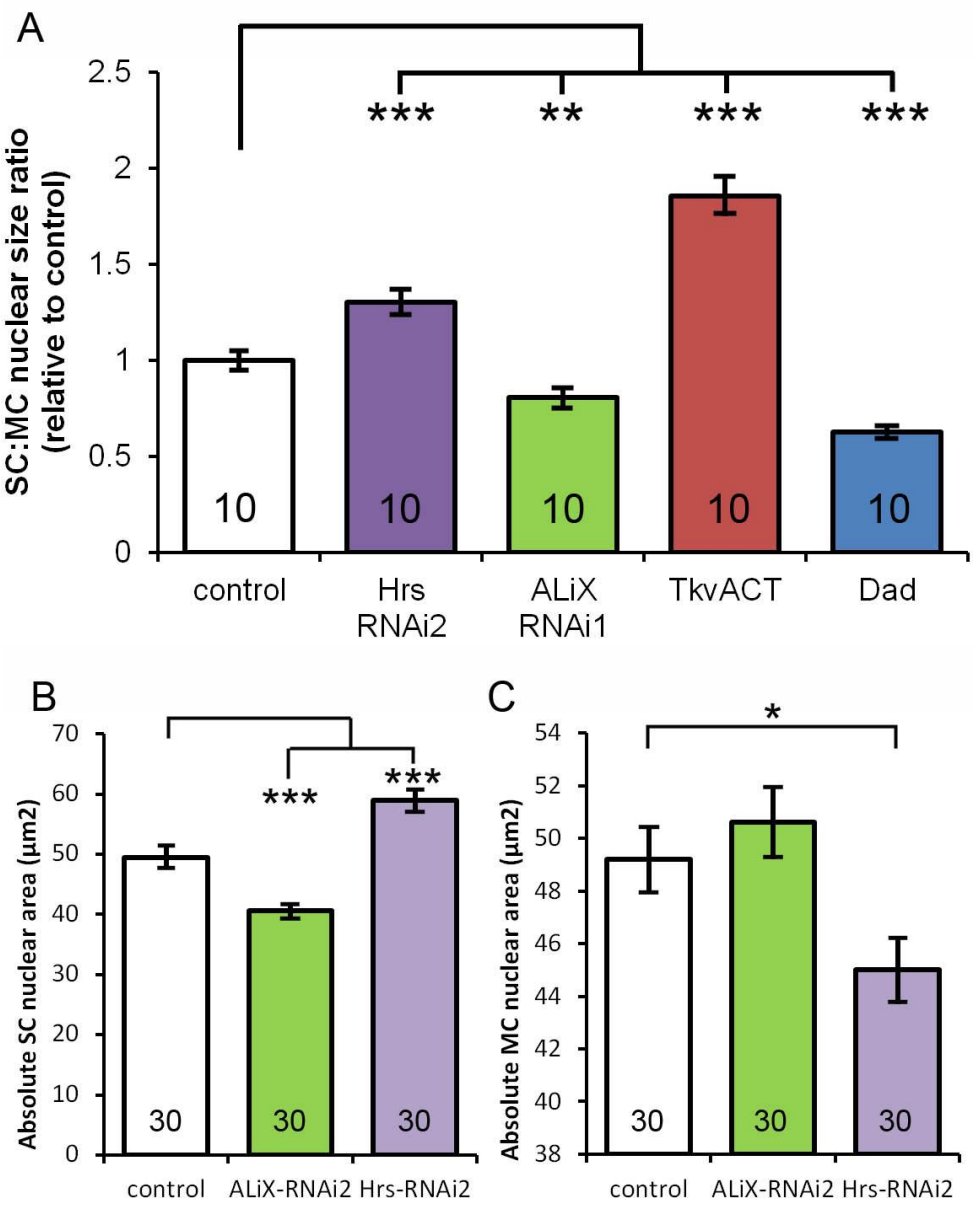


Figure 5.4. Effect of ESCRT knockdown on SC growth. (**A**) Growth of SCs relative to MCs in 6-day-old *esg^{ts}F/O> UAS-ALiX-RNAi1, UAS-Hrs-RNAi2, UAS-Dad or UAS-Tkv^{ACT}* virgin males, measured by the ratio of SC to MC nuclear size and normalised to control experiments carried out and imaged in parallel. Three SCs per gland were analysed and averaged across 'n' glands (numbers in bars). (**B** and **C**) Re-analysis of data from **A** showing absolute nuclear size of individual SCs (**B**) and MCs (**C**). MC numbers in **C** were averaged for each SC, 30 SCs measured across 10 glands. Data were analysed by pairwise comparisons using either a two-tailed unpaired Student's t test or the Mann Whitney U test for normal and non-parametric data sets, respectively; following Shapiro-Wilk test for normality. Error bars indicate ±SE.

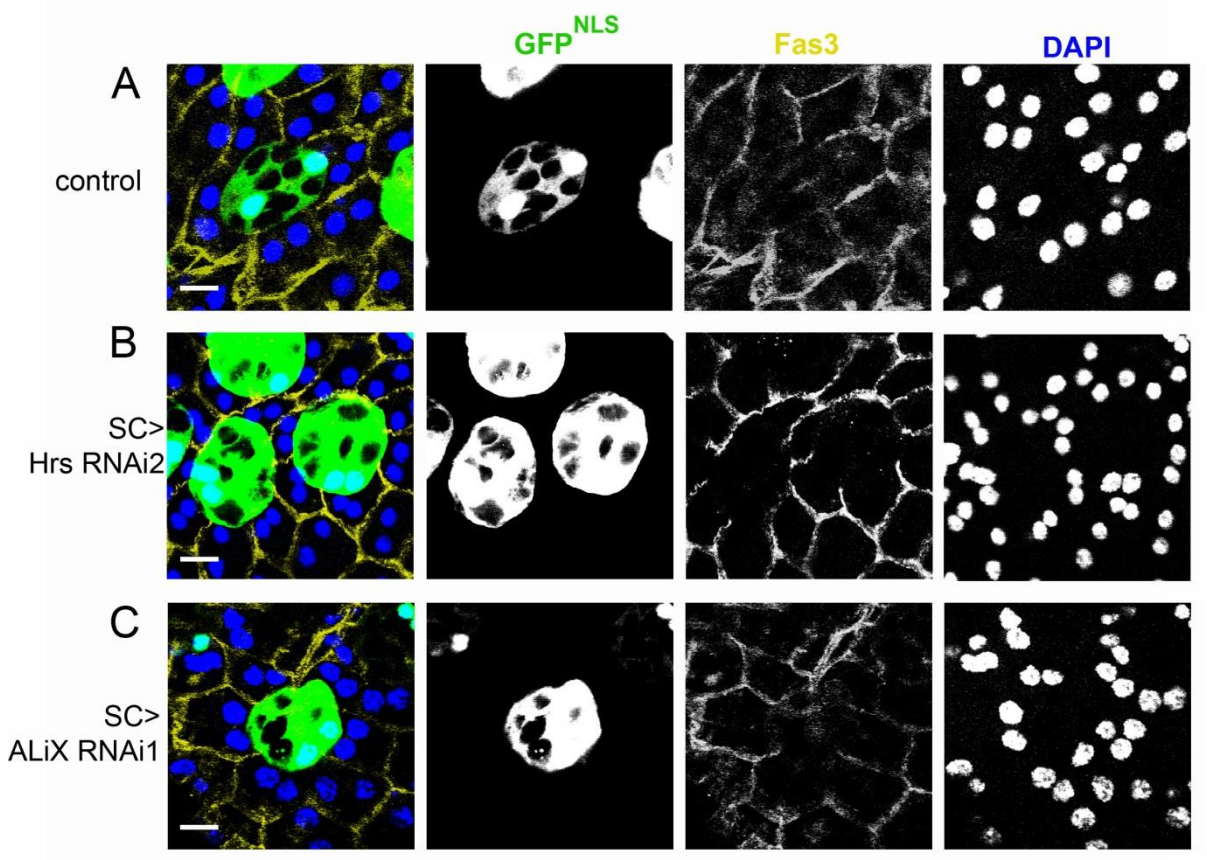


Figure 5.5. Effect of ESCRT knockdown on SC growth: exosome secretion is not required for normal post-developmental SC growth. Representative images of 6-day-old virgin males expressing nuclear GFP alone (**A**) or in combination with either *UAS-Hrs-RNAi2* (**B**) or *UAS-ALiX-RNAi1* (**C**), under the control of the *esg^{ts}F/O* system, stained for Fas3 (yellow) and with DAPI (blue). Control SC nuclei are smaller than MC nuclei at eclosion, but are larger by 6-days (**A**). Knockdown of *Hrs* by RNAi resulted in SCs with significantly larger nuclei relative to MCs (**B**) than control, whilst knockdown of *ALiX* by RNAi resulted in SCs with significantly smaller nuclei (**C**) than control. Scale bars, 10µm.

5.4 Discussion

5.4.1 BMP-dependent regulation of endolysosomal trafficking as a novel mechanism for controlling exosome secretion

This study has identified a novel role for BMP signalling in the regulation of exosome secretion. Unlike *Hrs* and *ALiX*, our data indicate that BMP signalling is not required for ILV formation. Therefore, BMP signalling is likely to regulate endolysosomal trafficking events, upstream or downstream of mMVBL formation, necessary for exosome secretion. To our knowledge, this is the first report describing a role for TGF-beta family signalling in the regulation of exosome secretion.

Whilst the observed reduction of mMVBL size in *Dad*-expressing SCs may explain the reduced number of exosomes secreted into the gland, we believe this relatively small size effect (≈15%) is unlikely to account for the large reduction in exosome secretion (≈90%). Moreover, small mMVBLs in *Dad*-expressing SCs were often completely filled with ILVs, indicating that these cells may continue to make normal numbers of ILVs that become densely packaged inside these compartments, although this was difficult to quantify due to reasons previously described (Section 3.4.3)

A simple interpretation of the observed effect of BMP signalling on ILVs is that BMP signalling is required for trafficking events leading to the fusion of mMVBLs with the plasma membrane. However, the increase in size of mMVBLs of SCs expressing the constitutively activated BMP receptor does not support such a model.

One alternative explanation is that BMP signalling is required for mMVBL maturation; whereby mMVBLs in *Dad*-expressing SCs fail to mature properly, blocking exosome secretion and therefore retaining CD63-GFP-positive ILVs. This role in endolysosomal trafficking and maturation is consistent with the effect of increasing BMP signalling in these cells, where a highly enlarged

acidic compartment lacking CD63-GFP puncta is formed: the ILVs may have been degraded following further acidification or rapidly secreted by a kiss-and-run mechanism. We have previously hypothesised that the acidic microenvironment inside mMVBLs can prevent GFP fluorescence (Section 3.3.2). Therefore, it will be important to use antibody staining inside these compartments to confirm a loss of CD63-GFP ILVs.

Nevertheless, a change in the rate of mMVBL maturation does not completely explain the observed changes in mMVBL size following up- or down-regulation of BMP signalling. Another possible explanation for this is that BMP signalling may regulate the rate of membrane trafficking into the endolysosomal system. In support of this, we observed an increase in iLEs in SCs with increased BMP signalling, consistent with an increased rate of endocytosis. Activation of the BMP receptor following ligand binding is believed to induce receptor internalisation (Chen 2009; Balogh et al. 2013). Therefore, Tkv^{ACT} may be constitutively and rapidly endocytosed when expressed in SCs, increasing the amount of membrane trafficking through the endosomal system leading to growth of mMVBLs, perhaps reflecting abnormally high activation of the receptor. Indeed, *Dad*-expressing SCs did not have reduced numbers of iLEs, suggesting that BMP signal transduction is not required for endocytosis or early endocytic maturation events. Furthermore, we observed SVs appearing to dock at the edge of the mMVBLs in SCs with increased BMP signalling, potentially feeding in membrane from the secretory pathway. Although *Dad*-expressing cells did not have increased numbers of SVs that would be expected if SV-mMVBL fusion was inhibited, the reduction in mMVBL size and SV number in Dad-expressing SCs could be explained by the reduction in SV synthesis, resulting in less membrane to feed mMVBL growth in these cells. Therefore, our data support a model in which mMVBL size is increased by delivery of newly synthesised proteins and membrane from both the secretory and endocytic pathways, and the rate of delivery to mMVBLs may be regulated by BMP signalling. They also suggest that BMP signalling may be required for macromolecular protein synthesis in the secretory system.

Alternatively, the reduction of SVs in Dad-expressing SCs could be explained by an increased rate of SV secretion. Further work could assess, by western blot analysis, the amount of SC secretory products such as ANCE in the seminal fluid of *Dad*- and Tkv^{ACT}- expressing SCs in order to address whether increased BMP signalling reduces secretion of proteins trafficked via the secretory pathway.

In summary, our data indicate that BMP signalling is not required for ILV formation, but instead regulates a key trafficking and/or maturation event governing mMVBL formation or secretion.

5.4.2 Exosome secretion is not required for cell growth

The opposing effects of *ALiX* and *Hrs* knockdown suggest that exosome secretion is not required for SC growth. To our knowledge, neither *ALiX* nor *Hrs* has been reported to have direct roles in the regulation of cell growth. Nevertheless, their role in protein sorting and ILV biogenesis implicates both factors in the regulation of growth factor receptor turnover, and thus indirectly in growth regulation. Growth factor signalling, e.g. via the activation of the EGFR or FGFR, at least partially mediates cell growth via the activation of the PI3K signalling cascade, culminating in the activation of the major growth regulator mTOR (Section 6.1.2.1). Previous studies have demonstrated roles for *Hrs* and *ALiX* in both the positive regulation of EGFR and FGFR receptor turnover as well as both the positive and negative regulation of growth factor signalling in various cellular contexts (Jékely et al. 2003; Schmidt et al. 2004; Chanut-Delalande et al. 2010). However, as previous work in the host lab reported no role for either EGFR, FGFR or PI3K signalling in the regulation of SC growth (Leiblich et al. 2012), *Hrs* and *ALiX* are unlikely to indirectly regulate SC growth through the regulation of these pathways. Nevertheless, alternative growth factor receptors, whose turnover is differentially regulated by *ALiX* and *Hrs*, may regulate growth in SCs.

In order to deliver comparable data to that previously published, we employed the method of *relative* nuclear size analysis previously employed by the host lab for the characterisation of BMP-dependent post-developmental SC growth (Leiblich et al. 2012) chosen to highlight the enhanced

growth rate of SCs relative to MCs, whilst controlling for variations between experimental runs. However, the well-characterised role for exosomes in intercellular signalling leads to the possibility that SC exosomes influence MC growth. However, as only *Hrs* knockdown and not *ALiX* knockdown reduced the absolute growth of surrounding MCs, this non-cell autonomous growth effect is unlikely to involve exosome-mediated signalling. Importantly, *Hrs* (and *ALiX*) knockdown produced similar effects on SC growth when absolute nuclear size measurements were analysed, reaffirming our conclusion that *ALiX* but not *Hrs* is required for SC growth.

5.4.3 Regulation of cell growth by endolysosomes

Several recent studies in mammalian cells as well as *in vivo* evidence in *Drosophila* have demonstrated a key role for endolysosomes in mTOR-regulated cell growth (Sancak et al. 2010; Ögmundsdóttir et al. 2012). mTORC1 activity is regulated by the activity of Rheb GTPases residing at the surface of endolysosomes (Sancak et al. 2008; Sancak et al. 2010). Rag GTPases and Proton Assisted Transporters also reside on the surface of endolysosomes and mediate the recruitment of mTORC1 in response to extracellular stimuli (cytokines, hormones and amino acids), where Rheb promotes mTORC1 activation and downstream signalling events culminating in cell growth (Sancak et al. 2008; Sancak et al. 2010; Ögmundsdóttir et al. 2012).

Based on the idea that mMVBLs in *Dad*-expressing SCs fail to mature, these cells could remain small because the mTORC1-activating compartments are not formed, whereas SCs with high BMP signalling may grow rapidly because they form mature lysosomes.

Interestingly, we noted a correlation between the size of mMVBLs and SC growth following modulation of BMP signalling and knockdown of *Hrs* or *ALiX*. Therefore, we hypothesise that the levels of growth-promoting components e.g. Rag and Rheb GTPases, PATs and mTORC1, recruited and activated at the surface of mMVBLs is proportional to their surface area and maturity. Consistent with such a model, previous work has characterised age-dependent growth of SCs

(Leiblich et al. 2012), which also correlates with the observed increase in mMVBL size with age of SCs reported in this study (Section 3.3.3). This model relies upon the assumption that endolysosomal surface area, and not extracellular stimuli, is the limiting factor governing SC growth. Further work attempting to uncouple mMVBL size and SC growth will be necessary to test whether mMVBL size regulates SC growth.

5.4.4 Reciprocal functions for BMP and Hrs in the regulation of late endosomal size

Consistent with our observations, previous studies have also shown that blocking endosomal maturation by knockdown of the ESCRT-0 component, *Hrs*, induces the formation of enlarged immature endosomal 'class E' compartments lacking ILVs (Piper et al. 1995; Chanut-Delalande et al. 2010). This increase in size is likely to be a direct consequence of reduced membrane internalisation and degradation as Hrs is critical for ILV budding through recruitment of downstream ESCRT components (Katzmann et al. 2003). Interestingly, in *Drosophila* this cellular phenotype is also associated with an increase in BMP signalling probably resulting from reduced receptor degradation (Jékely et al. 2003). Our data demonstrate that BMP signalling also promotes growth of mMVBLs, suggesting that there is a complex bidirectional interaction between mMVBL maturation and size, and the level of BMP signalling in SCs.

Although it is possible the observed effects of *Hrs* knockdown on mMVBL size and morphology are caused by increased BMP signalling following reduced receptor degradation, we believe this is unlikely given the reduction of mMVBL size of SC>*ALiX*-RNAi SCs despite a similar block of ILV formation. Assessing the level of BMP signalling and receptor turnover following *ALiX* and *Hrs* knockdown using a reporter construct and antibody staining with pulse chase analysis, respectively, would provide further insights into the role of BMP signalling on endolysosomal trafficking.

6. The role of RTK signalling in the regulation of exosome secretion.

6.1 Introduction

6.1.1 EGFR signalling

EGFR signalling mediates both long- and short- range intercellular signalling in a wide range of normal developmental and physiological processes (reviewed in (Shilo 2003) for *Drosophila*). By functioning as a long-range morphogen, EGF signalling can pattern large epithelial tissues (Goentoro et al. 2006). In addition to mediating cell fate decisions, EGF signalling has also been implicated in the regulation of cell migration, cell proliferation and cell death (Kurada et al. 1999; Shilo 2003). Consequently, EGFR is often mis-regulated in many cancers including breast (Mader et al. 2011) and prostate (Batra 2011), and EGFR-promoted cell motility has been implicated in metastasis (Lu et al. 2009).

6.1.1.1 EGFR signal transduction

Unlike mammals, which possess four EGF receptors, *Drosophila* EGFR is encoded by a single gene that gives rise to two isoforms, EGFR1/EGFR2 (Freeman 1998). EGFR1 and EGFR2 differ minimally only in their N terminal signal sequence (Clifford et al. 1994). The EGFR can be activated by one of four *Drosophila* ligands: spitz, vein, keren or gurken (Freeman 1998). With the exception of vein, the EGF ligands are synthesised as membrane-bound precursors that undergo processing in the ER and Golgi by Star and Rhomboid (Urban et al. 2002). This processing is essential to generate a signal-competent ligand through the release of soluble EGF into the intraluminal space of the ER and thus its extracellular secretion (Schweitzer et al. 1995; Urban et al. 2002). *spitz* is widely expressed throughout many developmental stages and across many tissues, and consequently is considered the primary EGFR ligand (Freeman 1998).

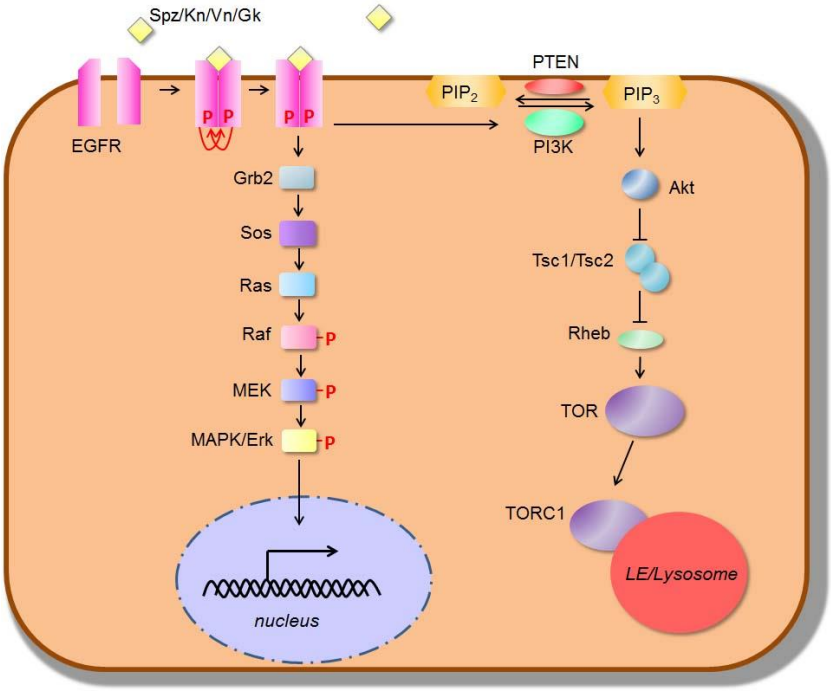


Figure 6.1.1. The core PI3K and EGFR signalling pathways and their interaction via EGFR-mediated PI3K recruitment. The EGFR has four potential ligands: spitz, keren and gurken are from the TGF-α family, whilst vein is a neuregulin. Ligand binding induces dimerization and autophosphorylation of the EGFR, leading to its full activation. Active EGFR recruits the adaptor, Grb2 (Growth factor receptor-bound 2), and initiates the Ras/Raf/MEK/MAPK signalling cascade resulting in the phosphorylation of ERK-MAPK (extracellular regulated kinase 1/mitogen activated kinase), which translocates to the nucleus to modulate target gene expression. Active EGFR can also recruit class I PI3K to the plasma membrane, which phosphorylates PIP_2 to PIP_3; this is antagonised by the activity of PTEN (Phosphatase and tensin homologue on chromosome ten). PIP_3 recruits downstream effectors including Akt, which inactivates Tsc1/Tsc2 (Tuberous Sclerosis 1/2) to relieve the repression of Rheb (Ras homologue enriched in brain). Rheb activity results in the activation of the mTOR complex upon translocation to the surface of late endosomes (LE) and lysosomes to regulate effectors that ultimately control cell growth via the stimulation of protein synthesis and transcription. Reviewed in (Mendoza et al. 2011).

EGFR signalling is initiated by ligand binding to the EGF receptor, inducing receptor homodimerisation and autophosphorylation. Activation of EGFR induces intercellular signalling through the induction of both the Ras (Rat sarcoma)/Raf (Rapidly accelerated fibrosarcoma)/MEK (Map Kinase Kinase) /ERK-MAPK (Extracellular signal Related Kinase, Mitogen-Activated Protein Kinase) (**Fig. 6.1.1**) as well as the PI3-Kinase (Phosphatidylinositol 3-Kinase)/Akt signal transduction cascades (Section 6.1.2). Active EGFR recruits the adaptor, Grb2 (Growth factor receptor-bound 2), Sos (Son of Sevenless) and the oncogene, Ras, to activate a protein phosphorylation cascade. This cascade culminates in the phosphorylation and activation of the major effector ERK-MAPK, which subsequently translocates to the nucleus to modulate target gene expression through activation of transcription factors, including in flies the ETS transcriptional activator *Pointed* (Fuchs et al. 2012). Depending on the developmental context, EGFR signalling can also induce non-transcriptional outcomes, such as promoting cell survival in the developing *Drosophila* eye by inhibiting the proapoptotic factor Hid (*Head involution defective*)(Bergmann et al. 1998; Kurada et al. 1999). Ras also functions upstream of the PI3K/Akt signalling pathway, resulting in additional crosstalk between these two cascades further downstream (Section 6.1.2.2) (Mendoza et al. 2011). The Ras/Raf/MEK/ERK-MAPK signal transduction cascade is also activated by other growth factors, such as FGF, as well as peptide hormones and neurotransmitters (Mendoza et al. 2011).

EGFR is often under complex feedback regulation, finely tuning EGFR signalling in both space and time (Shilo 2005). These feedback mechanisms can involve altering the expression of positive or negative regulators. Positive regulators include the ligands spitz and vein, whose expression is upregulated in response to EGFR signalling. During *Drosophila* oocyte patterning, EGFR signalling involves an autocrine positive feedback loop, in which transcription of the ligand, spitz, is a direct target of the active signalling cascade initiated by a paracrine gurken signal (Wasserman et al. 1998; Golembo et al. 1999).

Conversely, in a number of post-embryonic examples, the cells that produce EGF ligands are refractory to the signal such that signalling occurs in a paracrine fashion (Brodu et al. 2004; Frankfort et al. 2004; Shilo 2005). In these contexts, EGFR signalling initiates a negative feedback loop involving the transcription of negative regulators such as *sprouty* (Kim et al. 2004), *argos* (Golembo et al. 1996) or *kekkon* (Shilo 2005).

6.1.1.2 EGFR trafficking

Following activation of EGFR the receptor is rapidly internalised by endocytosis (Cohen et al. 1985). Some studies report the internalisation of the receptor is required to initiate signal transduction (Vieira et al. 1996), however other studies suggest EGFR signalling is independent of endocytosis (Kranenburg et al. 1999).

Mammalian cell lines experiments have demonstrated that EGFR undergoes constitutive internalisation and turnover at a basal rate independent of ligand binding, kinase activity and C-terminal regulatory regions (Wiley et al. 1991) (**Fig. 6.1.2**). However, the rate of EGFR endocytosis is up-regulated in response to ligand-binding in a kinase-dependent manner (Wiley et al. 1991). Lysosomal targeting of EGFR is dependent upon a distinct C terminal targeting sequence within the regulatory C-terminal region (specifically residues 945-991 in mammalian EGFR) (Opresko et al. 1995) and is independent of its kinase activity (Wiley et al. 1991; Opresko et al. 1995).

It has been suggested that RTKs can continue to signal from the surface of endosomes following endocytosis, until they are internalised onto ILVs, both in mammalian systems and *Drosophila* (Futter et al. 1996; Lloyd et al. 2002; Stuffers et al. 2009). In mammalian systems, blocking ILV formation results in the maintenance of (auto)phosphorylated EGF-EGFR complexes at the surface of endosomes, which continue to associate with downstream effectors (Ushiro et al. 1980; Wada et al. 1992). Both in mammalian cells and *Drosophila,* the inhibition of ESCRT function, by knockdown of ESCRT 0 component, *Hrs*, prevents down regulation of EGFR signalling (Lloyd et al. 2002; Chanut-Delalande et al. 2010), as does knockdown of ESCRT II component *Tsg101* in mammalian cells (Bache et al. 2006).

6.1.1.3 EGFR signalling regulates trafficking

Two pivotal studies have begun to dissect the regulation of intracellular membrane trafficking by extracellular cues. EGFR signalling has been shown to regulate endocytic trafficking through the regulation of the small GTPase Rab5. The Rab GAP RN-tre, whose activity is negatively regulated by EGFR signalling via the adaptor Eps8, regulates the activity of Rab5 (Lanzetti et al. 2000). RN-tre activity negatively regulates EGFR internalisation by stimulating Rab5 GTP hydrolysis, inhibiting endocytosis (Lanzetti et al. 2000). Furthermore, RIN1 (Rab and Rab Interactor 1) displays RabGEF activity which positively regulates the activity of Rab5, thus promoting early endocytic trafficking events (Tall et al. 2001). RIN1 is activated by Ras, the downstream effector of EGFR signalling. Thus, EGFR signalling promotes Rab5-dependent endocytic trafficking by activation of RIN1 through Ras, as well as inhibition of negative regulator RN-tre through Eps8.

6.1.1.4 EGFR and exosomes

Several studies have identified the EGF receptor as well as EGF ligands as cargos on vesicles secreted by both 'normal' and diseased cells (Sanderson et al. 2008; Adamczyk et al. 2011; Higginbotham et al. 2011; Beckler et al. 2013). In mammalian systems, the EGF ligand,

amphiregulin (AREG), is present on exosomes secreted by MDCK (Madin-Darby Canine Kidney) cells. Exosomal-AREG remains unprocessed and thus membrane-linked. Exosomal-AREG is competent to induce signalling in recipient cells following uptake, resulting in increased cancer cell invasiveness (Higginbotham et al. 2011). Specific isoforms of the mammalian EGFR have been identified on exosomes secreted by human keratinocyte HaCa T cells (Sanderson et al. 2008). Mutation of the oncogene Kras has been demonstrated to induce secretion of EGFR on exosomes, further suggesting exosomal-EGFR may be involved in tumorigenesis and cancer progression (Beckler et al. 2013).

It has not yet been established whether exosomal-EGF or exosomal-EGFR have signalling roles during 'normal' biology *in vivo*.

6.1.2 PI3K signalling

Phosphatidylinositol lipids are important second messengers, transducing extracellular cues into an intracellular response (Schink et al. 2013). A family of phosphoinositide 3-kinases (PI3Ks) catalyses the phosphorylation of inositol lipids at the D3 position of the inositol ring of different phosphoinositides (Costa et al. 2011). Further studies over many years in both vertebrate and invertebrate systems have identified a wide range of cellular roles for PI3K signalling, extending to cell survival, cell polarity and migration (Vanhaesebroeck 1996). At a tissue level, PI3K signalling is implicated in diverse physiological process including angiogenesis (Bing-Hua Jiang et al. 2009), cardiovascular homeostasis (Damilano et al. 2010), immunity (Okkenhaug 2013) and metabolic control (Foukas et al. 2011). This diversity is borne from the huge range of effectors that the three PI3K classes possess (Vanhaesebroeck et al. 2010; Costa et al. 2011).

The three classes of PI3K differ in their structure, enzymatic function and subcellular localisation (**Fig. 6.1.3**). Class I PI3K regulates the conversion of PtdIns(4,5)P_2 to PtdIns(3,4,5)P_3; Class II PI3K catalyses the conversion of PtdIns(4)P to PtdIns(3,4)P_2; Class III PI3K catalyses that conversion of

PtdIns to PtdIns(3)P (Vanhaesebroeck et al. 2010) . These lipid modifications are recognised by PH, PZ and FYVE domains in effector proteins, respectively. By modulating the lipid composition of membrane in specific subcellular compartments, PI3K can regulate the localisation and activity of its effectors (Vanhaesebroeck et al. 2010; Costa et al. 2011; Schink et al. 2013). The role of Class III PI3K in the regulation of endocytic trafficking is discussed in Section 1.3.5.2.

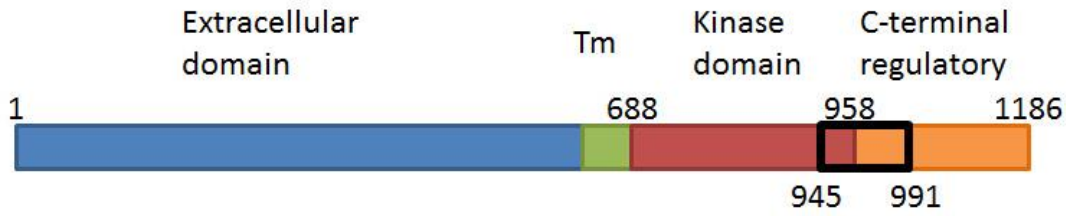


Figure 6.1.2. Schematic representation of EGFR. Numbers indicate amino acid residues numbered from N terminus. EGFR possess an extracellular ligand-binding domain (blue) and transmembrane domain (Tm, green), a kinase domain (red) and a C-terminal regulatory region. Residues 945-991 (black box) are required for occupancy-mediated lysosomal targeting. Figure adapted from (Opresko et al. 1995).

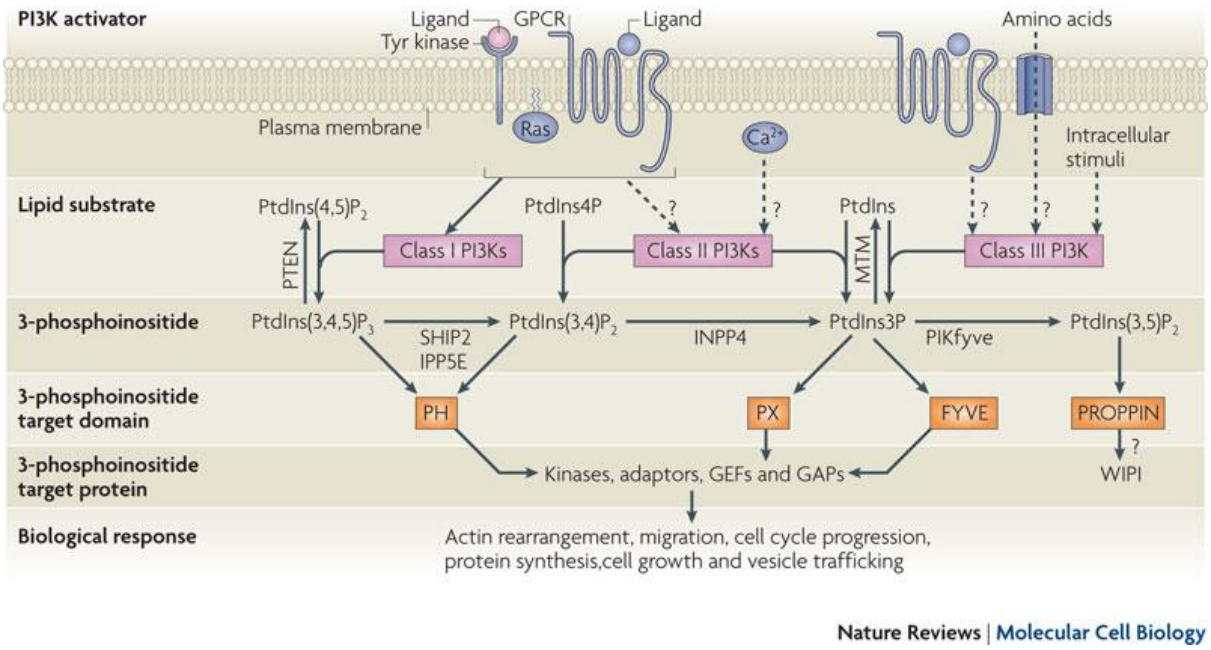


Figure 6.1.3. Isoform-specific lipid kinase activity of PI3K. Figure from (Vanhaesebroeck et al. 2010).

6.1.2.1 Class I PI3K in RTK signalling and cell growth

Class I PI3Ks are composed of a catalytic subunit p110 and a regulatory adaptor subunit e.g. p85, and are responsive to nutrient status through activation by Insulin Receptor signalling (Britton et al. 2002). Of the three classes of PI3Ks, only Class I is clearly regulated by RTK activation due to the presence of an SH2 domain, which recruits and directly activates the p110/p85 heterodimer following RTK autophosphorylation (Lindmo et al. 2006). In addition, Class I PI3K activity is also indirectly modulated by RTKs via the oncogene, Ras, via the presence of their Ras-binding domain (RBD) (Orme et al. 2006). The requirement for Ras-dependent PI3K activation for full PI3K activation *in vivo* has been shown in *Drosophila,* demonstrating the role of PI3K in the integration of multiple signals (Orme et al. 2006). *Drosophila* possesses one Class I PI3K, *Dp110*. The generation of PtdIns(3,4,5)P_3 at the plasma membrane is recognised by effector proteins containing PH domains, and results in the recruitment and activation of the serine-threonine protein kinase Akt and inactivation of the small GTPase regulators, TSC1 and TSC2 (Tuberous Sclerosis 1/2) (Vanhaesebroeck et al. 2010; Mendoza et al. 2011), as well as leading to altered regulation of RabGTPase GAPs and GEFs (Vanhaesebroeck et al. 2010).

Initial experiments identified a crucial role for PI3K in the regulation of cell growth and/or proliferation. The generation of PtdIns(3,4,5)P_3 at the plasma membrane by Class I PI3K initiates a transduction cascade through the recruitment and activation Akt and its downstream targets (mTORC1, GSK3 (Glycogen synthase kinase 3) and the Forkhead box family of transcription factors (FOXOs) (Leevers et al. 1996; Mendoza et al. 2011). Importantly, studies in *Drosophila* have shown that Class III PI3K catalytic subunit Vps34 activity is not required for TOR activation (Juhász et al. 2008). Class I PI3K activity is antagonised by the activity of the tumour suppressor, Pten (Phosphatase and Tensin Homologue), which dephosphorylates PtdIns(3,4,5)P_3 to PtdIns(4,5)P_2. Like PI3K, initial studies in *Drosophila* identified a key role for Pten in the regulation of cell growth and proliferation (Goberdhan et al. 1999), and it has also been shown to affect cell survival in tumour cells (Leslie et al. 2009). Cytosolic Pten is recruited to the plasma membrane via its C-

terminal C2 domain, which recognises PtdIns(3,4,5)P_3 created by the activity of Class I PI3K (Das et al. 2003). Furthermore, of the three splice variants of *Drosophila Pten* (*Pten1*-3), only Pten2 contains the PDZ-binding domain present in mammalian Pten, targeting it to specific regions of the plasma membrane which contain PDZ-domain-containing proteins such as dlg1 (Yamamoto et al. 2004).

6.1.2.2 Class I PI3K signalling and endocytic trafficking

PI3Ks play crucial roles throughout the endocytic pathway, regulating both early and late trafficking events. The PtdIns(3,4,5)P_3-enriched plasma membrane created by the activity of Class I PI3K has been shown to recruit RabGTPase GAPs and GEFs via their PH domains (Vanhaesebroeck et al. 2010). Rab5 interacts with both the mammalian Class I PI3K p110beta and the Class III PI3K Vps34, and their activities at the plasma membrane are necessary for the recruitment of Rab5 (Shin et al. 2005). Previous work has suggested a possible novel role for Class I PI3Ks in the production of PtdIns(3)P through its interaction with Rab5, although the physiological significance of this activity remains unexplored (Vanhaesebroeck et al. 2010).

6.1.2.3 PI3K, PTEN, cancer and exosomes

Due to its central role in the regulation of cell growth, proliferation and survival (Leevers et al. 1996; Goberdhan et al. 1999), the PI3K-Akt-mTOR pathway is one of the most commonly mis-regulated cascades in cancer (Fruman et al. 2014). Mutations in both *Pten* and the gene encoding the catalytic subunit of PI3K, *PI3KCA,* are frequently observed in a wide range of human cancers, including prostate (Assinder et al. 2009), as a result of their tumour suppressor and oncogenic activities, respectively (Fruman et al. 2014).

Interestingly, the down-regulation of Pten can also occur in the absence of genetic mutation (Parsons 2004; Gabriel et al. 2013). It has been proposed that one mechanism of reduced Pten protein expression involves the increased secretion of this tumour suppressor on exosomes

(Gabriel et al. 2013), which may modulate PI3K signalling in cancer cells. Pten incorporation into exosomes is stimulated by EGFR signalling in prostate cancer cells (Gabriel et al. 2013), suggesting complex interactions between oncogenic signalling pathways governing cancer cell exosome secretion.

Recent studies have implicated invadopodia, actin-rich cellular projections that function in extracellular matrix degradation by, and migration of, invasive cancer cells, in exosome secretion and have demonstrated a critical role for Class I PI3K in both invadopodia formation (Hoshino et al. 2012) and exosome secretion (Hoshino et al. 2013). The authors suggest that invadopodia create docking sites for MVBs and thus indirectly regulate exosome secretion through increasing surface area.

6.1.3 Aims and objectives

1. Investigate whether SC exosomes carry RTKs
2. Investigate whether EGFR and Class I PI3K signalling regulates exosome secretion in SCs
3. Characterise the role of EGFR and Class I PI3K signalling in the regulation of SC endocytic and secretory trafficking

6.2 Methods

See Sections 2.3.3-2.6 for live imaging of SCs and quantification of exosome secretion assays; SC compartments were counted as for Figs. 3.20 and 3.21. Although care was taken to count iLEs by eye as accurately as possible, the number of iLEs counted varied between experimental runs of control cells (see Fig. 6.B4 and 6.8B). Therefore effects of genetic manipulations on iLEs numbers should be interpreted with caution.

6.3 Results

6.3.1 SCs secrete EGFR-GFP and FGFR-GFP into the accessory gland lumen

Several studies report RTK signalling components associated with exosomes (Sanderson et al. 2008; Adamczyk et al. 2011; Higginbotham et al. 2011; Demory Beckler et al. 2013). Previous analysis of an enhancer trap line demonstrated specific expression of Breathless (Btl) (encoding *Drosophila* FGFR) in SCs (A. Leiblich and Z. Syed, unpublished). Data presented in this thesis suggests the EGFR is also expressed in SCs (indirect evidence from knockdown, section 6.3.2). To investigate whether exosomes secreted by SCs might carry RTKs, we expressed GFP-tagged EGFR and Btl specifically in SCs. In fixed glands, both EGFR-GFP and Btl-GFP localised to the limiting membrane of a subpopulation of large SC secretory compartments (**Fig 6.1B and 6.2A**). Fluorescent GFP puncta were also observed within one or two of these compartments per SC. However, the identity of these compartments was not investigated further, in part due to the non-uniform expression levels of EGFR-GFP in SCs within the same gland, when driven by *spi-Gal4* (**Fig. 6.1A**). The majority of EGFR-GFP and Btl-GFP was observed intracellularly; limited fluorescence was observed at the apical plasma membrane (**Fig. 6.1B and 6.1D**). A small number of EGFR-GFP and Btl-GFP puncta were observed in the gland lumen, suggesting that both the EGFR and FGFR are secreted, presumably on membrane-bound vesicles (**Fig. 6.1C-D, 6.2B**).

6.3.2 Autocrine EGFR signalling regulates endocytic and secretory trafficking events

Given the presence of EGFR-GFP on putative exosomes secreted by SCs, the SC-specific expression of the EGFR ligand, *spitz* in the AG (**Fig. 2.1**), as well as reports of EGFR modulating early endocytic trafficking events in mammalian cell line studies (Section 6.1.1.3), we analysed the effects of modulating EGFR signalling on the SC secretory and endocytic compartments by live cell imaging.

Modulating EGFR signalling in SCs expressing CD63-GFP had significant effects on endocytic and secretory compartment number, size and morphology (**Fig. 6.3 and 6.4**). As previously described (Section 3.3.3), SCs of 6-day-old AGs contain approximately 2-3 mMVBLs, the largest of which is approximately 10µm in diameter and contains numerous CD63-GFP-postive ILVs; approximately 4 iLEs and 20 non-acidic SVs (**Figure 6.3A and 6.4**). Expression of a constitutively active EGFR (*EGFR*^{ACT}), harbouring an A887T point mutation in the kinase domain (Lesokhin et al. 1999), produced a strong cellular phenotype affecting both secretory vacuole and late endosome formation (**Figure 6.3B**). However, this phenotype could not be quantified by our standard assays as the compartments could not be distinguished due to a lack of a clear CD63-GFP-positive limiting membrane. The diffuse expression of CD63-GFP throughout the cytosol suggests the presence of large amounts of small secretory membrane-bound vesicles that have not matured and/or fused to form distinct secretory vacuoles.

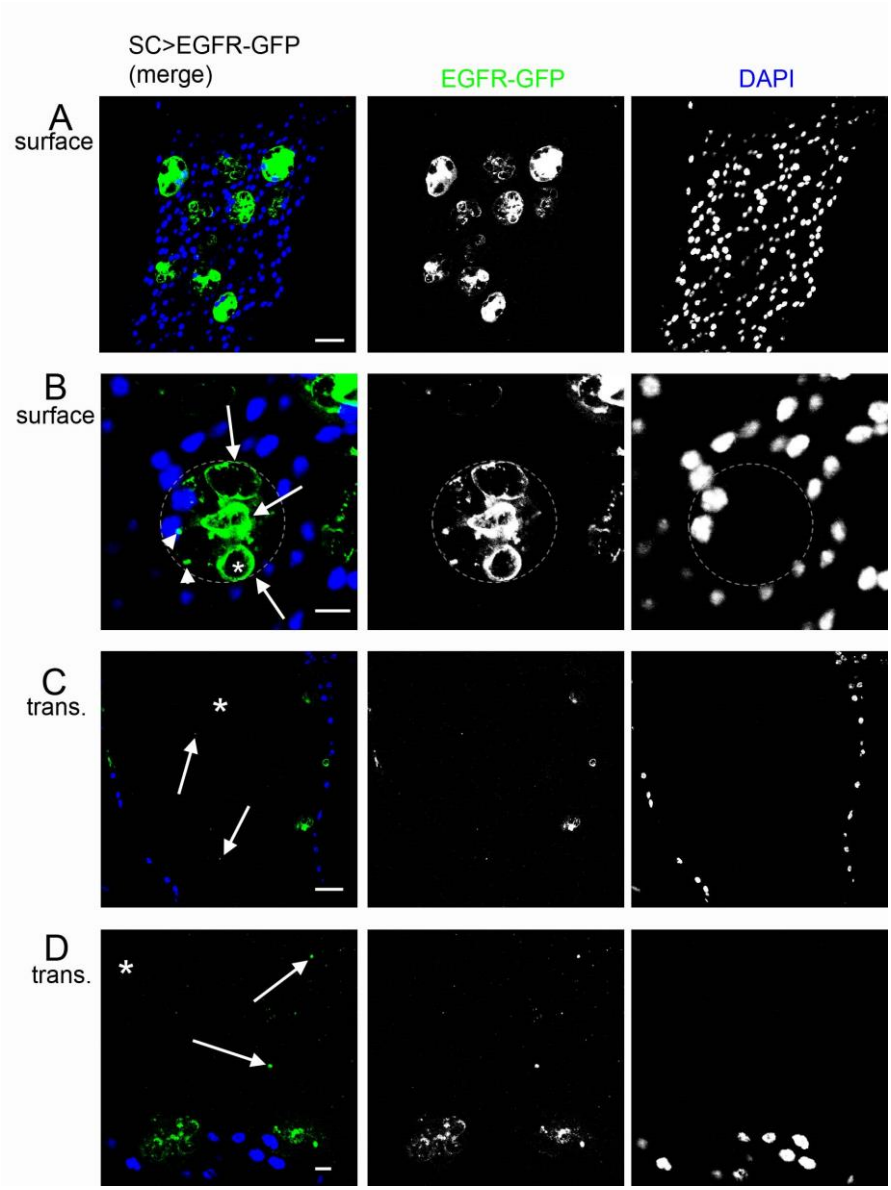


Figure 6.1. SCs secrete EGFR-GFP into the accessory gland lumen. 3-day-old *spi-Gal4, Tub-Gal80^{ts}; UAS-EGFR-GFP* virgin male AG stained with DAPI (blue). Flies were maintained at 18˚C until eclosion when they were shifted to 29˚C to induce transgene expression. EGFR-GFP localises to the limiting membrane of a subpopulation of large SC compartments (**B**, arrows), as well as small puncta both within (centre compartment in **B**) and outside (**B**, arrow heads) large intracellular compartments. EGFR-GFP is secreted into the gland lumen (**C** and **D**; *) as discrete puncta (**D**, arrows). **A** and **B** show surface images across the plane of the epithelium; **C** and **D** show transverse image through the gland revealing the surrounding epithelium in cross-section and the gland lumen (*). Limited EGFR-GFP was observed at the plasma membrane. Scale bars: (**A** and **C**) 20µm, (**B** and **D**) 5µm.

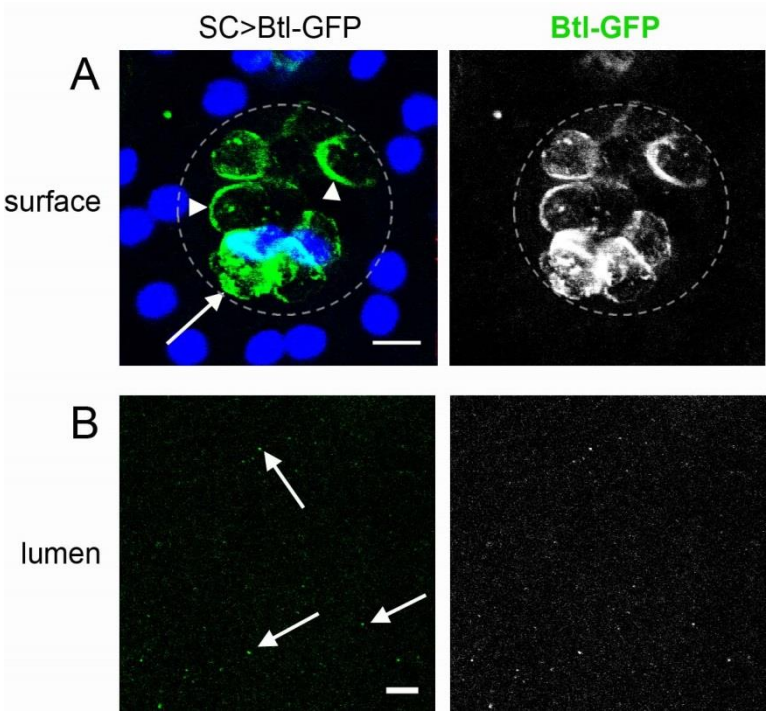


Figure 6.2. FGFR-GFP is secreted by SCs into the accessory gland lumen. 3-day-old virgin male expressing *UAS-Btl-GFP* under control of *spi-Gal4; Tub-Gal80^{ts}*. Flies were maintained at 18˚C until eclosion when they were shifted to 29˚C to induce transgene expression. Btl-GFP localises to the limiting membrane of many SC secretory compartments (**A**, arrow heads), some of which contain Btl-GFP puncta inside (**A**, arrow). (**B**) Btl-GFP puncta are also seen in the gland lumen (**B**, arrows). Approximate cell outline indicated in **A** by dashed circle; limited EGFR-GFP was observed at the plasma membrane. Scale bars, 5µm.

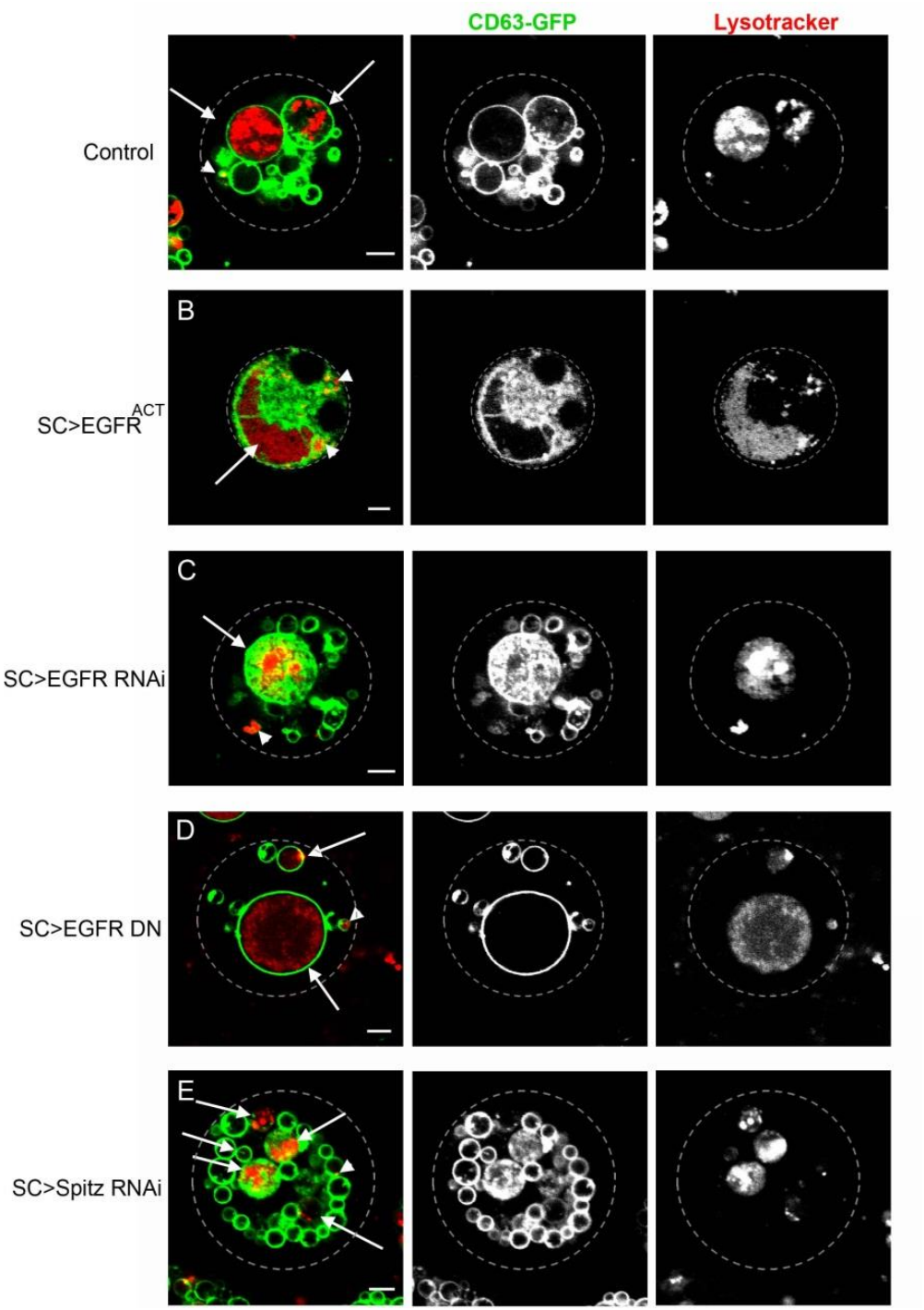


Figure 6.3. Modulating EGFR signalling in virgin males alters the morphology of SC endocytic and secretory compartments. Representative images of individual SCs expressing CD63-GFP from AGs dissected from 6-day-old virgin males, stained with Lysotracker-Red. *UAS-CD63-GFP, Tub-Gal80^{ts}; dsx-GAL4* males (co-expressing various transgenic constructs; control flies were obtained by crossing the above driver line to w^{1118}) were shifted to 29˚C at eclosion. (**A**) Control SCs expressing CD63-GFP contained several large acidic mMVBLs (arrows), which included a number of GFP puncta inside, as well as iLEs which were also CD63-GFP-positive (arrowheads). (**B**) SCs

expressing *EGFR*^{ACT} were severally malformed. mMVBLs (arrows) and iLEs (arrowheads) could not be easily distinguished due to the presence of CD63-GFP throughout the cell cytoplasm. (**C**) Knockdown of *EGFR* by RNAi induces large mMVBLs filled with CD63-GFP-positive ILVs (arrow). (**D**) SCs expressing an EGFR dominant negative construct (*EGFR-DN*) contain large mMVBLs which lack CD63-GFP ILVs (arrow). (**E**) *spitz*-RNAi-expressing SCs contain multiple small mMVBLs of normal morphology (arrows) and many of secretory vacuoles. Arrows indicate mMVBLs (acidic compartments greater than 2µm in diameter); arrowheads indicate iLEs (acidic compartments less than 2µm). Scale bars, 5µm. Approximate position of limiting membranes of individual SCs are indicated by dashed circle.

Down-regulation of EGFR signalling by modulating both the levels (**Fig. 6.3C**) and activity (**Fig. 6.3D**) of the EGFR produced surprisingly dissimilar effects of SC biology. Whilst both manipulations resulted in the formation of enlarged mMVBLs, mMVBLs of SCs expressing a dominant negative EGFR (*EGFR-DN*), harbouring a C-terminal truncation and lacking the entire kinase domain (Buff et al. 1998), contained no CD63-GFP ILVs, whilst mMVBLs of SCs expressing an RNAi construct targeting the EGFR were filled with ILVs. Furthermore, only SC>*EGFR*-RNAi cells contained significantly fewer iLEs than controls (**Fig 6.4B**), whilst only *EGFR DN*-expressing SCs contained significantly fewer SVs (**Fig 6.4C**). Unlike modulating signalling by manipulation of the receptor, knockdown of the EGFR ligand *spitz* by RNAi produced SCs with significantly more mMVBLs, which were significantly smaller than controls, as well as more SVs (**Fig. 6.3E and 6.4A**). Taken together, these data indicate that the level of EGFR signalling in SCs regulates multiple aspects of both secretory and late endosomal SC biology, presumably in an autocrine manner involving secretion of the ligand, spitz.

Given the strong effect of reducing EGFR signalling on SC endocytic compartments, we hypothesised that modulating EGFR signalling would affect exosome secretion. Indeed, several experiments utilising the lumen secretion assay employed previously (Section 3.3.9) demonstrated that modulating EGFR signalling could significantly affect numbers of exosomes secreted by SCs. However, unlike many other genetic manipulations (Section 3.3.9.2 and **Fig. 3.22**), the effect observed was not consistent between experiments (**Fig. 6.5A-D**) making it difficult to draw firm conclusions.

6.3.4 Class I PI3K signalling regulates endocytic and secretory trafficking events in SCs

PI3Ks have well-characterised roles regulating early (Class I and II) and late (Class III) endocytic trafficking events (Li et al. 1995; Vanhaesebroeck et al. 2010) and Class I PI3K activity promotes receptor-mediated endocytosis (Li et al. 1995) (Sections 1.3.5.2 and 6.1.2.2). In addition, Class I PI3K activity is stimulated by EGFR activation (Orme et al. 2006), which appears to alter SC

endolysosomal trafficking. To investigate the role of PI3K signalling in the regulation of intracellular membrane trafficking in SCs, we used live cell imaging to analyse the effects of modulating the activity and/or levels of the *Drosophila* Class I PI3K, Dp110, as well as its functional antagonist, Pten, in SCs expressing CD63-GFP (**Fig. 6.6 and 6.7**). Increasing Dp110 signalling by both RNAi-mediated knockdown of *Pten* and expression of a constitutively activated PI3K possessing a C-terminal farnesylation signal directing membrane targeting (CAAX; $Dp110^{ACT}$) (Leevers et al. 1996; Parrish et al. 2009), significantly increased the number of mMVBLs per SC; however, over-expression of wild-type *Dp110*, which can have weaker effects in other *in vivo* assays (Leevers et al. 1996), did not have the same effect (**Fig. 6.8A**). The size of mMVBLs was also affected by the level of PI3K signalling: over-expression of both *Dp110* and $Dp110^{ACT}$ significantly increased the size of mMVBLs (**Fig. 6.8D**). Conversely, down-regulating PI3K signalling by expression of a dominant negative Dp110 (*Dp110-DN*), harbouring a D954A point mutation in the ATP binding site, which renders the protein 'kinase-dead' (Leevers et al. 1996) reduced the size of mMVBLs. *Drosophila* possesses three *Pten* splice isoforms (1-3), only Pten2 contains a PDZ-binding domain also found in mammalian Pten (Yamamoto et al. 2004; Pinal et al. 2006). Interestingly, whilst expression of a Pten not containing the PDZ-binding domain significantly reduced the size of mMVBLs, expression of the PDZ-domain containing isoform (*PTEN-PDZ*; i.e. *Pten2*) did not have the same effect of mMVBL size (**Fig. 6.8D**).

In addition to affecting the size of mMVBLs, modulating the level of PI3K signalling also affected the morphology of the mMVBLs formed. In contrast to control SCs whose mMVBLs contained sporadic CD63-GFP-positive ILVs (**Fig. 6.6A and 6.7A**), the mMVBLs of *Dp110* and $Dp110^{ACT}$ SCs were filled with more CD63-GFP-positive ILVs (**Fig. 6.6B and 6.6D**). Conversely, mMVBLs of SCs expressing *Dp110-DN* did contain CD63-GFP-positive ILVs (**Fig. 6.6C**), an effect also observed following *ESCRT* knockdown (**Fig. 3.20**) or increased BMP signalling (**Fig. 5.2**)**.** The mMVBLs of SCs expressing *PTEN*-RNAi, *PTEN-PDZ* and *PTEN* contained variable numbers of GFP puncta (**Fig. 6.7**); we observed mMVBLs both filled, as well as void, of CD63-GFP within individual SCs following

expression of *PTEN* and *PTEN-PDZ*, whilst the mMVBLs of *PTEN*-RNAi SCs did not appear consistently different to control.

Modulating PI3K signalling also had effects on upstream endocytic trafficking. Over-expression of *Dp110, Dp110^{ACT}* or *PTEN*-RNAi all resulted in a significant increase in the number of iLEs per SC (**Fig. 6.8B**). Interestingly, down-regulating PI3K signalling had no effect on the number of mMVBLs or iLEs, with the exception of *PTEN-PDZ* expression, which displayed a small yet significant increase in the number of iLEs, although this effect varied greatly between SCs (**Figure 6.8A and 6.8B**).

Overall, these data suggest that PI3K signalling promotes late endosomal trafficking to drive the formation of large mMVBLs, potentially through increasing the rate of upstream endosomal trafficking resulting in the formation of more iLEs. However, PI3K signalling does not appear to be necessary for the formation and/or maturation of late endosomal compartments and its effects are more variable than those of many of the other genetic manipulations I have tested.

PI3K signalling had the opposite effect on SV formation. Down-regulating PI3K signalling by expression of either *PTEN* isoform *PTEN-PDZ* or *PTEN* significantly increased the number of SVs, although *Dp110-DN* had no effect on SV number (**Fig. 6.8D**). Conversely, expression of *Dp110* resulted in a small but significant decrease in the number of SVs, although other activating manipulations had no effect (**Figure 6.8D**). These data suggest that PI3K signalling in SCs may regulate endolysosomal trafficking and secretory vacuole formation and/or trafficking.

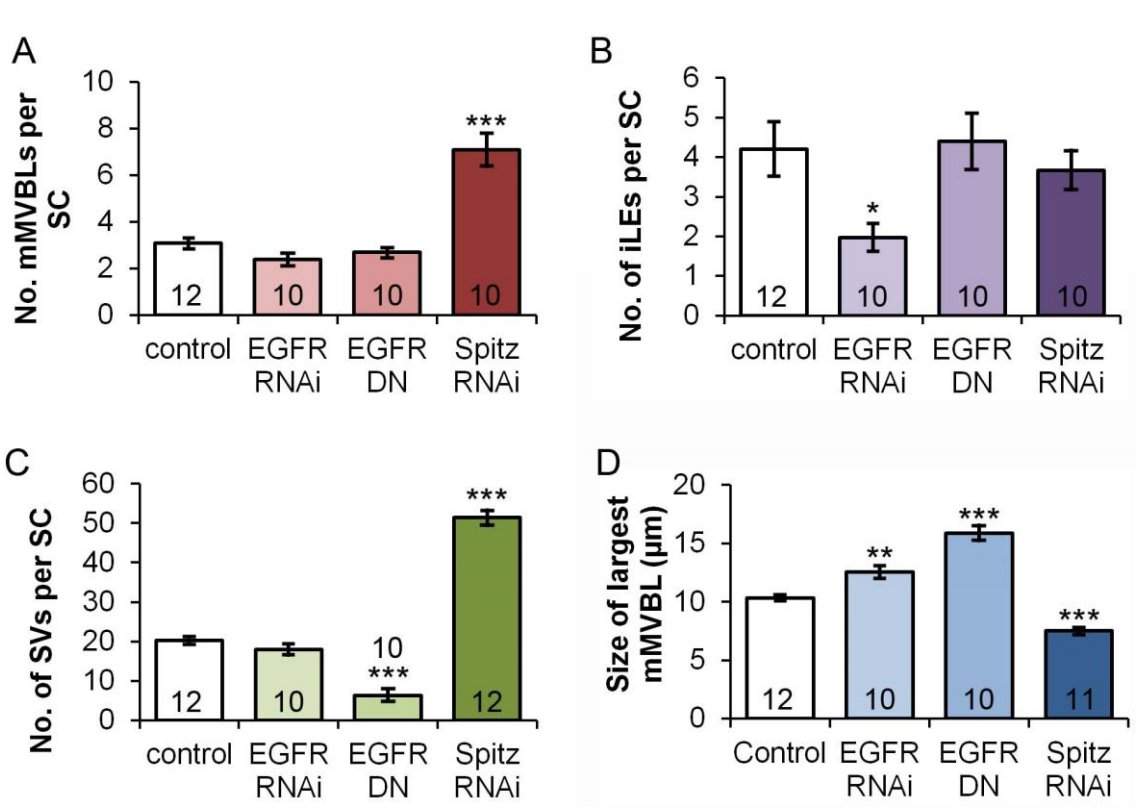


Figure 6.4. Modulating EGFR signalling alters the number and size of SC endocytic and secretory compartments. Different SC intracellular compartments from AGs of 6-day-old virgin males dissected and stained with Lysotracker-Red were quantified and measured. *UAS-CD63-GFP; Tub-Gal80^{ts}; dsx-GAL4* males (co-expressing various transgenic constructs; control flies were obtained by crossing the above driver line to *w*^{1118}) were shifted to 29˚C at eclosion. (**A**) Average number of mMVBLs per SC. SCs expressing s*pitz-RNAi* had significantly more mMVBLs. (**B**) Average number of iLEs per SC. Reducing levels of the EGFR by RNAi results in significantly fewer iLEs. (**C**) Average number of secretory vacuoles per SC. The number of SVs was significantly reduced following expression of *EGFR-DN*, but significantly increased following knockdown of the EGFR ligand, *spitz*. (**D**) Average size of the largest mMVBL in each SC, measured by the widest diameter (µm). Both expression of *EGFR-DN,* as well as knockdown of the receptor by RNAi (*EGFR*-RNAi), significantly increased the size of the largest mMVBL, whilst knockdown of the ligand (*spitz*-RNAi) significantly reduced the size of the largest mMVBL. Values indicate averages of 3 SCs per gland, averaged over *n* glands (number in bars). Error bars indicate ±SE. *p<0.05, **p<0.01; ***p<0.001; pairwise comparisons relative to control; data were analysed using either an unpaired two-tailed Student's t test or Mann-Whitney U test, for normally and non-normally distributed data sets, respectively.

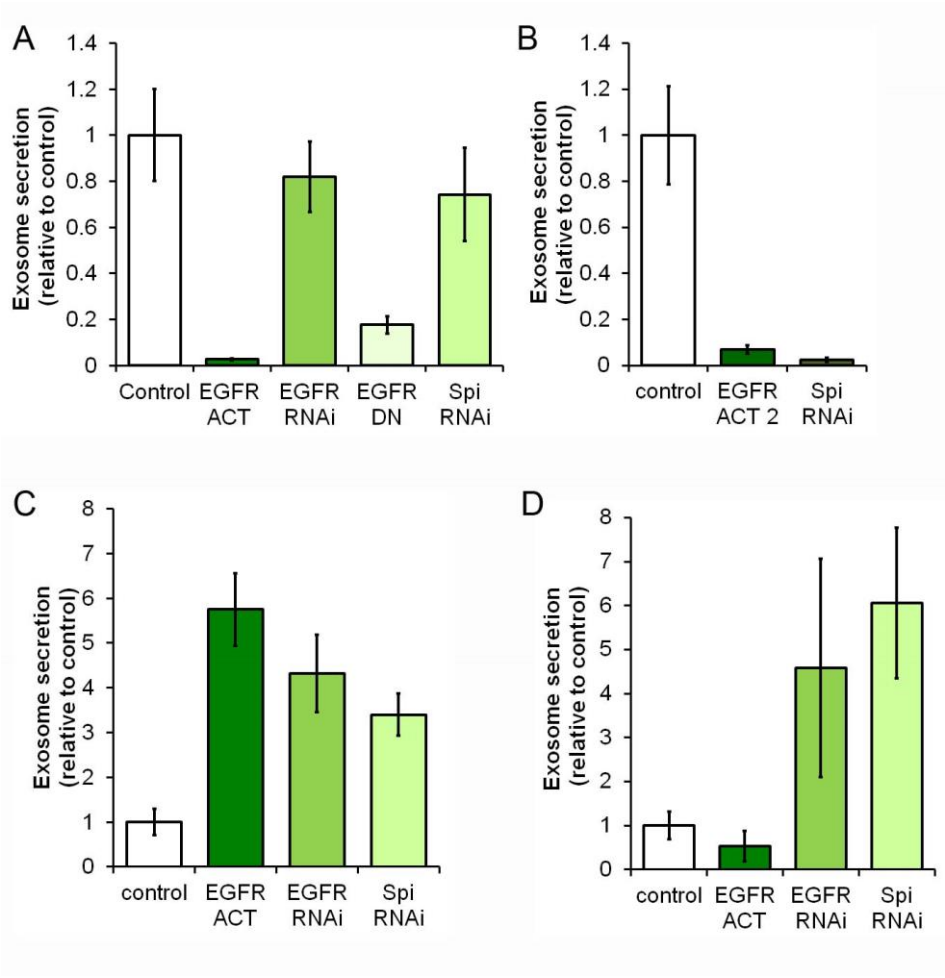


Figure 6.5. Modulating EGFR signalling alters CD63-GFP exosome secretion in a non-reproducible manner. (A-D) Quantifications of 4 independent experiments with their associated controls carried out simultaneously. The number of CD63-GFP-particles secreted into the gland lumen was assayed following genetic manipulation of EGFR signalling. The values represent the average particles in a 7225 μm^2 luminal area, averaged over 3 confocal sections at 5µm intervals for each gland, and then over 'n' glands (n>8). Exosome secretion provided relative to the control value for each independent experiment carried out simultaneously. *UAS-CD63-GFP, Tub-Gal80^{ts}; dsx-Gal4* males (co-expressing various transgenic constructs; control flies were obtained by crossing the above driver line to *w^{1118}*) were shifted to 29˚C at eclosion to induce post-developmental transgene expression and mated to 3 females at 2 days (to expel the stored luminal contents), allowed to recover for 24 hours and then dissected at 4 days. Error bars indicate ±SE. Statistical significance was not calculated due to the large inter-experimental variation observed.

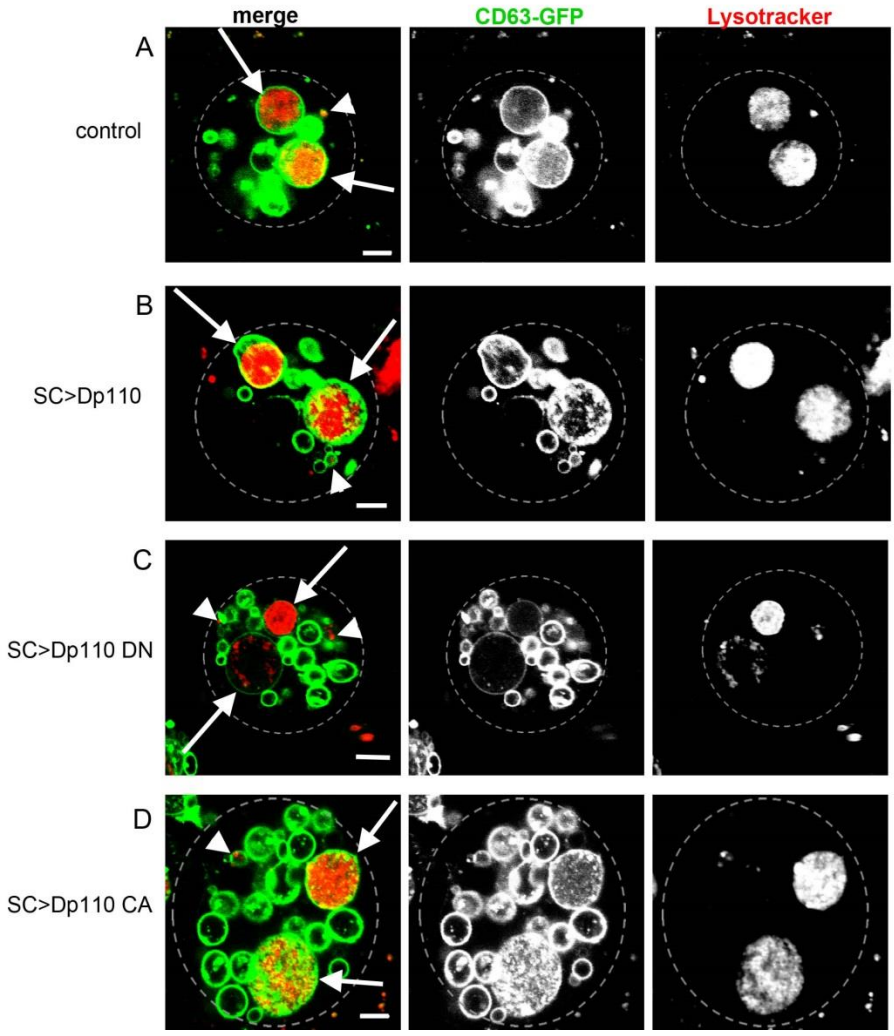


Figure 6.6. Modulating Class I PI3K (*Dp110*) signalling alters the morphology of endocytic and secretory compartments. Representative images of individual SCs expressing CD63-GFP (green) 6-day-old virgin male AGs, stained with Lysotracker-Red (red). *UAS-CD63-GFP, tub-Gal80^{ts}; dsx-Gal4* males (co-expressing various transgenic constructs; control flies were obtained by crossing the above driver line to *w^{1118}*) were shifted to 29˚C at eclosion. (**A**) Control SCs expressing CD63-GFP contained several large acidic mMVBLs (arrows) that include a number of GFP-positive puncta inside, as well as CD63-GFP-positive iLEs (arrowheads). (**B**) mMVBLs of SCs overexpressing *Dp110* did not appear morphologically different to controls. (**C**) SCs expressing a dominant-negative PI3K mutant (*Dp110-DN*) often contained a large mMVBL with a weakly labelled CD63-GFP-positive membrane (arrow). (**D**) SCs expressing a constitutively-activate PI3K mutant (*Dp110-CA*) contain large mMVBLs filled with CD63-GFP-positive ILVs (arrow). Arrows indicate mMVBLs (acidic compartments >2µm in diameter); arrowheads indicate iLEs (acidic compartments <2µm). Scale bars, 5µm. Approximate cell outlines marked with dashed circle.

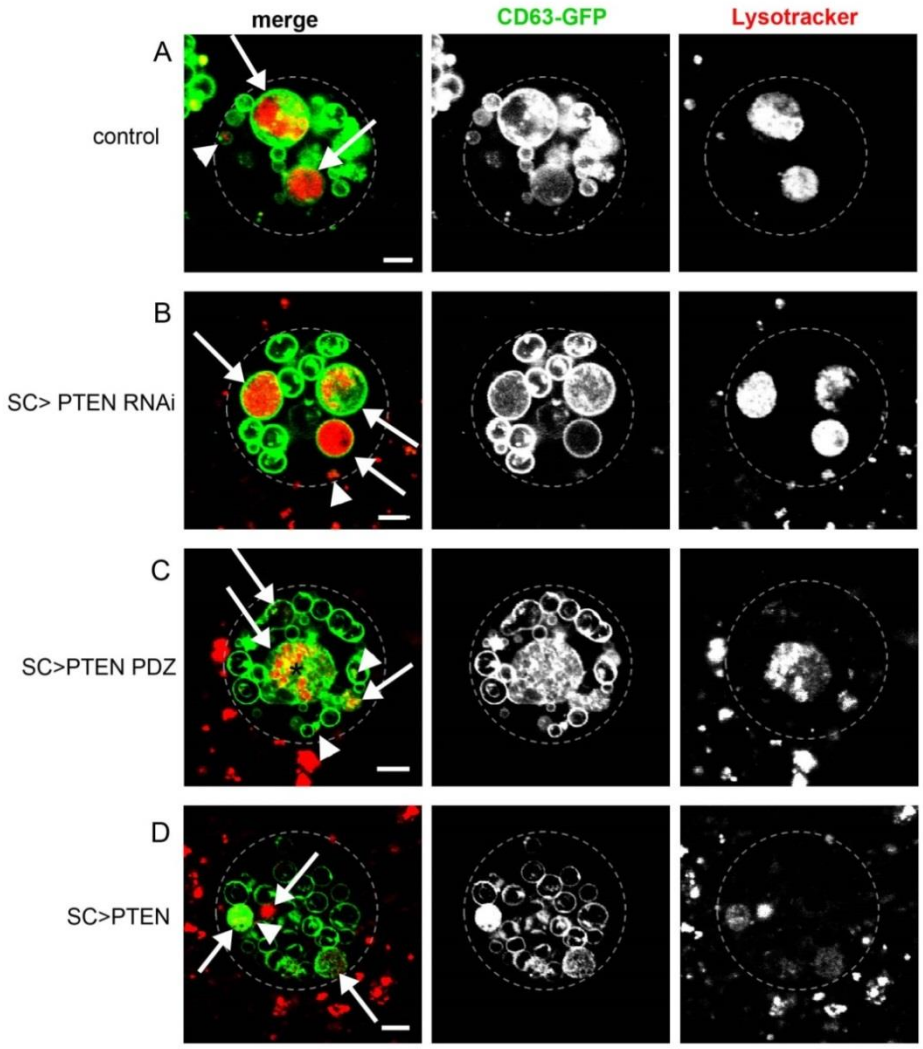


Figure 6.7. Modulating PTEN signalling alters the morphology of endocytic and secretory compartments. Representative images of individual SCs, expressing CD63-GFP (green) of 6-day-old virgin male AGs, stained with Lysotracker-Red (red). *UAS-CD63-GFP, tub-Gal80^{ts}; dsx-Gal4* males (co-expressing various transgenic constructs; control flies were obtained by crossing the above driver line to *w^{1118}*) were shifted to 29˚C at eclosion. (**A**) Control SCs expressing CD63-GFP contained several largest acidic mMVBLs (arrows), which included a number of GFP-positive puncta inside, as well as iLEs which were also CD63-GFP-positive (arrowheads). (**B**) SCs overexpressing *PTEN*-RNAi contain mMVBLs of 'normal' morphology (arrows). (**C**) SCs expressing *PTEN-PDZ* contain mMVBLs of variable morphology (arrows), some of which are completely filled with CD63-GFP (*). (**D**) SCs overexpressing a form of *PTEN* lacking the PDZ domain contain mMVBLs of 'normal' morphology with CD63-GFP ILVs (arrow). Arrows indicate mMVBLs (acidic compartments >2µm in diameter); arrowheads indicate iLEs (acidic compartments <2µm). Scale bars, 5µm. Approximate cell outlines marked with dashed circle.

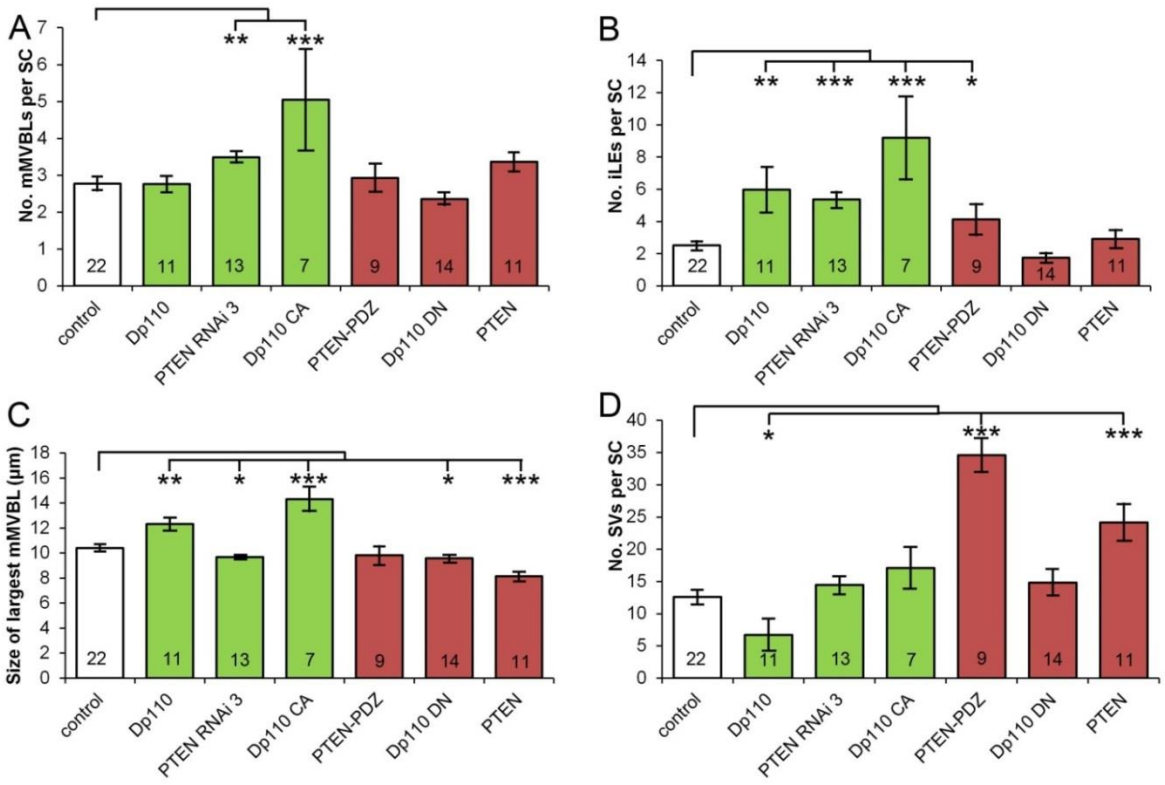


Figure 6.8. Modulating PI3K signalling alters the number and size of endocytic and secretory compartments. AGs dissected from 6-day-old virgin males were stained with Lysotracker-Red and the intracellular compartments of SCs were quantified and measured. *UAS-CD63-GFP, Tub-Gal80^{ts}; dsx-Gal4* males (co-expressing various transgenic constructs; control flies were obtained by crossing the above driver line to *w*^{1118}) were shifted to 29˚C at eclosion. (**A**) Average number of mMVBLs per SC. SCs expressing *Dp110-CA and PTEN*-RNAi contained significantly more mMVBLs. (**B**) Average number of iLEs per SC. SCs expressing *Dp110*, *Dp110-CA* and *PTEN*-RNAi. Surprisingly, the *PTEN-PDZ* transgene also induced a smaller, but significant increase in iLEs. (**C**) Average size of the largest mMVBL in each SC, measured by the widest diameter (µm). SCs expressing *Dp110* and *Dp110-CA* have significantly larger mMVBLs. Conversely, SCs expressing *Dp110-DN, PTEN* and (surprisingly) *PTEN*-RNAi had significantly smaller mMVBLs. (**D**) Average number of secretory vacuoles per SC. SCs expressing *Dp110* contained significantly less SVs, whilst SCs expressing either *PTEN-PDZ* or *PTEN* contained more SVs. Values indicate averages of 3 SCs per gland, averaged over *n* glands (number in bars). Error bars indicate ±SE. *p<0.05, **p<0.01; ***p<0.001; relative to control. Data were analysed using either an unpaired two-tailed Student's t-test or Mann-Whitney U Test, for normally and non-normally distributed data sets respectively. Control experiment carried out on simultaneously.

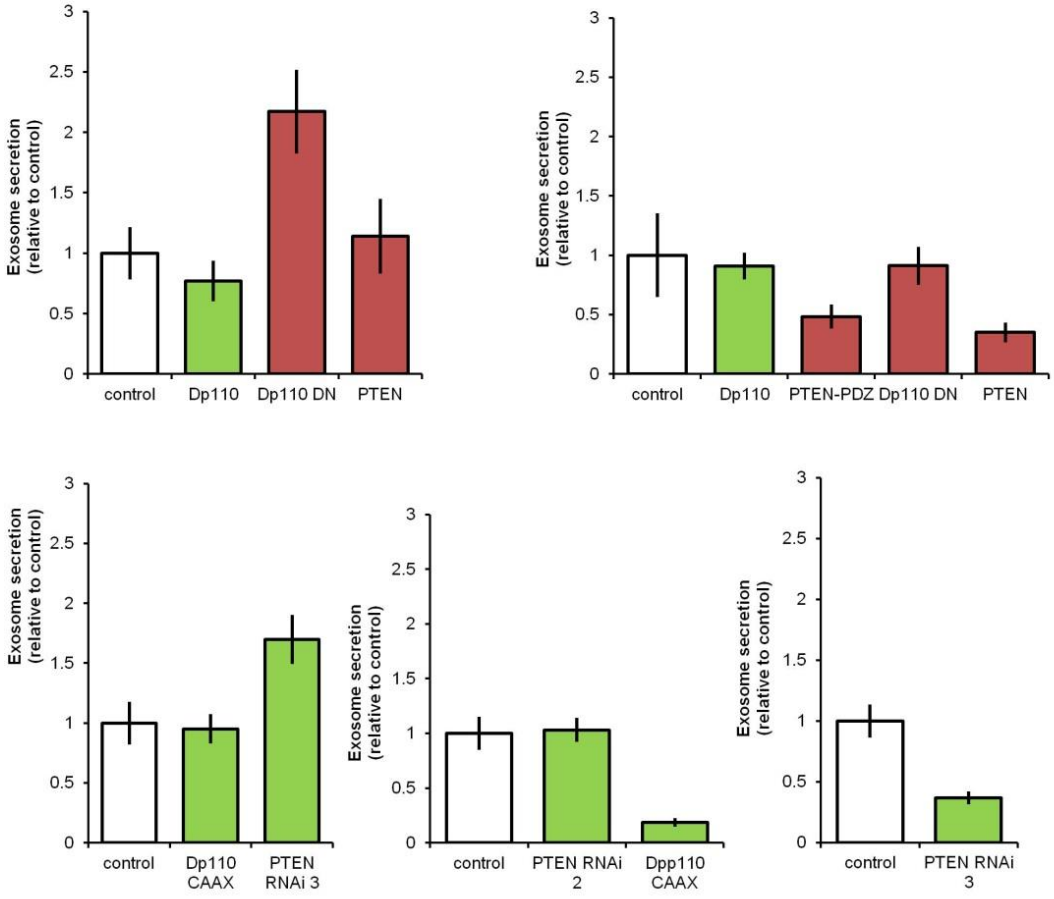


Figure 6.9. Modulating PI3K signalling alters CD63-GFP exosome secretion in a non-reproducible manner. (A-D) Quantifications of 5 independent experiments; the number of CD63-GFP-secreted particles into the gland lumen was assayed following genetic manipulation of PI3K signalling by expression of: Class I PI3K (*Dp110*), constitutively-activated PI3K (*Dp110 CAAX*), dominant negative PI3K (*Dp110 DN*), *PTEN* and PTEN containing a PDZ domain (*PTEN-PDZ*); as well as RNAi-mediated knockdown of PTEN (*PTEN* RNAi). The values represent the average particles in a 7225 μm^2 luminal area, averaged over 3 confocal sections at 5µm intervals, and then over 'n' glands (number above or in bars). Exosome secretion provided as a percentage of the control value for each independent experiment carried out simultaneously. *UAS-CD63-GFP, Tub-Gal80^{ts}; dsx-Gal4* males (co-expressing various transgenic constructs; control flies were obtained by crossing the above driver line to *w^{1118}*) were shifted to 29˚C at eclosion and mated to 3 females at 2 days (to expel the stored luminal contents), allowed to recover for 24 hours and then dissected at 4 days. Error bars indicate ±SE. Statistical significance was not calculated due to the large inter-experimental variation observed.

6.4 Discussion

Signalling by RTKs and their downstream targets in the PI3K signalling cascade has been implicated in membrane trafficking events in other systems (Wiley et al. 1991; Li et al. 1995; Wiedemann et al. 1998; Lanzetti et al. 2000; Shin et al. 2005; Vanhaesebroeck et al. 2010). I employed the SC system to study this in more detail, experiments that suggested potential roles in secretory and endocytic trafficking, but produced greater levels of experimental variation than other genetic manipulations.

6.4.1 The EGFR and FGFR are potential exosome cargos

EGFR-GFP and Btl-GFP were both secreted into the AG lumen in discrete puncta when expressed in SCs. As both RTKs are transmembrane receptors, it is likely that these fluorescent puncta represent membrane-bound vesicles secreted by SCs. As EGFR-GFP showed limited localisation to the apical plasma membrane of SCs, but was internalised in intracellular compartments, I conclude that EGFR-GFP at least is unlikely to be released on MVs shed from SCs. The presence of EGFR-GFP and Btl-GFP puncta inside large secretory compartments of SCs is consistent with them being ILVs in mMVBLs and therefore representing putative future exosomes. Live cell imaging of SCs stained with Lysotracker and expressing EGFR-GFP and Btl-GFP, as well as knockdown of *ESCRT* genes (see below), would allow identification of the compartments inside which these puncta form and reside, and thus provide further support of an exosomal identity.

In comparison to CD63-GFP (**Fig. 3.7 and 3.23A-B**), a very small number of EGFR-GFP- and Btl-GFP-positive puncta were observed in the AG lumen, suggesting that only a small proportion of SC exosomes carry the EGFR-GFP/Btl-GFP. Co-localisation studies with CD63 labelled with an alternative fluorophore (e.g. CD63-tdTomato) may provide insights into the nature of secreted EGFR-GFP- and Btl-GFP-containing structures and address whether these RTKs are present on CD63-GFP-positive or -negative exosomes. As EGFR sorting is classically considered to be ESCRT-

dependent (Chanut-Delalande et al. 2010), it will be necessary to investigate whether EGFR-GFP secretion is blocked by e.g. *Hrs* knockdown in order to confirm an exosomal identity.

It remains possible that the GFP secreted into the lumen in SC>EGFR-GFP and SC>Btl-GFP AGs has been cleaved from the RTK proper. However, as the GFP is fused to the intracellular/cytoplasmic C terminus of EGFR this would still require unconventional secretion mechanisms such as those provided by EVs for extracellular secretion. This idea could be tested using western analysis to screen for full-length fusion protein. I was unable to stain for endogenous EGFR or Btl in the AG using commercially available antibodies (data not shown), even though it is likely that SCs express Btl (*Btl-Gal4* reporter expression; Zain Syed, FHS project 2013) and EGFR (indirect evidence from SC>*EGFR*-RNAi*/spi*-RNAi phenotypes; Section 6.3.2). Therefore whether SC exosomes carry endogenous RTKs remains to be investigated.

I was also unable to obtain evidence for the secretion of membrane-bound spi-GFP (Tsruya et al. 2002) into the gland lumen (data not shown). However, we observed cytoplasmic localisation of this fusion protein, suggesting its high level expression may have affected normal secretory trafficking, a phenotype that would be consistent with the effects of other manipulations modulating EGFR and PI3K signalling (Section 6.4.3).

Several proteomic analyses of isolated mammalian exosomes secreted by cancer cells have identified EGF signalling components including both receptor (Adamczyk et al. 2011; Demory Beckler et al. 2013) and ligand (Higginbotham et al. 2011) as cargos, and these have been hypothesised to function in the modulation of the tumour microenvironment. Given our finding that SC exosomes have the potential to reprogramme females cells (Section 4.3.3), it is tempting to speculate that exosomal-EGFR may function in this process. However, it is important to note that mass spectrometry analysis of isolated exosomes secreted by *Drosophila* S2 and Kc167 cells have not identified any EGFR or FGFR components (Gross et al. 2012; Koles et al. 2012; Beckett et al. 2013), although these cells are clearly very different in phenotype from SCs. Overall, our data

indicate that RTKs may be present on *Drosophila* exosomes secreted by secondary cells, suggesting that exosomal RTKs may have a physiologically relevant signalling role *in vivo*.

6.4.1.1 Autocrine EGFR signalling by SCs

Despite uniform expression levels of *UAS-GFP^{NLS}* as well as *UAS-CD63-GFP* when driven by s*pi-Gal4 (+/- tub-Gal80^{ts}*) (**Fig. 2.1, 3.1 and 3.3**), I observed non-uniform expression of *UAS-EGFR-GFP* between different SCs in an individual AG when using this driver line. I speculate this is a phenotypic consequence of receptor overexpression, which might increase EGFR signalling levels. This could induce negative feedback mechanisms (Section 6.1.2), altering the expression level of the ligand *spitz*, whose promoter was used to drive transgene expression. A negative feedback mechanism involving the transcriptional down-regulation of EGFR ligands has not been previously reported in flies (Shilo 2005; Singh et al. 2005). Phenotypic analysis of EGFR-GFP expression by live cell imaging as well as the use of an alternative *Gal4* line to drive SC-specific expression may provide further insight into the nature of autocrine EGFR signalling in SCs.

6.4.2 Regulation of exosome secretion by EGFR and PI3K signalling

Despite identification of EGFR and PI3K signalling components on exosomes, their well-characterised oncogenic roles (Fruman et al. 2014) and the increase in exosome secretion during tumorigenesis (Higginbotham et al. 2011; Ge et al. 2012), there are no studies clearly implicating these signalling pathways in the regulation of exosome secretion. Unfortunately, I was unable to obtain reproducible effects on CD63-GFP secretion using the assay employed to effectively and reproducibly block exosome secretion by knockdown of ESCRT components (**Fig. 3.23**), when modulating either EGFR or PI3K signalling. Nevertheless, our findings demonstrate that SC exosome secretion is affected by the level of both EGFR and PI3K signalling, and that their roles in the regulation of exosome secretion appear to be complex, probably involving the regulation of multiple aspects of both endocytic and secretory membrane trafficking.

A recent study has implicated PI3K signalling in negative regulation of exosomes with angiogenesis-promoting properties secreted by endothelial cells (Ju et al. 2014). Oncogenic Ras mutations (Kras) in cancer cells lines, which can modulate PI3K signalling, have been suggested to increase secretion of exosomes carrying the EGF ligand, amphiregulin (Higginbotham et al. 2011). However, in both studies exosome number was inferred from western blot analysis of purified exosomes; therefore, it remains possible that in these systems, PI3K and EGFR regulate cargo loading into vesicles rather than vesicle biogenesis or secretion. My findings that modulation of both EGFR signalling and PI3K signalling affects the number of CD63-GFP-positive secreted puncta provides the first direct *in vivo* evidence of a potential role for such signalling in the regulation of CD63-positive exosome biogenesis or secretion, although the data presented in this study are not yet sufficiently consistent to identify the nature of this regulation.

The assay employed to quantify exosome secretion comprised a multiple-mating protocol involving a 24 hours recovery period after mating. However, an ELISA-based analysis method probing for the MC products has suggested that the AG secretory content does not return to 'virgin' levels until 3 days after a mating event (Buehner et al. 2009). Whilst this study only analysed replenishment of MC products, it is conceivable that SC secretion displays similar replenishment kinetics, although no direct comparison of MC and SC secretion rates has been carried out to date. We speculate that, as EGFR signalling in SCs is likely to involve complex autocrine feedback loops (Sections 6.1.2 and 6.4.1), our assay may either have been inadequate to capture the replenished, equilibrated state of AG secretions or reflects changes in several different PI3K-dependent processes, which ultimately lead to variable secretory outcomes. Modifying the assay either by increasing the refractory period (to a minimum of three days after mating) or by assaying secretion without pre-mating may produce more reproducible data to help clarify the roles of EGFR and PI3K signalling in CD63-GFP exosome secretion.

6.4.3 Regulation of endocytic trafficking by EGFR and PI3K signalling

The effects of modulating EGFR and PI3K signalling on endosomal trafficking are difficult to relate to exosome secretion without reproducible results from the exosome secretion assay. Consistent with previous studies showing a EGFR and PI3K signalling promoting endocytosis and downstream endocytic trafficking (Wiley et al. 1991; Li et al. 1995; Wiedemann et al. 1998; Lanzetti et al. 2000; Shin et al. 2005; Vanhaesebroeck et al. 2010) (Sections 6.1.2.2 and 6.1.1.3), the general trends observed in the data suggest that both EGFR and PI3K signalling drive endosomal trafficking and/or maturation in SCs. In addition, the data suggest their activity also influences aspects of the secretory compartment trafficking. Whether these effects on both the endocytic and secretory compartments are interdependent e.g. signalling driving membrane trafficking from the secretory pathway into the endosomal pathway, cannot be established from the data. Interestingly, Class I PI3K signalling activity at the Golgi had previous been shown to regulate membrane trafficking to lysosomal compartments (Wiedemann et al. 1998), although further experiments will be necessary to investigate whether PI3K is required for this process in SCs.

The different cellular phenotypes following modulation of their upstream components suggest that, although PI3K is likely to be downstream effector of the EGFR, as has been shown for many cell types (Section 6.1.1.1), there are likely to be additional effectors that also modulate endocytic trafficking events that are linked to one or both of these components. For instance, in addition to the PI3K/AKT/mTOR signal transduction cascade, EGFR also signals through the Ras/Raf/MEK/MAPK pathway (**Fig. 6.1.1**), which itself may regulate aspects of endolysosomal trafficking (Freeman 1998; Mendoza et al. 2011). Furthermore, FGFR is also expressed in SCs (Zain Syed, FHS project 2013) and would be predicted to regulate PI3K signalling, potentially in a redundant manner to EGFR (Vanhaesebroeck et al. 2010; Costa et al. 2011; Mendoza et al. 2011).

6.4.3.1 EGFR signalling regulates endocytic trafficking in SCs

The strong phenotypic effects on endocytic and secretory compartments of SCs resulting from *spitz* knockdown and the fact that *spi* is expressed in these cells (evidence from *spi-GAL4* enhancer trap expression; **Fig. 2.1** (Hayashi et al. 2002)) provide good evidence for an autocrine signalling loop regulating SC membrane trafficking. However, in the case of *spitz* knockdown, it is not possible to conclude whether the observed increase in mMVBLs and SVs results from reduced secretion, increased or altered endocytosis or a combination of these processes. Unfortunately, the more inconsistent phenotypes following EGFR knockdown and mutant construct expression does not help to clarify the role of EGFR signalling in these processes.

For example, reducing EGFR signalling by RNAi-mediated knockdown of *spitz* or *EGFR* had surprisingly different effects on the number and morphology of endocytic and secretory SC compartments. Whilst this discrepancy may be explained by differing knockdown levels of the RNAi constructs utilised, an alternative hypothesis is that the *EGFR*-RNAi phenotype reflects the greatest degree of EGFR signalling inhibition compared to *spitz* knockdown, since spitz is only one of several EGFR ligands and multiple ligands have been shown to mediate intercellular signalling in the same tissue (Golembo et al. 1999). Another possibility is that reduced *EGFR* expression increases the level of spitz via the feedback mechanism discussed above, a response that is not possible when *spi*-RNAi is expressed.

To study the roles of EGFR signalling in endocytic trafficking, we utilised expression of transgenic constructs harbouring mutated forms of the EGFR in order to up- and down- regulate the EGFR signalling pathway (i.e. *EGFR ACT* and *EGFR DN*). However, as EGFR activation has been shown to directly trigger endocytosis (Wiley et al. 1991), expression of such proteins may affect endocytic trafficking in a manner that is independent of signal transduction *per se*. This may also explain the differing cellular phenotypes produced following expression of a dominant negative-EGFR and

EGFR knockdown by RNAi. Therefore, it is difficult to ascertain whether some of the observed effects of EGFR protein overexpression are merely artefacts of high receptor levels.

Previous studies have suggested that EGFR-DN lacking the C terminal regulatory and kinase domains is not packaged into ILVs and degraded in cells lines, but is instead recycled back to the plasma membrane (Futter et al. 1996; Futter et al. 2001). The authors propose that downstream (Class III) PI3K activity required for ILVs biogenesis is reduced following *EGFR-DN* expression (Futter et al. 2001). Consistent with this, *EGFR-DN* expression blocked ILV biogenesis in SCs (**Fig. 6.3**). By contrast, residual EGFR expressed in the presence of *EGFR*-RNAi may be sufficient to permit (Class III) PI3K-dependent ILV formation, but prevent further MVB maturation required to degrade ILVs. It will important to investigate the role Class III PI3K in ILV biogenesis in SCs. Our findings suggest that expression of *EGFR-DN* has previously uncharacterised effects on both the secretory and endocytic pathways, and indeed that EGFR activity may be required for late endosomal maturation, which has implications for its use to block EGFR signalling in other systems.

6.4.3.2 PI3K activity regulates endocytic trafficking in SCs

Despite the lack of reproducibility when assaying exosome secretion, I did observe some general trends in SC cellular phenotypes after modulating the level of PI3K signalling. My data suggest that mMVBLs from SCs with increased PI3K signalling were generally larger than controls and for the activated PI3K construct, potentially contained many ILVs, perhaps suggesting that trafficking into endolysosomes is elevated in these genetic backgrounds, but subsequent maturation may be compromised.

PI3K signalling has well characterised roles in the regulation of cell growth in response to nutrient status and growth factor signalling via a signal transduction cascade that culminates in the activation of mTORC1 signalling at the surface of late endosomes and lysosomes (see Section

6.1.2.1). Interestingly, other work in the host lab has demonstrated a requirement for mTOR in the growth and maturation of mMVBL compartments (A. Leiblich, unpublished data). SCs expressing *mTOR*-RNAi or a combination of Tsc1 and Tsc2, negative regulators of mTORC1, possess smaller mMVBLs than control cells, which do not seem to fully mature. Similarly, we have demonstrated that reducing PI3K signalling by expression of *Dp110-DN* or *PTEN* over-expression also reduces the size of mMVBLs, and maturation of these compartments may also be affected when *PTEN* is over-expressed. Whilst it is tempting to speculate that PI3K exerts its effects on mMVBL growth and maturation via the AKT/mTOR signalling pathway, further epistasis studies will be required in order to characterise the regulation of endocytic trafficking in SCs by PI3K signalling. Nevertheless, these findings further support our hypothesis that mMVBL size regulates cell growth through the recruitment and activation of major cell growth regulators including mTOR to the surface of mMVBLs (Section 5.4.3). Although previous work suggested increasing PI3K signalling is not sufficient to increase SC growth (Leiblich et al. 2012), the effects of PI3K activation are now being reassessed with a wider range of transgenes to determine whether modulating PI3K signalling in other ways might induce growth effects.

7. MCs of the AG shed sex peptide-carrying microvesicles into the gland lumen

7.1 Introduction

7.1.1 MV biogenesis

The roles and regulation of MVs shed from the plasma membrane are less well studied than exosomes. MV shedding has been shown to be stimulated in response to extracellular cues (Heijnen et al. 1999; Wilson et al. 2004; Ducuing et al. 2013) and requires energy input as well as RNA and protein synthesis (Dainiak et al. 1991), suggesting that MV biogenesis is an active, regulated process. The mechanism by which membrane is shed from cells in distinct particles is largely unknown. However, several models of MV biogenesis have been proposed (Cocucci et al. 2009). These models can be subdivided into protein-driven and lipid-driven mechanisms. However, it is likely that a combination of protein- and lipid-dependent mechanisms contribute simultaneously.

Altering the asymmetrical organisation of certain lipids in plasma membrane has been proposed as a lipid-driven mechanism. This model followed the observation that the lipid composition of shed MVs was 'reversed' in comparison to the configuration at the plasma membrane (Frey et al. 2011). The lipid composition of the inner (cytoplasmic) and outer (extracellular) leaflets of the phospholipid bilayer are asymmetrical; the inner leaflet is enriched with phosphatidylserine (PS) and phosphatidylethanolamine (PE), whilst phosphatidylcholine (PC) and sphingolipids are segregated to the outer leaflet (Coleman et al. 2009; Sharom 2011). Since the former of these lipids are conical shaped and negatively charged, their asymmetric sorting into microdomains has been shown to induce membrane curvature (Morris 2010). As PS is found on the extracellular

face of shed MVs (Frey et al. 2011), it has been hypothesised that this lipid configuration could generate the outward membrane budding required to initiate MV biogenesis (Xu et al. 2013).

An additional lipid-driven MV biogenesis model has been proposed following a study that demonstrated a requirement for cholesterol in the formation of so-called synaptic-like microvesicles that bud from the apical surface of neuronal plasma membranes (Thiele et al. 2000). The mechanism proposed involves interactions between cholesterol-enriched lipid domains and certain proteins sorted into these domains inducing membrane curvature (Thiele et al. 2000). However, whether this mechanism has a role in MV budding from epithelial cells is yet to be investigated.

Specific proteins have also been implicated in several stages of MV biogenesis, from membrane budding to scission. Protein factors have been hypothesised to generate the physical force necessary to induce membrane curvature during the initial outward membrane budding. In a manner reminiscent of their activity during ILV formation inside MVBs, the ESCRT complex has been proposed to exert its membrane-deforming activity at the apical plasma membrane of *C. elegans tat-5* mutant embryos, which constitutively shed MVs from their embryonic surface (Wehman et al. 2011). The shedding of MVs in *tat-5* embryos is dependent upon members of the ESCRT-III complex as well as Rab11, which is hypothesised to mediate the apical delivery of the complex (Wehman et al. 2011). This model is supported by further reports of a requirement for ESCRT-III components in MV shedding in mammalian cells (Nabhan et al. 2012). ESCRT-dependent MVs secreted by *tat-5* mutants are larger than ILVs formed inside MVBs, suggesting that additional factors may specifically regulate ESCRT-dependent MV biogenesis (Wehman et al. 2011).

The oligomerisation of cytosolic proteins generating a protrusion force has also been proposed as MV biogenesis mechanism. *In vitro* studies have demonstrated that the polymerisation of such cytoplasmic proteins coupled to a membrane anchor is sufficient to drive MV shedding (Shen et al. 2011). Interestingly, *C. elegans* sperm have been shown to bud MVs from their limiting membrane. These MVs contain the Major Sperm Protein (MSP), a cytoskeletal factor whose polymerisation is required for the membrane deformation necessary for amoeboid motility (Italiano Jr et al. 1996). However, whether MSP polymerisation is required for MV shedding from sperm has not yet been addressed *in vivo.*

Cortical proteins that function in membrane abscission during cytokinesis have also been implicated in MV shedding. Cytoskeletal factors, including actin and myosin, have been shown to function in generating the contractile force necessary to draw together the membrane and form MVs (Muralidharan-Chari et al. 2009).

Finally, the activity of enzymatic proteins can regulate the lipid composition of the plasma membrane, thus contributing to lipid-driven MV biogenesis and demonstrating the likely co-operation between lipid- and protein-driven mechanisms. As described above, the lipid-asymmetry has been proposed to contribute to membrane curvature involved in MV shedding. Lipid asymmetry is itself regulated by the activity of phospholipid flippases and floppases that translocate phospholipids across the bilayer (Coleman et al. 2009; Frey et al. 2011; Sharom 2011). Interestingly, *tat-5* (which induces constitutive MV shedding in the *C. elegans* embryo when mutated) encodes a P4-ATPase, a family of lipid translocases/flippases (Folmer et al. 2009). However, whether specific cells modulate the activity of lipid translocases to actively regulate MV secretion has not yet been investigated.

The establishment of new in vivo models, such as the recently proposed for *Dictyolstelium*, which constitutively sheds MVs under normal growth conditions (Tatischeff 2013), will be critical in understanding the mechanisms of MV shedding, as well as their roles, in a normal physiological context.

7.1.2 Regulation of MV biogenesis

MV shedding has been proposed to occur in a constitutive manner (Cocucci et al. 2009). Nevertheless, an increase in intracellular calcium has been shown to rapidly increase shedding (Pasquet et al. 1996; Theopold et al. 1997; Bucki et al. 1998). Several studies have reported increased rates of EV secretion in response to extracellular stimuli (Heijnen et al. 1999; Wilson et al. 2004; Bianco et al. 2005). For example, the activation of cell surface purinergic receptors following ATP binding has been shown to stimulate EV secretion in microglia (Bianco et al. 2005).

A study of the regulation of MV secretion identified a member of the ADP-ribosylation factor family of small GTP binding proteins ARF6 as a novel positive regulator of MV shedding in tumour cells (Muralidharan-Chari et al. 2009). MV shedding involved increased ERK/MAPK signalling, a pathway which is stimulated by ARF6-mediated activation of Phospholipase D, which recruits ERK to the plasma membrane, and results in the phosphorylation of Myosin Light Chain (MLC) by MLC Kinase (MLCK), hypothesised to drive membrane abscission necessary for vesicle shedding. Interestingly, the mis-regulation of ARF6 has been implicated in cancer cell invasion and metastasis (Muralidharan-Chari et al. 2009), leading the authors to speculate that mis-regulated MV secretion contributes to this role of ARF6 in cancer progression (Muralidharan-Chari et al. 2009). This study suggests that the apical activation of the ERK/MAPK signalling pathway is sufficient to induce MV shedding; however, whether this is true for normal non-cancerous epithelial cells *in vivo* has not yet been addressed.

7.1.3 Roles of MVs

Although MVs have been hypothesised to function in a wide range of normal and disease-associated processes few studies have clearly identified specific physiological functions for them. Shed MVs have been implicated in coagulation, inflammation and tumourigenesis (Cocucci et al. 2009). The vesicles shed from specific cell types often harbour distinct cargo profiles (Cocucci et al. 2009), which are likely to reflect the proteins present on the plasma membrane of the specialised cell type of origin. Importantly, it has been demonstrated that not all components of a cell's apical plasma membrane are present on shed MVs, suggesting that highly selective cargo sorting mechanisms do exist (Muralidharan-Chari et al. 2009).

MVs have been implicated in promoting the extracellular transport of signalling molecules between distant cells. For example, MSP-MVs shed from the surface of *C. elegans* spermatocytes have been hypothesised to aid long-range MSP signalling, as MSP activates Eph receptors to promote oocytic meiosis maturation (Kosinski et al. 2005). In addition to this reproductive inter-organism signalling in invertebrates, mammalian placental cells have also been shown to secrete MVs, which have been hypothesised to function in mother-fetus crosstalk (Aharon et al. 2013).

MVs have been implicated in physical processes, including as clotting and coagulation (Bastida et al. 1984; Theopold et al. 1997; Heijnen et al. 1999; Franz et al. 2013). MVs shed from platelets selectively carry pro-coagulation factors (Sims et al. 1988; Heijnen et al. 1999; Del Conde et al. 2005). Pro-coagulation microvesicles have also been implicated in insect hemolymph coagulation (Theopold et al. 1997), suggesting an evolutionarily conserved role for MVs in the coagulation of circulating fluids. MVs isolated from the human seminal fluid have been shown to possess coagulant properties and are capable of activating the extrinsic coagulation pathway, suggesting a function in mating plug formation (Franz et al. 2013).

MVs have also been proposed to have additional reproductive functions. MVs have been implicated in sperm maturation in the male reproductive tract, a process by which sperm acquire the morphological and biochemical characteristics essential to be able to fertilise an oocyte. Following exit from the testes and vas deferens, sperm are stored in the epididymis where they undergo further maturation steps. However, many of the factors they acquire during this period (in which they are transcriptionally and translationally quiescent) are cytoplasmic or integral membrane proteins (Cooper 1998). It has been proposed that MVs secreted by the epididymis act as vehicles to allow the transport of these factors to sperm (Sullivan et al. 2013).

7.1.4 MVs and *Drosophila*

MVs secreted by *Drosophila* epithelial cells are yet to be identified. The initial identification of secreted membrane-bound vesicles in Drosophila utilised a GPI-anchored GFP transgene expressed in specific compartments of the developing wing imaginal disc (Greco et al. 2001). GPI-anchored proteins have been shown to slot into the external leaflet of the plasma membrane and cluster into lipid rafts (Rietveld et al. 1999; Muniz et al. 2000), lipid microdomains that have been shown to be enriched in exosomal and MV membranes (**Figs. 1.3 and 1.4**). These secreted particles were coined 'argosomes' (Greco et al. 2001) and were hypothesised to assist the transport of certain morphogens, including Wg and Hh (Panakova et al. 2005), across the plane of the epithelium during pattern formation (Greco et al. 2001).

Further studies refined the identity of these nanoparticles as 'lipoprotein particles' due to the presence of apolipophorins I and II on their limiting membrane (Panakova et al. 2005). These vesicles were shown to be distinct from the exosomes secreted by epithelial cells of the imaginal wing disc that can be marked with CD63-GFP (Panakova et al. 2005) and are also distinct from

MVs as they are composed of a single lipid leaflet, instead of a lipid bilayer shed directly from a plasma membrane. In the *Drosophila* larva, lipoprotein particles are primarily produced by the *Drosophila* fat body and are distributed via the hemolymph to the developing wing disc, for example, where they reversibly associate with secreted proteins or pick up membrane anchored cargos from the outer leaflet of cell membranes through GPI-anchor exchange (Panakova et al. 2005; Eugster et al. 2007). Both Wg and Hh are lipid-modified proteins (Willert et al. 2003; Gallet et al. 2006; Takada et al. 2006) and are also hypothesised to associate with membranes via interactions with GPI-anchored heparan sulphate proteoglycans (HSPGs) (The et al. 1999; Greco et al. 2001; Guerrero et al. 2007). These lipid modifications and interaction partners have important roles in long-range Wg and Hh signalling (The et al. 1999; Willert et al. 2003; Guerrero et al. 2007; Ducuing et al. 2013), leading to the hypothesis that they allow these factors to associate tightly with lipoprotein particle membranes (Panakova et al. 2005).

7.2 Methods

7.2.1 Electron microscopy

For structural EM, 3-day-old virgin w^{1118} males were dissected. AGs were fixed, processed and sectioned as described in Section 2.7.1.

For immuno-EM, 3-day-old *spi-Gal4; UAS-CD63-GFP* virgin males we dissected. AGs were fixed, processed, sectioned and stained (rabbit anti-GFP 1:2000) as described in Section 2.7.2.

7.2.2 Single-pair GFP transfer experiments

For single-pair mating experiments to analyse MV targets and SP-GFP localisation in the female reproductive tract, w^{1118} virgin females (2- to 10-days-old) were incubated with individual *SP-GFP* or *Acp26Aa-Gal4; UAS-GFP*^{GPI} 3-day-old virgin males and matings observed. Females were

dissected 20 minutes after the start of mating in 4% paraformaldehyde in PBS, fixed for a minimum of 30 minutes, washed for 30 minutes in PBST (females mated to SP-GFP males were also stained for a minimum of 30 minutes in TRITC-phalloidin in PBST; 1:400 dilution) and then mounted in PBS and Vectashield with DAPI (Vector Laboratories).

7.3 Results

7.3.1 SCs secrete GPI-anchored GFP into the AG lumen.

As EVs are enriched in lipid raft components (Raposo et al. 2013) including glycosylphosphatidylinositol (GPI)-anchored proteins (De Gassart et al. 2003), we expressed a GPI-anchored GFP fusion protein specifically in SCs. As expected for GPI-anchored proteins (Muniz et al. 2000), GFP^{GPI} localised to the SC plasma membrane (**Fig. 7.1A**), being enriched at the apical cell surface (**Fig. 7.1B**), and also at the limiting membrane of SVs (**Fig. 7.1A**). Surprisingly, GFP fluorescence was also observed inside the dense core of SVs (**Fig. 7.1A**). Interestingly, GFP^{GPI} was secreted into the gland lumen, where it could be seen in discrete fluorescent puncta of high intensity, as well as cigar shaped structures of approximately 0.5 to 10µm in length (**Fig. 7.1C**). These cigar-shaped structures exhibited weak intensity fluorescence. These data suggest that SCs may secrete two distinct membrane-bound vesicles that are enriched in lipid raft components to which GPI-anchored proteins bind.

7.3.2 MCs shed MVs into the AG lumen

To investigate whether MCs also secrete lipid raft-enriched EVs, we expressed GFP^{GPI} using the MC-specific driver *Acp26Aa-Gal4* (**Fig. 7.2A; Fig. 2.1D**). Large amounts of GFP^{GPI} were observed in the AG lumen (**Fig. 7.2B**), on apparent cigar-shaped structures, which we term microvesicles (MVs), ranging from 0.5 to 10µm in length (**Fig. 7.2B-D**). The lumen of larger vesicles was often

void of GFP^{GPI}, suggesting that GFP^{GPI} associates with the limiting membrane of these structures (**Fig. 7.2C**). GFP^{GPI} was enriched at the apical plasma membrane of MCs (**Fig. 7.2C**) and was not observed in intracellular MC compartments, consistent with reports that GPI^{GFP} usually traffics directly to the apical plasma membrane from the Golgi (Muniz et al. 2000). Our data suggest that the cigar-shaped MVs are shed from the apical plasma membrane of MCs.

Interestingly, the vesicles secreted into the lumen could not be stained using an anti-GFP antibody, despite apparent staining intracellularly in MCs, suggesting that the microenvironment of GFP^{GPI}, which should be exposed to the fluid phase within the AG lumen, is not permissive to antibody staining or that GFP structure is not sufficiently preserved in fixed AGs (**Fig. 7.2E**). Furthermore, attempts to stain the surface of these particles with Annexin V, which recognises exposed PS on the surface of MVs, were also unsuccessful (data not shown).

Importantly, vesicles of similar size and morphology were observed in electron micrographs of wild-type AGs (**Fig. 7.3A**), although they were not well preserved by many fixation procedures, suggesting their secretion is not an artefact of fusion protein expression. Interestingly, despite our inability to detect staining by immunofluorescence, anti-GFP immuno-EM demonstrated reactivity on the outer surface of these structures in the gland lumen (**Fig. 7.3B-C**). The surface of GFP^{GPI}-expressing MCs exhibits exaggerated budding of large protrusions containing GFP^{GPI} from the apical surface (**Fig. 7.3B**), which were not as prominent in wild-type glands (**Fig. 7.3A**), suggesting the expression of this fusion protein drives additional membrane budding.

7.3.3 MVs are transferred to the female reproductive tract during mating

To investigate whether MVs have a role in *Drosophila* reproduction, we analysed the localisation of MVs transferred into the female reproductive tract during mating. GFP^{GPI} was transferred to the female from approximately 15 minutes after the start of mating and could be observed until at least 1 hour after mating ends (**Fig. 7.4**; Rachel Patel, FHS project 2014). GFP^{GPI} fills the entire

uterus of females (**Fig. 7.4B**) and can also often be observed in the oviduct (**Fig. 7.4D**). Reducing the confocal sensitivity during imaging of fixed tissue revealed intense GFP fluorescence on the surface of intact MVs predominantly in the anterior mating plug, uterus and oviduct, as well as weaker diffuse and apparently soluble fluorescence throughout the reproductive tract (**Fig. 7.4C-D**), suggesting that many MVs remain intact during transfer but a proportion of GFP may be cleaved from the GPI anchor during and/or after mating. We did not observe GFP^{GPI} in sperm storage organs (data not shown), suggesting that MVs and at least one of their potential cargos do not interact with sperm.

7.3.4 Sex peptide is carried by MVs into the female

The large number of MVs transferred to females during mating led use to hypothesise that these particles might carry signalling molecules as cargos that could be responsible for one or more aspects of the female PMR. Sex peptide (SP) is considered the major regulator of the PMR and is produced primarily by MCs (Chapman et al. 2003; Kubli et al. 2012) (Section 1.4.3). *SP-GFP*, a C terminal GFP fusion transgene driven by the SP promoter, has been previously utilised in the *Drosophila* reproduction field; however, its localisation in both males and females has only been analysed at low magnification and apparently at high fluorescence detection settings (Villella et al. 2006; Minami et al. 2012; Tayler et al. 2012). High resolution confocal analysis of the AG lumen of *SP-GFP* males at low confocal gain settings revealed the presence of SP-GFP at the surface of the numerous cigar-shaped MVs in the gland lumen, presumably marking those predominantly shed by MCs and marked by GFP^{GPI} (**Figs. 7.5A-B, 7.2**). Interestingly, SP-GFP was not observed intracellularly nor indeed at the apical plasma membrane of MCs. Consistent with previous reports, SP-GFP is transferred into the female reproductive tract during mating (Villella et al. 2006) (**Fig. 7.6A-D**). SP-GFP remains associated with MVs in the anterior mating plug (**Fig. 7.6C**). Unlike GFP^{GPI} (**Fig. 7.4**), we observed an unusual pattern of SP-GFP fluorescence in other regions of the reproductive tract. In the posterior uterus, MV association of SP-GFP was still observed, but

in other regions, including the oviduct and spermathecae, it was associated with thin and irregular lines of staining, consistent with previous reports of SP associating with the long tails of sperm in the female uterus, where is 'hitchhikes' into the storage organs (**Fig. 7.6D-E**) (Peng et al. 2005).

In summary, we have identified SP as a cargo of lipid-raft-enriched MVs shed by MCs that are transferred into the female during mating. After mating, some SP is passed to sperm tails where it is thought to perform its key reproductive functions.

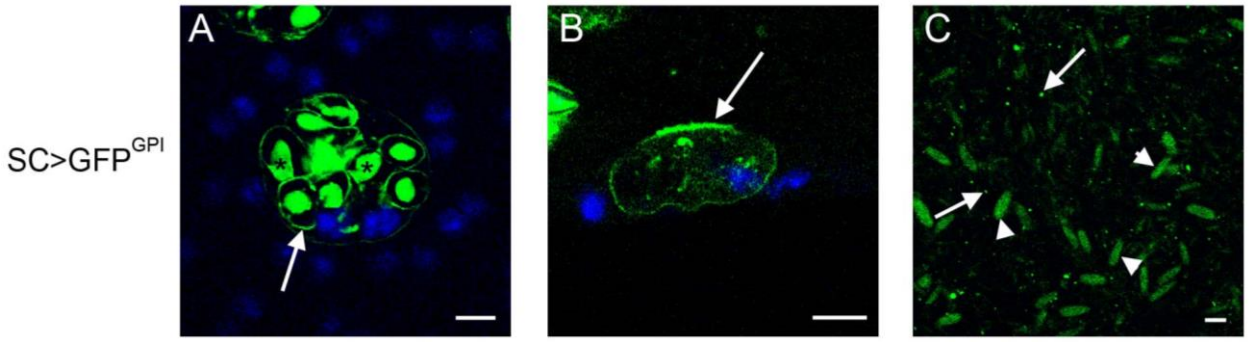


Figure 7.1. SCs secrete GPI-anchored GFP into the accessory gland lumen. Representative images of 3-day-old virgin *spi-Gal4; UAS-GFP^{GPI}* males, stained with DAPI (blue). GFP^{GPI} localises to the limiting membrane (**A**, arrows) and dense core (**A**, *) of SVs, as well as the plasma membrane (**A** and **B**). GFP^{GPI} accumulates at the apical plasma membrane of some SCs (**B**, arrow) and is also secreted into the gland lumen (**C**) in both discrete puncta (arrows) as well as large cigar-shaped vesicles (arrowheads). Scale bars: (**A** and **C**) 5µm and (**B**) 10µm.

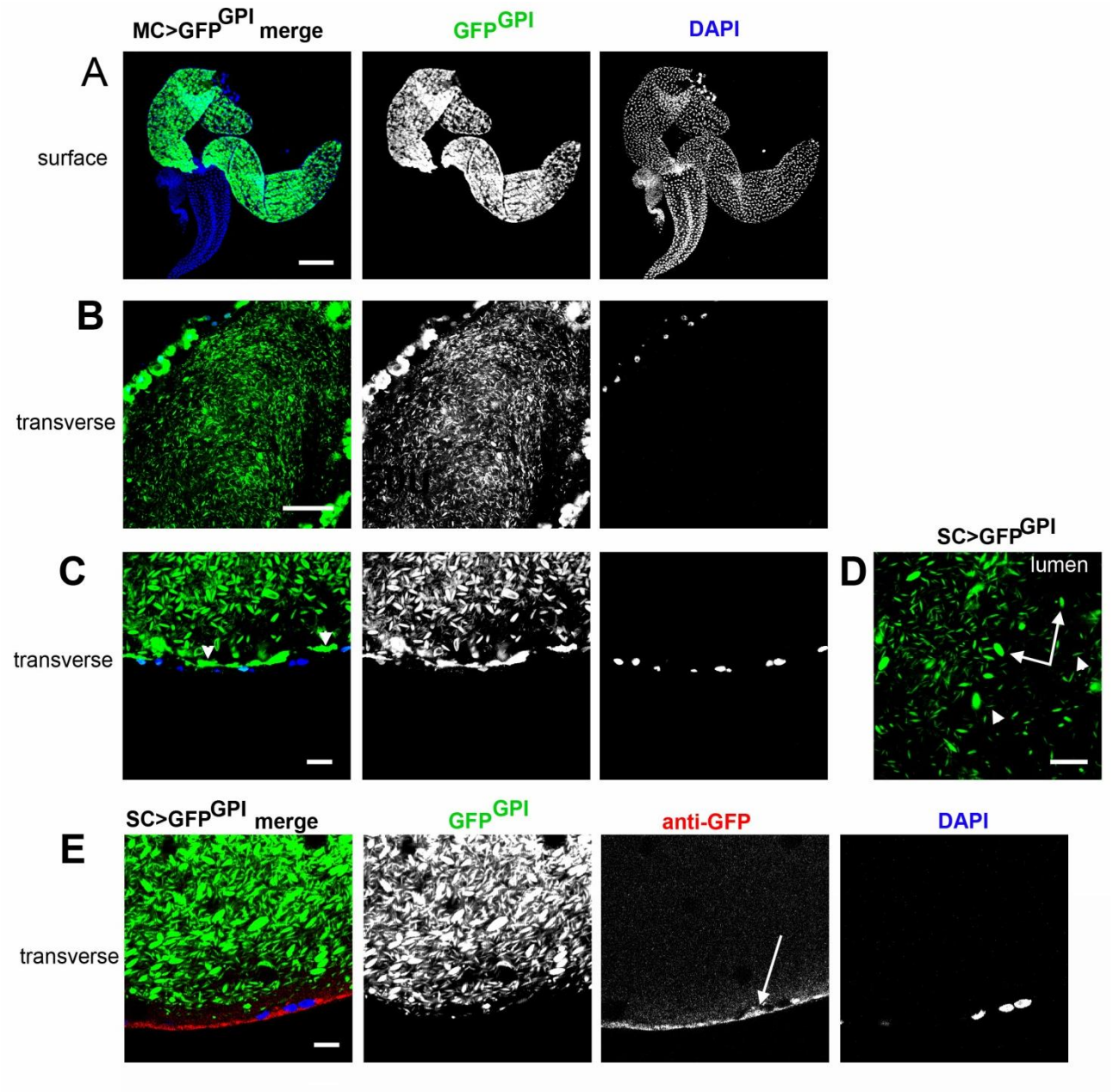


Figure 7.2. MCs shed GFP^{GPI}–containing MVs into the accessory gland lumen. 3-day-old virgin *Acp26Aa-Gal4; Tub-Gal80^{ts}, UAS-GFP^{GPI}* (co-expressed with *UAS-GFP^{NLS}*, **A-C**) stained with DAPI (**A-E**) and anti-GFP (**E**). GFP^{GPI} accumulates at the apical surface of MCs (**C**, arrowheads) and is found on cigar-shaped MVs, of various sizes, shed into the gland lumen (**D**, arrows). An anti-GFP antibody does not recognise the fluorescent GFP secreted into the gland lumen, although picks up weak fluorescence inside MCs (**E**, arrow). (**B-E**) show transverse images through the gland lumen (**D**) and epithelium (**B-C**; **E**). Scale bars: (**A**) 200µm, (**B**) 50µm, (**C** and **E**) 20µm, (**D**) 10µm.

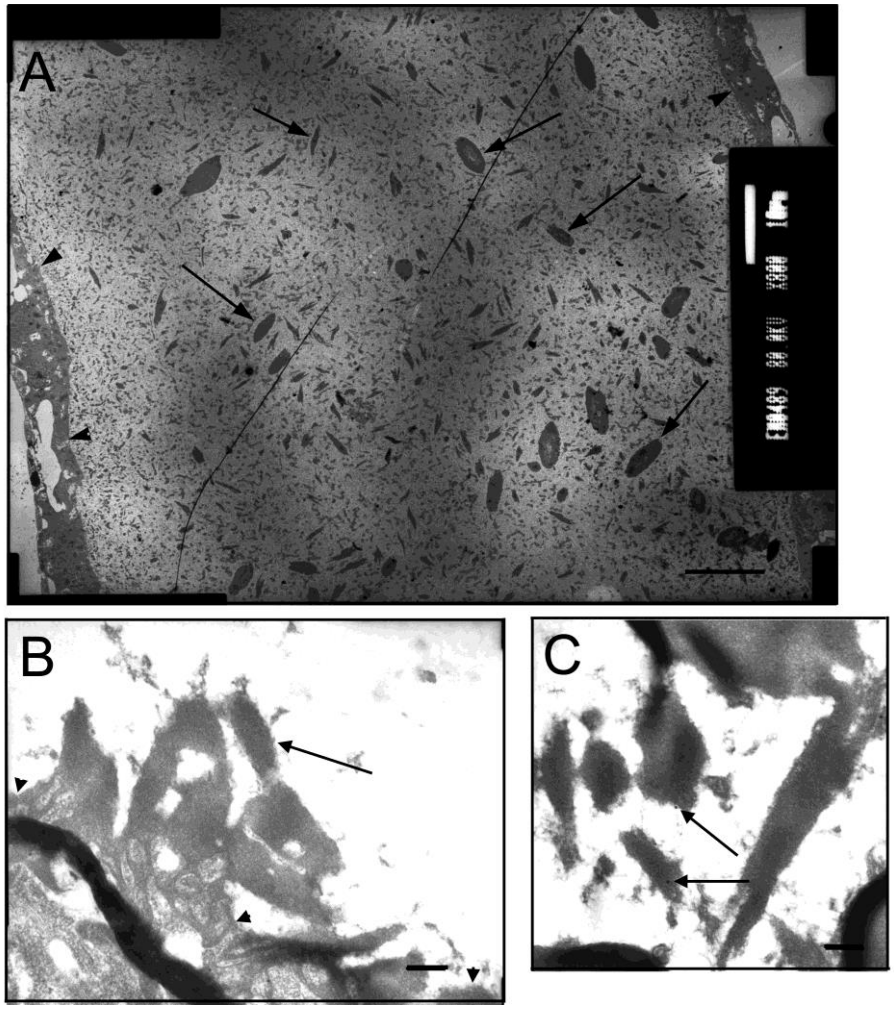


Figure 7.3. The AG lumen contains many large, cigar-shaped particles of various sizes, which appear to be shed by MCs. AGs were fixed and processed for standard transmission electron microscopy (**A**, **B**) or immune-EM (**C**). (**A**) AG of a 3-day-old virgin w^{1118} male sectioned transversely, showing large cigar-shaped vesicles in the gland lumen (arrows), arrowheads indicate apical surface of epithelium (cut in cross section). (**B-C**) AG of a 3-day-old virgin *Acp26Aa-Gal4; UAS-GFP*^{GPI} virgin male showing the MCs in cross-section (**B**, lower left of image, apical surface indicated by arrowheads) and lumen containing shed MVs (**C**). Large structures bleb into the lumen from the apical surface of MCs, in some rare cases exhibiting a bilayer-like structure at their surface (**B**, arrow). Anti-GFP immuno-EM stains MVs in the lumen (15nm gold particles; **C**, arrows). Artefactual electron dense folds are seen in both **B** and **C**. Scale bars: (**A)** 10µm, (**B)** 500nm, (**C)** 200nm. This work was carried out in collaboration with Prof. John Morris (DPAG, Oxford) and Katie Windsor (FHS project, 2013).

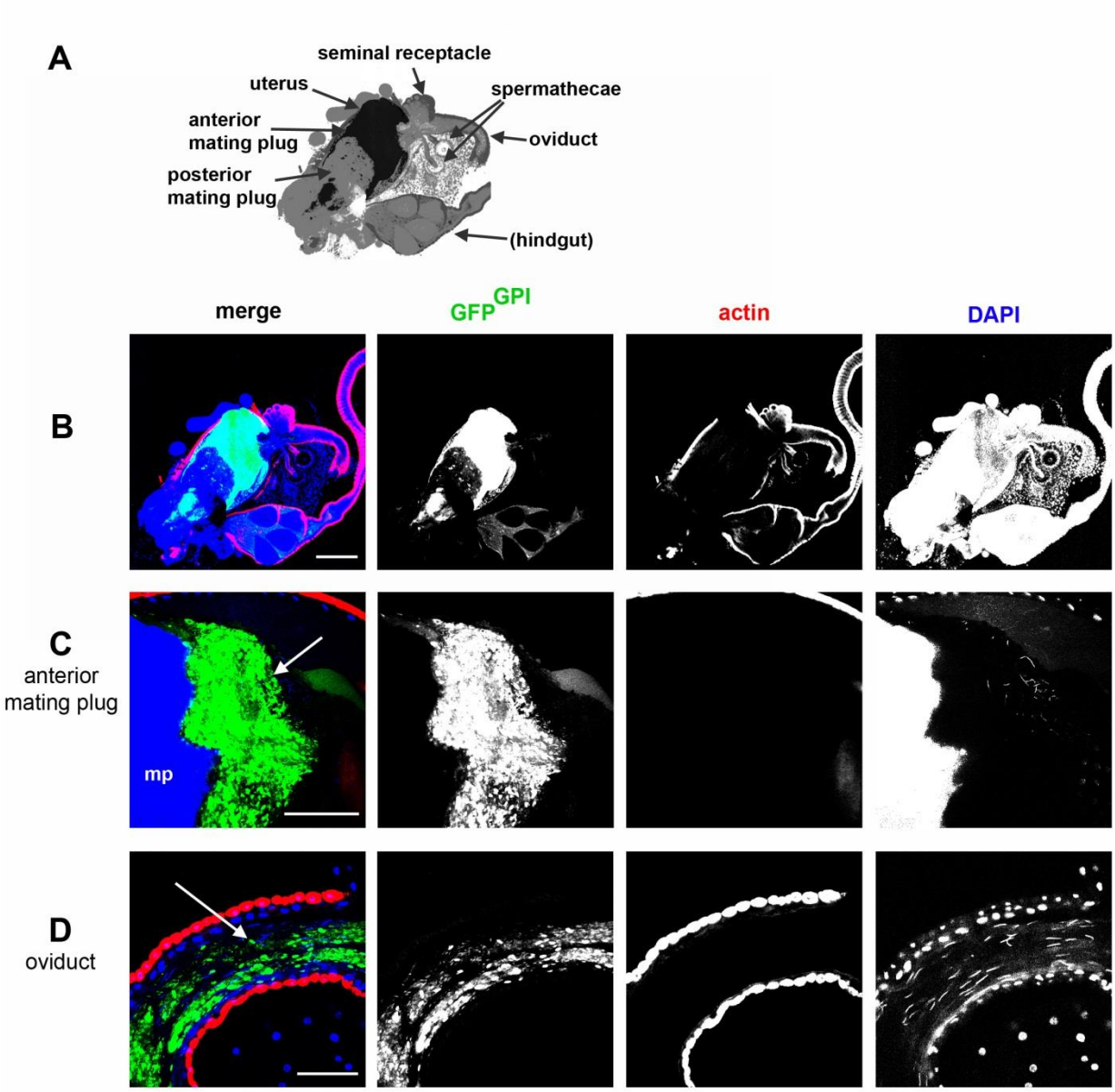


Figure 7.4. GFP^{GPI} MVs are transferred to the female reproductive tract during mating. *w^{1118}* (virgin) females mated to *spi-Gal4; UAS-GFP^{GPI}* virgin males and dissected 20 minutes after the start of mating (approximately immediately after the end of mating). Female reproductive tracts were stained with phalloidin (red) and DAPI (blue). GFP^{GPI}–MVs transferred to the female reproductive tract concentrate in the anterior mating plug (**C**, arrow), but are also found in the uterus and the proximal (relative to the uterus) oviduct (**D**, arrow). In **C,** mp= posterior mating plug (autofluorescent). GFP^{GPI} image in **B** is over-exposed to reveal presence of GFP in uterus, but highest levels are found in the anterior mating plug (revealed by lower exposure in **C**). Scale bars: (**B)** 200µm, (**C** and **D)** 50µm.

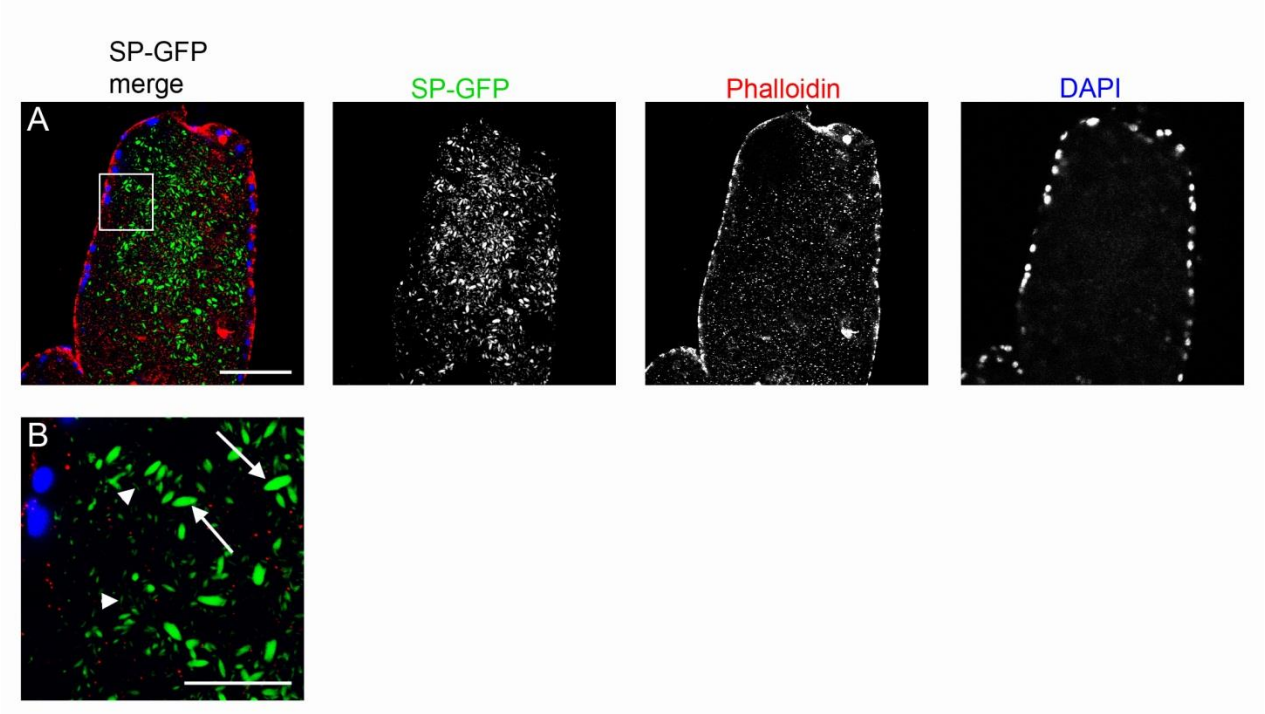


Figure 7.5. SP-GFP localises to MVs shed into the lumen of the gland. *SP-GFP* virgin male AG stained with phalloidin (red) and DAPI (blue). **B** shows the region of AG outlined in **A** (white box) at higher magnification. SP-GFP localises to both small (**B**, arrowheads) and larger (**B**, arrows) cigar-shaped vesicles in the lumen of the gland. Scale bars: (**A**) 50µm, (**B**) 10µm. This work was carried out in collaboration with Aaron Leiblich.

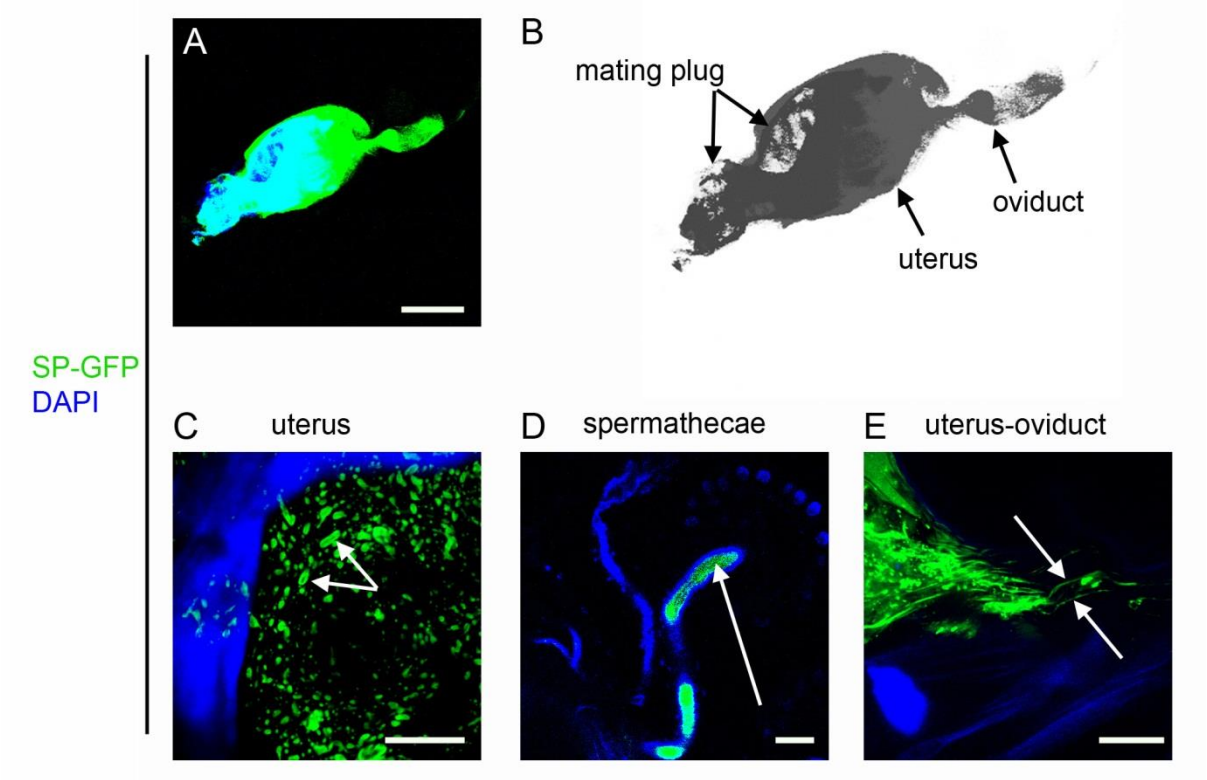


Figure 7.6. SP-GFP transferred to females is associated with MVs and is released to permit sperm binding. Reproductive tract of control w^{1118} female mated to *SP-GFP* male, dissected 15 minutes after the start of mating, and stained with DAPI (blue). SP-GFP (green) is found throughout the entire female reproductive tract (**A** and schematic **B**), including: the mating plug and uterus (**C**), where it remains associated with MVs (**C,** arrows); and in the ducts (**D**) leading to the spermathecae (out of confocal plane in **D**) and oviduct (**E**), where it probably associates with both the heads and long tails of sperm (**D** and **E,** arrows). Scale bars: (**A**) 200µm, (**C-E**) 20µm. This work was carried out in collaboration with Aaron Leiblich.

7.4 Discussion

7.4.1 Lipid raft-enriched MVs are predominantly shed by MCs

We have utilised confocal and electron microscopy to identify the presence of large, cigar-shaped microparticles in the *Drosophila* seminal fluid that can be marked by expressing GFP^{GPI} in MCs. Although we observed an increase in the amount of membrane budding from the surface of MCs expressing GFP^{GPI}, there are three lines of evidence supporting their endogenous presence in the AG lumen of wild type flies. Firstly, we observed particles of a similar shape and size during EM analysis of the wild type AG luminal content. Secondly, additional work has shown that imaging of Lysotracker-stained wild type AGs also consistently reveals cigar-shaped structures in the lumen of wild type glands (Mark Wainwright, pers. comm.). Lastly, GFP-tagged SP, whose expression was driven by its endogenous promoter, was observed at the surface of cigar shaped vesicles in the gland lumen despite not accumulating at the MC surface.

The accumulation of the lipid-raft marker GFP^{GPI} at the apical plasma membrane of MCs led us to assign these particles as MVs, which we hypothesise are shed from their surface. These particles have a large range of sizes, from a few hundred nanometres to several micrometres, as well as an asymmetrical morphology; these characteristics are consistent with those previously reported for isolated MVs in other systems (Cocucci et al. 2009; Raposo et al. 2013). Nevertheless, the AG particles uniformly exhibit an unusual cigar shape, and many are much larger than isolated MVs reported in the literature (typically up to 1µm in diameter; (Heijnen et al. 1999; Taraboletti et al. 2002; Cocucci et al. 2009)). It is possible that these differences result from the *in vivo* approach utilised in this study compared to the *in vitro* approaches utilised in such publications, which employ crude isolation procedures prior to EM analysis and are therefore subject to experimental artefacts influencing their morphology (Conde-Vancells et al. 2008; György et al. 2011; Raposo et al. 2013) (Section 1.3.3).

Interestingly, we were unable to obtain good evidence for the budding of large vesicles (>2µm length) into the lumen from the apical surface of MCs in wild type AGs using EM analysis. However, we did observe numerous small (0.5µm width by 1µm length) protrusions emanating from the surface of both MCs and SCs. Given the large size range of MVs present in the gland lumen, we hypothesize that larger vesicles may form by fusion after secretion. Indeed, the fact that many are much larger than the size usually reported for shed MVs (e.g. 100nm-1µm (Heijnen et al. 1999; Taraboletti et al. 2002; Cocucci et al. 2009)), is consistent with this idea. Notably, our data suggest that expression of the fusion protein GFP^{GPI} itself increases the amount of MV shedding. As lipid-lipid and lipid-protein interactions have been implicated in the biogenesis of shed MVs (section 7.1.1), it is possible that the high-level expression of a GPI-anchored protein induces membrane curvature (Thiele et al. 2000; Contreras et al. 2003; Markvoort et al. 2007; Staneva et al. 2009).

GFP^{GPI} accumulated to a lesser extent at the apical surface of SCs than that of MCs, and we found no evidence for budding of GFP^{GPI} from the apical plasma membrane of SCs. Nevertheless, we did observe GFP^{GPI} on MVs in the gland lumen when this was expressed specifically in SCs, albeit at much weaker levels, suggesting that both cell types may contribute to MVs in the seminal fluid. An alternative hypothesis is that the GFP^{GPI} from SCs is transferred to MVs (shed by MCs) once it is secreted. Further work in the host lab has demonstrated a large degree of variability in the number of GFP^{GPI} MVs secreted into the gland lumen and also supports our previous assumption that expression of this construct affects normal MV secretion (Mark Wainwright, unpublished). Unfortunately, the huge number, asymmetric shape and variable size of these particles prevented their accurate quantification in the AG lumen. As previously mentioned, the *Drosophila* seminal fluid is unsuitable for quantitative EV analysis techniques such as NTA (Section 1.3.3), which require large volumes of fluid. Therefore, it is not possible the accurately estimate the relative contributions of the two cells types to MVs, although it is likely that given their large number in the AG epithelium, MCs give rise to at least the majority of MVs produced.

7.4.2 GFP^{GPI} vesicles in the AG lumen are unlikely to be lipoprotein particles

An alternative identity for these microparticles is that of lipoprotein particles, extracellular structures composed of apolipophorins, cholesterol and a lipid monolayer, which have well-characterised roles in the delivery of lipoproteins and lipids in the hemolymph (Palm et al. 2012). GFP^{GPI} has been previously demonstrated to associate with extracellular lipoprotein particles when expressed specifically in regions of the developing wing disc. It has been suggested that GFP^{GPI} at the limiting membrane of these epithelial cells is 'picked up' by circulating lipoprotein particles produced by the fat body (Panakova et al. 2005).

Apolipophorins are expressed at high levels in many tissues in the adult fly (Chintapalli et al. 2007); however, expression in the AG is low (Data from FlyAtlas; Lipophorin CG11064). Furthermore, the observed increase in membrane shedding following expression of GFP^{GPI} suggests MCs are capable of shedding MVs from their surface. Therefore, we favour a model in which they are produced from budding of the apical plasma membrane of MCs. Unfortunately, as previously mentioned, membrane preservation proved challenging during sample processing and preparation for EM. Therefore, to date, we have been unable to ascertain by EM analysis the nature of the limiting membrane of these structures in the gland lumen, which would shed light on their identity. Therefore, we cannot exclude the possibility that lipoprotein particles are produced outside the AG and are transported via the hemolymph into the AG, particularly as it has been shown that lipoprotein particles are capable of crossing biological barriers, including the blood-brain barrier (Brankatschk et al. 2010). Expression of GFP^{GPI} in the fat body will be important to investigate the possibility that these particles in the AG lumen are lipoprotein particles transported in the hemolymph after production in the fat body.

The association of key signalling proteins with lipoprotein particles has been directly demonstrated in *Drosophila* for both Hedgehog (Hh) and Wingless (Wg) (Panakova et al. 2005). If the lipoprotein particle identity of vesicles present in the AG lumen can be confirmed, our

findings would suggest these microparticles can also be utilised for the long range inter-organism transmission of signals in reproduction. It would then be interesting to investigate whether their cargo SP binds lipophorins and whether this interaction is required for its loading onto the surface of these particles.

7.4.3 SCs may also secrete a distinct EV marked by GFP^{GPI}

Unlike MCs, where GFP^{GPI} localised exclusively to the apical plasma membrane, GFP^{GPI} in SCs was also present at the limiting membrane of SVs. Surprisingly, we also observed GFP^{GPI} in the dense core of SVs. *Drosophila* ANCE possesses mammalian Angiotensin Converting Enzyme (ACE)-like peptidase activity and has therefore been suggested to cleave the C termini of seminal fluid proteins (Rylett et al. 2007). Given its localisation inside the dense core of SVs, it is possible that ANCE is responsible for the cleavage of GFP^{GPI}, releasing the GFP moiety from its membrane anchor. An alternative explanation is that the electron dense core of SVs is composed of densely compacted membrane and not soluble proteins. Although both *Drosophila* ANCE and mammalian ACE are secreted into the extracellular space, mammalian ACE has been shown to be synthesised as a membrane-bound precursor that is cleaved from its C-terminal membrane anchor at the apical plasma membrane, releasing soluble ACE into the extracellular space (Hooper 1991). However, the lack of homology between the C terminal regions of mammalian and *Drosophila* ANCE have led to the assumption that *Drosophila* ANCE is not produced as a membrane-bound precursor (Tatei et al. 1995), which has been demonstrated by expression in COS-7 cell lines (Cornell 1995). This makes it unlikely that membrane attachment explains why ANCE is located in SC dense cores because it does not appear to be membrane-bound.

We were unable to obtain convincing evidence for the presence of GFP^{GPI} in SC mMVBLs in fixed cells. Interestingly, we observed intense, discrete GFP^{GPI} puncta in the lumen of the AG only when this fusion protein was expressed in SCs and not in MCs. As exosomes are also enriched in lipid raft components including GPI-anchored proteins (Cocucci et al. 2009), and given our previous

characterisation of CD63-GFP exosomes, demonstrating SC-specific exosome secretion (Section 3.3.1), we hypothesise that these GFP^{GPI}-marked puncta might be exosomes. We attempted to express both GFP^{GPI} and CD63-mCherry in SCs; however, CD63-mCherry aggregated and was not correctly trafficked out of SCs (data not shown). Live cell imaging would address whether GFP^{GPI} also localises to mMVBLs and thus provide support for its incorporation into exosomes. However, it remains possible that GFP^{GPI} expression induces membrane budding either inside mMVBLs or in SVs, as we observed at the apical plasma membrane (Sections 7.3.2 and 7.4.1), and so this remains an area that requires further investigation.

7.4.4 A role of AG MVs in reproductive signalling

This preliminary study has identified potential roles for seminal fluid MVs in reproduction based on our novel finding that they carry the key PMR regulator, sex peptide, and also contribute to the mating plug, which blocks immediate remating. The host lab is now employing a candidate screen in order to identify factors required for MV shedding in the AG (Mark Wainwright). Once such factor(s) have been identified it will be important to assay the effect(s) of blocking MV secretion in males on all aspects of reproduction, as this will assess whether MV secretion is necessary for fertility and whether MVs play a central role in reproduction.

7.4.4.1 MVs carry SP into the female during mating

Despite its similar localisation on MVs in the AG lumen, unlike GFP^{GPI}, SP-GFP did not accumulate at the apical plasma membrane of MCs. This observation is consistent with the identification of an N-terminal signal peptide designating SP for extracellular secretion (Chen et al. 1988). Therefore, we hypothesise that soluble SP is secreted into the gland lumen, where it associates with the surface of MVs.

Our study has revealed for the first time that the major PMR regulator SP is delivered on MVs into the female reproductive tract, where it binds sperm. We found no evidence for the association of GFP^{GPI} with sperm heads or tails, suggesting that MVs do not fuse with sperm. Instead SP is presumably temporarily released from MVs into the female tract lumen to be associated with sperm.

7.4.4.2 MVs in the *Drosophila* seminal fluid contribute to the mating plug

The localisation of MC-derived MVs in the anterior mating plug is consistent with previous findings that formation of the anterior mating plug requires products of the AG (Lung et al. 2001). Our identification of membranous particles in this structure suggests that MVs may form a physical scaffold, although it is likely that coagulation requires Acps and/or female factors.

My study only analysed the localisation of one Acp: SP (Acp70A). *Drosophila* seminal fluid carries at least 112 Acps, many of which have important signalling functions regulating many aspects of the PMR (Ram et al. 2007). Many Acps, including SP, ovulin and Acp36De, require processing events in either the AG or female in order to carry out their signalling function (Peng et al. 2005; Laflamme et al. 2012). It is likely that many of the numerous proteases present in the seminal fluid are synthesized as inactive zymogens that require N-terminal cleavage for full activation. Indeed, a proteolytic cascade has been shown to be central in the induction of the PMR, culminating in the cleavage of ovulin and Acp36De (Laflamme et al. 2012). It is tempting to speculate that one or more of these processing events leads to the release of such molecules from their association with MVs, which may function to concentrate these proteins in specific regions of the reproductive tract, such as the posterior uterus, where several Acps transit into the hemolymph (Lung et al. 1999).

7.4.5 A conserved role for MVs in coagulation

Shed MVs have been shown to have important roles in both insect hemolymph and mammalian blood coagulation (Fox et al. 1991; Pasquet et al. 1996; Theopold et al. 1997). Interestingly, *Drosophila* hemolymph also contains MVs shed from the surface of hemocytes (Theopold et al. 1997). MVs shed into human seminal fluid have also been shown to carry coagulant factors such a tissue factor (TF) (Heijnen et al. 1999; Franz et al. 2013). Our findings suggest an evolutionarily conserved role for MVs in seminal fluid coagulation and clotting. It is important to note that TF has also been identified on prostate-derived exosomes secreted into the seminal fluid, suggesting that in humans, multiple types of EV may function in seminal fluid coagulation even in species that do not form a mating plug *per se* (Fernández et al. 1997).

I have identified the presence of microparticles in seminal fluid that carry SP into the female during mating. Although further work is required to definitively ascertain whether they are *bona fide* microvesicles, the *Drosophila* AG may provide a new genetic model system in which MV biogenesis and cargo loading can be studied in an unparalleled manner *in vivo*.

8. Concluding remarks

8.1 Summary of findings

My thesis work has identified several membrane-bound EVs secreted by the AG and suggested that they may mediate a surprising range of important reproductive roles. The analysis has revealed a surprising degree of cell type-specificity in exosome secretion and potentially MV shedding (Sections 3.3.1, 7.3.1 and 7.3.2). MCs shed MVs that carry the key PMR regulator SP into the female during mating (Section 7.3.4), whilst SCs specifically secrete exosomes (Section 3.3.1). The unusual biology of SCs has permitted the study of endocytic and secretory cell biology by confocal microscopy (Section 3.3). Knockdown of ESCRT components has provided strong genetic evidence for the exosomal identity of CD63-GFP-positive vesicles as well as shown that these are made by conserved mechanisms in *Drosophila* (Baietti et al. 2012; Colombo et al. 2013) (Section 3.3.9). Quantitative analysis of exosome secretion in the AG lumen also revealed novel roles for BMP, PI3K and EGFR signalling in the regulation of exosome secretion (Sections 5.3.1, 6.3.2 and 6.3.3).

Blocking exosome secretion prevents males from inducing specific aspects of the PMR (Section 4.3.4); males without SC exosomes fail to fully reprogramme female behaviour after mating, suggesting that exosomes may carry critical signalling molecules responsible for this function. As exosomes are likely to carry nucleic acids, receptors, signal transducers and effectors, they harbour the potential to reprogramme target cells. Our identification of a direct interaction between male exosomes and female epithelial cells opens up the interesting possibility that the reprogramming activity of exosomes acts directly on female cells.

All in all, my study represents the most detailed analysis of *in vivo* exosome biogenesis and function in any genetic organism to date and provides the first genetic system to study the normal formation and functions of shed microvesicles in a living animal. The accessory gland and the tools I have generated should provide the basis for further studies that will inform our

understanding of EV function not only in flies, but also in human health and disease. It has already provided the preliminary data for about £1M of basic science funding, and current grant proposals are now seeking to exploit the more translational aspects of the work to understand the roles of EVs in diseases such as cancer.

8.2 Implications for past, present and future exosome studies

Current mammalian cell line studies of exosomes often employ the use Nanoparticle Tracking Analysis (NTA), a method sensitive enough to measure particle size and number (Van Der Pol et al. 2013), to accurately analyse EVs isolated from cell culture. Unfortunately, the AG contains only nanolitre volumes of secretions, making it impractical to employ standard exosome analysis techniques like ultracentrifugation and Nanosight Tracker Analysis (Vlassov et al., 2012). Nevertheless, the power of the AG *in vivo* system in which the particles are not subjected to harsh isolation protocols which have significant effects of their morphology and biochemistry (Momen-Heravi et al. 2013) provides alternative information regarding their physiological functions (see Chapter 4).

The power of *Drosophila* genetics can now be utilised to identify novel regulators of exosome biogenesis and secretion using the new model system I have established in the AG. This *in vivo* system should provide invaluable novel insights into the regulation of exosome secretion under physiological conditions; for example the roles of major signalling pathways in epithelial exosome biogenesis and secretion are poorly understood, yet my studies have already highlighted functions for several pathways in these processes and suggest potential significance in disease (see Section 8.5).

Interestingly, my findings question the use of cancer cell lines utilised in several previous publications to study normal exosome biogenesis and secretion regulation (Baietti et al. 2012; Colombo et al. 2013). My results indicate that the modulation of several signalling pathways mis-

regulated in cancer initiation and/or progression, including BMP, EGFR and PI3K signalling, influence multiple aspects of intracellular trafficking. This strongly suggests that use of cancer cell lines for such studies may produce artefactual results that do not reflect normal physiological processes in healthy cells. In addition, my work indicates that although it is now well established that endocytic and endolysosomal trafficking regulates aspects of several different signalling cascades (Sections 1.3, 5.1.2, 6.1.1.2 and 6.1.2.3), this signalling also strongly regulates these trafficking events, potentially providing important feedback regulation and new mechanisms for different signalling cascades to interact with one another.

8.3 Implications for cell biology

The unusually large size of SCs and their endocytic and secretory compartments permitted the study of dynamic membrane trafficking processes involved in the exosome secretion pathway in an unparalleled manner using standard confocal microscopy. Improvements in super-resolution and high speed imaging techniques should now be utilised to study such processes in SCs at higher spatial and temporal resolution. SCs can now be employed to further study endolysosomal maturation as well as secretory vacuole maturation and dense core formation, which may provide critical insights relevant to other glandular, secretory cell types, such as beta-cells.

8.4 Implications for reproductive biology

The polygamous reproductive strategy of *Drosophila* has given rise to sexual conflict between males and females regarding how often a female mates. In addition to stimulating female egg production, a male aims to prevent the mating of females to subsequent males, in order to ensure he sires the maximum number of her offspring, by producing a mating plug and altering her behaviour. Both these latter processes are dependent upon factors secreted by cells of the AG that until now have been believed to be proteinaceous in nature. However, my studies have revealed unexpected roles for EVs in both these processes: exosomes carry an, as yet,

unidentified factor(s) critical for the maintenance of male rejection behaviours (Chapter 4.3.4); whilst MVs may contribute to the physical formation of the anterior mating plug and also carry the major rejection behaviour signal, SP (Chapter 7.3.4).

Drosophila genes encoding seminal fluid components have unusually high rates of sequence divergence (Haerty et al. 2007). This has been hypothesized to reflect the strong selective pressure acting on Acps to ensure reproductive success in the face of sexual conflict (Begun et al. 2000). I hypothesise that the secretion of EVs into the seminal fluid has evolved under this strong adaptive pressure in order to remove the restriction on the type of molecule that can be transferred from males to females. In addition to secreted protein, EVs allow the transfer of integral membrane proteins, cytoplasmic factors and nucleic acids to females and thus increases the diversity of molecules that can be utilised by males as part of their reproductive strategy. In addition, the employment of EVs to carry cargos in the seminal fluid is a powerful method for storing and then transferring numerous components essential for fertility within a solution filled with proteases, since protein cargos may be protected and/or concentrated by EVs.

The critical active signalling molecule(s) carried by SC exosomes responsible for their role in the maintenance of the PMR is yet to be identified. Despite the requirement for both BMP signalling and exosome secretion in SCs in order to reprogramme female behaviour, we have no evidence for the secretion of either receptor (Tkv-GFP) or ligand (Dpp-GFP and Gbb-GFP) on SC exosomes (A. Leiblich, unpublished data). As exosomes can be loaded with a huge range of factors, including nucleic acids such as DNAs, mRNAs, miRNAs, as well as signalling proteins such as receptors, ligands and signal transducers, it is likely that SC exosomes do not carry just one signalling molecule but rather a complex assortment that may work interdependently in order to carry out their functions. We have identified candidate cargos that may be involved in this process (EGFR and FGFR; Chapter 6.3.1) and further work will now be required to investigate whether these have a role in the maintenance of female remating behaviours. Importantly, delivering membrane-bound receptors to female cells may allow males to influence which cells respond to

soluble ligands in seminal fluid, independently of female receptor expression, thus promoting the male's sexual conflict strategy.

Our findings also raise the interesting possibility that male-derived exosomes may also interact with female epithelial cells in mammals. Further characterisation of this target cell interaction, as well as an investigation into potential interactions of exosomes with neuronal and immune cells, in *Drosophila* may shed further light on the mechanism of exosome function in reproduction.

Interestingly, further to the identification of SP as a MV cargo, additional work in the lab has demonstrated a requirement for SP in MV formation (Mark Wainwright, unpublished). Knockdown of SP by RNAi results in the formation of very large (>50µm) aberrant structures in the AG lumen we hypothesise to form by MV fusion. Although SP does not have a mammalian homologue, these findings raise the interesting possibility that the association of secreted proteins with the surface of MVs is critical for their stability.

8.5 Implications for cancer cell biology

Exosomes have been implicated in angiogenesis, cell growth and modulation of the immune response (Admyre et al. 2007; Mineo et al. 2012; Webber et al. 2014). Cancer cells are thought to secrete increased numbers exosomes and therefore may exploit the signalling capabilities of these vesicles to manipulate their microenvironment (Tavoosidana et al. 2011; Ge et al. 2012). Crucially, our *in vivo* studies have demonstrated that exosome secretion by cells in an epithelial tissue is regulated by the BMP, EGFR and PI3K signalling pathways (Sections 5.3.1, 6.3.2 and 6.3.3). Numerous studies have implicated the mis-regulation of all three of these signalling pathways in the induction and progression of cancer (Parsons 2004; Assinder et al. 2009; Juárez et al. 2011), although characterisation of the molecular mechanisms resulting in tumorigenesis remains incomplete. We have demonstrated that exosome secretion is responsive to extracellular signals in healthy cells and tissues, and hypothesise that oncogenic mutations allow

cell-autonomous regulation of exosome secretion in order for cancer cells to exploit this process to manipulate their microenvironment by reprogramming neighbouring and distant cells.

Many aspects of normal SC biology parallel that of cancer cells, including post-developmental cell growth, delamination and migration and the secretion of large quantities of EVs. We have identified the BMP signalling pathway as a major regulator of all these processes in SCs (Section 5.3.1, (Leiblich et al. 2012)). Our results have indicated a correlation between cell and late endosomal/lysosomal size that we hypothesise may result from alterations in the recruitment and activation of the growth-promoting mTORC1 complex at late endosomal membranes (Section 5.4.3; see below). BMP signalling has been implicated in initiation, progression and metastasis in several cancers, including the prostate (Assinder et al. 2009), for many years. Recent studies have now detected the secretion of exosomal TGF-β by cancer cells, and exosomal TGF-β has also been implicated in manipulation of the tumour microenvironment (Yu et al. 2013; Webber et al. 2014). My study has demonstrated a previously unidentified role for TGF-β signalling in regulation of exosome secretion. Although we were unable to investigate whether increased BMP signalling increases exosome secretion in the AG, further experiments in mammalian cell lines may provide insight into a potential secretion-promoting role for this signalling pathway. Future work should address whether mis-regulated BMP signalling in cancer cells also contributes to cancer progression by increasing secretion of exosomes capable of reprogramming neighbouring cells.

Work by another DPhil student in the host lab has recently indicated a requirement for mTOR in mMVBL maturation and exosome secretion (Aaron Leiblich, unpublished data), further indicating a strong relationship between cell growth and exosome secretion. Although additional work is required in order to unpick the role of PI3K signalling in the regulation of CD63-GFP exosome secretion by SCs, preliminary translational experiments by our collaborators have shown that both PI3K signalling and rapamycin-resistant mTORC1 are required for CD63-GFP-positive exosome secretion in colorectal cancer cells, implicating the PI3K/Akt/mTORC1 signalling pathway

in exosome regulation (Sumeth Perera, Goberdhan Lab). Further studies in the AG will be critical provide additional genetic evidence in favour of such a mechanism.

Work by our collaborators and others (Ju et al. 2014) have demonstrated a role for PI3K signalling in the release of angiogenesis-promoting exosomes; exosomes secreted by PI3K/mTORC1-inhibited cells exhibit angiogenesis-promoting activity (unpublished data; Sumeth Perera, Goberdhan lab). These preliminary data link PI3K and mTORC1 signalling to the modulation of the stromal microenvironment and raise the interesting possibility, which future work in the host lab and also by collaborators will address, that an additional and adaptive role of PI3K/mTORC1 mis-regulation in tumorigenesis involves exosome secretion.

Interestingly, in several cancer cell lines both mTORC1 and PI3K inhibition result in a simultaneous increase in the proportion of exosomes containing the lipid raft-associated cytosolic protein, caveolin-1 (Sumeth Perera and Shih-Jung Fan, unpublished data), raising the exciting possibility that cells can alter the 'flavour' of exosomes they secrete in response to extracellular signals such as growth factor signalling and nutritional status. Although CD63-GFP was utilised in the majority of this thesis (Chapters 3-6) and *Drosophila* do not possess a caveolin homologue, this study has potentially identified an additional lipid-raft associated SC exosome marker, GFP^{GPI} (Section 7.3.1). It will also be important to identify endogenous markers of different exosome populations present in the AG. In addition to current work screening tagged tetraspanins (Mark Wainwight), there are several lipid rafts components such a flotillin, which has been identified as a specific cargo of a distinct ALiX-independent exosome population (Baietti et al. 2012), that are promising endogenous candidates to mark a other populations of exosomes in *Drosophila.*

As several studies have indicated different exosome populations utilise distinct mechanisms of biogenesis and secretion (Section 1.3.5), the SC may provide a powerful system in which multiple populations can be visualised simultaneously in order to investigate their differential regulation. Furthermore, as it is likely that different exosome populations carry unique combinations of

cargos, they may also carry out distinct signalling functions in reproduction. Currently, since I have focused on the regulation of CD63-GFP-positive exosomes, my analysis may have missed other ESCRT- and BMP-independent exosomes in SCs that perform other roles in reprogramming the female PMR. Therefore, in years to come, the AG may provide a system in which the specific roles of distinct exosome populations can be tested *in vivo* using genetic techniques.

9. Bibliography

Aalberts, M., E. Sostaric, R. Wubbolts, M. W. M. Wauben, E. N. M. Nolte-'T Hoen, B. M. Gadella, T. A. E. Stout and W. Stoorvogel (2013). Spermatozoa recruit prostasomes in response to capacitation induction. *Biochimica et Biophysica Acta (BBA) - Proteins and Proteomics* **1834**(11): 2326-2335.

Aalberts, M., T. A. E. Stout and W. Stoorvogel (2014). Prostasomes: Extracellular vesicles from the prostate. *Reproduction* **147**(1): R1-R14.

Aalberts, M., F. M. F. Van Dissel-Emiliani, N. P. H. Van Adrichem, M. Van Wijnen, M. H. M. Wauben, T. A. E. Stout and W. Stoorvogel (2012). Identification of distinct populations of prostasomes that differentially express prostate stem cell antigen, annexin a1, and glipr2 in humans. *Biology of Reproduction* **86**(3): 82, 81-88.

Aberle, H., A. P. Haghighi, R. D. Fetter, B. D. Mccabe, T. R. Magalhães and C. S. Goodman (2002). *Wishful thinking* encodes a BMP type II receptor that regulates synaptic growth in *Drosophila. Neuron* **33**(4): 545-558.

Adachi-Yamada, T., M. Nakamura, K. Irie, Y. Tomoyasu, Y. Sano, E. Mori, S. Goto, N. Ueno, Y. Nishida and K. Matsumoto (1999). P38 mitogen-activated protein kinase can be involved in transforming growth factor β superfamily signal transduction in *Drosophila* wing morphogenesis. *Molecular and Cellular Biology* **19**(3): 2322-2329.

Adell, A. Y., and D. Teis (2011). Assembly and disassembly of the ESCRT-III membrane scission complex. *FEBS Letters* **585**(20): 3191-3196.

Adamczyk, K. A., S. Klein-Scory, M. M. Tehrani, U. Warnken, W. Schmiegel, M. Schnölzer and I. Schwarte-Waldhoff (2011). Characterization of soluble and exosomal forms of the EGFR released from pancreatic cancer cells. *Life Sciences* **89**(9–10): 304-312.

Admyre, C., S. M. Johansson, K. R. Qazi, J.-J. Filén, R. Lahesmaa, M. Norman, E. P. A. Neve, A. Scheynius and S. Gabrielsson (2007). Exosomes with immune modulatory features are present in human breast milk. *The Journal of Immunology* **179**(3): 1969-1978.

Affolter, M. and K. Basler (2007). The decapentaplegic morphogen gradient: From pattern formation to growth regulation. *Nat Rev Genet* **8**(9): 663-674.

Aharon, A. and B. Brenner (2013). Placenta-derived microparticles. *Thrombosis Research* **131**(0): S22-S24.

Aigaki, T., I. Fleischmann, P.-S. Chen and E. Kubli (1991). Ectopic expression of sex peptide alters reproductive behavior of female d. Melanogaster. *Neuron* **7**(4): 557-563.

Al-Nedawi, K., B. Meehan, J. Micallef, V. Lhotak, L. May, A. Guha and J. Rak (2008). Intercellular transfer of the oncogenic receptor egfrviii by microvesicles derived from tumour cells. *Nat Cell Biol* **10**(5): 619-624.

Alexandre, C., A. Baena-Lopez and J.-P. Vincent (2014). Patterning and growth control by membrane-tethered wingless. *Nature* **505**(7482): 180-185.

Alvarado, D., A. H. Rice and J. B. Duffy (2004). Bipartite inhibition of drosophila epidermal growth factor receptor by the extracellular and transmembrane domains of kekkon1. *Genetics* **167**(1): 187-202.

Alvarez-Erviti, L., Y. Seow, H. Yin, C. Betts, S. Lakhal and M. J. A. Wood (2011). Delivery of sirna to the mouse brain by systemic injection of targeted exosomes. *Nat Biotech* **29**(4): 341-345.

Araujo, H. and E. Bier (2000). Sog and dpp exert opposing maternal functions to modify toll signaling and pattern the dorsoventral axis of the drosophila embryo. *Development* **127**(16): 3631-3644.

Arienti, G., E. Carlini and C. A. Palmerini (1997). Fusion of human sperm to prostasomes at acidic ph. *Journal of Membrane Biology* **155**(1): 89-94.

Arvidson, G., G. Ronquist, G. Wikander and A.-C. Öjteg (1989). Human prostasome membranes exhibit very high cholesterol/phospholipid ratios yielding high molecular ordering. *Biochimica et Biophysica Acta (BBA) - Biomembranes* **984**(2): 167-173.

Asea, A., C. Jean-Pierre, P. Kaur, P. Rao, I. M. Linhares, D. Skupski and S. S. Witkin (2008). Heat shock protein-containing exosomes in mid-trimester amniotic fluids. *Journal of Reproductive Immunology* **79**(1): 12-17.

Assinder, S. J., Q. Dong, Z. Kovacevic and D. R. Richardson (2009). The tgf-β, pi3k/akt and pten pathways: Established and proposed biochemical integration in prostate cancer. *Biochem J* **417**(2): 411-421.

Avila, F. W., K. Ravi Ram, M. C. Bloch Qazi and M. F. Wolfner (2010). Sex peptide is required for the efficient release of stored sperm in mated drosophila females. *Genetics* **186**(2): 595-600.

Avila, F. W. and M. F. Wolfner (2009). Acp36de is required for uterine conformational changes in mated drosophila females. *Proceedings of the National Academy of Sciences* **106**(37): 15796-15800.

Babst, M., D. J. Katzmann, E. J. Estepa-Sabal, T. Meerloo and S. D. Emr (2002). Escrt-iii: An endosome-associated heterooligomeric protein complex required for mvb sorting. *Developmental Cell* **3**(2): 271-282.

Babst, M., D. J. Katzmann, W. B. Snyder, B. Wendland and S. D. Emr (2002). Endosome-associated complex, escrt-ii, recruits transport machinery for protein sorting at the multivesicular body. *Developmental cell* **3**(2): 283-289.

Bache, K. G., S. Stuffers, L. Malerød, T. Slagsvold, C. Raiborg, D. Lechardeur, S. Wälchli, G. L. Lukacs, A. Brech and H. Stenmark (2006). The escrt-iii subunit hvps24 is required for degradation but not silencing of the epidermal growth factor receptor. *Molecular Biology of the Cell* **17**(6): 2513-2523.

Baietti, M. F., Z. Zhang, E. Mortier, A. Melchior, G. Degeest, A. Geeraerts, Y. Ivarsson, F. Depoortere, C. Coomans, E. Vermeiren, P. Zimmermann and G. David (2012). Syndecan-syntenin-alix regulates the biogenesis of exosomes. *Nat Cell Biol* **14**(7): 677-685.

Bailey, J. M., P. K. Singh and M. A. Hollingsworth (2007). Cancer metastasis facilitated by developmental pathways: Sonic hedgehog, notch, and bone morphogenic proteins. *Journal of Cellular Biochemistry* **102**(4): 829-839.

Bairatia, A. (1968). Structure and ultrastructure of the male reproductive system in drosophila melanogaster. *nitore Zoologico Italiano - Italian Journal of Zoology* **2**(3-4): 105-182.

Baker, M. A., B. Nixon, N. Naumovski and R. J. Aitken (2012). Proteomic insights into the maturation and capacitation of mammalian spermatozoa. *Systems Biology in Reproductive Medicine* **58**(4): 211-217.

Ballard, S. L., J. Jarolimova and K. A. Wharton (2010). Gbb/bmp signaling is required to maintain energy homeostasis in drosophila. *Developmental Biology* **337**(2): 375-385.

Balogh, P., S. Katz and A. L. Kiss (2013). The role of endocytic pathways in tgf-β signaling. *Pathology & Oncology Research* **19**(2): 141-148.

Bampton, E. T. W., C. G. Goemans, D. Niranjan, N. Mizushima and A. M. Tolkovsky (2005). The dynamics of autophagy visualised in live cells: From autophagosome formation to fusion with endo/lysosomes. *Autophagy* **1**(1): 23-36.

Bastida, E., A. Ordinas, G. Escolar and G. Jamieson (1984). Tissue factor in microvesicles shed from u87mg human glioblastoma cells induces coagulation, platelet aggregation, and thrombogenesis. *Blood* **64**(1): 177-184.

Batra, M. M. a. S. K. (2011). Frequent gene products and molecular pathways altered in prostate cancer– and metastasis-initiating cells and their progenies and novel promising multitargeted therapies. *Mol Med.* **17**(9-10): 949-964.

Beckett, K., S. Monier, L. Palmer, C. Alexandre, H. Green, E. Bonneil, G. Raposo, P. Thibault, R. L. Borgne and J.-P. Vincent (2013). Drosophila s2 cells secrete wingless on exosome-like vesicles but the wingless gradient forms independently of exosomes. *Traffic* **14**(1): 82-96.

Begun, D. J., P. Whitley, B. L. Todd, H. M. Waldrip-Dail and A. G. Clark (2000). Molecular population genetics of male accessory gland proteins in drosophila. *Genetics* **156**(4): 1879-1888.

Bergmann, A., J. Agapite, K. Mccall and H. Steller (1998). The Drosophila gene hid is a direct molecular target of ras-dependent survival signaling. *Cell* **95**(3): 331-341.

Bertram, M. J., G. A. Akerkar, R. L. Ard, C. Gonzalez and M. F. Wolfner (1992). Cell type-specific gene expression in the Drosophila melanogaster male accessory gland. *Mechanisms of Development* **38**(1): 33-40.

Bertram M. J., D. M. Neubaum, Wolfner MF. (1996). Localization of the Drosophila male accessory gland protein acp36de in the mated female suggests a role in sperm storage. *Insect Biochem Mol Biol.* **26**(8-9): 971-980.

Betz, C. and M. N. Hall (2013). Where is mTOR and what is it doing there? *The Journal of Cell Biology* **203**(4): 563-574.

Beyenbach, K. W. and H. Wieczorek (2006). The V-type H+ atpase: Molecular structure and function, physiological roles and regulation. *Journal of Experimental Biology* **209**(4): 577-589.

Bianco, F., E. Pravettoni, A. Colombo, U. Schenk, T. Möller, M. Matteoli and C. Verderio (2005). Astrocyte-derived ATP induces vesicle shedding and IL-1β release from microglia. *The Journal of Immunology* **174**(11): 7268-7277.

Bobinac D, M. I., Zoricić S, Spanjol J, Dordević G, Mustać E, Fuckar Z. (2005). Expression of bone morphogenetic proteins in human metastatic prostate and breast cancer. *Croat Med J.* **46**(3): 389-396.

Bornemann, D. J., S. Park, S. Phin and R. Warrior (2008). A translational block to hspg synthesis permits bmp signaling in the early *Drosophila* embryo. *Development* **135**(6): 1039-1047.

Boswell, R. E. and A. P. Mahowald (1985). Tudor, a gene required for assembly of the germ plasm in *Drosophila melanogaster*. *Cell* **43**(1): 97-104.

Brand, A. H. and N. Perrimon (1993). Targeted gene expression as a means of altering cell fates and generating dominant phenotypes. *Development* **118**(2): 401-415.

Brankatschk, M. and S. Eaton (2010). Lipoprotein particles cross the blood–brain barrier in *Drosophila. The Journal of Neuroscience* **30**(31): 10441-10447.

Bright, N. A., M. J. Gratian and J. P. Luzio (2005). Endocytic delivery to lysosomes mediated by concurrent fusion and kissing events in living cells. *Current biology : CB* **15**(4): 360-365.

Britton, J. S., W. K. Lockwood, L. Li, S. M. Cohen and B. A. Edgar (2002). *Drosophila's* insulin/pi3-kinase pathway coordinates cellular metabolism with nutritional conditions. *Developmental Cell* **2**(2): 239-249.

Brodu, V., P. R. Elstob and A. P. Gould (2004). EGF receptor signaling regulates pulses of cell delamination from the *Drosophila* ectoderm. *Developmental Cell* **7**(6): 885-895.

Brouwers, J. F., M. Aalberts, J. W. A. Jansen, G. Van Niel, M. H. Wauben, T. A. E. Stout, J. B. Helms and W. Stoorvogel (2013). Distinct lipid compositions of two types of human prostasomes. *Proteomics.* **13**(10-11): 1660-1666.

Brummel, T. J., V. Twombly, G. Marqués, J. L. Wrana, S. J. Newfeld, L. Attisano, J. Massagué, M. B. O'connor and W. M. Gelbart (1994). Characterization and relationship of dpp receptors encoded by the saxophone and thick veins genes in drosophila. *Cell* **78**(2): 251-261.

Bucci, C., P. Thomsen, P. Nicoziani, J. Mccarthy and B. Van Deurs (2000). Rab7: A key to lysosome biogenesis. *Molecular Biology of the Cell* **11**(2): 467-480.

Bucki, R., C. Bachelot-Loza, A. Zachowski, F. Giraud and J.-C. Sulpice (1998). Calcium induces phospholipid redistribution and microvesicle release in human erythrocyte membranes by independent pathways. *Biochemistry* **37**(44): 15383-15391.

Buff, E., A. Carmena, S. Gisselbrecht, F. Jimenez and A. M. Michelson (1998). Signalling by the *Drosophila* epidermal growth factor receptor is required for the specification and diversification of embryonic muscle progenitors. *Development* **125**(11): 2075-2086.

Burgess, J., L. M. Del Bel, C.-I. J. Ma, B. Barylko, G. Polevoy, J. Rollins, J. P. Albanesi, H. Krämer and J. A. Brill (2012). Type II phosphatidylinositol 4-kinase regulates trafficking of secretory granule proteins in *Drosophila*. *Development* **139**(16): 3040-3050.

Caby, M.-P., D. Lankar, C. Vincendeau-Scherrer, G. Raposo and C. Bonnerot (2005). Exosomal-like vesicles are present in human blood plasma. *International Immunology* **17**(7): 879-887.

Chanut-Delalande, H., A. C. Jung, M. M. Baer, L. Lin, F. Payre and M. Affolter (2010). The Hrs/stam complex acts as a positive and negative regulator of RTK signaling during *Drosophila* development. *PLoS ONE* **5**(4): e10245.

Chapman, T., J. Bangham, G. Vinti, B. Seifried, O. Lung, M. F. Wolfner, H. K. Smith and L. Partridge (2003). The sex peptide of *Drosophila melanogaster*: Female post-mating responses analyzed by using RNA interference. *Proceedings of the National Academy of Sciences* **100**(17): 9923-9928.

Chapman, T., D. M. Neubaum, M. F. Wolfner and L. Partridge (2000). The role of male accessory gland protein Acp36De in sperm competition in *Drosophila melanogaster*. *Proceedings of the Royal Society of London. Series B: Biological Sciences* **267**(1448): 1097-1105.

Chen, P. S., E. Stumm-Zollinger, T. Aigaki, J. Balmer, M. Bienz and P. Böhlen (1988). A male accessory gland peptide that regulates reproductive behavior of female *D. melanogaster*. *Cell* **54**(3): 291-298.

Chen, W., Y. Feng, D. Chen and A. Wandinger-Ness (1998). Rab11 is required for trans-golgi network–to–plasma membrane transport and a preferential target for GDP dissociation inhibitor. *Molecular Biology of the Cell* **9**(11): 3241-3257.

Chen, Y.-G. (2009). Endocytic regulation of TGF-β signaling. *Cell Res* **19**(1): 58-70.

Chintapalli, V. R., J. Wang and J. A. T. Dow (2007). Using flyatlas to identify better *Drosophila melanogaster* models of human disease. *Nat Genet* **39**(6): 715-720.

Christianson, H. C., K. J. Svensson and M. Belting (2014). Exosome and microvesicle mediated phene transfer in mammalian cells. *Seminars in Cancer Biology*. pii: S1044-579X(14)00055-8. [Epub ahead of print]

Clayton, A., A. Turkes, S. Dewitt, R. Steadman, M. D. Mason and M. B. Hallett (2004). Adhesion and signaling by b cell-derived exosomes: The role of integrins. *The FASEB Journal*.

Clifford, R. and T. Schüpbach (1994). Molecular analysis of the drosophila egf receptor homolog reveals that several genetically defined classes of alleles cluster in subdomains of the receptor protein. *Genetics* **137**(2): 531-550.

Cocucci, E., G. Racchetti and J. Meldolesi (2009). Shedding microvesicles: Artefacts no more. *Trends in Cell Biology* **19**(2): 43-51.

Cohen, S. and R. A. Fava (1985). Internalization of functional epidermal growth factor:Receptor/kinase complexes in a-431 cells. *Journal of Biological Chemistry* **260**(22): 12351-12358.

Coleman, J. A., M. C. M. Kwok and R. S. Molday (2009). Localization, purification, and functional reconstitution of the p4-atpase atp8a2, a phosphatidylserine flippase in photoreceptor disc membranes. *Journal of Biological Chemistry* **284**(47): 32670-32679.

Colombo, M., C. Moita, G. Van Niel, J. Kowal, J. Vigneron, P. Benaroch, N. Manel, L. F. Moita, C. Théry and G. Raposo (2013). Analysis of ESCRT functions in exosome biogenesis, composition and secretion highlights the heterogeneity of extracellular vesicles. *Journal of Cell Science* **126**(24): 5553-5565.

Conde-Vancells, J., E. Rodriguez-Suarez, N. Embade, D. Gil, R. Matthiesen, M. Valle, F. Elortza, S. C. Lu, J. M. Mato and J. M. Falcon-Perez (2008). Characterization and comprehensive proteome profiling of exosomes secreted by hepatocytes. *Journal of Proteome Research* **7**(12): 5157-5166.

Contreras, F.-X., A.-V. Villar, A. Alonso, R. N. Kolesnick and F. M. Goñi (2003). Sphingomyelinase activity causes transbilayer lipid translocation in model and cell membranes. *Journal of Biological Chemistry* **278**(39): 37169-37174.

Cooper, T. G. (1998). Interactions between epididymal secretions and spermatozoa. *J Repro Fertil Suppl* **53**: 119-136.

Cornell, W. T., N. S. Lamango, D. Coates, P. Corvol, F. Soubrier, J. Hoheise, H. Lehrach, R. E. Isaac. (1995). Cloning and expression of an evolutionary conserved single-domain angiotensin converting enzyme from *Drosophila melanogaster*. *J Biol Chem.* **270**(23): 13613-13619.

Corrigan, L., S. Redhai, A. Leiblich, S., S. M. W. Perera, R. Patel, C. Gandy, S. M. Wainwright, J. F. Morris, F. Hamdy, D. C. I. Goberdhan and C. Wilson (2014). BMP-regulated exosomes from *Drosophila* male reproductive glands reprogramme female behaviour. *JCB*, in press.

Costa, C. and E. Hirsch (2011). More than just kinases: The scaffolding function of PI3K. Phosphoinositide 3-kinase in health and disease. C. Rommel, B. Vanhaesebroeck and P. K. Vogt, Springer Berlin Heidelberg. **346:** 171-181.

Dainiak, N. and S. Sorba (1991). Intracellular regulation of the production and release of human erythroid-directed lymphokines. *The Journal of Clinical Investigation* **87**(1): 213-220.

Damilano, F., A. Perino and E. Hirsch (2010). Pi3k kinase and scaffold functions in heart. *Annals of the New York Academy of Sciences* **1188**(1): 39-45.

Das, S., J. E. Dixon and W. Cho (2003). Membrane-binding and activation mechanism of pten. *Proceedings of the National Academy of Sciences* **100**(13): 7491-7496.

De Gassart, A., C. Géminard, B. Février, G. Raposo and M. Vidal (2003). Lipid raft-associated protein sorting in exosomes. *Blood* **102**(13): 4336-4344.

Del Conde, I., C. N. Shrimpton, P. Thiagarajan and J. A. López (2005). Tissue-factor–bearing microvesicles arise from lipid rafts and fuse with activated platelets to initiate coagulation. *Blood* **106**(5): 1604-1611.

Delprato, A., E. Merithew and D. G. Lambright (2004). Structure, exchange determinants, and family-wide rab specificity of the tandem helical bundle and Vps9 domains of rabex-5. *Cell* **118**(5): 607-617.

Demory Beckler, M., J. N. Higginbotham, J. L. Franklin, A.-J. Ham, P. J. Halvey, I. E. Imasuen, C. Whitwell, M. Li, D. C. Liebler and R. J. Coffey (2013). Proteomic analysis of exosomes from mutant Kras colon cancer cells identifies intercellular transfer of mutant Kras. *Molecular & Cellular Proteomics* **12**(2): 343-355.

Denzer, K., M. Van Eijk, M. J. Kleijmeer, E. Jakobson, C. De Groot and H. J. Geuze (2000). Follicular dendritic cells carry MHC class II-expressing microvesicles at their surface. *The Journal of Immunology* **165**(3): 1259-1265.

Di Noto, G., L. Paolini, A. Zendrini, A. Radeghieri, L. Caimi and D. Ricotta (2013). C-Src enriched serum microvesicles are generated in malignant plasma cell dyscrasia. *PLoS ONE* **8**(8): e70811.

Dibenedetto, A. J., H. A. Harada and M. F. Wolfner (1990). Structure, cell-specific expression, and mating-induced regulation of a *Drosophila melanogaster* male accessory gland gene. *Developmental Biology* **139**(1): 134-148.

Dietzl, G., D. Chen, F. Schnorrer, K.-C. Su, Y. Barinova, M. Fellner, B. Gasser, K. Kinsey, S. Oppel, S. Scheiblauer, A. Couto, V. Marra, K. Keleman and B. J. Dickson (2007). A genome-wide transgenic rnai library for conditional gene inactivation in *Drosophila*. *Nature* **448**(7150): 151-156.

Dores, M. R., M. M. Paing, H. Lin, W. A. Montagne, A. Marchese and J. Trejo (2012). AP-3 regulates Par1 ubiquitin-independent MVB/lysosomal sorting via an ALiX-mediated pathway. *Molecular Biology of the Cell* **23**(18): 3612-3623.

Ducuing, A., B. Mollereau, J. D. Axelrod and S. Vincent (2013). Absolute requirement of cholesterol binding for hedgehog gradient formation in *Drosophila. Biology Open* **2**(6): 596-604.

Duijvesz, D., K. E. Burnum-Johnson, M. A. Gritsenko, A. M. Hoogland, M. S. Vredenbregt-Van Den Berg, R. Willemsen, T. Luider, L. Paša-Tolić and G. Jenster (2013). Proteomic profiling of exosomes leads to the identification of novel biomarkers for prostate cancer. *PLoS ONE* **8**(12): e82589.

Edgar, J. R., E. R. Eden and C. E. Futter (2013). Hrs- and CD63-dependent competing mechanisms make different sized endosomal intraluminal vesicles. *Traffic*. **15**(2): 197-211.

Eden, E.R., I. J. White and C. E. Futter. (2009). Down-regulation of epidermal growth factor receptor signalling within multivesicular bodies. *Biochem Soc Trans.* **37**(1): 173-177.

Eugster, C., D. Panáková, A. Mahmoud and S. Eaton (2007). Lipoprotein-heparan sulfate interactions in the hh pathway. *Developmental Cell* **13**(1): 57-71.

Fabiani, R., L. Johansson, ö. Lundkvist and G. Ronquist (1994). Enhanced recruitment of motile spermatozoa by prostasome inclusion in swim-up medium. *Human Reproduction* **9**(8): 1485-1489.

Fader, C. M., A. Savina, D. Sánchez and M. I. Colombo (2005). Exosome secretion and red cell maturation: Exploring molecular components involved in the docking and fusion of multivesicular bodies in K562 cells. *Blood Cells, Molecules, and Diseases* **35**(2): 153-157.

Falguières, T., P.-P. Luyet, C. Bissig, C. C. Scott, M.-C. Velluz and J. Gruenberg (2008). In vitro budding of intralumenal vesicles into late endosomes is regulated by ALiX and Tsg101. *Molecular Biology of the Cell* **19**(11): 4942-4955.

Fan, Y., A. Rafaeli, C. Gileadi, E. Kubli and S. W. Applebaum (1999). *Drosophila melanogaster* sex peptide stimulates juvenile hormone synthesis and depresses sex pheromone production in helicoverpa armigera. *Journal of Insect Physiology* **45**(2): 127-133.

Fernandez-Borja, M., R. Wubbolts, J. Calafat, H. Janssen, N. Divecha, S. Dusseljee and J. Neefjes (1999). Multivesicular body morphogenesis requires phosphatidyl-inositol 3-kinase activity. *Current Biology* **9**(1): 55-58.

Fernández, J. A., M. J. Heeb, K. P. Radtke and J. H. Griffin (1997). Potent blood coagulant activity of human semen due to prostasome-bound tissue factor. *Biology of Reproduction* **56**(3): 757-763.

Flis, V. V. and G. Daum (2013). Lipid transport between the endoplasmic reticulum and mitochondria. *Cold Spring Harbor Perspectives in Biology* **5**(6): pii: a013235.

Folmer, D. E., R. P. J. O. Elferink and C. C. Paulusma (2009). P4 ATPases - lipid flippases and their role in disease. *Biochimica et Biophysica Acta (BBA) - Molecular and Cell Biology of Lipids* **1791**(7): 628-635.

Foukas, L. and D. Withers (2011). Phosphoinositide signalling pathways in metabolic regulation. Curr Top Microbiol Immunol. 346:115-41.

Fox, J. E., C. D. Austin, C. C. Reynolds and P. K. Steffen (1991). Evidence that agonist-induced activation of calpain causes the shedding of procoagulant-containing microvesicles from the membrane of aggregating platelets. *Journal of Biological Chemistry* **266**(20): 13289-13295.

Frankfort, B. J. and G. Mardon (2004). Senseless represses nuclear transduction of egfr pathway activation. *Development* **131**(3): 563-570.

Franz, C., A. N. Böing, C. M. Hau, M. Montag, T. Strowitzki, R. Nieuwland and B. Toth (2013). Procoagulant tissue factor-exposing vesicles in human seminal fluid. *Journal of Reproductive Immunology* **98**(1–2): 45-51.

Freeman, M. (1996). Reiterative use of the EGF receptor triggers differentiation of all cell types in the *Drosophila* eye. *Cell* **87**(4): 651-660.

Freeman, M. (1998). Complexity of EGF receptor signalling revealed in *Drosophila*. *current Opinion in Cell Biology* **8**(4): 407-411.

Frey, B. and U. Gaipl (2011). The immune functions of phosphatidylserine in membranes of dying cells and microvesicles. *Seminars in Immunopathology* **33**(5): 497-516.

Fruman, D. A. and C. Rommel (2014). PIK and cancer: Lessons, challenges and opportunities. *Nat Rev Drug Discov* **13**(2): 140-156.

Fuchs, A., L. S. Cheung, E. Charbonnier, S. Y. Shvartsman and G. Pyrowolakis (2012). Transcriptional interpretation of the EGF receptor signaling gradient. *Proceedings of the National Academy of Sciences* **109**(5): 1572-1577.

Fujimoto, T. (1996). Gpi-anchored proteins, glycosphingolipids, and sphingomyelin are sequestered to caveolae only after crosslinking. *Journal of Histochemistry & Cytochemistry* **44**(8): 929-941.

Futter, C. E., L. M. Collinson, J. M. Backer and C. R. Hopkins (2001). Human Vps34 is required for internal vesicle formation within multivesicular endosomes. *The Journal of Cell Biology* **155**(7): 1251-1264.

Futter, C. E., A. Pearse, L. J. Hewlett and C. R. Hopkins (1996). Multivesicular endosomes containing internalized EGF-EGF receptor complexes mature and then fuse directly with lysosomes. *The Journal of Cell Biology* **132**(6): 1011-1023.

Gabriel, K., A. Ingram, R. Austin, A. Kapoor, D. Tang, F. Majeed, T. Qureshi and K. Al-Nedawi (2013). Regulation of the tumor suppressor Pten through exosomes: A diagnostic potential for prostate cancer. *PLoS ONE* **8**(7): e70047.

Gallet, A., L. Ruel, L. Staccini-Lavenant and P. P. Thérond (2006). Cholesterol modification is necessary for controlled planar long-range activity of hedgehog in *Drosophila* epithelia. *Development* **133**(3): 407-418.

Garside, V., A. Chang, A. Karsan and P. Hoodless (2013). Co-ordinating notch, BMP, and TGF-β signaling during heart valve development. *Cellular and Molecular Life Sciences* **70**(16): 2899-2917.

Ge, R., E. Tan, S. Sharghi-Namini and H. Asada (2012). Exosomes in cancer microenvironment and beyond: Have we overlooked these extracellular messengers? *Cancer Microenvironment* **5**(3): 323-332.

Ghazi-Tabatabai, S., S. Saksena, J. M. Short, A. V. Pobbati, D. B. Veprintsev, R. A. Crowther, S. D. Emr, E. H. Egelman and R. L. Williams (2008). Structure and disassembly of filaments formed by the ESCRT-III subunit Vps24. *Structure* **16**(9): 1345-1356.

Ghossoub, R., F. Lembo, A. Rubio, C. B. Gaillard, J. Bouchet, N. Vitale, J. Slavík, M. Machala and P. Zimmermann (2014). Syntenin-ALiX exosome biogenesis and budding into multivesicular bodies are controlled by ARF6 and PLD2. *Nat Commun* **5:**3477.

Gligorov, D., J. L. Sitnik, R. K. Maeda, M. F. Wolfner and F. Karch (2013). A novel function for the hox gene *Abd-B* in the male accessory gland regulates the long-term female post-mating response in *Drosophila. PLoS Genet* **9**(3): e1003395.

Goberdhan, D. C. (2010). Intracellular amino acid sensing and mTOR1-regulated growth: New ways to block an old target? *Curr Opin Investig Drugs.* **11**(12): 1360-1367.

Goberdhan, D. C. I., N. Paricio, E. C. Goodman, M. Mlodzik and C. Wilson (1999). *Drosophila* tumor suppressor Pten controls cell size and number by antagonizing the chico/PI3-Kinase signaling pathway. *Genes & Development* **13**(24): 3244-3258.

Goentoro, L. A., G. T. Reeves, C. P. Kowal, L. Martinelli, T. Schüpbach and S. Y. Shvartsman (2006). Quantifying the gurken morphogen gradient in *Drosophila* oogenesis. *Developmental Cell* **11**(2): 263-272.

Golembo, M., R. Schweitzer, M. Freeman and B. Z. Shilo (1996). Argos transcription is induced by the *Drosophila* EGF receptor pathway to form an inhibitory feedback loop. *Development* **122**(1): 223-230.

Golembo, M., T. Yarnitzky, T. Volk and B.-Z. Shilo (1999). Vein expression is induced by the EGF receptor pathway to provide a positive feedback loop in patterning the *Drosophila* embryonic ventral ectoderm. *Genes & Development* **13**(2): 158-162.

Greco, V., M. Hannus and S. Eaton (2001). Argosomes: A potential vehicle for the spread of morphogens through epithelia. *Cell* **106**(5): 633-645.

Gross, J. C., V. Chaudhary, K. Bartscherer and M. Boutros (2012). Active wnt proteins are secreted on exosomes. *Nat Cell Biol* **14**(10): 1036-1045.

Guerrero, I., and C. Chiang (2007). A conserved mechanism of hedgehog gradient formation by lipid modifications. *Trends in Cell Biology* **17**(1): 1-5.

Gusachenko, O. N., M. A. Zenkova and V. V. Vlassov (2013). Nucleic acids in exosomes: Disease markers and intercellular communication molecules. *Biochemistry (Moscow)* **78**(1): 1-7.

György, B., T. Szabó, M. Pásztói, Z. Pál, P. Misják, B. Aradi, V. László, É. Pállinger, E. Pap, Á. Kittel, G. Nagy, A. Falus and E. Buzás (2011). Membrane vesicles, current state-of-the-art: Emerging role of extracellular vesicles. *Cellular and Molecular Life Sciences* **68**(16): 2667-2688.

Haerty, W., S. Jagadeeshan, R. J. Kulathinal, A. Wong, K. Ravi Ram, L. K. Sirot, L. Levesque, C. G. Artieri, M. F. Wolfner, A. Civetta and R. S. Singh (2007). Evolution in the fast lane: Rapidly evolving sex-related genes in *Drosophila. Genetics* **177**(3): 1321-1335.

Hanson, P. I., R. Roth, Y. Lin and J. E. Heuser (2008). Plasma membrane deformation by circular arrays of ESCRT-III protein filaments. *The Journal of Cell Biology* **180**(2): 389-402.

Häsemeyer, M., N. Yapici, U. Heberlein and B. J. Dickson (2009). Sensory neurons in the *Drosophila* genital tract regulate female reproductive behavior. *Neuron* **61**(4): 511-518.

Hata, A., G. Lagna, J. Massagué and A. Hemmati-Brivanlou (1998). Smad6 inhibits BMP/Smad1 signaling by specifically competing with the Smad4 tumor suppressor. *Genes & Development* **12**(2): 186-197.

Hayashi, S., K. Ito, Y. Sado, M. Taniguchi, A. Akimoto, H. Takeuchi, T. Aigaki, F. Matsuzaki, H. Nakagoshi, T. Tanimura, R. Ueda, T. Uemura, M. Yoshihara and S. Goto (2002). Getdb, a database compiling expression patterns and molecular locations of a collection of gal4 enhancer traps. *genesis* **34**(1-2): 58-61.

Hayes, S., A. Chawla and S. Corvera (2002). Tgf-β receptor internalization into EEA1-enriched early endosomes: role in signaling to Smad2. *The Journal of Cell Biology* **158**(7): 1239-1249.

Hazawa, M., K. Tomiyama, A. Saotome-Nakamura, C. Obara, T. Yasuda, T. Gotoh, I. Tanaka, H. Yakumaru, H. Ishihara and K. Tajima (2014). Radiation increases the cellular uptake of exosomes through CD29/CD81 complex formation. *Biochemical and Biophysical Research Communications* **446**(4): 1165-1171.

Hegde, R. S. and S.-W. Kang (2008). The concept of translocational regulation. *The Journal of Cell Biology* **182**(2): 225-232.

Heifetz, Y., L. N. Vandenberg, H. I. Cohn and M. F. Wolfner (2005). Two cleavage products of the *Drosophila* accessory gland protein ovulin can independently induce ovulation. *Proceedings of the National Academy of Sciences of the United States of America* **102**(3): 743-748.

Heijnen, H. F. G., A. E. Schiel, R. Fijnheer, H. J. Geuze and J. J. Sixma (1999). Activated platelets release two types of membrane vesicles: Microvesicles by surface shedding and exosomes derived from exocytosis of multivesicular bodies and secretory granules. *Blood* **94**(11): 3791-3799.

Helms, J. B. and C. Zurzolo (2004). Lipids as targeting signals: Lipid rafts and intracellular trafficking. *Traffic* **5**(4): 247-254.

Hemler, M. E. (2003). Tetraspanin proteins mediate cellular penetration, invasion, and fusion events and define a novel type of membrane microdomain. *Annual Review of Cell and Developmental Biology* **19**(1): 397-422.

Henderson, K. D. and D. J. Andrew (1998). Identification of a novel *Drosophila* Smad on the X chromosome. *Biochemical and Biophysical Research Communications* **252**(1): 195-201.

Hennig, K. M., J. Colombani and T. P. Neufeld (2006). Tor coordinates bulk and targeted endocytosis in the *Drosophila melanogaster* fat body to regulate cell growth. *The Journal of Cell Biology* **173**(6): 963-974.

Herndon, L. A. and M. F. Wolfner (1995). A *Drosophila* seminal fluid protein, Acp26Aa, stimulates egg laying in females for 1 day after mating. *Proceedings of the National Academy of Sciences* **92**(22): 10114-10118.

Higginbotham, J. N., M. Demory Beckler, J. D. Gephart, J. L. Franklin, G. Bogatcheva, G.-J. Kremers, D. W. Piston, G. D. Ayers, R. E. Mcconnell, M. J. Tyska and R. J. Coffey (2011). Amphiregulin exosomes increase cancer cell invasion. *Current Biology* **21**(9): 779-786.

Hirota, Y., T. Kuronita, H. Fujita and Y. Tanaka (2007). A role for Rab5 activity in the biogenesis of endosomal and lysosomal compartments. *Biochemical and Biophysical Research Communications* **364**(1): 40-47.

Hoodless, P. A., T. Haerry, S. Abdollah, M. Stapleton, M. B. O'connor, L. Attisano and J. L. Wrana (1996). Madr1, a mad-related protein that functions in BMP2 signaling pathways. *Cell* **85**(4): 489-500.

Hooper, N. (1991). Angiotensin converting enzyme: Implications from molecular biology for its physiological functions. *Int J Biochem.* **23**(7-8): 641-647.

Hoshino, D., J. Jourquin, S. W. Emmons, T. Miller, M. Goldgof, K. Costello, D. R. Tyson, B. Brown, Y. Lu, N. K. Prasad, B. Zhang, G. B. Mills, W. G. Yarbrough, V. Quaranta, M. Seiki and A. M. Weaver (2012). Network analysis of the focal adhesion to invadopodia transition identifies a PI3K-PKCα invasive signaling axis. *Sci. Signal.* **5**(241): ra66-.

Hoshino, D., Kellye C. Kirkbride, K. Costello, Emily S. Clark, S. Sinha, N. Grega-Larson, Matthew J. Tyska and Alissa M. Weaver (2013). Exosome secretion is enhanced by invadopodia and drives invasive behavior. *Cell Reports* **5**(5): 1159-1168.

Hsu, C., Y. Morohashi, S.-i. Yoshimura, N. Manrique-Hoyos, S. Jung, M. A. Lauterbach, M. Bakhti, M. Grønborg, W. Möbius, J. Rhee, F. A. Barr and M. Simons (2010). Regulation of exosome secretion by Rab35 and its GTPase-activating proteins TBC1D10a–c. *The Journal of Cell Biology* **189**(2): 223-232.

Hudson, J. B., S. D. Podos, K. Keith, S. L. Simpson and E. L. Ferguson (1998). The *Drosophila medea* gene is required downstream of *dpp* and encodes a functional homolog of human *smad4. Development* **125**(8): 1407-1420.

Huotari, J. and A. Helenius (2011). Endosome maturation. *EMBO J* **30**(17): 3481-3500.

Inoue, H., T. Imamura, Y. Ishidou, M. Takase, Y. Udagawa, Y. Oka, K. Tsuneizumi, T. Tabata, K. Miyazono and M. Kawabata (1998). Interplay of signal mediators of decapentaplegic (dpp): Molecular characterization of mothers against dpp, medea, and daughters against dpp. *Molecular Biology of the Cell* **9**(8): 2145-2156.

Italiano Jr, J. E., T. M. Roberts, M. Stewart and C. A. Fontana (1996). Reconstitution *in vitro* of the motile apparatus from the amoeboid sperm of ascaris shows that filament assembly and bundling move membranes. *Cell* **84**(1): 105-114.

Jékely, G. and P. Rørth (2003). Hrs mediates downregulation of multiple signalling receptors in *Drosophila. EMBO rep.* **4**(12):1163-8.

Jiang, B. H. and L. Z. Liu (2009). Chapter 2 PI3K/Pten signaling in angiogenesis and tumorigenesis. *Advances in cancer research.* F. V. W. George and K. George, Academic Press. **102:** 19-65.

Jiang, H., P. H. Patel, A. Kohlmaier, M. O. Grenley, D. G. Mcewen and B. A. Edgar (2009). Cytokine/JAK/Stat signaling mediates regeneration and homeostasis in the *Drosophila* midgut. *Cell* **137**(7): 1343-1355.

Ju, R., Z. W. Zhuang, J. Zhang, A. A. Lanahan, T. Kyriakides, W. C. Sessa and M. Simons (2014). Angiopoietin-2 secretion by endothelial cell exosomes: Regulation by the phosphatidylinositol 3-kinase (PI3K)/Akt/endothelial nitric oxide synthase (eNos) and syndecan-4/syntenin pathways. *Journal of Biological Chemistry* **289**(1): 510-519.

Juárez, P. and T. A. Guise (2011). Tgf-β in cancer and bone: Implications for treatment of bone metastases. *Bone* **48**(1): 23-29.

Juhász, G., J. H. Hill, Y. Yan, M. Sass, E. H. Baehrecke, J. M. Backer and T. P. Neufeld (2008). The class III PI(3)K Vps34 promotes autophagy and endocytosis but not tor signaling in *Drosophila. The Journal of Cell Biology* **181**(4): 655-666.

Kajimoto, T., T. Okada, S. Miya, L. Zhang and S.-i. Nakamura (2013). Ongoing activation of sphingosine 1-phosphate receptors mediates maturation of exosomal multivesicular endosomes. *Nat Commun* **4**:2712.

Kalb, J. M., A. J. Dibenedetto and M. F. Wolfner (1993). Probing the function of *Drosophila melanogaster* accessory glands by directed cell ablation. *Proceedings of the National Academy of Sciences* **90**(17): 8093-8097.

Kamiya, Y., K. Miyazono and K. Miyazawa (2008). Specificity of the inhibitory effects of Dad on Tgf-β family type I receptors, Thickveins, Saxophone, and Baboon in *Drosophila. FEBS Letters* **582**(17): 2486-2500.

Katoh, K., H. Shibata, H. Suzuki, A. Nara, K. Ishidoh, E. Kominami, T. Yoshimori and M. Maki (2003). The ALG-2-interacting protein ALiX associates with CHMP4b, a human homologue of yeast Snf7 that is involved in multivesicular body sorting. *Journal of Biological Chemistry* **278**(40): 39104-39113.

Katzmann, D. J., M. Babst and S. D. Emr (2001). Ubiquitin-dependent sorting into the multivesicular body pathway requires the function of a conserved endosomal protein sorting complex, ESCRT-I. *Cell* **106**(2): 145-155.

Katzmann, D. J., C. J. Stefan, M. Babst and S. D. Emr (2003). Vps27 recruits ESCRT machinery to endosomes during MVB sorting. *The Journal of Cell Biology* **162**(3): 413-423.

Kawase, E., M. D. Wong, B. C. Ding and T. Xie (2004). Gbb/BMP signaling is essential for maintaining germline stem cells and for repressing bam transcription in the *Drosophila* testis. *Development* **131**(6): 1365-1375.

Kelly, R. W., P. Holland, G. Skibinski, C. Harrison, L. McMillan, T. Hargreave, and K. James (1991). Extracellular organelles (prostasomes) are immunosuppressive components of human semen. *Clin Exp Immunol.* **86**(3): 550-556.

Kershaw-Young, C. M., X. Druart, J. Vaughan and W. M. C. Maxwell (2012). B-nerve growth factor is a major component of Alpaca seminal plasma and induces ovulation in female Alpacas. *Reproduction, Fertility and Development* **24**(8): 1093-1097.

Khalsa, O., J. W. Yoon, S. Torres-Schumann and K. A. Wharton (1998). Tgf-beta/BMP superfamily members, Gbb-60a and Dpp, cooperate to provide pattern information and establish cell identity in the *Drosophila* wing. *Development* **125**(14): 2723-2734.

Kharaziha, P., S. Ceder, Q. Li and T. Panaretakis (2012). Tumor cell-derived exosomes: A message in a bottle. *Biochimica et Biophysica Acta (BBA) - Reviews on Cancer* **1826**(1): 103-111.

Kim, H. J. and D. Bar-Sagi (2004). Modulation of signalling by sprouty: A developing story. *Nat Rev Mol Cell Biol* **5**(6): 441-450.

Kim J, M. S., M. Le, D. Bedore, D.T. Umetsu, D. Di Vizio, M.R. Freeman (2014). Enhanced shedding of extracellular vesicles from amoeboid prostate cancer cells: Potential effects on the tumor microenvironment. *Cancer Biology & Therapy* **15**: 409-418.

Kirilly, D., E. P. Spana, N. Perrimon, R. W. Padgett and T. Xie (2005). BMP signaling is required for controlling somatic stem cell self-renewal in the *Drosophila* ovary. *Developmental Cell* **9**(5): 651-662.

Koles, K., J. Nunnari, C. Korkut, R. Barria, C. Brewer, Y. Li, J. Leszyk, B. Zhang and V. Budnik (2012). Mechanism of evenness interrupted (evi)-exosome release at synaptic boutons. *Journal of Biological Chemistry* **287**(20): 16820-16834.

Korkut, C., B. Ataman, P. Ramachandran, J. Ashley, R. Barria, N. Gherbesi and V. Budnik (2009). Trans-synaptic transmission of vesicular wnt signals through evi/wntless. *Cell* **139**(2): 393-404.

Kosinski, M., K. Mcdonald, J. Schwartz, I. Yamamoto and D. Greenstein (2005). *C. elegans* sperm bud vesicles to deliver a meiotic maturation signal to distant oocytes. *Development* **132**(15): 3357-3369.

Köttgen, M., A. Hofherr, W. Li, K. Chu, S. Cook, C. Montell and T. Watnick (2011). *Drosophila* sperm swim backwards in the female reproductive tract and are activated via Trpp2 ion channels. *PLoS ONE* **6**(5): e20031.

Kranenburg, O., I. Verlaan and W. H. Moolenaar (1999). Dynamin is required for the activation of mitogen-activated protein (MAP) kinase by MAP Kinase Kinase. *Journal of Biological Chemistry* **274**(50): 35301-35304.

Kruse, K., P. Pantazis, T. Bollenbach, F. Jülicher and M. González-Gaitán (2004). Dpp gradient formation by dynamin-dependent endocytosis: Receptor trafficking and the diffusion model. *Development* **131**(19): 4843-4856.

Krüttner, S., B. Stepien, J. N. Noordermeer, M. A. Mommaas, K. Mechtler, B. J. Dickson and K. Keleman (2012). *Drosophila* CPEB Orb2a mediates memory independent of its RNA-binding domain. *Neuron* **76**(2): 383-395.

Kubli, E. (2003). Sex-peptides: Seminal peptides of the *Drosophila* male. *Cellular and Molecular Life Sciences CMLS* **60**(8): 1689-1704.

Kubli, E. and D. Bopp (2012). Sexual behavior: How sex peptide flips the postmating switch of female flies. *Current Biology* **22**(13): R520-R522.

Kurada, P. and K. White (1999). Epidermal growth factor receptor: Its role in *Drosophila* eye differentiation and cell survival. *Apoptosis* **4**(4): 239-243.

Laflamme, B. A., K. Ravi Ram and M. F. Wolfner (2012). The *Drosophila melanogaster* seminal fluid protease "seminase" regulates proteolytic and post-mating reproductive processes. *PLoS Genet* **8**(1): e1002435.

Laflamme, B. A. and M. F. Wolfner (2013). Identification and function of proteolysis regulators in seminal fluid. *Molecular Reproduction and Development* **80**(2): 80-101.

Lance, R. S., R. R. Drake and D. A. Troyer (2011). Multiple recognition assay reveals prostasomes as promising plasma biomarkers for prostate cancer. *Expert Review of Anticancer Therapy* **11**(9): 1341-1343.

Lanzetti, L., V. Rybin, M. G. Malabarba, S. Christoforidis, G. Scita, M. Zerial and P. P. Di Fiore (2000). The Eps8 protein coordinates EGF receptor signalling through Rac and trafficking through Rab5. *Nature* **408**(6810): 374-377.

Leevers, S. J., D. Weinkove, L. K. Macdougall, E. Hafen and M. D. Waterfield (1996). The *Drosophila* phosphoinositide 3-kinase Dp110 promotes cell growth. *EMBO J* **15**(23): 6584-6594.

Leiblich, A., L. Marsden, C. Gandy, L. Corrigan, R. Jenkins, F. Hamdy and C. Wilson (2012). Bone morphogenetic protein- and mating-dependent secretory cell growth and migration in the *Drosophila* accessory gland. *Proceedings of the National Academy of Sciences* **109**(47): 19292-19297.

Leslie, N. R., H. Maccario, L. Spinelli and L. Davidson (2009). The significance of Pten's protein phosphatase activity. *Advances in Enzyme Regulation* **49**(1): 190-196.

Lesokhin, A. M., S.-Y. Yu, J. Katz and N. E. Baker (1999). Several levels of EGF receptor signaling during photoreceptor specification in wild-type, Ellipse, and null mutant *Drosophila. Developmental Biology* **205**(1): 129-144.

Letsou, A., K. Arora, J. L. Wrana, K. Simin, V. Twombly, J. Jamal, K. Staehling-Hampton, F. M. Hoffmann, W. M. Gelbart, J. Massagué and M. B. O'connor (1995). Drosophila dpp signaling is mediated by the punt gene product: A dual ligand-binding type II receptor of the Tgfβ receptor family. *Cell* **80**(6): 899-908.

Li, G., C. D'souza-Schorey, M. A. Barbieri, R. L. Roberts, A. Klippel, L. T. Williams and P. D. Stahl (1995). Evidence for phosphatidylinositol 3-kinase as a regulator of endocytosis via activation of Rab5. *Proceedings of the National Academy of Sciences* **92**(22): 10207-10211.

Liégeois, S., A. Benedetto, J.-M. Garnier, Y. Schwab and M. Labouesse (2006). The V0-atpase mediates apical secretion of exosomes containing hedgehog-related proteins in *Caenorhabditis elegans. The Journal of Cell Biology* **173**(6): 949-961.

Lindmo, K. and H. Stenmark (2006). Regulation of membrane traffic by phosphoinositide 3-kinases. *Journal of Cell Science* **119**(4): 605-614.

Liu, H. and E. Kubli (2003). Sex-peptide is the molecular basis of the sperm effect in *Drosophila melanogaster. Proceedings of the National Academy of Sciences* **100**(17): 9929-9933.

Llorente, A., M. C. De Marco and M. A. Alonso (2004). Caveolin-1 and MAL are located on prostasomes secreted by the prostate cancer PC-3 cell line. *Journal of Cell Science* **117**(22): 5343-5351.

Lloyd, T. E., Richard Atkinson, Mark N. Wu, Yi Zhou, Giuseppa Pennetta and H. J. Bellen (2002). Hrs regulates endosome membrane invagination and tyrosine kinase receptor signaling in *Drosophila*. *Cell* **108**(2): 261-269.

Lu, X. and Y. Kang (2009). Epidermal growth factor signalling and bone metastasis. *Br J Cancer* **102**(3): 457-461.

Ludwig, A.-K. and B. Giebel (2012). Exosomes: Small vesicles participating in intercellular communication. *The International Journal of Biochemistry; Cell Biology* **44**(1): 11-15.

Lung, O. and M. F. Wolfner (1999). *Drosophila* seminal fluid proteins enter the circulatory system of the mated female fly by crossing the posterior vaginal wall. *Insect Biochemistry and Molecular Biology* **29**(12): 1043-1052.

Lung, O. and M. F. Wolfner (2001). Identification and characterization of the major *Drosophila melanogaster* mating plug protein. *Insect Biochemistry and Molecular Biology* **31**(6–7): 543-551.

Mader, C. C., M. Oser, M. A. O. Magalhaes, J. J. Bravo-Cordero, J. Condeelis, A. J. Koleske and H. Gil-Henn (2011). An EGFR–Src–Arg–cortactin pathway mediates functional maturation of invadopodia and breast cancer cell invasion. *Cancer Research* **71**(5): 1730-1741.

Mair, W., C. M. Sgrò, A. P. Johnson, T. Chapman and L. Partridge (2004). Lifespan extension by dietary restriction in female *Drosophila melanogaster* is not caused by a reduction in vitellogenesis or ovarian activity. *Experimental Gerontology* **39**(7): 1011-1019.

Manning, A. (1962). A sperm factor affecting the receptivity of *Drosophila melanogaster f*emales. *Nature* **194**(4825): 252-253.

Markus, B. (2011). MVB vesicle formation: ESCRT-dependent, ESCRT-independent and everything in between. *Current Opinion in Cell Biology* **23**(4): 452-457.

Markvoort, A. J., A. F. Smeijers, K. Pieterse, R. A. Van Santen and P. A. J. Hilbers (2007). Lipid-based mechanisms for vesicle fission. *The Journal of Physical Chemistry B* **111**(20): 5719-5725.

Marmion, R. A., M. Jevtic, A. Springhorn, G. Pyrowolakis and N. Yakoby (2013). The *Drosophila* BMPRII, *wishful thinking*, is required for eggshell patterning. *Developmental Biology* **375**(1): 45-53.

Marois, E., A. Mahmoud and S. Eaton (2006). The endocytic pathway and formation of the wingless morphogen gradient. *Development* **133**(2): 307-317.

Massagué, J., L. Attisano and J. L. Wrana (1994). The tgf-β family and its composite receptors. *Trends in Cell Biology* **4**(5): 172-178.

Matsuo, H., J. Chevallier, N. Mayran, I. Le Blanc, C. Ferguson, J. Fauré, N. S. Blanc, S. Matile, J. Dubochet, R. Sadoul, R. G. Parton, F. Vilbois and J. Gruenberg (2004). Role of LBPA and ALiX in multivesicular liposome formation and endosome organization. *Science* **303**(5657): 531-534.

Mccabe, B. D., G. Marqués, A. P. Haghighi, R. D. Fetter, M. L. Crotty, T. E. Haerry, C. S. Goodman and M. B. O'connor (2003). The BMP homolog Gbb provides a retrograde signal that regulates synaptic growth at the *Drosophila* neuromuscular junction. *Neuron* **39**(2): 241-254.

Mcguire, S. E., Z. Mao and R. L. Davis (2004). Spatiotemporal gene expression targeting with the target and gene-switch systems in *Drosophila. Sci. STKE* **2004**(220): pl6-.

Mendoza M. C., E. Emrah Er and J. Blenis (2011). The Ras-erk and PI3K-mTOR pathways: Cross-talk and compensation. *trends in Biochemical Sciences* **36**(6): 320-328.

Michel, M., I. Raabe, A. P. Kupinski, R. Perez-Palencia and C. Bokel (2011). Local Bmp receptor activation at adherens junctions in the *Drosophila* germline stem cell niche. *Nat Commun* **2**: 415.

Miller, A. (1950). The internal anatomy and histology of the imago of *Drosophila melanogaster,* Biology of *Drosophila*. *Cold Spring Harbor Laboratory Press*: 420-534.

Minami, R., M. Wakabayashi, S. Sugimori, K. Taniguchi, A. Kokuryo, T. Imano, T. Adachi-Yamada, N. Watanabe and H. Nakagoshi (2012). The homeodomain protein *defective proventriculus* is essential for male accessory gland development to enhance fecundity in *Drosophila. PLoS ONE* **7**(3): e32302.

Mineo, M., S. Garfield, S. Taverna, A. Flugy, G. De Leo, R. Alessandro and E. Kohn (2012). Exosomes released by K562 chronic myeloid leukemia cells promote angiogenesis in a Src-dependent fashion. *Angiogenesis* **15**(1): 33-45.

Minogue, S., M. G. Waugh, M. A. De Matteis, D. J. Stephens, F. Berditchevski and J. J. Hsuan (2006). Phosphatidylinositol 4-kinase is required for endosomal trafficking and degradation of the EGF receptor. *Journal of Cell Science* **119**(3): 571-581.

Misra, S. and J. H. Hurley (1999). Crystal structure of a phosphatidylinositol 3-phosphate-specific membrane-targeting motif, the FYVE domain of Vps27p. *Cell* **97**(5): 657-666.

Miura, S., A. P. Singh and Y. Mishina (2010). BMPR1a is required for proper migration of the AVE through regulation of Dkk1 expression in the pre-streak mouse embryo. *Developmental Biology* **341**(1): 246-254.

Möbius, W., E. Van Donselaar, Y. Ohno-Iwashita, Y. Shimada, H. F. G. Heijnen, J. W. Slot and H. J. Geuze (2003). Recycling compartments and the internal vesicles of multivesicular bodies harbor most of the cholesterol found in the endocytic pathway. *Traffic* **4**(4): 222-231.

Momen-Heravi, F., L. Balaj, S. Alian,P. Y. Mantel, A. E. Halleck, A. J. Trachtenberg, C. E. Soria, S. Oquin, C. M. Bonebreak, E. Saracoglu, J. Skog, W. P. Kuo. (2013). Current methods for the isolation of extracellular vesicles. *Biol Chem* **394**(10): 1253-1262.

Monsma, H. H., M. F. Wolfner. (1990). Synthesis of two *Drosophila* male accessory gland proteins and their fate after transfer to the female during mating. *Dev Biol* **142**(2): 465-475.

Morelli, A. E., A. T. Larregina, W. J. Shufesky, M. L. G. Sullivan, D. B. Stolz, G. D. Papworth, A. F. Zahorchak, A. J. Logar, Z. Wang, S. C. Watkins, L. D. Falo and A. W. Thomson (2004). Endocytosis, intracellular sorting, and processing of exosomes by dendritic cells. *Blood* **104**(10): 3257-3266.

Morris, R. J. (2010). Ionic control of the metastable inner leaflet of the plasma membrane: Fusions natural and artefactual. *FEBS Letters* **584**(9): 1665-1669.

Morrison, C. D., J. G. Parvani and W. P. Schiemann (2013). The relevance of the Tgf-β paradox to EMT-MET programs. *Cancer Letters* **341**(1): 30-40.

Moshitzky P, F. I., Chaimov N, Saudan P, Klauser S, Kubli E, Applebaum SW. (1996). Sex-peptide activates juvenile hormone biosynthesis in the *Drosophila melanogaster* corpus allatum. *Arch Insect Biochem Physiol.* **32**(3-4): 363-374.

Mueller, T. D. and J. Nickel (2012). Promiscuity and specificity in Bmp receptor activation. *FEBS Letters* **586**(14): 1846-1859.

Muniz, M. and H. Riezman (2000). Intracellular transport of GPI-anchored proteins. *EMBO J* **19**(1): 10-15.

Muralidharan-Chari, V., J. W. Clancy, A. Sedgwick and C. D'souza-Schorey (2010). Microvesicles: Mediators of extracellular communication during cancer progression. *Journal of Cell Science* **123**(10): 1603-1611.

Muralidharan-Chari, V., H. Hoover, J. Clancy, J. Schweitzer, M. A. Suckow, V. Schroeder, F. J. Castellino, J. S. Schorey and C. D'souza-Schorey (2009). Adp-ribosylation factor 6 regulates tumorigenic and invasive properties in vivo. *Cancer Research* **69**(6): 2201-2209.

Nabhan, J. F., R. Hu, R. S. Oh, S. N. Cohen and Q. Lu (2012). Formation and release of Arrestin domain-containing protein 1-mediated microvesicles (ARMMS) at plasma membrane by recruitment of Tsg101 protein. *Proceedings of the National Academy of Sciences* **109**(11): 4146-4151.

Nakayama S, K. K., Aigaki T. (1997). Ectopic expression of sex-peptide in a variety of tissues in *Drosophila* females using the p[Gal4] enhancer-trap system. . *Mol Gen Genet.* **254**(4): 449-455.

Narasimha M., A. Uv, A. Krejci, N. H. Brown and S. J. Bray (2008). Grainy head promotes expression of septate junction proteins and influences epithelial morphogenesis *J Cell Sci* **121**: 747-752.

Neul, J. L. and E. L. Ferguson (1998). Spatially restricted activation of the Sax receptor by Scw modulates Dpp/Tkv signaling in *Drosophila* dorsal–ventral patterning. *Cell* **95**(4): 483-494.

Ni, J.-Q., M. Markstein, R. Binari, B. Pfeiffer, L.-P. Liu, C. Villalta, M. Booker, L. Perkins and N. Perrimon (2008). Vector and parameters for targeted transgenic RNA interference in *Drosophila* melanogaster. *Nat Meth* **5**(1): 49-51.

Nichols, B. (2003). Caveosomes and endocytosis of lipid rafts. *Journal of Cell Science* **116**(23): 4707-4714.

Nickerson, D. P., M. West, R. Henry and G. Odorizzi (2010). Regulators of Vps4 ATPase activity at endosomes differentially influence the size and rate of formation of intralumenal vesicles. *Molecular Biology of the Cell* **21**(6): 1023-1032.

Ninov, N., S. Menezes-Cabral, C. Prat-Rojo, C. Manjón, A. Weiss, G. Pyrowolakis, M. Affolter and E. Martín-Blanco (2010). Dpp signaling directs cell motility and invasiveness during epithelial morphogenesis. *Current Biology* **20**(6): 513-520.

Nishi, T. and M. Forgac (2002). The vacuolar (H+)-ATPases — nature's most versatile proton pumps. *Nat Rev Mol Cell Biol* **3**(2): 94-103.

O' Connor, M. B., D. Umulis, H. G. Othmer and S. S. Blair (2006). Shaping Bmp morphogen gradients in the *Drosophila* embryo and pupal wing. *Development* **133**(2): 183-193.

Odorizzi, G., D. J. Katzmann, M. Babst, A. Audhya and S. D. Emr (2003). Bro1 is an endosome-associated protein that functions in the MVB pathway in *Saccharomyces cerevisiae*. *Journal of Cell Science* **116**(10): 1893-1903.

Ögmundsdóttir, M. H., S. Heublein, S. Kazi, B. Reynolds, S. M. Visvalingam, M. K. Shaw and D. C. I. Goberdhan (2012). Proton-assisted amino acid transporter PAT1 complexes with RAG GTPases and activates TORC1 on late endosomal and lysosomal membranes. *PLoS ONE* **7**(5): e36616.

Okkenhaug, K. (2013). Signaling by the phosphoinositide 3-kinase family in immune cells. *Annual Review of Immunology* **31**(1): 675-704.

Olguín, P., A. Glavic and M. Mlodzik (2011). Intertissue mechanical stress affects frizzled-mediated planar cell polarity in the *Drosophila* notum epidermis. *Current Biology* **21**(3): 236-242.

Opresko, L. K., C.-P. Chang, B. H. Will, P. M. Burke, G. N. Gill and H. S. Wiley (1995). Endocytosis and lysosomal targeting of epidermal growth factor receptors are mediated by distinct sequences independent of the tyrosine kinase domain. *Journal of Biological Chemistry* **270**(9): 4325-4333.

Orlean, P. and A. K. Menon (2007). Thematic review series: Lipid posttranslational modifications. GPI anchoring of protein in yeast and mammalian cells, or: how we learned to stop worrying and love glycophospholipids. *Journal of Lipid Research* **48**(5): 993-1011.

Orme, M. H., S. Alrubaie, G. L. Bradley, C. D. Walker and S. J. Leevers (2006). Input from ras is required for maximal pi(3)k signalling in drosophila. *Nat Cell Biol* **8**(11): 1298-1302.

Ostrowski, M., N. B. Carmo, S. Krumeich, I. Fanget, G. Raposo, A. Savina, C. F. Moita, K. Schauer, A. N. Hume, R. P. Freitas, B. Goud, P. Benaroch, N. Hacohen, M. Fukuda, C. Desnos, M. C. Seabra, F. Darchen, S. Amigorena, L. F. Moita and C. Thery (2010). Rab27a and Rab27b control different steps of the exosome secretion pathway. *Nat Cell Biol* **12**(1): 19-30.

Palm, W., J. L. Sampaio, M. Brankatschk, M. Carvalho, A. Mahmoud, A. Shevchenko and S. Eaton (2012). Lipoproteins in *Drosophila melanogaster* —assembly, function, and influence on tissue lipid composition. *PLoS Genet* **8**(7): e1002828.

Palmerini, C. A., E. Carlini, A. Nicolucci and G. Arienti (1999). Increase of human spermatozoa intracellular Ca^{2+}concentration after fusion with prostasomes. *Cell Calcium* **25**(4): 291-296.

Panakova, D., H. Sprong, E. Marois, C. Thiele and S. Eaton (2005). Lipoprotein particles are required for hedgehog and wingless signalling. *Nature* **435**(7038): 58-65.

Park, K.-H., B.-J. Kim, J. Kang, T.-S. Nam, J. M. Lim, H. T. Kim, J. K. Park, Y. G. Kim, S.-W. Chae and U.-H. Kim (2011). Ca^{2+} signaling tools acquired from prostasomes are required for progesterone-induced sperm motility. *Sci. Signal.* **4**(173): ra31-.

Parker, G. A. (1970). Sperm competition and its evolutionary consequences in the insects. *Biological Reviews* **45**(4): 525-567.

Parolini, I., C. Federici, C. Raggi, L. Lugini, S. Palleschi, A. De Milito, C. Coscia, E. Iessi, M. Logozzi, A. Molinari, M. Colone, M. Tatti, M. Sargiacomo and S. Fais (2009). Microenvironmental pH is a key factor for exosome traffic in tumor cells. *Journal of Biological Chemistry* **284**(49): 34211-34222.

Parrish, J. Z., P. Xu, C. C. Kim, L. Y. Jan and Y. N. Jan (2009). The microRNA *bantam* functions in epithelial cells to regulate scaling growth of dendrite arbors in *Drosophila* sensory neurons. *Neuron* **63**(6): 788-802.

Parsons, R. (2004). Human cancer, Pten and the PI-3 Kinase pathway. *Seminars in Cell & Developmental Biology* **15**(2): 171-176.

Paschen, S. A. and W. Neupert (2001). Protein import into mitochondria. *IUBMB Life* **52**(3-5): 101-112.

Pashkova, N., L. Gakhar, S. C. Winistorfer, A. B. Sunshine, M. Rich, M. J. Dunham, L. Yu and R. C. Piper (2013). The yeast *ALiX* homolog *Bro1* functions as a ubiquitin receptor for protein sorting into multivesicular endosomes. *Developmental Cell* **25**(5): 520-533.

Pasquet, J.-M., J. Dachary-Prigent and A. T. Nurden (1996). Calcium influx is a determining factor of calpain activation and microparticle formation in platelets. *European Journal of Biochemistry* **239**(3): 647-654.

Pasquet, J.-M., F. Toti, A. T. Nurden and J. Dachary-Prigent (1996). Procoagulant activity and active calpain in platelet-derived microparticles. *Thrombosis Research* **82**(6): 509-522.

Patterson, J. Y. (1943). Studies in the genetics of *Drosophila*. Iii. *The Drosophilidae of the Southwest.*: 55.

Peng, J., S. Chen, S. Büsser, H. Liu, T. Honegger and E. Kubli (2005). Gradual release of sperm bound sex-peptide controls female postmating behavior in *Drosophila*. *Current Biology* **15**(3): 207-213.

Peng, J., P. Zipperlen and E. Kubli (2005). *Drosophila* sex-peptide stimulates female innate immune system after mating via the Toll and IMD pathways. *Current Biology* **15**(18): 1690-1694.

Pilch, B. and M. Mann (2006). Large-scale and high-confidence proteomic analysis of human seminal plasma. *Genome Biology* **7**(5): R40.

Pilpel, N., I. Nezer, S. W. Applebaum and Y. Heifetz (2008). Mating-increases trypsin in female drosophila hemolymph. *Insect Biochemistry and Molecular Biology* **38**(3): 320-330.

Pinal, N., D. C. I. Goberdhan, L. Collinson, Y. Fujita, I. M. Cox, C. Wilson and F. Pichaud (2006). Regulated and polarized PtdIns(3,4,5)P accumulation is essential for apical membrane morphogenesis in photoreceptor epithelial cells. *Current Biology* **16**(2): 140-149.

Piper, R. C., A. A. Cooper, H. Yang and T. H. Stevens (1995). Vps27 controls vacuolar and endocytic traffic through a prevacuolar compartment in *Saccharomyces cerevisiae*. *The Journal of Cell Biology* **131**(3): 603-617.

Pols, M. S. and J. Klumperman (2009). Trafficking and function of the tetraspanin CD63. *Experimental Cell Research* **315**(9): 1584-1592.

Pons-Rejraji, H., C. Artonne, B. Sion, F. Brugnon, M. Canis, L. Janny and G. Grizard (2011). Prostasomes: Inhibitors of capacitation and modulators of cellular signalling in human sperm. *International Journal of Andrology* **34**(6pt1): 568-580.

Principe, D. R., J. A. Doll, J. Bauer, B. Jung, H. G. Munshi, L. Bartholin, B. Pasche, C. Lee and P. J. Grippo (2014). Tgf-β: Duality of function between tumor prevention and carcinogenesis. *Journal of the National Cancer Institute* **106**(2).

Pryor, P. R., B. M. Mullock, N. A. Bright, S. R. Gray and J. P. Luzio (2000). The role of intraorganellar Ca^{2+} in late endosome–lysosome heterotypic fusion and in the reformation of lysosomes from hybrid organelles. *The Journal of Cell Biology* **149**(5): 1053-1062.

Pryor, P. R., B. M. Mullock, N. A. Bright, M. R. Lindsay, S. R. Gray, S. C. W. Richardson, A. Stewart, D. E. James, R. C. Piper and J. P. Luzio (2004). Combinatorial snare complexes with Vamp7 or vamp8 define different late endocytic fusion events. *EMBO Rep* **5**(6): 590-595.

Qi, H., M. M. Moran, B. Navarro, J. A. Chong, G. Krapivinsky, L. Krapivinsky, Y. Kirichok, I. S. Ramsey, T. A. Quill and D. E. Clapham (2007). All four CatSper ion channel proteins are required for male fertility and sperm cell hyperactivated motility. *Proceedings of the National Academy of Sciences* **104**(4): 1219-1223.

Raftery, L. A. and D. J. Sutherland (1999). Tgf-β family signal transduction in drosophila development: From mad to smads. *Developmental Biology* **210**(2): 251-268.

Raiborg, C., K. G. Bache, D. J. Gillooly, I. H. Madshus, E. Stang and H. Stenmark (2002). Hrs sorts ubiquitinated proteins into clathrin-coated microdomains of early endosomes. *Nat Cell Biol* **4**(5): 394-398.

Ram, K. R. and M. F. Wolfner (2007). Sustained post-mating response in *Drosophila melanogaster* requires multiple seminal fluid proteins. *PLoS Genet* **3**(12): e238.

Ram, K. R. and M. F. Wolfner (2009). A network of interactions among seminal proteins underlies the long-term postmating response in *Drosophila. Proceedings of the National Academy of Sciences* **106**(36): 15384-15389.

Ramteke, A., H. Ting, C. Agarwal, S. Mateen, R. Somasagara, A. Hussain, M. Graner, B. Frederick, R. Agarwal and G. Deep (2013). Exosomes secreted under hypoxia enhance invasiveness and stemness of prostate cancer cells by targeting adherens junction molecules. *Molecular Carcinogenesis.* doi: 10.1002/mc.22124. [Epub ahead of print]

Rana, S., S. Yue, D. Stadel and M. Zöller (2012). Toward tailored exosomes: The exosomal tetraspanin web contributes to target cell selection. *The International Journal of Biochemistry & Cell Biology* **44**(9): 1574-1584.

Raposo, G. and W. Stoorvogel (2013). Extracellular vesicles: Exosomes, microvesicles, and friends. *The Journal of Cell Biology* **200**(4): 373-383.

Ravi Ram, K., S. Ji and M. F. Wolfner (2005). Fates and targets of male accessory gland proteins in mated female drosophila melanogaster. *Insect Biochemistry and Molecular Biology* **35**(9): 1059-1071.

Ravi Ram, K., L. K. Sirot and M. F. Wolfner (2006). Predicted seminal astacin-like protease is required for processing of reproductive proteins in *Drosophila melanogaster. Proceedings of the National Academy of Sciences* **103**(49): 18674-18679.

Ravi Ram, K. and M. F. Wolfner (2007). Seminal influences: *Drosophila* Acps and the molecular interplay between males and females during reproduction. *Integrative and Comparative Biology* **47**(3): 427-445.

Raymond, C. K., I. Howald-Stevenson, C. A. Vater and T. H. Stevens (1992). Morphological classification of the yeast vacuolar protein sorting mutants: evidence for a prevacuolar compartment in class E Vps mutants. *Molecular Biology of the Cell* **3**(12): 1389-1402.

Rexhepaj, A., H. Liu, J. Peng, Y. Choffat and E. Kubli (2003). The sex-peptide DUP99b is expressed in the male ejaculatory duct and in the cardia of both sexes. *European Journal of Biochemistry* **270**(21): 4306-4314.

Rezával, C., H. J. Pavlou, A. J. Dornan, Y.-B. Chan, E. A. Kravitz and S. F. Goodwin (2012). Neural circuitry underlying *Drosophila* female postmating behavioral responses. *Current Biology* **22**(13): 1155-1165.

Rideout, E. J., A. J. Dornan, M. C. Neville, S. Eadie and S. F. Goodwin (2010). Control of sexual differentiation and behavior by the *doublesex* gene in *Drosophila melanogaster*. *Nat Neurosci* **13**(4): 458-466.

Rietveld, A., S. Neutz, K. Simons and S. Eaton (1999). Association of sterol- and glycosylphosphatidylinositol-linked proteins with *Drosophila* raft lipid microdomains. *Journal of Biological Chemistry* **274**(17): 12049-12054.

Rink, J., E. Ghigo, Y. Kalaidzidis and M. Zerial (2005). Rab conversion as a mechanism of progression from early to late endosomes. *Cell* **122**(5): 735-749.

Robertis, R. D. a. E. M. D. (2011). Endocytic control of growth factor signalling: Multivesicular bodies as signalling organelles. *Nat Rev Mol Cell Biol* **13**(1): 53-60.

Ronquist, G. and I. Brody (1985). The prostasome: Its secretion and function in man. *Biochimica et Biophysica Acta (BBA) - Reviews on Biomembranes* **822**(2): 203-218.

Ronquist, G. K., A. Larsson, A. Stavreus-Evers and G. Ronquist (2012). Prostasomes are heterogeneous regarding size and appearance but affiliated to one DNA-containing exosome family. *The Prostate* **72**(16): 1736-1745.

Ronquist, K. G., B. Ek, A. Stavreus-Evers, A. Larsson and G. Ronquist (2013). Human prostasomes express glycolytic enzymes with capacity for ATP production. *American Journal of Physiology - Endocrinology and Metabolism* **304**(6): E576-E582.

Rosenfeld, J. L., R. H. Moore, K.-P. Zimmer, E. Alpizar-Foster, W. Dai, M. N. Zarka and B. J. Knoll (2001). Lysosome proteins are redistributed during expression of a GTP-hydrolysis-defective Rab5a. *Journal of Cell Science* **114**(24): 4499-4508.

Rylett, C. M., M. J. Walker, G. J. Howell, A. D. Shirras and R. E. Isaac (2007). Male accessory glands of *Drosophila melanogaster* make a secreted angiotensin I-converting enzyme (ance), suggesting a role for the peptide-processing enzyme in seminal fluid. *Journal of Experimental Biology* **210**(20): 3601-3606.

Sabharanjak S., P. Sharma, R. G. Parton and S. Mayor (2002). Gpi-anchored proteins are delivered to recycling endosomes via a distinct Cdc42-regulated, clathrin-independent pinocytic pathway. *Dev Cell* **2**(4): 411-423.

Sadoul, R. (2006). Do ALiX and ALG-2 really control endosomes for better or for worse? *Biology of the Cell* **98**(1): 69-77.

Sancak, Y., L. Bar-Peled, R. Zoncu, A. L. Markhard, S. Nada and D. M. Sabatini (2010). Ragulator-RAG complex targets mTORC1 to the lysosomal surface and is necessary for its activation by amino acids. *Cell* **141**(2): 290-303.

Sancak, Y., T. R. Peterson, Y. D. Shaul, R. A. Lindquist, C. C. Thoreen, L. Bar-Peled and D. M. Sabatini (2008). The rag gtpases bind raptor and mediate amino acid signaling to mTORC1. *Science* **320**(5882): 1496-1501.

Sanderson, M. P., S. Keller, A. Alonso, S. Riedle, P. J. Dempsey and P. Altevogt (2008). Generation of novel, secreted epidermal growth factor receptor (EGFR/Erbb1) isoforms via metalloprotease-dependent ectodomain shedding and exosome secretion. *Journal of Cellular Biochemistry* **103**(6): 1783-1797.

Sato, M. and T. B. Kornberg (2002). FGF is an essential mitogen and chemoattractant for the air sacs of the *Drosophila* tracheal system. *Developmental Cell* **3**(2): 195-207.

Saudan, P., K. Hauck, M. Soller, Y. Choffat, M. Ottiger, M. Spörri, Z. Ding, D. Hess, P. M. Gehrig, S. Klauser, P. Hunziker and E. Kubli (2002). Ductus ejaculatorius peptide 99b (DUP99b), a novel *Drosophila melanogaster* sex-peptide pheromone. *European Journal of Biochemistry* **269**(3): 989-997.

Savina, A., C. M. Fader, M. T. Damiani and M. I. Colombo (2005). Rab11 promotes docking and fusion of multivesicular bodies in a calcium-dependent manner. *Traffic* **6**(2): 131-143.

Savina, A., M. Vidal and M. I. Colombo (2002). The exosome pathway in K562 cells is regulated by Rab11. *Journal of Cell Science* **115**(12): 2505-2515.

Schink, K. O., C. Raiborg and H. Stenmark (2013). Phosphatidylinositol 3-phosphate, a lipid that regulates membrane dynamics, protein sorting and cell signalling. *BioEssays* **35**(10): 900-912.

Schmidt, M. H. H., D. Hoeller, J. Yu, F. B. Furnari, W. K. Cavenee, I. Dikic and O. Bögler (2004). ALiX/aip1 antagonizes epidermal growth factor receptor downregulation by the Cbl-SETA/Cin85 complex. *Molecular and Cellular Biology* **24**(20): 8981-8993.

Schmidt O. and D. Teis (2012). The ESCRT machinery. *Curr Biol* **22**(4): R116-R120.

Schmidt, T., Y. Choffat, S. Klauser and E. Kubli (1993). The *Drosophila melanogaster* sex-peptide: A molecular analysis of structure-function relationships. *Journal of Insect Physiology* **39**(5): 361-368.

Schmidt T., E. Stumm-Zollinger and P. S. Chen (1985). Protein metabolism of *Drosophila melanogaster* male accessory glands—iii: Stimulation of protein synthesis following copulation. *Insect Biochem* **15**(3): 391-401.

Scott C. C., F. Vacca and J. Gruenberg (2014). Endosome maturation, transport and functions. *Seminars in Cell & Developmental Biology*. **31**:2-10.

Schroeder, B., S. Srivatsan, A. Shaw, D. Billadeau and M. A. Mcniven (2012). Cin85 phosphorylation is essential for EGFR ubiquitination and sorting into multivesicular bodies. *Molecular Biology of the Cell* **23**(18): 3602-3611.

Schweitzer, R., M. Shaharabany, R. Seger and B. Z. Shilo (1995). Secreted spitz triggers the DER signaling pathway and is a limiting component in embryonic ventral ectoderm determination. *Genes & Development* **9**(12): 1518-1529.

Sharom, F. J. (2011). Flipping and flopping—lipids on the move. *IUBMB Life* **63**(9): 736-746.

Sheldon H., Hiekamp E., H. Turley, R. Dragovic, P. Thomas, C. E. Oon, R. Leek, M. Edelmann, B. Kessler, R. C. Sainson, I. Sargent, J. L. Li, A. L. Harris (2010). New mechanism for notch signaling to endothelium at a distance by delta-like 4 incorporation into exosomes. *Blood* **116**(13): 2385-2394.

Shen, B., N. Wu, J.-M. Yang and S. J. Gould (2011). Protein targeting to exosomes/microvesicles by plasma membrane anchors. *Journal of Biological Chemistry* **286**(16): 14383-14395.

Shilo, B.-Z. (2003). Signaling by the *Drosophila* epidermal growth factor receptor pathway during development. *Experimental Cell Research* **284**(1): 140-149.

Shilo, B.-Z. (2005). Regulating the dynamics of EGF receptor signaling in space and time. *Development* **132**(18): 4017-4027.

Shin, H.-W., M. Hayashi, S. Christoforidis, S. Lacas-Gervais, S. Hoepfner, M. R. Wenk, J. Modregger, S. Uttenweiler-Joseph, M. Wilm, A. Nystuen, W. N. Frankel, M. Solimena, P. De Camilli and M. Zerial (2005). An enzymatic cascade of Rab5 effectors regulates phosphoinositide turnover in the endocytic pathway. *The Journal of Cell Biology* **170**(4): 607-618.

Simons, K. and E. Ikonen (1997). Functional rafts in cell membranes. *Nature* **387**(6633): 569-572.

Simons, K. and D. Toomre (2000). Lipid rafts and signal transduction. *Nat Rev Mol Cell Biol* **1**(1): 31-39.

Sims, P. J., E. M. Faioni, T. Wiedmer and S. J. Shattil (1988). Complement proteins C5B-9 cause release of membrane vesicles from the platelet surface that are enriched in the membrane receptor for coagulation factor Va and express prothrombinase activity. *Journal of Biological Chemistry* **263**(34): 18205-18212.

Singh, A. B. and R. C. Harris (2005). Autocrine, paracrine and juxtacrine signaling by EGFR ligands. *Cellular Signalling* **17**(10): 1183-1193.

Sirot, L. K., M. C. Hardstone, M. E. H. Helinski, J. M. C. Ribeiro, M. Kimura, P. Deewatthanawong, M. F. Wolfner and L. C. Harrington (2011). Towards a semen proteome of the dengue vector mosquito: Protein identification and potential functions. *PLoS Negl Trop Dis* **5**(3): e989.

Sirot L. K., Mariana F. Wolfner and a. S. Wigby (2011). Protein-specific manipulation of ejaculate composition in response to female mating status in *Drosophila melanogaster*. *PNAS* **108**(24): 9922-9926.

Sirot L. K., N. A. B., Anthony C. Fiumera, and Mariana F. Wolfner (2009). Seminal fluid protein depletion and replenishment in the fruit fly, *Drosophila melanogaster*: An ELISA-based method for tracking individual ejaculates. *Behav Ecol Sociobiol.* **63**(10): 1505-1513.

Sitnik, J. L., C. Francis, K. Hens, R. Huybrechts, M. F. Wolfner and P. Callaerts (2014). Neprilysins: An evolutionarily conserved family of metalloproteases that play important roles in reproduction in *Drosophila*. *Genetics* **196**(3): 781-797.

Skibinski G, K. R., D. Harkiss, K. James (1992). Immunosuppression by human seminal plasma--extracellular organelles (prostasomes) modulate activity of phagocytic cells. *Am J Reprod Immunol.* **28**(2): 97-103.

Smith, R. (1984). Sperm competition and the evolution of animal mating systems. *Academic, New York*. ISBN-13: 978-0126525700.

Soller, M., M. Bownes and E. Kubli (1999). Control of oocyte maturation in sexually mature *Drosophila* females. *Developmental Biology* **208**(2): 337-351.

Sönnichsen, B., S. De Renzis, E. Nielsen, J. Rietdorf and M. Zerial (2000). Distinct membrane domains on endosomes in the recycling pathway visualized by multicolor imaging of Rab4, Rab5, and Rab11. *The Journal of Cell Biology* **149**(4): 901-914.

Sorkin, A., L. K. Goh. (2008). Endocytosis and intracellular trafficking of Erbbs. *Exp Cell Res.* **314**(17): 3093-3106.

Staneva, G., A. Momchilova, C. Wolf, P. J. Quinn and K. Koumanov (2009). Membrane microdomains: role of ceramides in the maintenance of their structure and functions. *Biochimica et Biophysica Acta (BBA) - Biomembranes* **1788**(3): 666-675.

Stenmark, H. (2009). Rab GTPases as coordinators of vesicle traffic. *Nat Rev Mol Cell Biol* **10**(8): 513-525.

Stenmark, H., R. G. Parton, O. Stelle-Mortimer, A. Lutcke, J. Gruenberg and M. Zerial (1994). Inhibition of Rab5 GTPase activity stimulates membrane fusion in endocytosis. *EMBO J* **13**(6): 1287-1296.

Stuffers, S., C. Sem Wegner, H. Stenmark and A. Brech (2009). Multivesicular endosome biogenesis in the absence of ESCRTs. *Traffic* **10**(7): 925-937.

Sullivan, R. and F. Saez (2013). Epididymosomes, prostasomes, and liposomes: Their roles in mammalian male reproductive physiology. *Reproduction* **146**(1): R21-R35.

Sullivan, R., F. Saez, J. Girouard and G. Frenette (2005). Role of exosomes in sperm maturation during the transit along the male reproductive tract. *Blood Cells, Molecules, and Diseases* **35**(1): 1-10.

Suster, M. L., L. Seugnet, M. Bate and M. B. Sokolowski (2004). Refining Gal4-driven transgene expression in *Drosophila* with a Gal80 enhancer-trap. *genesis* **39**(4): 240-245.

Tall, G. G., M.Alejandro Barbieri, P. D. Stahl and B. F. Horazdovsky. (2001). Ras-activated endocytosis is mediated by the Rab5 guanine nucleotide exchange activity of Rin1. *Dev Cell* **1**(1): 73-82.

Takada, R., Y. Satomi, T. Kurata, N. Ueno, S. Norioka, H. Kondoh, T. Takao and S. Takada (2006). Monounsaturated fatty acid modification of Wnt protein: Its role in Wnt secretion. *Development* **11**(6): 791-801.

Tamai, K., M. Shiina, N. Tanaka, T. Nakano, A. Yamamoto, Y. Kondo, E. Kakazu, J. Inoue, K. Fukushima, K. Sano, Y. Ueno, T. Shimosegawa and K. Sugamura (2012). Regulation of hepatitis C virus secretion by the Hrs-dependent exosomal pathway. *Virology* **422**(2): 377-385.

Tamai, K., N. Tanaka, T. Nakano, E. Kakazu, Y. Kondo, J. Inoue, M. Shiina, K. Fukushima, T. Hoshino, K. Sano, Y. Ueno, T. Shimosegawa and K. Sugamura (2010). Exosome secretion of dendritic cells is regulated by Hrs, an ESCRT-0 protein. *Biochemical and Biophysical Research Communications* **399**(3): 384-390.

Tandler, B., D. L. Williamson and L. Ehrman (1968). Unusual filamentous structures in the paragonia of male *Drosophila*. *The Journal of cell biology* **38**(2): 329-336.

Taraboletti, G., S. D'ascenzo, P. Borsotti, R. Giavazzi, A. Pavan and V. Dolo (2002). Shedding of the matrix metalloproteinases Mmp-2, Mmp-9, and Mt1-Mmp as membrane vesicle-associated components by endothelial cells. *The American Journal of Pathology* **160**(2): 673-680.

Tatei, K., H. Cai, Y. Tony Ip and M. Levine (1995). Race: A *Drosophila* homologue of the angiotensin converting enzyme. *Mechanisms of Development* **51**(2–3): 157-168.

Tatischeff, I. (2013). Assets of the non-pathogenic microorganism *Dictyostelium discoideum* as a model for the study of eukaryotic extracellular vesicles. *F1000Research* **2**(73).

Tavoosidana, G., G. Ronquist, S. Darmanis, J. Yan, L. Carlsson, D. Wu, T. Conze, P. Ek, A. Semjonow, E. Eltze, A. Larsson, U. D. Landegren and M. Kamali-Moghaddam (2011). Multiple recognition assay reveals prostasomes as promising plasma biomarkers for prostate cancer. *Proceedings of the National Academy of Sciences* **108**(21): 8809-8814.

Tayler, T. D., D. A. Pacheco, A. C. Hergarden, M. Murthy and D. J. Anderson (2012). A neuropeptide circuit that coordinates sperm transfer and copulation duration in *Drosophila.* *Proceedings of the National Academy of Sciences* **109**(50): 20697-20702.

The, I., Y. Bellaiche and N. Perrimon (1999). Hedgehog movement is regulated through tout velu–dependent synthesis of a heparan sulfate proteoglycan. *Molecular Cell* **4**(4): 633-639.

Theopold, U. and O. Schmidt (1997). *Helix pomatia* Lectin and Annexin V, two molecular probes for insect microparticles: Possible involvement in hemolymph coagulation. *Journal of Insect Physiology* **43**(7): 667-674.

Thiele, C., M. J. Hannah, F. Fahrenholz and W. B. Huttner (2000). Cholesterol binds to synaptophysin and is required for biogenesis of synaptic vesicles. *Nat Cell Biol* **2**(1): 42-49.

Tian, T., Y.-L. Zhu, F.-H. Hu, Y.-Y. Wang, N.-P. Huang and Z.-D. Xiao (2012). Dynamics of exosome internalization and trafficking. *Journal of Cellular Physiology* **228**(7):1487-95.

Trajkovic, K., C. Hsu, S. Chiantia, L. Rajendran, D. Wenzel, F. Wieland, P. Schwille, B. Brügger and M. Simons (2008). Ceramide triggers budding of exosome vesicles into multivesicular endosomes. *Science* **319**(5867): 1244-1247.

Tsruya, R., A. Schlesinger, A. Reich, L. Gabay, A. Sapir and B.-Z. Shilo (2002). Intracellular trafficking by star regulates cleavage of the drosophila EGFR receptor ligand spitz. *Genes & Development* **16**(2): 222-234.

Tsuneizumi, K., T. Nakayama, Y. Kamoshida, T. B. Kornberg, J. L. Christian and T. Tabata (1997). Daughters against dpp modulates Dpp organizing activity in *Drosophila* wing development. *Nature* **389**(6651): 627-631.

Tsudaa M., K.-H. Seong and T. Aigakia (2006). Posh, a scaffold protein for JNK signaling, binds to ALG-2 and ALiX in drosophila. *FEBS Letters* **580**(13): 3296-3330.

Urban, S., J. R. Lee and M. Freeman (2002). A family of rhomboid intramembrane proteases activates all *Drosophila* membrane-tethered EGF ligands. *EMBO J* **21**(16):4277-86.

Ushiro, H. and S. Cohen (1980). Identification of phosphotyrosine as a product of epidermal growth factor-activated protein kinase in A-431 cell membranes. *Journal of Biological Chemistry* **255**(18): 8363-8365.

Van Der Pol, E., F. Coumans, Z. Varga, M. Krumrey and R. Nieuwland (2013). Innovation in detection of microparticles and exosomes. *Journal of Thrombosis and Haemostasis* **11**: 36-45.

Van Der Pol, E., F. A. W. Coumans, A. E. Grootemaat, C. Gardiner, I. L. Sargent, P. Harrison, A. Sturk, T. G. Van Leeuwen and R. Nieuwland (2014). Particle size distribution of exosomes and microvesicles determined by transmission electron microscopy, flow cytometry, nanoparticle tracking analysis, and resistive pulse sensing. *Journal of Thrombosis and Haemostasis* **12**(7): 1182-1192.

Van Deurs B., P. K. Holm, L. Kayser, K. Sandvig. (1995). Delivery to lysosomes in the human carcinoma cell line HEp-2 involves an actin filament-facilitated fusion between mature endosomes and preexisting lysosomes. *Eur J Cell Biol* **66**(4): 309-323.

Van niel, G., S. Charrin, S. Simoes, M. Romao, L. Rochin, P. Saftig, Michael S. Marks, E. Rubinstein and G. Raposo (2011). The tetraspanin CD63 regulates ESCRT-independent and -dependent endosomal sorting during melanogenesis. *Developmental Cell* **21**(4): 708-721.

Muralidharan-Chari, V., J. Clancy, C. Plou, M. Romao, P. Chavrier, G. Raposo and D'Souza Schorey (2009). Arf6-regulated shedding of tumor cell-derived plasma membrane microvesicles. *Curr Biol* **19**: 1875-1885.

Vanhaesebroeck, B., J. Guillermet-Guibert, M. Graupera and B. Bilanges (2010). The emerging mechanisms of isoform-specific PI3K signalling. *Nat Rev Mol Cell Biol* **11**(5): 329-341.

Vanhaesebroeck B, S. R., Waterfield MD. (1996). The study of phosphoinositide 3-kinase function. *Cancer Surv,* **27**: 249-270.

Vanlandingham, P. A. and B. P. Ceresa (2009). Rab7 regulates late endocytic trafficking downstream of multivesicular body biogenesis and cargo sequestration. *Journal of Biological Chemistry* **284**(18): 12110-12124.

Vida, T. and B. Gerhardt (1999). A cell-free assay allows reconstitution of Vps33p-dependent transport to the yeast vacuole/lysosome. *The Journal of Cell Biology* **146**(1): 85-98.

Vieira, A. V., C. Lamaze and S. L. Schmid (1996). Control of EGF receptor signaling by clathrin-mediated endocytosis. *Science* **274**(5295): 2086-2089.

Villella, A., J.-B. Peyre, T. Aigaki and J. Hall (2006). Defective transfer of seminal-fluid materials during matings of semi-fertile *fruitless* mutants in *Drosophila*. *Journal of Comparative Physiology A* **192**(12): 1253-1269.

Visconti, P. E., H. Galantino-Homer, X. Ning, G. D. Moore, J. P. Valenzuela, C. J. Jorgez, J. G. Alvarez and G. S. Kopf (1999). Cholesterol efflux-mediated signal transduction in mammalian sperm: B-cyclodextrins initiate transmembrane signaling leading to an increase in protein tyrosine phosphorylation and capacitation. *Journal of Biological Chemistry* **274**(5): 3235-3242.

Vitelli, R., M. Santillo, D. Lattero, M. Chiariello, M. Bifulco, C. B. Bruni and C. Bucci (1997). Role of the small GTPase Rab7 in the late endocytic pathway. *Journal of Biological Chemistry* **272**(7): 4391-4397.

Wada, I., W. H. Lai, B. I. Posner and J. J. Bergeron (1992). Association of the tyrosine phosphorylated epidermal growth factor receptor with a 55-kd tyrosine phosphorylated protein at the cell surface and in endosomes. *The Journal of Cell Biology* **116**(2): 321-330.

Walker, M., C. Rylett, J. Keen, N. Audsley, M. Sajid, A. Shirras and R. E. Isaac (2006). Proteomic identification of *Drosophila melanogaster* male accessory gland proteins, including a pro-cathepsin and a soluble gamma-glutamyl transpeptidase. *Proteome Science* **4**(1): 9.

Wang, Y.-C. and E. L. Ferguson (2005). Spatial bistability of Dpp-receptor interactions during *Drosophila* dorsal-ventral patterning. *Nature* **434**(7030): 229-234.

Wasserman, J. D. and M. Freeman (1998). An autoregulatory cascade of egf receptor signaling patterns the *Drosophila* egg. *Cell* **95**(3): 355-364.

Webber, J., R. Steadman, M. D. Mason, Z. Tabi and A. Clayton (2010). Cancer exosomes trigger fibroblast to myofibroblast differentiation. *Cancer Research* **70**(23): 9621-9630.

Webber, J. P., L. K. Spary, A. J. Sanders, R. Chowdhury, W. G. Jiang, R. Steadman, J. Wymant, A. T. Jones, H. Kynaston, M. D. Mason, Z. Tabi and A. Clayton (2014). Differentiation of tumour-promoting stromal myofibroblasts by cancer exosomes. *Oncogene*. doi: 10.1038/onc.2013.560. [Epub ahead of print]

Wegener, C., L. Malerød, N. Pedersen, C. Prodiga, O. Bakke, H. Stenmark and A. Brech (2010). Ultrastructural characterization of giant endosomes induced by GTPase-deficient Rab5. *Histochemistry and Cell Biology* **133**(1): 41-55.

Wehman, A. M., C. Poggioli, P. Schweinsberg, B. D. Grant and J. Nance (2011). The P4-ATPase tat-5 inhibits the budding of extracellular vesicles in *C. elegans* embryos. *Current Biology* **21**(23): 1951-1959.

Wemmer, M., I. Azmi, M. West, B. Davies, D. Katzmann and G. Odorizzi (2011). Bro1 binding to Snf7 regulates ESCRT-III membrane scission activity in yeast. *The Journal of Cell Biology* **192**(2): 295-306.

Wiedemann, C. and S. Cockcroft (1998). Vesicular transport: Sticky fingers grab a lipid. *Nature* **394**(6692): 426-427.

Wigby, S. and T. Chapman (2005). Sex peptide causes mating costs in female *Drosophila melanogaster. Current Biology* **15**(4): 316-321.

Wiley, H. S., J. J. Herbst, B. J. Walsh, D. A. Lauffenburger, M. G. Rosenfeld and G. N. Gill (1991). The role of tyrosine kinase activity in endocytosis, compartmentation, and down-regulation of the epidermal growth factor receptor. *Journal of Biological Chemistry* **266**(17): 11083-11094.

Willert, K., J. D. Brown, E. Danenberg, A. W. Duncan, I. L. Weissman, T. Reya, J. R. Yates and R. Nusse (2003). Wnt proteins are lipid-modified and can act as stem cell growth factors. *Nature* **423**(6938): 448-452.

Wilson, H. L., S. E. Francis, S. K. Dower and D. C. Crossman (2004). Secretion of intracellular IL-1 receptor antagonist (type 1) is dependent on P2X7 receptor activation. *The Journal of Immunology* **173**(2): 1202-1208.

Wolfner, M. F. (1997). Tokens of love: Functions and regulation of *Drosophila* male accessory gland products. *Insect Biochemistry and Molecular Biology* **27**(3): 179-192.

Wollert, T. and J. H. Hurley (2010). Molecular mechanism of multivesicular body biogenesis by ESCRT complexes. *Nature* **464**(7290): 864-869.

Wollert, T., C. Wunder, J. Lippincott-Schwartz and J. H. Hurley (2009). Membrane scission by the ESCRT-III complex. *Nature* **458**(7235): 172-177.

Wubbolts, R., R. S. Leckie, P. T. M. Veenhuizen, G. Schwarzmann, W. Möbius, J. Hoernschemeyer, J.-W. Slot, H. J. Geuze and W. Stoorvogel (2003). Proteomic and biochemical analyses of human B cell-derived exosomes: Potential implications for their function and multivesicular body formation. *Journal of Biological Chemistry* **278**(13): 10963-10972.

Xu, J., S. Lamouille and R. Derynck (2009). Tgf-β-induced epithelial to mesenchymal transition. *Cell Res* **19**(2): 156-172.

Xu, P., R. D. Baldridge, R. J. Chi, C. G. Burd and T. R. Graham (2013). Phosphatidylserine flipping enhances membrane curvature and negative charge required for vesicular transport. *The Journal of Cell Biology* **202**(6): 875-886.

Xue, L. and M. Noll (2000). Drosophila female sexual behavior induced by sterile males showing copulation complementation. *Proceedings of the National Academy of Sciences* **97**(7): 3272-3275.

Xue, L. and M. Noll (2002). Dual role of the pax gene paired in accessory gland development of *Drosophila. Development* **129**(2): 339-346.

Yamamoto, Y., K. Irie, M. Asada, A. Mino, K. Mandai and Y. Takai (2004). Direct binding of the human homologue of the *Drosophila* disc large tumor suppressor gene to seven-pass transmembrane proteins, tumor endothelial marker 5 (Tem5), and a novel Tem5-like protein. *Oncogene* **23**(22): 3889-3897.

Yang, C. H., S. Rumpf, Y. Xiang, M. D. Gordon, W. Song, L. Y. Jan and Y.-N. Jan (2009). Control of the postmating behavioral switch in *Drosophila* females by internal sensory neurons. *Neuron* **61**(4): 5190526.

Yapici, N., Y.-J. Kim, C. Ribeiro and B. J. Dickson (2008). A receptor that mediates the post-mating switch in *Drosophila* reproductive behaviour. *Nature* **451**(7174): 33-37.

Ye, L., J. M. Lewis-Russell., H.G. Kyanaston and W.G. Jiang (2007). Bone morphogenetic proteins and their receptor signaling in prostate cancer. *Histol Histopathol* **22**(10): 1129-1147.

Yousefian, J., T. Troost, F. Grawe, T. Sasamura, M. Fortini and T. Klein (2013). Dmon1 controls recruitment of Rab7 to maturing endosomes in *Drosophila. Journal of Cell Science* **126**(7): 1583-1594.

Yu, L., F. Yang, L. Jiang, Y. Chen, K. Wang, F. Xu, Y. Wei, X. Cao, J. Wang and Z. Cai (2013). Exosomes with membrane-associated Tgf-β1 from gene-modified dendritic cells inhibit murine EAE independently of MHC restriction. *European Journal of Immunology* **43**(9): 2461-2472.

Zecca, M., K. Basler and G. Struhl (1995). Sequential organizing activities of engrailed, hedgehog and decapentaplegic in the *Drosophila* wing. *Development* **121**(8): 2265-2278.

Zhang, J., K. L. Schulze, P. R. Hiesinger, K. Suyama, S. Wang, M. Fish, M. Acar, R. A. Hoskins, H. J. Bellen and M. P. Scott (2007). Thirty-one flavors of *Drosophila* rab proteins. *Genetics* **176**(2): 1307-1322.

Published August 25, 2014

This article has original data in the JCB Data Viewer
http://jcb-dataviewer.rupress.org/jcb/browse/8152

BMP-regulated exosomes from *Drosophila* male reproductive glands reprogram female behavior

Laura Corrigan,[1] Siamak Redhai,[1] Aaron Leiblich,[1,2] Shih-Jung Fan,[1] Sumeth M.W. Perera,[1] Rachel Patel,[1] Carina Gandy,[1] S. Mark Wainwright,[1] John F. Morris,[1] Freddie Hamdy,[2] Deborah C.I. Goberdhan,[1] and Clive Wilson[1]

[1]Department of Physiology, Anatomy and Genetics and [2]Nuffield Department of Surgical Sciences, University of Oxford, Oxford OX1 3QX, England, UK

Male reproductive glands secrete signals into seminal fluid to facilitate reproductive success. In *Drosophila melanogaster*, these signals are generated by a variety of seminal peptides, many produced by the accessory glands (AGs). One epithelial cell type in the adult male AGs, the secondary cell (SC), grows selectively in response to bone morphogenetic protein (BMP) signaling. This signaling is involved in blocking the rapid remating of mated females, which contributes to the reproductive advantage of the first male to mate. In this paper, we show that SCs secrete exosomes, membrane-bound vesicles generated inside late endosomal multivesicular bodies (MVBs). After mating, exosomes fuse with sperm (as also seen in vitro for human prostate-derived exosomes and sperm) and interact with female reproductive tract epithelia. Exosome release was required to inhibit female remating behavior, suggesting that exosomes are downstream effectors of BMP signaling. Indeed, when BMP signaling was reduced in SCs, vesicles were still formed in MVBs but not secreted as exosomes. These results demonstrate a new function for the MVB–exosome pathway in the reproductive tract that appears to be conserved across evolution.

Introduction

In addition to sperm, seminal fluid contains multiple factors secreted by male reproductive glands that activate sperm (Rodríguez-Martínez et al., 2011) and can influence female physiology and behavior (Kershaw-Young et al., 2012). In *Drosophila melanogaster*, the paired accessory glands (AGs) secrete peptides that perform such functions (Wolfner, 1997). Sex peptide (SP) is one key product that in females can induce enhanced egg laying (Chapman et al., 2003), gradual release of sperm from storage organs (Liu and Kubli, 2003; Peng et al., 2005; Avila et al., 2010), and reduced receptivity to remating (Chen et al., 1988). This latter effect directly conflicts with female reproductive interests, leading us to investigate whether males use unconventional signaling strategies to achieve this.

Each AG is composed of a monolayered epithelium encased by a muscular sheath, which contracts during mating to expel the luminal contents. The epithelium is composed of two distinct binucleate cell types (DiBenedetto et al., 1990; Bertram et al., 1992). There are ∼1,000 main cells (MCs), which secrete signaling proteins such as SP (Chapman et al., 2003; Kubli, 2003). Scattered among MCs in the distal tip of the gland are roughly 40 secondary cells (SCs). SCs are unusually large, vacuole-filled cells, ∼25 µm in diameter, whose cell biology remains relatively uncharacterized (Rylett et al., 2007; Leiblich et al., 2012). SCs have an important modulatory influence on the maintenance of postmating female responses (Minami et al., 2012; Gligorov et al., 2013). One aspect of this, reduced receptivity to remating, is regulated by SC-specific bone morphogenetic protein (BMP) signaling (Leiblich et al., 2012) via an unknown mechanism.

Exosomes are secreted membrane-bound, nanosized (40–100 nm) vesicles generated in late endosomal multivesicular bodies (MVBs; Raposo and Stoorvogel, 2013; Christianson et al., 2014). They are thought to mediate short- and long-range intercellular signaling events in biological contexts, such as immune (Théry et al., 2009) and tumor cell signaling (Ge et al.,

D.C.I. Goberdhan and C. Wilson contributed equally to this paper.

Correspondence to Clive Wilson: clive.wilson@dpag.ox.ac.uk

Abbreviations used in this paper: AG, accessory gland; ANCE, angiotensin-converting enzyme I; BMP, bone morphogenetic protein; ESCRT, endosomal sorting complex required for transport; Evi, Evenness Interrupted; iLE, immature late endosome; ILV, intraluminal vesicle; MC, main cell; mMVBL, maturing MVB or lysosome; MVB, multivesicular body; SC, secondary cell; SP, sex peptide; SV, secretory vacuole; UAS, upstream activating sequence.

© 2014 Corrigan et al. This article is distributed under the terms of an Attribution–Noncommercial–Share Alike–No Mirror Sites license for the first six months after the publication date (see http://www.rupress.org/terms). After six months it is available under a Creative Commons License (Attribution–Noncommercial–Share Alike 3.0 Unported license, as described at http://creativecommons.org/licenses/by-nc-sa/3.0/).

The Rockefeller University Press $30.00
J. Cell Biol. Vol. 206 No. 5 671–688
www.jcb.org/cgi/doi/10.1083/jcb.201401072

THE JOURNAL OF CELL BIOLOGY

Downloaded from jcb.rupress.org on October 5, 2014

Published August 25, 2014

2012; Azmi et al., 2013). Exosomes can carry ligands, receptors, intracellular signaling molecules, lipids, and nucleic acids, allowing them to participate in a wide range of functions at the cell surface or when their contents are discharged into target cells through fusion or endocytosis (Raposo and Stoorvogel, 2013; Christianson et al., 2014). They are probably secreted into the extracellular milieu by all cells and enter body fluids, such as plasma and urine (Nilsson et al., 2009; Lance et al., 2011; Properzi et al., 2013; Record et al., 2014).

Prostate-derived exosomes (or prostasomes) have reported functions in healthy and tumorigenic prostate (Ronquist, 2012; Soekmadji et al., 2013). In vitro studies suggest roles for prostasomes and epididymis-derived exosomes (epididymosomes) in promoting motility during sperm capacitation (Palmerini et al., 1999; Park et al., 2011; Aalberts et al., 2013) and maturation (Sullivan and Saez, 2013), respectively. In these ex vivo experiments, prostasomes fuse specifically to the head/neck region of sperm, potentially under pH control (Arienti et al., 1997; Park et. al., 2011; Aalberts et al., 2013).

Here, we demonstrate that SCs of the AG secrete exosomes in vivo. The very large size of SC endolysosomal compartments allows aspects of exosome biogenesis to be visualized in living tissue for the first time, revealing remarkably dynamic membrane deformation and fusion events. Secreted exosomes fuse with sperm in vivo in females after mating, phenocopying reported properties of human prostasomes in vitro (Arienti et al., 1997; Park et al., 2011). Furthermore, SC-derived exosomes interact with epithelial cells in the female reproductive tract and are required to induce changes in female remating behavior controlled by BMP signaling. Secretion, but not formation, of SC-derived exosomes requires BMP signaling, highlighting endolysosomal trafficking as a key regulator of SC function. Thus, regulated secretion of exosomes in the AG provides an essential part of the armory promoting male-specific interests during *Drosophila* reproduction.

Results

SCs secrete CD63-GFP–marked puncta into the AG lumen

Each AG secretes into a large lumen, which opens at its proximal end into the ejaculatory duct (Fig. 1, A–C). We expressed a GFP-tagged tetraspanin, CD63, a mammalian transmembrane exosome marker used previously to mark fly exosomes (Panáková et al., 2005; Gross, et al., 2012), independently in MCs and SCs (Figs. 1, A–C; and S1, A and B) using the GAL4/upstream activating sequence (UAS) system (Brand and Perrimon, 1993). In SCs of 3-d-old males, CD63-GFP localized to the limiting membrane of all large (>2-µm diameter) vacuoles and, in some cells, to the apical plasma membrane (Fig. 1 F). Not all vacuoles were identical, however; the majority appeared to be compartments previously described as secretory vacuoles (SVs; Rylett et al., 2007) because they had a dense core containing the secreted protease angiotensin-converting enzyme I (ANCE; Fig. 1, E and F). CD63-GFP–positive puncta, presumably representing intraluminal vesicles (ILVs), were also observed inside many vacuoles, especially in live specimens. These puncta were typically most prominent in at least one acidic compartment, stained with the vital acid-sensitive dye LysoTracker red (Fig. 1, G and H).

The AG lumen contained GFP-marked puncta (Figs. 1, C and D; and S1, A and F), which were not observed when CD63-GFP was expressed in the large number of MCs in the AG (Fig. S1 B), suggesting that only SCs secrete this tagged membrane protein. Overexpressed cytoplasmic GFP was sometimes incorporated into puncta inside SC vacuoles (Fig. S1 C), indicating that the puncta are not induced by CD63-GFP expression. Furthermore, another tagged, nonexosomal membrane protein, CD8-RFP, which labels all vacuolar compartments and is internalized in some of them, was not secreted (Fig. S1, D and E), suggesting that CD63-GFP is packaged into intraluminal structures and selectively secreted. In support of this, luminal vesicles ∼40 nm in diameter, as well as other particulate material, were observed by transmission EM in the AG lumen of wild-type males (Fig. S2 G).

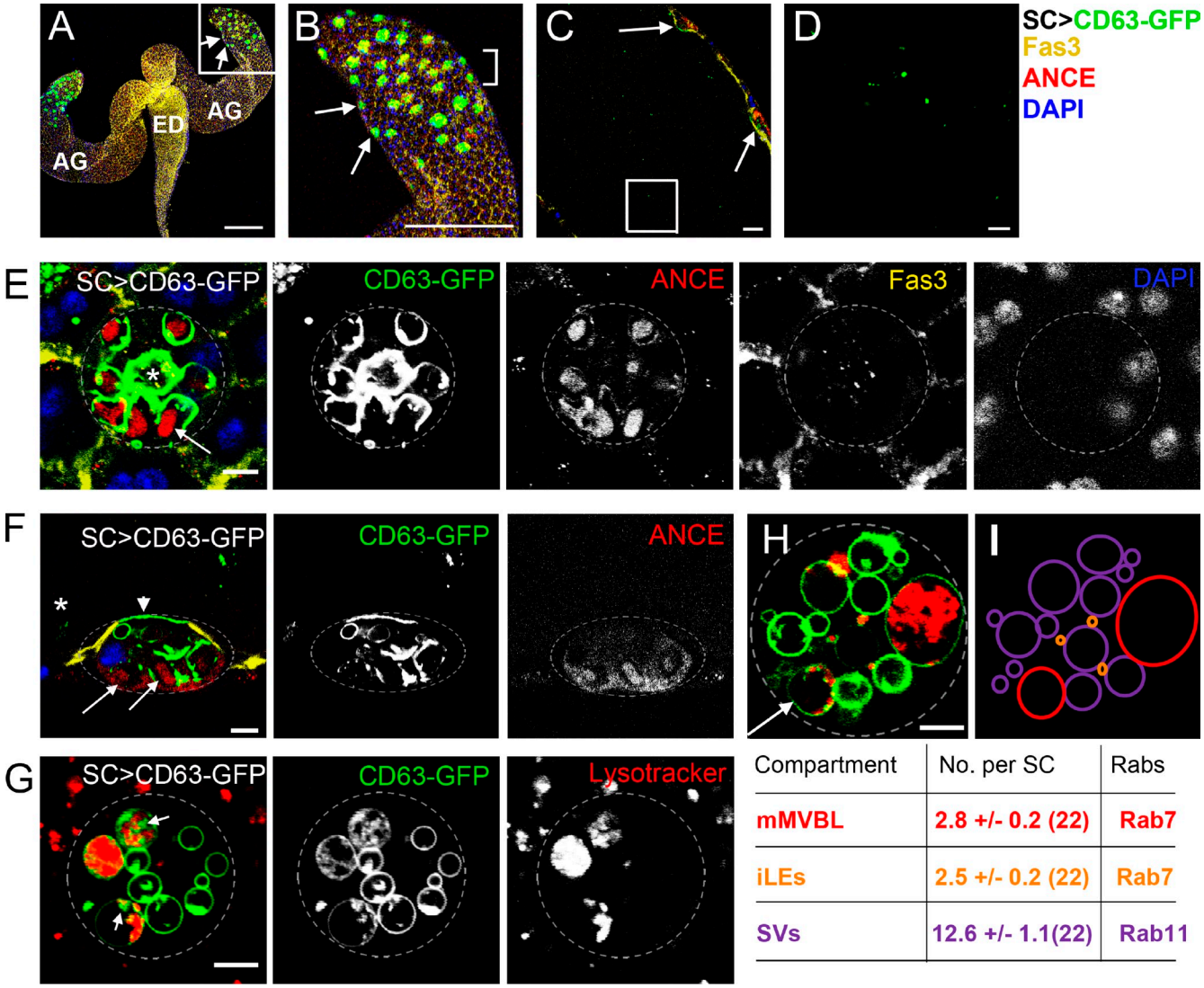
CD63-GFP–positive puncta are located inside late endosomes and lysosomes

We analyzed the large SC compartments in more detail using LysoTracker red–stained living glands. Counting vacuoles by scanning through multiple focal planes revealed remarkably consistent numbers of large (>2 µm) and small (<2 µm) CD63-positive acidic compartments and large nonacidic CD63-positive compartments in each SC of 6-d-old adults (Fig. 1 I). Both classes of acidic compartments were also visible in non–CD63-GFP–expressing SCs (Figs. S1, G versus H; and 2, A–C) and therefore were not induced by CD63-GFP expression. We hypothesized that the smaller apical acidic compartments were immature late endosomes (iLEs; CD63-GFP$^+$/LysoTracker$^+$ and <2 µm; Fig. 1 I), and the large acidic compartments, at least one of which contained small CD63-GFP–positive puncta, were unusually large (≤10 µm in 6-d-old SCs) maturing MVBs or lysosomes (mMVBLs; CD63-GFP$^+$/LysoTracker$^+$ and >2 µm; Fig. 1 I). In addition, some, but not all, nonacidic SV compartments (CD63-GFP$^+$/Lysotracker$^-$ and >2 µm; Fig. 1 I) contained larger CD63-GFP–positive intraluminal structures.

In each SC, an anti-CD63 antibody, which cross-reacted with fluorescent GFP puncta in the AG lumen (Fig. S2, B and C), also stained most of the lumen of either one or two compartments, which contained only sporadic fluorescent GFP puncta (Fig. S2 A). These compartments were ANCE negative and therefore not SVs. We reasoned that they were acidic compartments in which the microenvironment must partially inhibit fluorescence of internalized GFP. To confirm that SCs have giant vesicle-containing compartments, we analyzed SC ultrastructure by transmission EM (Fig. S2, E–I). In addition to the SV compartments previously reported by Rylett et al. (2007), SCs possessed one or two less electron-dense compartments containing vesicles ∼40 nm in diameter, an appropriate size to be precursors of secreted exosomes (Fig. S2 I). The ultrastructure of these large compartments was difficult to preserve in fixed, sectioned material, but because they are not filament- and ANCE core-containing SVs, we conclude that they must represent the acidic vesicle-containing compartments we observe in live specimens.

Downloaded from jcb.rupress.org on October 5, 2014

Published August 25, 2014



Compartment	No. per SC	Rabs
mMVBL	2.8 +/- 0.2 (22)	Rab7
iLEs	2.5 +/- 0.2 (22)	Rab7
SVs	12.6 +/- 1.1(22)	Rab11

Figure 1. **SCs secrete CD63-GFP–positive, exosome-like puncta.** (A–D) Paired accessory glands (AG) expressing CD63-GFP in SCs connect to the ejaculatory duct (ED; A). Images of different magnifications show surface sections of SCs within the AG epithelium (B; from square in A, arrows mark two SCs), a transverse section through the lumen (C; bracketed region in B, arrows mark two SCs), and CD63-GFP–positive puncta in the lumen (D; square in C; an image at higher confocal gain setting is shown in Fig. S1 F). (E and F) High magnification images of surface (E) and transverse (F; asterisk marks the lumen containing GFP puncta) sections through the SC show that CD63-GFP is also found at the apical plasma membrane (arrowhead; F) and the limiting membrane of SC vacuoles, the majority of which have a dense ANCE-positive core (highlighted with arrows). One or two CD63-GFP–lined compartments per SC lack an ANCE-stained core but contain fluorescent puncta (E, asterisk). Fasciclin3 (Fas3) marks septate junctions at the cell surface, and DAPI marks nuclei (note that SCs and MCs are binucleate). (G and H) Vital staining of SCs with LysoTracker red reveals CD63-GFP–positive puncta (putative ILVs; arrows) in large acidic compartments (mMVBLs), distinguishing them from other compartment classes, such as the more abundant secretory vacuoles (SVs) and immature late endosomes (iLEs). All images show SCs from 3-d-old males incubated at 28.5°C after eclosion. (I) Schematic representation of compartments within SC in H; values below indicate the mean total numbers of each compartment in 6-d-old control SCs counted from multiple sections along the apical–basal axis; the numbers of SCs analyzed are given in brackets. Approximate outline of the SC is marked in E–H. Bars: (A and B) 200 nm; (C) 20 µm; (D–H) 5 µm.

We performed more detailed live-imaging analysis of these large acidic and nonacidic SC compartments to confirm their identity, using selected ubiquitously expressed YFP-tagged Rab GTPases (Marois et al., 2006) that regulate endocytic trafficking and exosome secretion (Savina et al., 2002; Fader et al., 2005; Stenmark, 2009; Koles et al., 2012; Beckett et al., 2013). SCs typically contained two or three large vacuoles lined with Rab7-YFP, most of which were acidic (Fig. 2 A). Importantly, because all large acidic compartments were Rab7 positive ($n > 50$ cells), this confirms that the acidic compartments with CD63-GFP–positive puncta are either MVBs or lysosomes containing undegraded GFP. In support of this, these large acidic compartments were also lined by a GFP fusion with type II phosphatidylinositol kinase (PI4KII-GFP; Fig. S2 D), which marks late endosomes and lysosomes in other *Drosophila* secretory cells (Burgess et al., 2012).

Rab11-YFP, a marker for exocytic and recycling endocytic membranes, which regulates exosome secretion in flies (Chen et al., 1998; Koles et al., 2012; Beckett et al., 2013), localized to the limiting membrane of nonacidic SVs (Fig. 2 B). However, expression of this marker induced loss of large mMVBLs in most SCs (10/13 cells); overexpression of wild-type Rab11 therefore

Downloaded from jcb.rupress.org on October 5, 2014

Published August 25, 2014

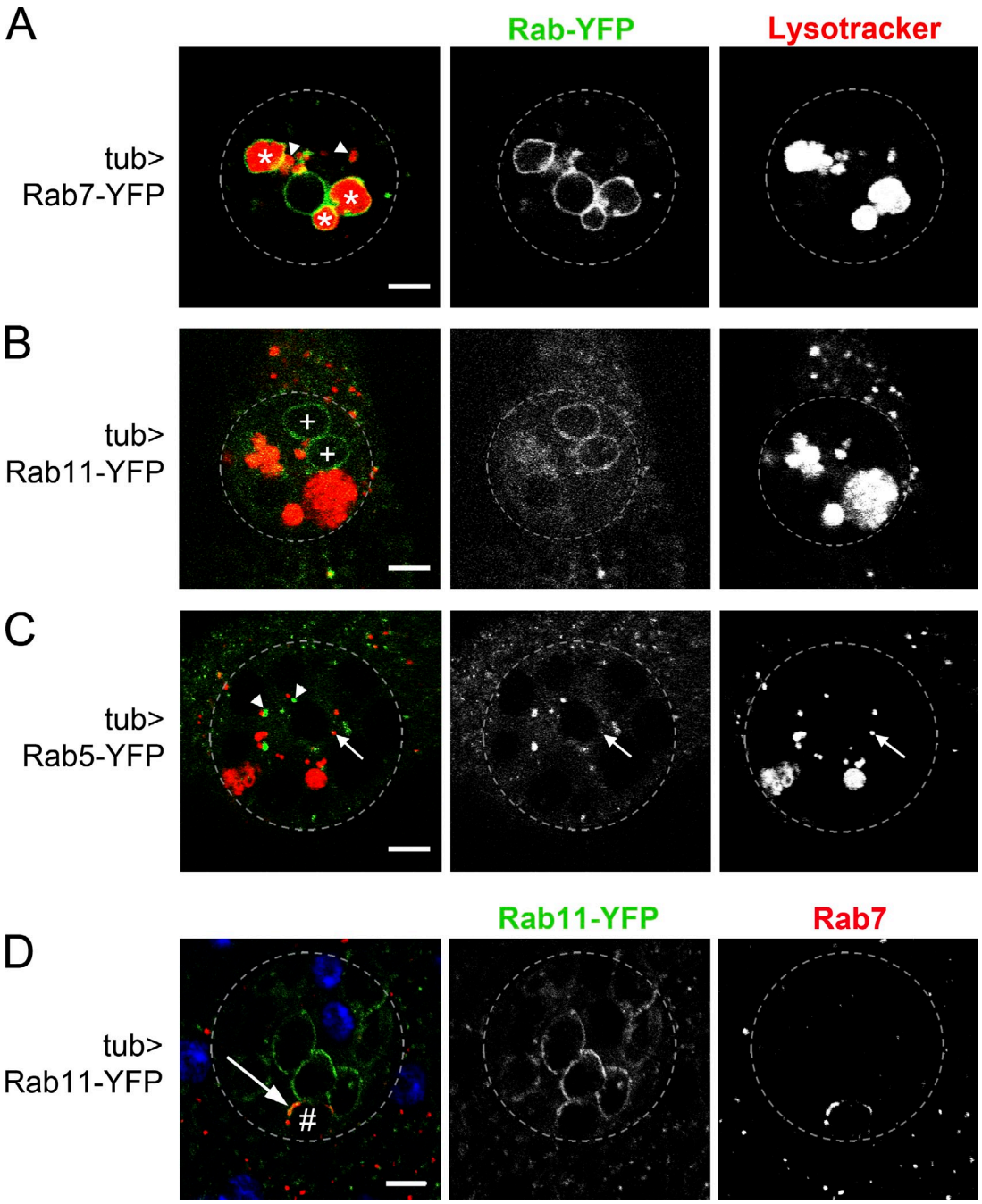


Figure 2. **Rab GTPase signatures define different SC subcellular compartments.** (A–D) SCs from 3-d-old males expressing different Rab-YFP constructs and stained with LysoTracker red. SCs have 5–10 small acidic Rab7-YFP–positive iLEs (A, arrowheads; most of these are usually located more apically than this confocal section; see Fig. 3) and 2.4 ± 0.9 (n = 11) Rab7-YFP–positive large vacuoles, 85% of which are acidic mMVBLs (A, asterisks; similar numbers [2.9 ± 0.5, n = 9] of large acidic compartments are seen in CD63-GFP–expressing SCs at this stage). Other Rab-YFP lines reveal Rab11-YFP–positive, nonacidic SVs (B, +; and D), many Rab5-YFP–positive small nonacidic compartments (C, arrowheads), and more rarely (4/16 SCs), a Rab5-YFP–positive small acidic compartment (C, arrows). In some fixed tub>Rab11-YFP SCs stained for Rab7, Rab7 colocalizes with Rab11-YFP in parts of the limiting membrane (D, arrow) of a single SV (D, #). DAPI stains nuclei (blue). Approximate outline of SC is marked in all images. Bars, 5 µm.

alters trafficking to mMVBLs, as has been found in other systems (Savina et al., 2002, 2005). Finally, Rab5-YFP, a marker for early endosomes, mainly localized to many small (<2 µm) nonacidic, centrally clustered compartments, often in close proximity to iLEs (Fig. 2 C). Interestingly, large nonacidic Rab7-YFP–positive vacuoles were typically in contact with acidic Rab7-YFP–positive iLEs (Fig. 2 A), consistent with a model in which the former compartments might derive from Rab11-positive vacuoles by fusion with iLEs. In support of this, we found Rab7 colocalizes with Rab11-YFP at the limiting membrane of a subpopulation of Rab11-YFP–lined SVs (Fig. 2 D). In conclusion, SCs contain unusually large secretory and acidic vacuoles, permitting the in vivo analysis of these compartments at high spatial resolution. At least one large acidic compartment in each SC contains CD63-positive puncta (Fig. 1, G and H), and equivalent large vesicle–containing structures are also observed by EM (Fig. S2).

Downloaded from jcb.rupress.org on October 5, 2014

Published August 25, 2014

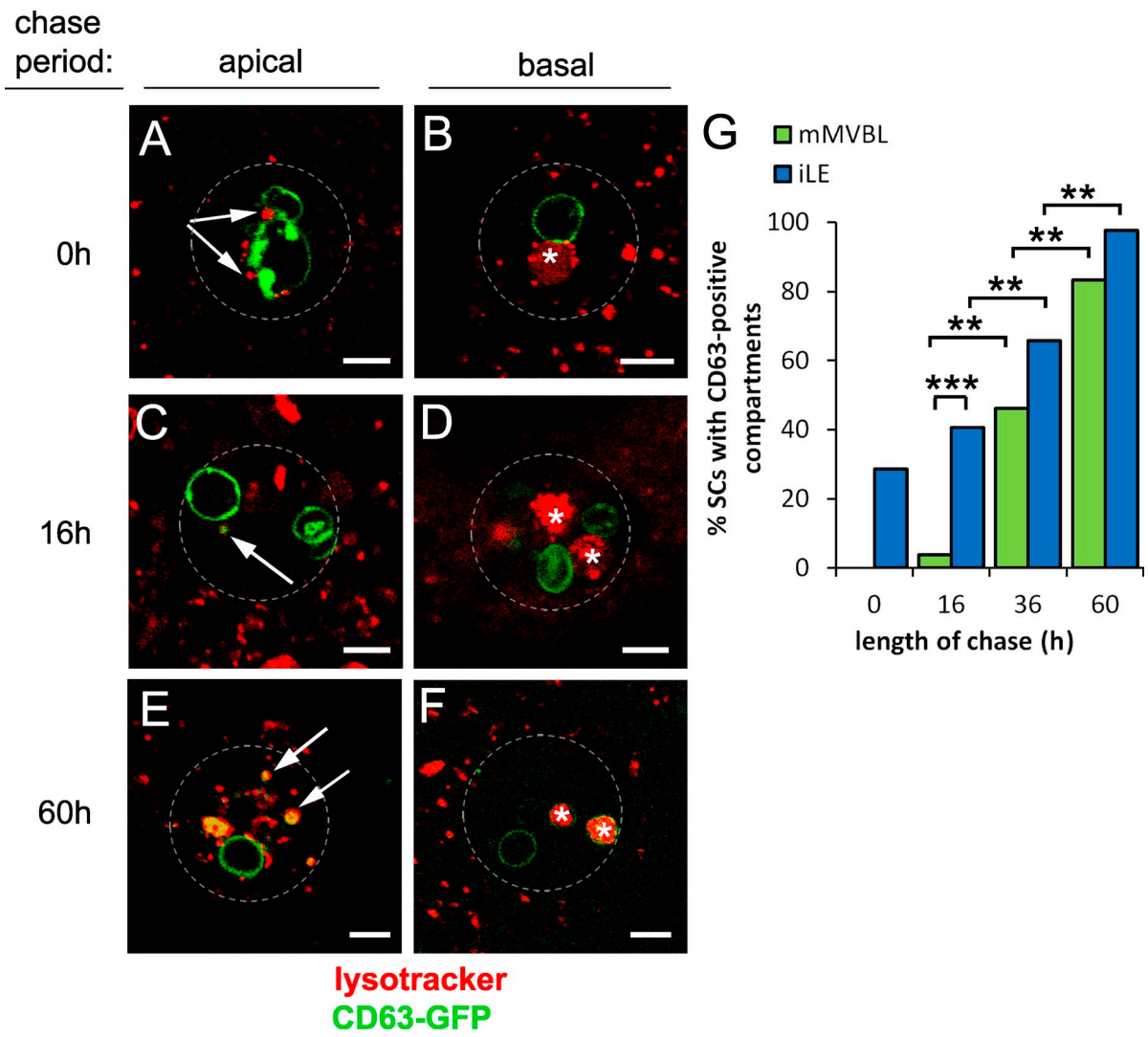


Figure 3. **CD63-GFP traffics from secretory to endocytic compartments in SCs.** (A–G) An 8-h pulse (at 28.5°C) of CD63-GFP expression was chased at 18°C for 0–60 h in virgin males, and proportions of cells with one or more LysoTracker red–positive iLEs (arrows in A, C, and E in apical sections; GFP positive in C and E) and mMVBLs (asterisks in B, D, and F in more basal views) that were CD63-GFP–positive were scored (G). Data shown are from a single representative experiment out of two repeats. The images in A–F are shown again in Fig. S3 alongside the corresponding single color channel images. Approximate outline of SC is marked in all images. **, $P < 0.01$; ***, $P < 0.001$; $n > 24$, pairwise comparisons, Fisher's exact test. Bars, 5 µm.

Endolysosomal and secretory compartments in SCs are highly dynamic

We followed CD63-GFP trafficking through the secretory and endolysosomal systems using a pulse–chase approach. Induction of a short (8 h) pulse of CD63-GFP expression, by inhibiting the temperature-sensitive GAL4 transcriptional repressor GAL80^{ts} at 28.5°C, followed by a chase period at 18°C of 0–60 h, revealed rapid labeling of two (1.9 ± 0.2, $n = 17$) nonacidic SVs, presumably receiving newly synthesized CD63-GFP from the Golgi (Figs. 3, A and B; and S3, A and B). Some iLEs were also GFP positive immediately after the pulse. During the early part of the time course, a greater proportion of SCs contained labeled iLEs than labeled mMVBLs ($P = 0.001$, $n > 27$), and this trend continued at later time points (Figs. 3, A–G; and S3, A–F), supporting our model in which CD63-GFP traffics first to the iLEs and subsequently to mMVBLs.

Strikingly, real-time confocal imaging of SCs revealed nonacidic SVs fusing with mMVBLs and rapid exchange of limiting membrane components (Fig. 4 A and Video 1). Although the internal contents of these compartments did not mix freely, these findings suggest a surprising level of exchange between SVs and mMVBLs and might explain how CD63-GFP–positive structures accumulate in SVs (Fig. 1, E–H).

As discussed previously, anti-CD63 staining indicates that GFP in many CD63-positive ILVs does not fluoresce (Fig. S2 A). However, inward invaginations of the CD63-GFP–labeled limiting membrane into the mMVBL lumen were observed in time-lapse videos, and occasionally, it appeared that new fluorescent ILVs might be formed from these (Fig. 4 B and Video 2). Therefore, some steps in ILV formation can be visualized by confocal microscopy in the large mMVBLs of living SCs, allowing us to screen for genetic manipulations that block these processes.

Downloaded from jcb.rupress.org on October 5, 2014

Published August 25, 2014

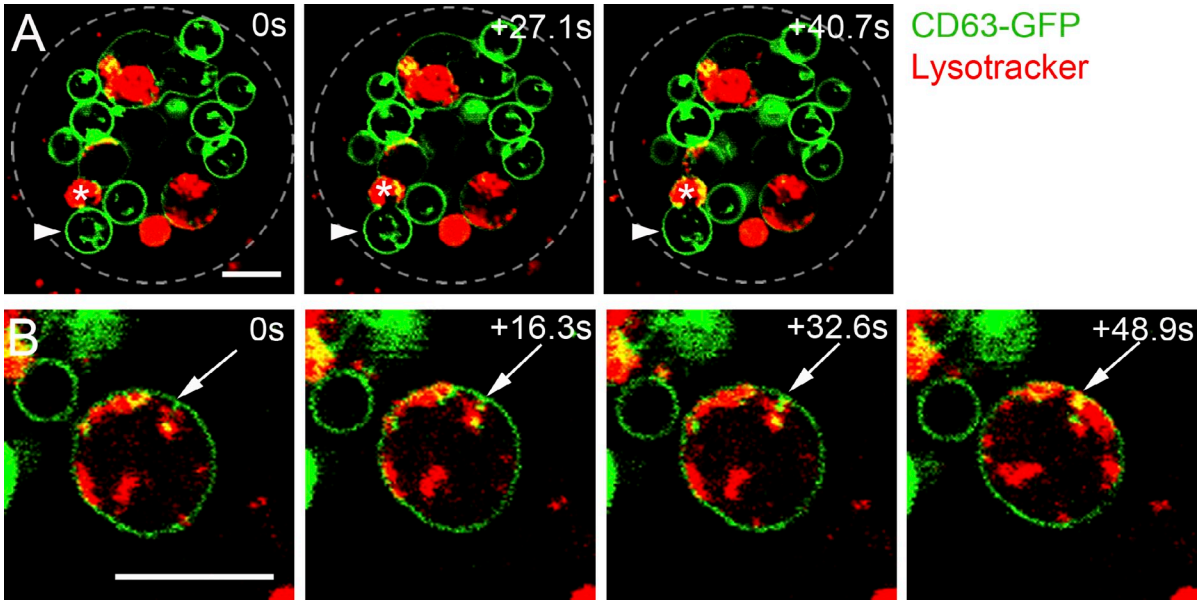


Figure 4. **Real-time imaging reveals dynamic endolysosomal trafficking events.** (A and B) Time-lapse imaging of 3-d-old *SC>CD63-GFP* males stained with LysoTracker red. (A) An mMVBL containing ILVs (asterisks) fuses with a large nonacidic SV (arrowheads; Video 1). Approximate outline of SC is marked. (B) A CD63-GFP–marked protrusion invaginates from the mMVBL membrane (arrows; 0 s) and seems to form a CD63-GFP–positive punctum in the next frame. Later, a line of peripheral acidic microdomains is seen below (48.9 s; see also Video 2). Bars, 5 µm.

Endosomal sorting complex required for transport (ESCRT)-dependent secretion of exosomes in SCs

To assess whether CD63-GFP–positive puncta in the AG lumen are exosomes derived from mMVBLs of SCs, we specifically blocked expression or function of a broad range of molecules in SCs, which in other systems are implicated in exosome biogenesis. The ESCRT complex has well-characterized roles in ILV formation, although ESCRT-independent mechanisms have also been reported (Trajkovic et al., 2008). Hrs is a component of the ESCRT-0 complex directly involved in protein sorting into ILVs and ILV formation through subsequent recruitment of downstream ESCRTs (Lloyd et al., 2002; Katzmann et al., 2003). Several recent studies demonstrate a role for Hrs in ESCRT-dependent exosome secretion in mammals and flies (Tamai et al., 2010; Gross et al., 2012; Colombo et al., 2013). ALiX (ALG-2–interacting protein X) interacts with several ESCRT complex proteins (Matsuo et al., 2004; Odorizzi, 2006). Recent knockdown studies in mammalian cells indicate that it is required in exosome biogenesis (Matsuo et al., 2004; Baietti et al., 2012), but this has not been investigated in flies. Fluorescent ILVs inside mMVBLs were almost completely absent in SCs expressing either *Hrs-RNAi* or *ALiX-RNAi* constructs, unlike controls (Fig. 5, B–D). The number of CD63-GFP–positive puncta secreted into the AG lumen was also drastically reduced ($P < 0.001$, $n > 9$; Fig. 5 A). mMVBLs in *ALiX-RNAi*– and *Hrs-RNAi*–expressing SCs were smaller and larger than controls, respectively (Fig. 5 I). These genotypes had normal numbers of iLEs (Fig. 5 H), but *Hrs-RNAi*–expressing SCs had significantly fewer mMVBLs (Fig. 5 G). Importantly, these *ESCRT* knockdown SCs still synthesized equivalent levels of the SC-specific CD63-GFP fusion protein by Western blot analysis of whole glands (Fig. 5 J) but transferred much less protein to females upon mating (Fig. 5 K), consistent with the reduced secretion of this exosome marker.

An alternative explanation for these results is that *ESCRT* knockdown affects all secretion by SCs. However, the SC-specific production (Rylett et al., 2007) of the secreted, nonexosomal protease ANCE (Figs. 5 J and S4, B–D), its secretion into the AG lumen (Fig. S4, E–G), and its transfer into females (Fig. 5 K) were not affected by *ALiX* or *Hrs* knockdown, showing that these treatments selectively affect the exosome biogenesis pathway in SCs.

To provide further evidence that SCs produce CD63-positive exosomes, we modulated the activities of three Rabs previously implicated in exosome secretion: Rab11 (Savina et al., 2002; Koles et al., 2012; Beckett et al., 2013), Rab35 (Hsu et al., 2010), and Rab27 (Ostrowski et al., 2010). Expression of dominant-negative Rab11-YFP (*Rab11DN*; Zhang et al., 2007), *Rab11-RNAi*, *Rab35-RNAi*, and one of two *Rab27-RNAi*'s significantly reduced the number of secreted GFP-positive puncta (Figs. 5 A and S5, A and B). Previous studies have indicated that Rab35 and Rab27 do not regulate secretion of exosomes carrying the cargo receptor Evenness Interrupted (Evi) in *Drosophila* S2 cells (Koles et al., 2012; Beckett et al., 2013), suggesting multiple exosome secretion routes in flies as well as mammals. Indeed, expression of two different RNAi's targeting *Evi*, which is required to produce Wingless-containing exosomes (Beckett et al., 2013) but is not required for CD63-GFP–positive exosome secretion in flies (Gross et al., 2012), did not affect the number of secreted puncta in the gland lumen (Fig. 5 A). Finally, the number of secreted puncta was also significantly reduced when *Rab7-RNAi* or dominant-negative Rab7-YFP (*Rab7DN*; Zhang et al., 2007) was expressed in SCs (Fig. 5 A), implicating late endolysosomal trafficking events in secretion. Based on these extensive genetic data,

Downloaded from jcb.rupress.org on October 5, 2014

Published August 25, 2014

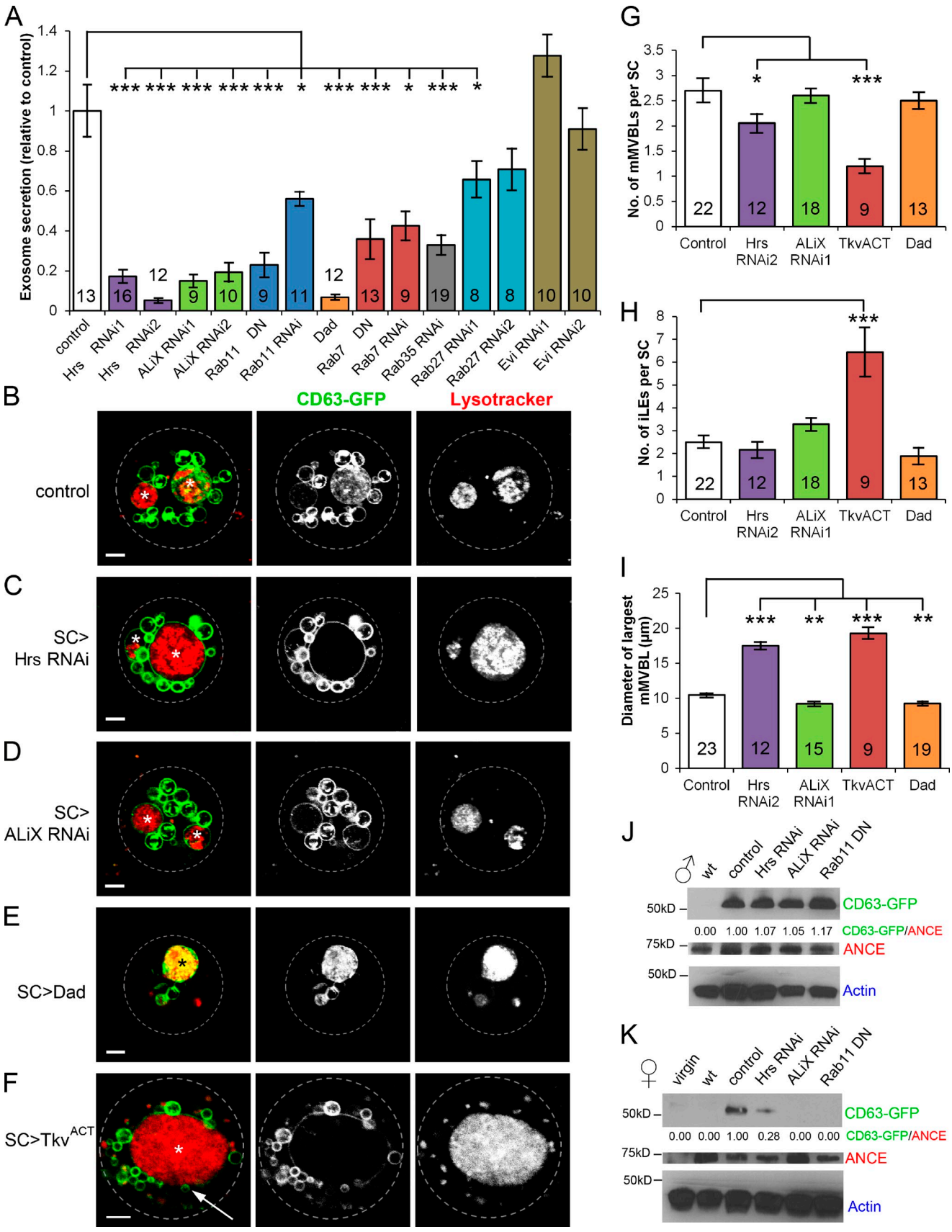


Figure 5. **ESCRTs, Rab GTPases, and BMP signaling regulate the exosome biogenesis pathway.** (A) The numbers of CD63-GFP–positive puncta secreted into the AG lumen were significantly reduced in *SC>Hrs-RNAi*, *SC>ALiX-RNAi*, *SC>Rab11DN*, *SC>Rab11-RNAi*, *SC>Dad*, *SC>Rab7-DN*, *SC>Rab7-RNAi*, *SC>Rab27-RNAi1*, and *SC>Rab35-RNAi* males compared with control (number of glands above or in the bars) but not *SC>Rab27-RNAi2* and

Downloaded from jcb.rupress.org on October 5, 2014

Published August 25, 2014

we conclude that SCs secrete CD63-GFP–positive exosomes whose biogenesis and secretion are regulated by evolutionarily conserved molecular mechanisms.

Interestingly, despite the large number of CD63-GFP–positive exosomes in the AG lumen, they did not seem to fuse with MCs in most of the gland (Fig. S5 C). However, we did observe occasional GFP puncta inside MC neighbors of SCs at the distal tip of each AG (Fig. S5 D). The regionalized nature of this uptake indicates that it may be mediated by contact-dependent transfer between SCs and MCs, rather than transfer via the AG lumen.

SC exosomes fuse with sperm and interact with epithelial cells in the female reproductive tract

We investigated whether the interaction between SC exosomes and target cells primarily takes place after mating. *SC>CD63-GFP* males transferred fluorescent puncta into the lumen of the female reproductive tract during mating (Fig. 6, A–D). Multiply mated males of 11 d and older can sporadically transfer SCs to females (Leiblich et al., 2012). Importantly, all mating experiments performed in our current study were with 4-d-old males; we never observed transfer of fluorescent SCs in >50 mated females that we imaged, indicating that SC transfer is not involved in the phenotypes observed.

Several seminal peptides target specific regions of the female reproductive tract and/or sperm after mating (Peng et al., 2005; Ravi Ram et al., 2005). Isolated human prostasomes fuse with the sperm midpiece in vitro, delivering Ca^{2+} signaling molecules implicated in sperm motility (Fabiani et al., 1994; Park et al., 2011). We also detected colocalization of CD63-GFP and sperm heads in the female reproductive tract after mating (Fig. 6, D and E). Analysis of confocal z series images revealed narrow rings of GFP surrounding the sperm head (Fig. 6 F), as might be expected after exosome–sperm fusion. These events were most commonly observed at 20 min after the start of mating (88% [14/16] mated females; Fig. 6 H) in the anterior portion of the female reproductive tract where sperm and exosomes accumulated, either in the anterior uterus (9/16) or the oviduct (5/16). This fusion frequency is almost certainly underestimated: first, because CD63-GFP is likely to rapidly diffuse and dissipate over the sperm surface after fusion, so the GFP fluorescence signal will rapidly become undetectable, and second, because there may be additional fusion to sperm tails. Although tools were not available to fluorescently colabel exosomes and sperm tails, pairs of short parallel fluorescent lines or extended irregular lines of GFP fluorescence were always seen in the female reproductive tract lumen (100%, $n = 8$; Fig. 6, F and G; and Video 3), which might represent such events. We did not observe CD63-GFP in sperm storage organs, though as discussed previously in this paper, GFP may dissipate after fusion to sperm before entering these structures.

Interestingly, we noted accumulation of CD63-GFP exosomes at the surface of the reproductive tract either in the uterus or oviduct in 40% of females (Fig. 7; $n = 34$), suggesting that SC exosomes also interact with female epithelial cells. In some cases, fluorescent aggregates made contact with the epithelium (Fig. 7 C and Video 4), whereas in others, dispersed puncta aligned along the epithelial surface (Fig. 7 D). These interactions may reflect docking to female cell targets, either before internalization via endocytosis (Morelli et al., 2004) or possibly as part of a cell surface signaling mechanism. In summary, SC-derived exosomes do not seem to fuse to the AG epithelium in virgin males but do fuse to sperm and interact with female epithelial cells after mating.

SC exosomes modulate female receptivity to remating

In contrast to virgin females, recently mated *Drosophila* females will reject a courting male (Wolfner, 1997). We have previously shown that BMP signaling in SCs is required for full induction of this female postmating behavior (Leiblich et al., 2012). We hypothesized that SC-derived exosomes might be involved in this function. Remarkably, blocking exosome production, using SC-specific expression of either *ALiX-RNAi* or dominant-negative Rab11, reduced the ability of males to prevent female remating (Fig. 8 A). Importantly, and similar to our observations when BMP signaling is blocked in SCs (Leiblich et al., 2012), we did not see any significant effect on egg laying, fecundity, or mating behavior for *SC>ALiX-RNAi* males (mating times, but not egg laying or fecundity, were reduced for *Rab11DN*; Fig. 8, B–F). Therefore, exosome secretion from SCs appears to be required to fully induce long-term postmating reprogramming of female behavior.

BMP signaling regulates endolysosomal trafficking and is required for exosome secretion

Blocking SC function and development affects multiple aspects of fecundity (Minami et al., 2012, Gligorov et al., 2013), but reduced BMP signaling and loss of exosome secretion in

SC>Evi-RNAi males. DN, dominant negative. (B–F) SCs from 6-d-old virgin males stained with LysoTracker red. (G–I) Different intracellular compartments were subsequently counted and measured. mMVBLs (asterisks) in SCs expressing CD63-GFP and *Hrs-RNAi* (C) or *ALiX-RNAi* (D) contain very few CD63-GFP–positive ILVs (internal puncta), unlike controls (B), and are altered in size (I). Reducing levels of BMP signaling in SCs (Dad overexpression; E) results in significantly smaller mMVBLs (I), typically containing a higher density of internalized fluorescent CD63-GFP than controls. SCs expressing an activated form of the BMP receptor Tkv^{ACT} (F) contain fewer mMVBLs (G), which are larger (I), and typically surrounded by multiple SVs (e.g., arrow). They also contain more iLEs (H). (G–I) Mean number of mMVBLs (G) and iLEs (H) and mean diameter of largest mMVBL (I) in SCs of different genotypes (I). Quantification in G–I is from a mean of three cells per gland, averaged over *n* glands (numbers in bars). (J) Western analysis of AG protein extracts from w^{1118} (wild type [wt]) and flies expressing *SC>CD63-GFP* with or without (control) different transgenes. (K) Western analysis of protein extracts from reproductive tracts dissected from females mated to males of the same genotypes. CD63-GFP/ANCE is the ratio of signals from Western blots. Full-length CD63-GFP protein is observed in males and females. Error bars indicate ±SE; *, $P < 0.05$; **, $P < 0.01$; ***, $P < 0.001$ relative to control. Data were analyzed using either an unpaired two-tailed Student's *t* test or Mann–Whitney *U* test, for normally and nonnormally distributed datasets, respectively. Approximate outline of SC is marked. Bars, 5 µm.

Downloaded from jcb.rupress.org on October 5, 2014

Published August 25, 2014

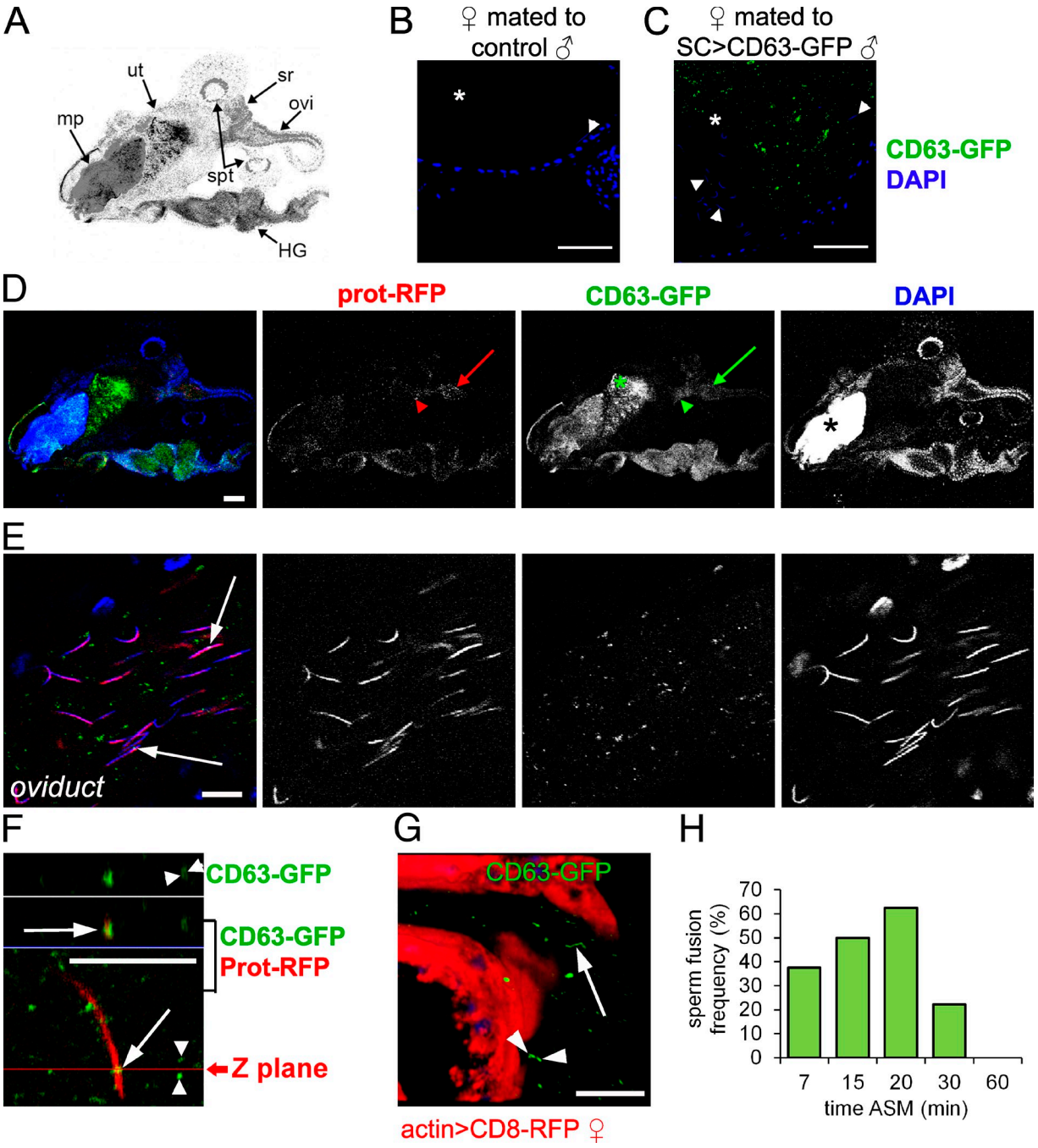


Figure 6. **SC exosomes interact with sperm in females.** (A) Schematic of female reproductive tract in D showing mating plug (mp), uterus (ut), oviduct (ovi), and sperm storage organs (spermathecae [spt] and seminal receptacle [sr]) as well as the autofluorescent hindgut (HG). (B and C) w^{1118} female reproductive tract dissected 20 min after mating to either a control w^{1118} (B) or *SC>CD63-GFP* (C) male, imaged under identical confocal settings. Images show lumen of the female uterus (asterisks) containing sperm whose heads are visible with DAPI staining (arrowheads). (D and E) Female reproductive tracts 20 min after mating to a *protamineB-RFP; SC>CD63-GFP* male. (D) ProtamineB-RFP (prot-RFP), which marks sperm heads, accumulates in the anterior uterus (red arrowhead) and oviduct (red arrow). Most CD63-GFP–positive exosomes localize to the posterior uterus (green asterisk), but they can also be seen in the anterior uterus (green arrowhead) and oviduct (green arrow). The autofluorescent mating plug (closed asterisk) is shown. (E) CD63-GFP–positive exosomes colocalize with sperm heads marked by protamineB-RFP (open arrows). (F) Orthogonal view of a z stack through near-complete ring of CD63-GFP fused to ProtamineB-RFP sperm head (arrows). The confocal image below the blue line shows part of the female reproductive tract lumen. The two images above the blue line, separated by a white line, are green (top) and red/green (bottom) z stacks captured in the z plane marked in the bottom image. Note multiple pairs of parallel GFP-positive lines (arrowheads), potentially produced by sperm tail fusion. (G) These (arrowheads) and irregular extended lines of fluorescence (arrow) are also seen in G, which shows a maximum 3D projection image of a z stack from a female anterior uterus and oviduct where the epithelium is marked by actin>CD8-RFP (also shown in Video 3). (H) Female reproductive tracts were dissected and fixed at specific times after the start of mating to *SC>CD63-GFP* males. The frequency of exosome–sperm interaction events within the female reproductive tract was analyzed (n = 8 for each time point after the start of mating [ASM]). Only fusions to the sperm heads are included. Bars: (B and C) 50 µm; (D) 200 µm; (E and F) 5 µm; (G) 20 µm.

Downloaded from jcb.rupress.org on October 5, 2014

Published August 25, 2014

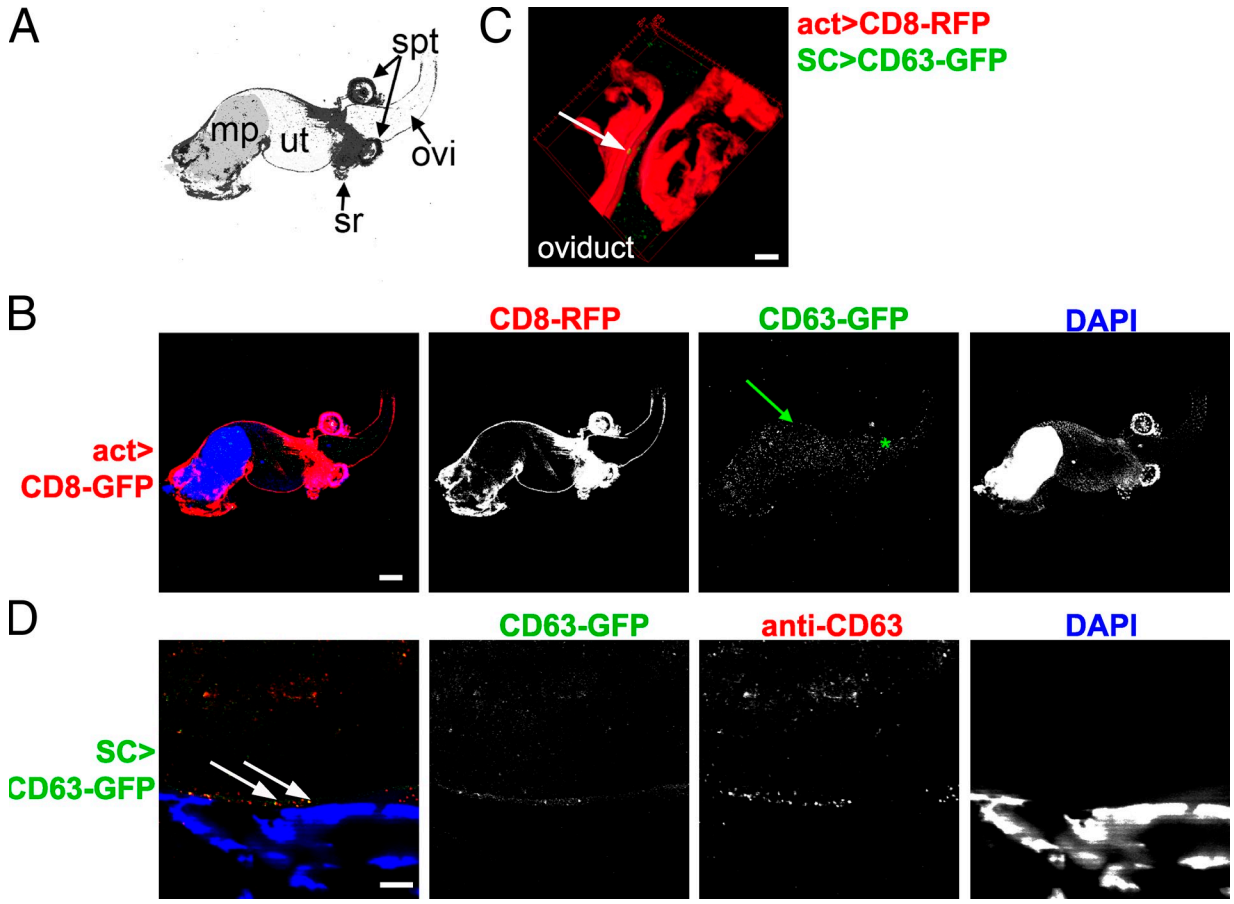


Figure 7. **SC exosomes interact with female epithelial cells.** (A) Schematic of female reproductive tract shown in B. mp, posterior mating plug (autofluorescent); ut, uterus; sr, seminal receptacle; spt, spermathecae; ovi, oviduct. (B–D) *actin>CD8-RFP*–expressing (B and C) or wild-type (D) females mated to *SC>CD63-GFP* males. (B) CD63-GFP exosomes are found in the uterus (green arrow) and oviduct (green asterisk). (C and D) These exosomes accumulate at the apical surface of female reproductive tract epithelial cells (arrows), which are either marked with CD8-RFP (C; Video 4) or unmarked (D). DAPI stains nuclei. In D, the reproductive tract is stained with an antibody against human CD63 to confirm that GFP and CD63 colocalize. Specific spermathecal cells exhibit weak autofluorescence. Bars: (B) 200 µm; (C) 20 µm; (D) 5 µm.

these cells specifically modulate female remating behavior. One possible explanation is that BMP signaling controls exosome production. Remarkably, antagonizing BMP signaling by expression of the negative regulator Dad almost completely blocked CD63-GFP–labeled exosome secretion (Fig. 5 A), strongly supporting this idea. Unfortunately, it was not possible to test the effect of elevated BMP signaling on exosome secretion by expression of a constitutively activated form of the BMP type I receptor Thickveins (Tkv^{ACT}, containing a Q199D substitution; Hoodless et al., 1996). The hypertrophic SCs induced by expression of this construct protrude into the AG lumen and shed large amounts of GFP-positive cellular debris (Leiblich et al., 2012), interfering with exosome counting.

We tested whether BMP signaling might modulate exosome secretion by altering endolysosomal trafficking in SCs, using live imaging of CD63-GFP–expressing cells. In contrast to the effect of *ALiX* and *Hrs* knockdown (Fig. 5, C and D), mMVBLs in *Dad*-expressing SCs contained unusually high levels of internalized CD63-GFP (Fig. 5 D), indicating that BMP signaling is not required for ILV formation but must control a key trafficking and/or maturation event from the mMVBL to the plasma membrane and lysosomes, where GFP fluorescence would be lost. Indeed, SCs overexpressing Tkv^{ACT} had significantly fewer, but much larger, mMVBLs ($P = 0.04$; Fig. 5, G and I) with no intraluminal fluorescence, supporting this model. Numbers of iLEs were elevated (Fig. 5 H), and more of these cells than control cells (17/19 versus 16/31; $P = 0.003$, Fisher's exact test) contained multiple SVs clustered around the enlarged mMVBL, consistent with the idea that there is increased bulk trafficking into the large acidic compartment. We therefore conclude that BMP signaling controls a key endolysosomal trafficking step in SCs required for exosome secretion, and this potentially explains the role of SC-specific BMP signaling in modulating female postmating behavior.

Because BMP signaling drives SC growth, as measured by relative size of SC versus neighboring MC nuclei (Leiblich et al., 2012), we tested whether exosome formation or secretion might be involved in this. Interestingly, although nuclei of SCs expressing either *ALiX-RNAi* or *Rab11DN* were reduced in size, nuclear size was increased in *Hrs-RNAi*–expressing SCs (Fig. 9). This suggests that ESCRT-dependent ILV formation is not required for SC growth.

Downloaded from jcb.rupress.org on October 5, 2014

Published August 25, 2014

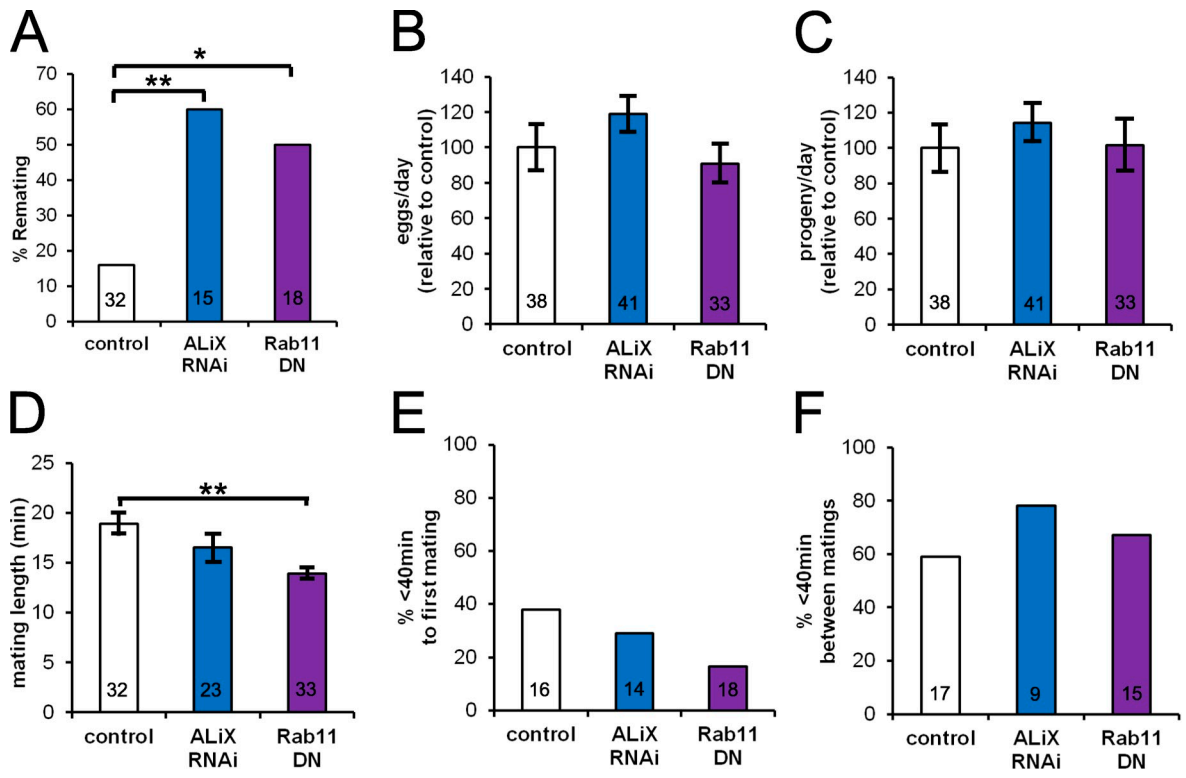


Figure 8. **Knockdown of *ALiX* in SCs selectively affects female postmating receptivity to other males.** (A) Proportion of premated 4-d-old males of different genotypes unable to prevent all females it subsequently mates with from remating (*, $P < 0.05$; **, $P < 0.01$, Fisher's exact test). (B and C) Egg counts (B) and progeny counts (C) from mated females before remating experiments were performed (analyzed by unpaired two-tailed Student's *t* test after a Shapiro–Wilk test to confirm normality). (D–F) Mating times (D; **, $P < 0.01$, Student's *t* test), proportion of males that mate within the first 40 min of exposure to females (E) or remate within 40 min of the end of previous mating (F), were also analyzed (using Fisher's exact test for E and F). Values inside bars show the number of males tested (*n*). Error bars indicate ±SE. Data shown are from a single representative experiment out of two repeats. DN, dominant negative.

Discussion

Seminal fluid synthesized by male reproductive glands has a powerful influence on fertility, affecting multiple sperm activities and altering female behavior, in some cases directly conflicting with female reproductive interests. Several previous studies have revealed an important function for seminal peptides in *Drosophila* (Chen et al., 1988; Wolfner, 1997) and mammals (Park et al., 2011; Kershaw-Young et al., 2012) in these processes. However, in this study, we present the first in vivo evidence that exosomes also play a key role and identify a completely novel role for BMP signaling in regulating this process.

SCs secrete exosomes: A new in vivo model to study exosome biogenesis

Exosome biogenesis, secretion, and uptake have been previously studied in *Drosophila* (Gross et al., 2012; Koles et al., 2012; Beckett et al., 2013). However, the small size of exosomes, MVBs, and fly tissues makes these processes difficult to analyze in vivo. The AG contains only nanoliter volumes of secretions, making it impractical to use standard exosome analysis techniques, such as ultracentrifugation and Nanosight Tracking Analysis (Vlassov et al., 2012). Like other studies in flies, we used genetic and imaging approaches to test the identity of SC-specific CD63-positive puncta. In addition, we used Western blot analysis of transferred seminal fluid and live imaging of giant MVBs in SCs to test our hypothesis that SCs produce exosomes.

We primarily used the human CD63-GFP tetraspanin marker in our analysis. However, GFP-positive puncta were also observed in large secretory compartments of SCs expressing cytosolic GFP, and exosome-sized vesicles in MVBs and the AG lumen were observed in EM analysis of wild-type glands (Fig. S2), confirming their presence in nontransgenic flies. Because exosomes can be loaded with many cellular components, our findings provide a potential explanation for the observation that AGs of several insects, including *Drosophila*, secrete intracellular proteins (Walker et al., 2006; Sirot et al., 2011).

Other evidence strongly supports the idea that CD63-positive puncta secreted from SCs are exosomes and not vesicles shed from the plasma membrane. This includes the observation that CD63-positive puncta are found inside both acidic Rab7-positive MVB-like compartments as well as nonacidic Rab11-positive vacuoles and require the ESCRT and ESCRT-associated proteins Hrs and ALiX, as well as several Rabs linked to mammalian exosome secretion, to be formed and secreted. Secreted puncta counts have been used previously in flies to study genetic control of exosome secretion (Gross et al., 2012). A criticism of this approach is that reduced puncta numbers may merely reflect aggregation. However, the transfer of CD63-GFP to females was drastically reduced in mutant backgrounds, arguing

Downloaded from jcb.rupress.org on October 5, 2014

Published August 25, 2014

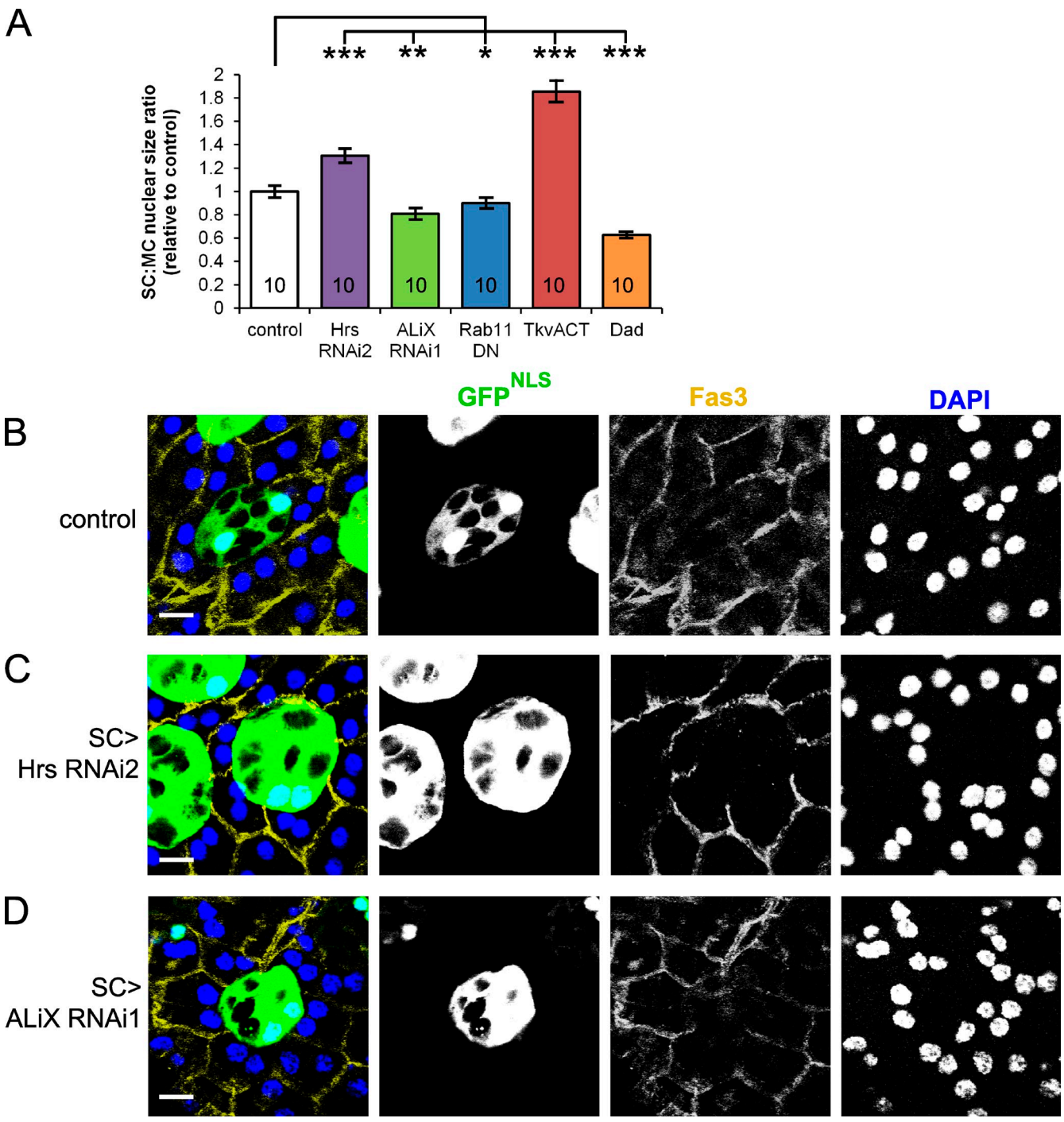


Figure 9. ***ALiX* and *Hrs* have different effects on SC growth.** (A) Growth of SCs relative to MCs in 6-d-old males expressing different transgenes in SCs, as measured by the ratio of SC to MC nuclear size and normalized to controls. Values inside bars show number of males tested (*n*). DN, dominant negative. (B–D) SCs in 6-d-old males expressing either GFP linked to a nuclear localization sequence (GFP^{NLS}) alone (B) or in combination with either *Hrs-RNAi* (C) or *ALiX-RNAi* (D), under the control of the *esgF/O*^{ts} driver. Control SC nuclei are smaller than MC nuclei at eclosion but grow to be larger by 6 d (B). Data for A were analyzed using the Student's *t* test or Mann–Whitney *U* test (*, $P < 0.05$; **, $P < 0.01$; ***, $P < 0.001$, $n = 10$) after a Shapiro–Wilk test for normality. Error bars indicate ±SE. Bars, 10 µm.

against a simple aggregation model. Furthermore, because genetic manipulation of ESCRT function does not alter other secretory processes in SCs (Figs. 5 K and S4), this strongly implicates the endocytic pathway in secretion of tagged CD63.

Studies of exosomes in *Drosophila* as well as mammals already suggest that multiple exosome subtypes exist and may be regulated differently, e.g., different roles for ALiX (Baietti et al., 2012 versus Colombo et al., 2013), Hrs (Edgar et al., 2014), and Evi (Beckett et al., 2013). If different exosome subtypes are made in SCs, these cells should offer an ideal system to study their differential regulation.

The remarkably large size of endosomal compartments in SCs provides new opportunities to study exosome biogenesis in vivo. To date, many studies of the intracellular exosome

Downloaded from jcb.rupress.org on October 5, 2014

Published August 25, 2014

biogenesis machinery and endolysosomal trafficking in higher eukaryotes have relied on expressing an activated form of Rab5 (Stenmark et al., 1994; Hirota et al., 2007; Wegner et al., 2010; Dores et al., 2012; Schroeder et al., 2012) or addition of the ionophore monensin (Savina et al., 2002) in cell culture to artificially enlarge the endolysosomal compartments, disrupting normal trafficking events. Hence, our new SC in vivo model should allow us to reinvestigate previously reported regulators of exosome biogenesis and identify functional differences in trafficking phenotypes, as we have seen for *Hrs* and *ALiX*.

Our study has already revealed a surprisingly dynamic interaction between the secretory and endolysosomal systems in SCs. Communication between these compartments using vesicular transport and tubulation processes has been reported in other cell types in flies and mammals (Savina et al., 2005; Minogue et al., 2006; Burgess et al., 2012), but our study suggests that direct fusion can also be involved. Indeed, our data are also consistent with mMVBLs forming after fusion between SVs and iLEs (Fig. 2 D), suggesting that fusion events may play a critical role in establishing distinct compartments within SCs. In light of this dynamic flux between compartments, it remains unclear whether CD63-GFP–labeled exosomes might be released by the classical route involving mMVBL fusion to the plasma membrane or via an intermediate secretory compartment.

SC exosomes have complex physiological functions

Although most analysis of the fly AG has highlighted roles for MC products, such as SP (Chen et al.,1988; Chapman et al., 2003), in reprogramming female postmating responses, several recent studies have also suggested a central but poorly defined function for SCs (Leiblich et al., 2012; Minami et al., 2012; Gligorov et al., 2013). A transcriptional program regulated by the *Hox* gene *Abd-B* controls vacuole formation in SCs (Gligorov et al., 2013). Our findings now indicate that at least one of the effects mediated by SCs, altered receptivity to remating, requires exosome secretion.

It is difficult to accurately estimate the frequency of SC exosome–sperm fusion events in each female fly because they can probably only be visualized transiently, and many may involve fusion to the very long sperm tail. Sperm play an essential role as mediators of SP-dependent postmating effects in females (Liu and Kubli, 2003; Peng et al., 2005), so it is plausible that exosome fusion to sperm may modulate specific SP functions. Another appealing hypothesis is that SC exosomes also interact with the female reproductive tract to influence female behavior. However, whatever the target tissues, our data clearly demonstrate a role for SC exosomes in female reprogramming. Furthermore, like human prostasomes (Arienti et al., 1997; Park et al., 2011), SC exosomes fuse with sperm, highlighting possible conserved roles for exosomes in male reproductive biology. In prostate cancer, prostasomes are inappropriately secreted into the bloodstream (Sahlén et al., 2004; Tavoosidana et al., 2011), so that other cells in the body may be subjected to these powerful reprogramming functions, potentially supporting tumor–stroma interactions and metastasis (Ronquist et al., 2010; Ge et al., 2012).

BMP-dependent regulation of endolysosomal trafficking and exosome secretion

Reducing BMP signaling in SCs inhibits exosome secretion and leads to the formation of a novel mMVBL compartment that is filled with fluorescent CD63-GFP. A simple interpretation of this result is that MVBL compartments in these cells do not mature properly, blocking exosome secretion. Consistent with this, increasing BMP signaling in these cells produces a highly enlarged acidic compartment.

Previous studies have shown that blocking endosomal maturation by knockdown of the early ESCRT component Hrs increases the size of immature endosomal class E compartments lacking ILVs and also results in increased BMP signaling (Piper et al., 1995; Jékely and Rørth, 2003; Chanut-Delalande et al., 2010). Our data demonstrate that elevated BMP signaling increases mMVBL size, suggesting that there is a complex bidirectional interaction between mMVBL maturation and size and the level of BMP signaling in SCs.

Our findings are consistent with a model in which BMP signaling also controls SC growth by driving endolysosomal trafficking and maturation events. Late endosomes and lysosomes have previously been shown to house major nutrient sensors and cell growth machinery, including the mTORC1 complex (Goberdhan, 2010; Ögmundsdóttir et al., 2012), which is activated by intraluminal amino acids. Interestingly, the growth rate of knockdown cells with reduced ESCRT function appears to correlate with mMVBL size (Fig. 5 I) rather than exosome secretion rate. We now need to test whether growth in these cells is mTORC1 dependent.

Whatever the explanation for the growth defects in SCs, our data very clearly implicate BMP signaling in the regulation of endolysosomal trafficking and exosome secretion. It will now be important to test whether BMP signaling plays a similar role in mammalian glands that secrete exosomes, such as prostate and breast, and determine whether this role is affected in diseases such as cancer.

Materials and methods

Fly stocks

The following stocks were used: *esgF/O^{ts}* (*esg-GAL4 tub-GAL80^{ts} UAS-FLP/CyO; UAS-GFP$_{nls}$ actin>FRT>CD2>FRT>GAL4/TM6* [Jiang et al., 2009]; a gift from B. Edgar, Center for Molecular Biology, University of Heidelberg, Heidelberg, Germany; *esg-GAL4^{NP7397}*, *tubP-GAL80^{ts}*, *P{UAS-FLP1.D}*, *P{UAS-GFP.nls}*, and *actin>FRT>CD2>FRT>GAL4/TM6* are described in FlyBase), *UAS–CD63-GFP* (Panáková et al., 2005; a C-terminal fusion of full-length human CD63 with pEGFP-C1, which was then inserted into the pUAST vector [Brand and Perrimon, 1993]; see FlyBase; a gift from S. Eaton, Max Planck Institute of Molecular Cell Biology and Genetics, Dresden, Germany), *tub-rab11-YFP*, *tub-rab7-YFP*, and *tub-rab5-YFP* (gifts from J.-P. Vincent, Medical Research Council National Institute for Medical Research, London, England, UK), *Acp26Aa-GAL4* (Chapman et al., 2003; ∼1.4-kb fragment upstream of the *Acp26Aa* coding region fused to GAL4; a gift from M. Wolfner, Cornell University, Ithaca, NY), *dsx-GAL4* (Rideout et al., 2010; a GAL4 gene trap inserted into the first coding exon of the *dsx* gene; a gift from S. Goodwin, University of Oxford, England, UK), *spi-GAL4* (Hayashi et al., 2002; *spi^{NP0261}*; see FlyBase), *UAS–ALiX-RNAi* (RNAi1, v32047 [Vienna Drosophila Resource Center]; RNAi2, HMS00298 [Bloomington Drosophila Stock Center] containing nonoverlapping target sequences; Dietzl et al., 2007; Ni et al., 2008), *UAS–Hrs-RNAi* (RNAi1, HMS00841 [Bloomington Drosophila Stock Center]; RNAi2, HMS00842 [Bloomington Drosophila Stock Center]; Ni et al., 2008), *UASp-YFP.Rab11.S25N* (Zhang et al., 2007; see FlyBase),

Downloaded from jcb.rupress.org on October 5, 2014

Published August 25, 2014

UASp-YFP.Rab7.T22N (Zhang et al., 2007; see FlyBase), *UAS–Rab35-RNAi* (JF02978), *UAS–Rab27-RNAi* (JF02165 [RNAi1] and HMS01523 [RNAi2] containing nonoverlapping target sequences), *UAS–Rab11-RNAi* (JF02812), *UAS–Rab7-RNAi* (JF02377), and *UAS–evi-RNAi* (RNAi1, 5214 [Vienna Drosophila Resource Center; Ni et al., 2008]; RNAi2 was a gift from J.-P. Vincent; Bloomington Drosophila Stock Center and Vienna Drosophila Resource Center RNAi lines are described in FlyBase), *protamineB-RFP-160* (Köttgen et al., 2011; full-length C-terminal fusion of *protamineB* and its upstream promoter to RFP; a gift from J. Belote, Syracuse University, Syracuse, NY), *tub-PI4KII-GFP* (Burgess et al., 2012; full-length *PI4KII* [LD24833] subcloned into a modified pCaSpeR4 vector containing the αTub84B promoter and with mEGFP inserted at its N-terminal end; a gift from J. Brill, The Hospital for Sick Children, Toronto, Ontario, Canada), *UAS-Dad* (Tsuneizumi et al., 1997; $Dad^{Scer\backslash UAS.cTa}$ in FlyBase), and *UAS-*Tkv^{QD} (Hoodless et al., 1996; full-length Thickveins coding sequence carrying a Q199D mutation cloned in the pUAST vector). *UAS–CD8-RFP*, *actin-GAL4*, and *tub-GAL80*^{ts} were obtained from the Bloomington Drosophila Stock Center. A *spi-GAL4* driver line (with or without *tub-GAL80*^{ts}), which expresses only in SCs within the AG, was used in all experiments except for exosome lumen counts (*dsx-GAL4 tub-GAL80*^{ts}; again specific for SCs in AG epithelium) and mating experiments, for which *esgF/O*^{ts} was used because it gives highly specific SC expression within the entire male reproductive system (Leiblich et al., 2012).

Classification of different vacuolar compartments in SCs

In living SCs, subcellular structures and intracompartment puncta are much better preserved than in fixed tissue (compare Fig. 1, E and G), so wherever possible, live staining was used for classifying and counting compartments. We expressed several UAS-regulated tagged markers for endolysosomal compartments in SCs, e.g., HRP-Lamp (Juhász et al., 2008) and spin-GFP (Sweeney and Davis, 2002), but they all altered the ratios of acidic and nonacidic compartments in these cells, so we could not use them as an additional tool to confirm our conclusion that large acidic compartments in SCs are late endosomes or lysosomes. CD63-GFP puncta that could be seen in the large acidic compartments of SCs were strongly fluorescent. This is consistent with observations in mammalian cells, in which CD63 is typically concentrated into ILVs within acidic MVBs before secretion (Escola et al., 1998).

Pulse–chase experiments

A short (8 h) pulse of CD63-GFP expression was induced by inhibiting the temperature-sensitive GAL4 transcriptional repressor GAL80^{ts} at 28.5°C. This was followed by a chase period at 18°C of 0–60 h. Note that the CD63-GFP transcript is likely to persist once the pulse has ended, and so, new fusion protein expression will continue during the chase period.

Analysis of exosome secretion and regulation

Because the AG lumen contains only nanoliter volumes of secreted fluid of complex composition (Fig. S2 G), including the exosomes made from just 40 SCs, it was not practical to use standard isolation approaches (Vlassov et al., 2012) to study SC exosomes. For in vivo exosome quantification and analysis of ANCE staining in the AG lumen (Figs. 5 and S4, respectively), newly eclosed males were incubated at 28.5°C to induce transgene expression. After 2 d, each male was mated to three w^{1118} virgin females overnight, after which the females were removed, and males were left for a further day before being dissected and fixed at 4 d after eclosion. This procedure allowed stored contents of the AG lumen to be partly expelled and replenished at least 2–3× during the period of transgene expression. Each test experiment was performed simultaneously with a control for direct comparison. The observation that blocking ESCRT-dependent events in SCs drastically reduces the levels of CD63-GFP in the AG lumen in young males after multiple matings without affecting expression in the gland (Fig. 5) strongly argues that shedding of membrane debris does not take place in these experiments. We used two RNAi's against Evi, a trafficking molecule required for secretion of Wingless on exosomes (Beckett et al., 2013), but not for CD63-positive exosome secretion (Gross et al., 2012), to test for nonspecific effects of modulating trafficking and RNAi overexpression. Although Evi is transcribed in many tissues in adults (Chintapalli et al., 2007), we have not confirmed that it is transcribed in SCs because an in situ hybridization method has not been developed for AG.

Mating experiments to analyze exosome transfer

For single-mating experiments to analyze exosome targets in the female reproductive tract (Figs. 6 and 7), w^{1118} or w^{1118}*; actin-GAL4; UAS–CD8-RFP* virgin females (2–10 d old) were placed with individual 3-d-old *spi-GAL4; UAS–CD63-GFP* ± *protamineB-RFP* virgin males, and matings were observed. Dissections of reproductive organs from females in 4% paraformaldehyde in PBS were performed at a known time after the start of mating. Dissected reproductive tracts were fixed for 30 min and then washed in PBST-0.03% (PBS and 0.03% Triton X-100) for 20 min before mounting in Vectashield with DAPI (Vector Laboratories). When dissected at 7 min after the start of mating, 2/8 female reproductive tracts did not contain CD63-GFP exosomes, suggesting that, despite sperm transfer from the testes, the contents of the AG had not yet been transferred to these individuals.

Sperm tails can also be marked in living flies with GFP-tagged proteins (Santel et al., 1997). However, although we constructed a UAS–CD63-mCherry transgenic line to study exosome fusion to sperm tails, we were unable to use this fly line successfully because the latter fusion protein aggregates in SCs and disrupts membrane trafficking.

Multiple-mating experiments

For analysis of the physiological role of exosomes in reproduction (Fig. 8), multiple-mating experiments were performed as previously reported (Leiblich et al., 2012); this protocol is described in this paragraph. Control and test experiments were always performed simultaneously to account for variations in food and other conditions. Newly eclosed virgin males (*esgF/O*^{ts}*>ALiX-RNAi 1*, *esgF/O*^{ts}*>Rab11DN*, or *esgF/O*^{ts}) were shifted to 28.5°C to induce transgene expression. Individual males were then added after 3 d to five 2–10-d-old virgin w^{1118} females (for a specific group of control and test flies, females were of identical age) overnight at 28.5°C. The next morning, these females were then replaced with three 2–5-d-old virgin w^{1118} females for 3 h and watched to score timing of mating events, after which the females were separated and incubated at 25°C. For crosses in which at least two females had mated, these females were transferred to separate, fresh vials on each of the next 3 d. Egg counts and progeny counts were recorded for each vial. Each female was then introduced to a dominantly marked (*CyO Roi*) white-eyed male and left for 3 h. Remating events were confirmed by the presence of *CyO Roi* progeny. The absence of effects on egg laying and fertility in males in which exosome secretion is inhibited supports the conclusion that the secretion of most seminal proteins is unaffected by this treatment.

LysoTracker staining

Glands were dissected in ice-cold PBS and left in ice-cold 5 µM LysoTracker red DND-99 (Invitrogen) in PBS for 5 min. They were then washed in ice-cold PBS for 5 min and mounted in PBS using a coverslip bridge for imaging. These specimens were imaged within 1 h but showed no signs of cell death or deterioration over several hours.

Preparation of AGs for antibody staining

The age of dissected flies is given as days after eclosion at 28.5°C. Immunostaining of the AG was performed as previously reported (Leiblich et al., 2012). Dissections were performed in 4% paraformaldehyde in PBS with a minimum total fixation period of 15 min followed by a 20-min wash in PBST-0.3% and then a 30-min wash in PBSTG-male (PBST-0.3% and 10% goat serum). All washes were performed at room temperature (22°C).

Preparation of female reproductive tract for staining

Females were dissected at a fixed time after the start of mating in ice-cold PBS and then fixed in 4% paraformaldehyde in PBS at 22°C. Tracts were washed for 6 × 5 min in PBST-0.3% before incubation in 100 µl chitinase solution (*Streptomyces griseus*; Sigma-Aldrich; 6 U/ml in PBST-0.3%) for 2 h at 22°C (Lung and Wolfner, 1999). Tracts were washed in PBST-0.3% for 6 × 5 min and then refixed for 20 min at 22°C. They were washed again in PBST-0.3% (3 × 5 min) and then blocked for 2 h with gentle shaking at room temperature in 100 µl PBSTG-female (PBS, 0.5% Triton X-100, 3% goat serum, and 0.1% BSA). All washes were performed at room temperature (22°C).

Immunostaining

Samples were incubated with primary antibodies (diluted in the appropriate PBST) overnight at 4°C before washing in appropriate PBST (6 × 10 min). They were then incubated for 2 h at 22°C with fluorescently conjugated donkey secondary antibodies (1:400 dilution; Alexa Fluor 649 and Cy3 labeled; Jackson ImmunoResearch Laboratories, Inc.) before six further 10-min washes in PBST. Stained glands were mounted in Vectashield with DAPI. The following primary antibodies were used: mouse anti–discs large (1:10 dilution of supernatant; Developmental Studies Hybridoma Bank), mouse anti-CD63 (1:10; Developmental Studies Hybridoma Bank), rabbit anti-GFP (1:1,000; catalog no. 6556; Abcam), mouse anti-Fas3

Downloaded from jcb.rupress.org on October 5, 2014

Published August 25, 2014

(1:10; Developmental Studies Hybridoma Bank; Narasimha et al., 2008), polyclonal rabbit anti-Rab7 (1:3,000; Tanaka and Nakamura, 2008; a gift from A. Nakamura, RIKEN Center for Developmental Biology, Kobe, Japan), and rat anti-ANCE (1:2,000; Rylett et al., 2007; a gift from E. Isaac, University of Leeds, Leeds, England, UK). All washes were performed at room temperature (22°C). Fluorescent GFP puncta were more readily observed in the female reproductive tract, perhaps because the luminal microenvironment (e.g., pH) affects fluorescence levels.

Western blot analysis

Protein extraction. For male AG samples, 3-d-old virgin *dsx-GAL4; tubGAL80^{ts}; UAS–CD63-GFP* males (incubated at 29°C from eclosion) expressing *UAS–ALiX-RNAi*, *UAS–Hrs-RNAi*, or *UAS-Rab11DN* constructs were dissected in ice-cold PBS. *w^{1118}* virgin males were used as a negative control.

For female samples, these males were introduced to single *w^{1118}* virgin females, and matings were observed. The whole female reproductive tracts with the ovaries removed were dissected in ice-cold PBS immediately after the end of mating. *w^{1118}* virgin females and *w^{1118}* females mated to *w^{1118}* males were used as a negative controls.

AG proteins were extracted by homogenizing the glands using a polycarbonate pestle on ice in 100 µl lysis buffer (radioimmunoprecipitation assay buffer; Sigma-Aldrich) supplemented with antiprotease and antiphosphatase cocktails (Sigma-Aldrich). The crude lysates were centrifuged briefly (300 *g*; 5 min), and the protein-containing supernatant was extracted. Proteins were quantified using a bicinchoninic acid assay kit (Thermo Fisher Scientific).

Blotting. Blotting of AG proteins was performed as previously described (Rylett et al., 2007), with minor alterations; the protocol is described in this paragraph. Samples containing 2.5 µg homogenized protein (made up to 15 µl) were added to 5 µl of 4× sampling buffer (0.2 M Tris-HCl, pH 6.8, 12% SDS, 40% glycerol, 20% β-mercaptoethanol, and 0.008% bromophenol blue) and heated to 95°C for 5 min. Proteins were separated using 10% mini-Protean TGX precast gels (Bio-Rad Laboratories) for 30 min along with a prestained ladder (Precision Plus Protein Dual Color Standards). Separated proteins were transferred to a polyvinylidene fluoride membrane (Immobilon-P; EMD Millipore) at 100 V for 1 h. The polyvinylidene fluoride membrane was then blocked for 1 h in 5% skimmed milk in TBS with Tween 20 (TBST) and then incubated with the anti-ANCE antibody (Rylett at al. 2007) at a 1:1,000 dilution, anti-GFP at 1:500 (rabbit; ab6556; Abcam), or anti-actin 1:10,000 (rabbit; 04-1040; EMD Millipore) in 5% milk in TBST overnight at 4°C. The membrane was washed in TBST for 3 × 5 min, incubated at room temperature for 1 h with a HRP-conjugated anti–rabbit secondary antibody (W4018; Promega) at 1:20,000 in 5% milk in TBST, and then washed in TBST for 3 × 5 min. Bound anti-ANCE, anti-GFP, or anti-actin antibody was detected using a SuperSignal West Pico Chemiluminescent Substrate kit (Thermo Fisher Scientific) as described in the manufacturer's instructions. Photographic films were exposed to the membrane for 30 s to 1 min before film development. Band intensities were calculated using ImageJ (National Institutes of Health).

Imaging

Live and fixed samples were imaged on a scanning confocal microscope (LSM 510 Meta [Axioplan 2]; Carl Zeiss), using LSM 510 Meta software. Low magnification images (Figs. 1, A and B; 6 D; and 7 B) were obtained using the 10× dry objective (0.45 NA Plan Apochromat); all other confocal images were obtained using the 63× objective (1.4 NA oil differential interference contrast Plan Apochromat) with immersion oil (Carl Zeiss). All live imaging was performed at 16°C. Fixed imaging was performed at 21°C. Details of fluorochromes used in individual experiments are described in the immunostaining procedure and figure legends.

Largest mMVBL diameter was measured on ImageJ by selecting the widest diameter of the largest compartment in a confocal z series. Quantifications of secreted CD63-GFP puncta (Figs. 5 A and S4 A) were performed using ImageJ particle analysis. Fluorescence intensity analysis of lumen content (Fig. S4 G) was performed using Photoshop (Adobe) software (gray intensity mean). Time series Videos 1 and 2 were recorded using LSM Image Browser after cropping video frames. Maximal projection image processing was performed on ImageJ, and rotating 3D projections shown in Videos 3 and 4 were recorded using the ImageJ 3D Viewer to process confocal z series image files. All other confocal images were processed using LSM Image Browser.

For exosome lumen counts and ANCE staining intensity quantification, three stacked confocal images of the lumen were obtained at 5-µm intervals within the central third of each gland at a 1.7× zoom, using the 63× objective. Glands were imaged at gain settings to minimize background staining and, for exosome counts, were repeated at a lower gain setting (Fig. S4 A) to confirm that decreased numbers of puncta did not represent a reduced number of more intensely fluorescent structures. *Rab11DN* is not secreted into the AG lumen (Fig. S5, B versus A), so the limited number of fluorescent puncta in the lumen in this genetic background represents CD63-GFP–positive structures. The values represent the mean particles in a 7,225-µm^2 luminal area, averaged over a minimum of nine glands, and calculated as a percentage of the control value from a parallel experiment.

For nuclear size data, 10 glands for each genotype were analyzed. For each gland, the areas of nuclei for three different SCs, and for each SC, nuclear areas for three surrounding MCs, were measured using ImageJ by outlining nuclei and measuring the enclosed area. For each SC, the mean nuclear size of neighboring MCs was calculated, and relative nuclear size values were obtained by dividing each SC value by the corresponding MC value. These ratios were averaged across 10 glands to give the mean nuclear size ratio. Individual experimental genotypes were always analyzed in parallel with a control that did not express the transgene.

EM

3-d-old *w^{1118}* male reproductive tracts were dissected out and stored overnight in fixative containing 2.5% glutaraldehyde and 4% formaldehyde in PBS, pH 7.2, washed with PBS, postfixed with 1% osmium tetroxide, dehydrated, and embedded in Spurr's epoxy resin between two sheets of polythene. Ultrathin sections were prepared with an ultratome (Ultracut S; Reichert), mounted on formvar-coated slot grids, stained with 2% uranyl acetate and lead citrate, and examined with an electron microscope (1010; JEOL) operated at 80 kV. Although several methodologies for fixation were tested, membranes in AG preparations were often poorly preserved.

Statistical analysis

All compartment and exosome counts, as well as nuclear and mMVBL size measurements, involved analysis of SCs from multiple independent animals and were repeated in at least three separate experiments. Data were analyzed using Excel (Microsoft) or SPSS (IBM). Normality of the data was assessed using a Shapiro–Wilk test. Based on this test, data were analyzed using a two-tailed unpaired Student's *t* test or Mann–Whitney *U* test for single-pair comparisons. Remating data and mating times (Fig. 8) were analyzed using Fisher's exact test. Remating results shown are from a single representative experiment including pooled data collected from crosses set up over several days. These experiments were repeated twice.

Online supplemental material

Fig. S1 shows SC-specific secretion of CD63-GFP exosomes and characterization of SC vacuolar compartments. Fig. S2 shows colocalization of GFP with the anti-CD63 antibody signal, except in specific mMVBLs. Fig. S3 shows individual channels from a pulse–chase analysis in Fig. 3 (A–F). Fig. S4 shows the effects of knocking down membrane trafficking regulators on ANCE secretion. Fig. S5 shows transfer of SC-specific CD63-GFP to neighboring MCs and the absence of Rab11-YFP on exosomes. Video 1 depicts a live-imaging sequence showing an acidic mMVBL fusing to a nonacidic SV in SCs (Fig. 4 A). Video 2 depicts a live-imaging sequence showing invagination of a CD63-GFP–positive membrane from the mMVBL limiting membrane (Fig. 4 B). Video 3 shows a rotating 3D projection of the image shown in Fig. 6 G. Video 4 shows a rotating 3D projection of the image in Fig. 7 C. Online supplemental material is available at http://www.jcb.org/cgi/content/full/jcb.201401072/DC1. Additional data are available in the JCB DataViewer at http://dx.doi.org/10.1083/jcb.201401072.dv.

We thank Stephen Goodwin, Suzanne Eaton, Mariana Wolfner, Jean-Paul Vincent, Elwyn Isaac, Bruce Edgar, Akira Nakamura, Julie Brill, and John Belote for stocks and reagents; Bloomington Drosophila Stock Center, Vienna Drosophila Resource Center, and Drosophila Genomics Resource Center stock centers for flies; Developmental Studies Hybridoma Bank, Iowa for monoclonal antibodies; Ana-Maria Vallés, Richard Parton, and the Micron Oxford Bioimaging facility for assistance with live imaging; and Yael Heifitz for advice regarding female reproductive tract staining.

This work was supported by the Wellcome Trust (092927/Z/10/Z and a studentship to L. Corrigan), the Oxford Cancer Research Centre (OCRC; Cancer Research UK clinical training fund), Cancer Research UK (C38302/A12278) through the OCRC Development Fund, the Biotechnology and Biological Sciences Research Council (BB/K017462/1), a Medical Research Council studentship to S. Redhai, and a studentship to S.M.W. Perera from The British Province of the Society of Jesus (626791).

The authors declare no competing financial interests.

Submitted: 17 January 2014
Accepted: 31 July 2014

Downloaded from jcb.rupress.org on October 5, 2014

Published August 25, 2014

References

Aalberts, M., E. Sostaric, R. Wubbolts, M.W.M. Wauben, E.N.M. Nolte-'t Hoen, B.M. Gadella, T.A.E. Stout, and W. Stoorvogel. 2013. Spermatozoa recruit prostasomes in response to capacitation induction. *Biochim. Biophys. Acta*. 1834:2326–2335. http://dx.doi.org/10.1016/j.bbapap.2012.08.008

Arienti, G., E. Carlini, and C.A. Palmerini. 1997. Fusion of human sperm to prostasomes at acidic pH. *J. Membr. Biol.* 155:89–94. http://dx.doi.org/10.1007/s002329900160

Avila, F.W., K. Ravi Ram, M.C. Bloch Qazi, and M.F. Wolfner. 2010. Sex peptide is required for the efficient release of stored sperm in mated *Drosophila* females. *Genetics*. 186:595–600. http://dx.doi.org/10.1534/genetics.110.119735

Azmi, A.S., B. Bao, and F.H. Sarkar. 2013. Exosomes in cancer development, metastasis, and drug resistance: a comprehensive review. *Cancer Metastasis Rev.* 32:623–642. http://dx.doi.org/10.1007/s10555-013-9441-9

Baietti, M.F., Z. Zhang, E. Mortier, A. Melchior, G. Degeest, A. Geeraerts, Y. Ivarsson, F. Depoortere, C. Coomans, E. Vermeiren, et al. 2012. Syndecan-syntenin-ALIX regulates the biogenesis of exosomes. *Nat. Cell Biol.* 14:677–685. http://dx.doi.org/10.1038/ncb2502

Beckett, K., S. Monier, L. Palmer, C. Alexandre, H. Green, E. Bonneil, G. Raposo, P. Thibault, R. Le Borgne, and J.-P. Vincent. 2013. *Drosophila* S2 cells secrete wingless on exosome-like vesicles but the wingless gradient forms independently of exosomes. *Traffic*. 14:82–96.

Bertram, M.J., G.A. Akerkar, R.L. Ard, C. Gonzalez, and M.F. Wolfner. 1992. Cell type-specific gene expression in the *Drosophila melanogaster* male accessory gland. *Mech. Dev.* 38:33–40. http://dx.doi.org/10.1016/0925-4773(92)90036-J

Brand, A.H., and N. Perrimon. 1993. Targeted gene expression as a means of altering cell fates and generating dominant phenotypes. *Development*. 118:401–415.

Burgess, J., L.M. Del Bel, C.-I.J. Ma, B. Barylko, G. Polevoy, J. Rollins, J.P. Albanesi, H. Krämer, and J.A. Brill. 2012. Type II phosphatidylinositol 4-kinase regulates trafficking of secretory granule proteins in *Drosophila*. *Development*. 139:3040–3050. http://dx.doi.org/10.1242/dev.077644

Chanut-Delalande, H., A.C. Jung, M.M. Baer, L. Lin, F. Payre, and M. Affolter. 2010. The Hrs/Stam complex acts as a positive and negative regulator of RTK signaling during *Drosophila* development. *PLoS ONE*. 5:e10245. http://dx.doi.org/10.1371/journal.pone.0010245

Chapman, T., J. Bangham, G. Vinti, B. Seifried, O. Lung, M.F. Wolfner, H.K. Smith, and L. Partridge. 2003. The sex peptide of *Drosophila melanogaster*: female post-mating responses analyzed by using RNA interference. *Proc. Natl. Acad. Sci. USA*. 100:9923–9928. http://dx.doi.org/10.1073/pnas.1631635100

Chen, P.S., E. Stumm-Zollinger, T. Aigaki, J. Balmer, M. Bienz, and P. Böhlen. 1988. A male accessory gland peptide that regulates reproductive behavior of female *D. melanogaster*. *Cell*. 54:291–298. http://dx.doi.org/10.1016/0092-8674(88)90192-4

Chen, W., Y. Feng, D. Chen, and A. Wandinger-Ness. 1998. Rab11 is required for trans-golgi network-to-plasma membrane transport and a preferential target for GDP dissociation inhibitor. *Mol. Biol. Cell*. 9:3241–3257. http://dx.doi.org/10.1091/mbc.9.11.3241

Chintapalli, V.R., J. Wang, and J.A.T. Dow. 2007. Using FlyAtlas to identify better *Drosophila melanogaster* models of human disease. *Nat. Genet.* 39:715–720. http://dx.doi.org/10.1038/ng2049

Christianson, H.C., K.J. Svensson, and M. Belting. 2014. Exosome and microvesicle mediated phene transfer in mammalian cells. *Semin. Cancer Biol.* http://dx.doi.org/10.1016/j.semcancer.2014.04.007

Colombo, M., C. Moita, G. van Niel, J. Kowal, J. Vigneron, P. Benaroch, N. Manel, L.F. Moita, C. Théry, and G. Raposo. 2013. Analysis of ESCRT functions in exosome biogenesis, composition and secretion highlights the heterogeneity of extracellular vesicles. *J. Cell Sci.* 126:5553–5565. http://dx.doi.org/10.1242/jcs.128868

DiBenedetto, A.J., H.A. Harada, and M.F. Wolfner. 1990. Structure, cell-specific expression, and mating-induced regulation of a *Drosophila melanogaster* male accessory gland gene. *Dev. Biol.* 139:134–148. http://dx.doi.org/10.1016/0012-1606(90)90284-P

Dietzl, G., D. Chen, F. Schnorrer, K.-C. Su, Y. Barinova, M. Fellner, B. Gasser, K. Kinsey, S. Oppel, S. Scheiblauer, et al. 2007. A genome-wide transgenic RNAi library for conditional gene inactivation in *Drosophila*. *Nature*. 448:151–156. http://dx.doi.org/10.1038/nature05954

Dores, M.R., M.M. Paing, H. Lin, W.A. Montagne, A. Marchese, and J. Trejo. 2012. AP-3 regulates PAR1 ubiquitin-independent MVB/lysosomal sorting via an ALIX-mediated pathway. *Mol. Biol. Cell*. 23:3612–3623. http://dx.doi.org/10.1091/mbc.E12-03-0251

Edgar, J.R., E.R. Eden, and C.E. Futter. 2014. Hrs- and CD63-dependent competing mechanisms make different sized endosomal intraluminal vesicles. *Traffic*. 15:197–211. http://dx.doi.org/10.1111/tra.12139

Escola, J.M., M.J. Kleijmeer, W. Stoorvogel, J.M. Griffith, O. Yoshie, and H.J. Geuze. 1998. Selective enrichment of tetraspan proteins on the internal vesicles of multivesicular endosomes and on exosomes secreted by human B-lymphocytes. *J. Biol. Chem.* 273:20121–20127. http://dx.doi.org/10.1074/jbc.273.32.20121

Fabiani, R., L. Johansson, O. Lundkvist, and G. Ronquist. 1994. Enhanced recruitment of motile spermatozoa by prostasome inclusion in swim-up medium. *Hum. Reprod.* 9:1485–1489.

Fader, C.M., A. Savina, D. Sánchez, and M.I. Colombo. 2005. Exosome secretion and red cell maturation: Exploring molecular components involved in the docking and fusion of multivesicular bodies in K562 cells. *Blood Cells Mol. Dis.* 35:153–157. http://dx.doi.org/10.1016/j.bcmd.2005.07.002

Ge, R., E. Tan, S. Sharghi-Namini, and H.H. Asada. 2012. Exosomes in cancer microenvironment and beyond: Have we overlooked these extracellular messengers? *Cancer Microenviron*. 5:323–332. http://dx.doi.org/10.1007/s12307-012-0110-2

Gligorov, D., J.L. Sitnik, R.K. Maeda, M.F. Wolfner, and F. Karch. 2013. A novel function for the Hox gene *Abd-B* in the male accessory gland regulates the long-term female post-mating response in *Drosophila*. *PLoS Genet.* 9:e1003395. http://dx.doi.org/10.1371/journal.pgen.1003395

Goberdhan, D.C. 2010. Intracellular amino acid sensing and mTORC1-regulated growth: new ways to block an old target? *Curr. Opin. Investig. Drugs*. 11:1360–1367.

Gross, J.C., V. Chaudhary, K. Bartscherer, and M. Boutros. 2012. Active Wnt proteins are secreted on exosomes. *Nat. Cell Biol.* 14:1036–1045. http://dx.doi.org/10.1038/ncb2574

Hayashi, S., K. Ito, Y. Sado, M. Taniguchi, A. Akimoto, H. Takeuchi, T. Aigaki, F. Matsuzaki, H. Nakagoshi, T. Tanimura, et al. 2002. GETDB, a database compiling expression patterns and molecular locations of a collection of Gal4 enhancer traps. *Genesis*. 34:58–61. http://dx.doi.org/10.1002/gene.10137

Hirota, Y., T. Kuronita, H. Fujita, and Y. Tanaka. 2007. A role for Rab5 activity in the biogenesis of endosomal and lysosomal compartments. *Biochem. Biophys. Res. Commun.* 364:40–47. http://dx.doi.org/10.1016/j.bbrc.2007.09.089

Hoodless, P.A., T. Haerry, S. Abdollah, M. Stapleton, M.B. O'Connor, L. Attisano, and J.L. Wrana. 1996. MADR1, a MAD-related protein that functions in BMP2 signaling pathways. *Cell*. 85:489–500. http://dx.doi.org/10.1016/S0092-8674(00)81250-7

Hsu, C., Y. Morohashi, S. Yoshimura, N. Manrique-Hoyos, S. Jung, M.A. Lauterbach, M. Bakhti, M. Grønborg, W. Möbius, J. Rhee, et al. 2010. Regulation of exosome secretion by Rab35 and its GTPase-activating proteins TBC1D10A–C. *J. Cell Biol.* 189:223–232. http://dx.doi.org/10.1083/jcb.200911018

Jékely, G., and P. Rørth. 2003. Hrs mediates downregulation of multiple signalling receptors in *Drosophila*. *EMBO Rep.* 4:1163–1168. http://dx.doi.org/10.1038/sj.embor.7400019

Jiang, H., P.H. Patel, A. Kohlmaier, M.O. Grenley, D.G. McEwen, and B.A. Edgar. 2009. Cytokine/Jak/Stat signaling mediates regeneration and homeostasis in the *Drosophila* midgut. *Cell*. 137:1343–1355. http://dx.doi.org/10.1016/j.cell.2009.05.014

Juhász, G., J.H. Hill, Y. Yan, M. Sass, E.H. Baehrecke, J.M. Backer, and T.P. Neufeld. 2008. The class III PI(3)K Vps34 promotes autophagy and endocytosis but not TOR signaling in *Drosophila*. *J. Cell Biol.* 181:655–666. http://dx.doi.org/10.1083/jcb.200712051

Katzmann, D.J., C.J. Stefan, M. Babst, and S.D. Emr. 2003. Vps27 recruits ESCRT machinery to endosomes during MVB sorting. *J. Cell Biol.* 162:413–423. http://dx.doi.org/10.1083/jcb.200302136

Kershaw-Young, C.M., X. Druart, J. Vaughan, and W.M.C. Maxwell. 2012. β-Nerve growth factor is a major component of alpaca seminal plasma and induces ovulation in female alpacas. *Reprod. Fertil. Dev.* 24:1093–1097. http://dx.doi.org/10.1071/RD12039

Koles, K., J. Nunnari, C. Korkut, R. Barria, C. Brewer, Y. Li, J. Leszyk, B. Zhang, and V. Budnik. 2012. Mechanism of evenness interrupted (Evi)-exosome release at synaptic boutons. *J. Biol. Chem.* 287:16820–16834. http://dx.doi.org/10.1074/jbc.M112.342667

Köttgen, M., A. Hofherr, W. Li, K. Chu, S. Cook, C. Montell, and T. Watnick. 2011. *Drosophila* sperm swim backwards in the female reproductive tract and are activated via TRPP2 ion channels. *PLoS ONE*. 6:e20031. http://dx.doi.org/10.1371/journal.pone.0020031

Kubli, E. 2003. Sex-peptides: seminal peptides of the *Drosophila* male. *Cell. Mol. Life Sci.* 60:1689–1704. http://dx.doi.org/10.1007/s00018-003-3052

Lance, R.S., R.R. Drake, and D.A. Troyer. 2011. Multiple recognition assay reveals prostasomes as promising plasma biomarkers for prostate cancer. *Expert Rev. Anticancer Ther.* 11:1341–1343. http://dx.doi.org/10.1586/era.11.134

Leiblich, A., L. Marsden, C. Gandy, L. Corrigan, R. Jenkins, F. Hamdy, and C. Wilson. 2012. Bone morphogenetic protein- and mating-dependent

Downloaded from jcb.rupress.org on October 5, 2014

Published August 25, 2014

secretory cell growth and migration in the *Drosophila* accessory gland. *Proc. Natl. Acad. Sci. USA*. 109:19292–19297. http://dx.doi.org/10.1073/pnas.1214517109

Liu, H., and E. Kubli. 2003. Sex-peptide is the molecular basis of the sperm effect in *Drosophila melanogaster*. *Proc. Natl. Acad. Sci. USA*. 100:9929–9933. http://dx.doi.org/10.1073/pnas.1631700100

Lloyd, T.E., R. Atkinson, M.N. Wu, Y. Zhou, G. Pennetta, and H.J. Bellen. 2002. Hrs regulates endosome membrane invagination and tyrosine kinase receptor signaling in *Drosophila*. *Cell*. 108:261–269. http://dx.doi.org/10.1016/S0092-8674(02)00611-6

Lung, O., and M.F. Wolfner. 1999. *Drosophila* seminal fluid proteins enter the circulatory system of the mated female fly by crossing the posterior vaginal wall. *Insect Biochem. Mol. Biol.* 29:1043–1052. http://dx.doi.org/10.1016/S0965-1748(99)00078-8

Marois, E., A. Mahmoud, and S. Eaton. 2006. The endocytic pathway and formation of the Wingless morphogen gradient. *Development*. 133:307–317. http://dx.doi.org/10.1242/dev.02197

Matsuo, H., J. Chevallier, N. Mayran, I. Le Blanc, C. Ferguson, J. Fauré, N.S. Blanc, S. Matile, J. Dubochet, R. Sadoul, et al. 2004. Role of LBPA and Alix in multivesicular liposome formation and endosome organization. *Science*. 303:531–534. http://dx.doi.org/10.1126/science.1092425

Minami, R., M. Wakabayashi, S. Sugimori, K. Taniguchi, A. Kokuryo, T. Imano, T. Adachi-Yamada, N. Watanabe, and H. Nakagoshi. 2012. The homeodomain protein defective proventriculus is essential for male accessory gland development to enhance fecundity in *Drosophila. PLoS ONE*. 7:e32302. http://dx.doi.org/10.1371/journal.pone.0032302

Minogue, S., M.G. Waugh, M.A. De Matteis, D.J. Stephens, F. Berditchevski, and J.J. Hsuan. 2006. Phosphatidylinositol 4-kinase is required for endosomal trafficking and degradation of the EGF receptor. *J. Cell Sci.* 119:571–581. http://dx.doi.org/10.1242/jcs.02752

Morelli, A.E., A.T. Larregina, W.J. Shufesky, M.L.G. Sullivan, D.B. Stolz, G.D. Papworth, A.F. Zahorchak, A.J. Logar, Z. Wang, S.C. Watkins, et al. 2004. Endocytosis, intracellular sorting, and processing of exosomes by dendritic cells. *Blood*. 104:3257–3266. http://dx.doi.org/10.1182/blood-2004-03-0824

Narasimha, M., A. Uv, A. Krejci, N.H. Brown, and S.J. Bray. 2008. Grainy head promotes expression of septate junction proteins and influences epithelial morphogenesis. *J. Cell Sci.* 121:747–752. http://dx.doi.org/10.1242/jcs.019422

Ni, J.-Q., M. Markstein, R. Binari, B. Pfeiffer, L.-P. Liu, C. Villalta, M. Booker, L. Perkins, and N. Perrimon. 2008. Vector and parameters for targeted transgenic RNA interference in *Drosophila melanogaster*. *Nat. Methods*. 5:49–51. http://dx.doi.org/10.1038/nmeth1146

Nilsson, J., J. Skog, A. Nordstrand, V. Baranov, L. Mincheva-Nilsson, X.O. Breakefield, and A. Widmark. 2009. Prostate cancer-derived urine exosomes: a novel approach to biomarkers for prostate cancer. *Br. J. Cancer*. 100:1603–1607. http://dx.doi.org/10.1038/sj.bjc.6605058

Odorizzi, G. 2006. The multiple personalities of Alix. *J. Cell Sci.* 119:3025–3032. http://dx.doi.org/10.1242/jcs.03072

Ögmundsdóttir, M.H., S. Heublein, S. Kazi, B. Reynolds, S.M. Visvalingam, M.K. Shaw, and D.C.I. Goberdhan. 2012. Proton-assisted amino acid transporter PAT1 complexes with Rag GTPases and activates TORC1 on late endosomal and lysosomal membranes. *PLoS ONE*. 7:e36616. http://dx.doi.org/10.1371/journal.pone.0036616

Ostrowski, M., N.B. Carmo, S. Krumeich, I. Fanget, G. Raposo, A. Savina, C.F. Moita, K. Schauer, A.N. Hume, R.P. Freitas, et al. 2010. Rab27a and Rab27b control different steps of the exosome secretion pathway. *Nat. Cell Biol.* 12:19–30. http://dx.doi.org/10.1038/ncb2000

Palmerini, C.A., E. Carlini, A. Nicolucci, and G. Arienti. 1999. Increase of human spermatozoa intracellular Ca2+ concentration after fusion with prostasomes. *Cell Calcium*. 25:291–296. http://dx.doi.org/10.1054/ceca.1999.0031

Panáková, D., H. Sprong, E. Marois, C. Thiele, and S. Eaton. 2005. Lipoprotein particles are required for Hedgehog and Wingless signalling. *Nature*. 435:58–65. http://dx.doi.org/10.1038/nature03504

Park, K.-H., B.-J. Kim, J. Kang, T.-S. Nam, J.M. Lim, H.T. Kim, J.K. Park, Y.G. Kim, S.-W. Chae, and U.-H. Kim. 2011. Ca2+ signaling tools acquired from prostasomes are required for progesterone-induced sperm motility. *Sci. Signal*. 4:ra31. http://dx.doi.org/10.1126/scisignal.2001595

Peng, J., S. Chen, S. Büsser, H. Liu, T. Honegger, and E. Kubli. 2005. Gradual release of sperm bound sex-peptide controls female postmating behavior in *Drosophila. Curr. Biol.* 15:207–213. http://dx.doi.org/10.1016/j.cub.2005.01.034

Piper, R.C., A.A. Cooper, H. Yang, and T.H. Stevens. 1995. VPS27 controls vacuolar and endocytic traffic through a prevacuolar compartment in *Saccharomyces cerevisiae. J. Cell Biol.* 131:603–617. http://dx.doi.org/10.1083/jcb.131.3.603

Properzi, F., M. Logozzi, and S. Fais. 2013. Exosomes: the future of biomarkers in medicine. *Biomarkers Med.* 7:769–778. http://dx.doi.org/10.2217/bmm.13.63

Raposo, G., and W. Stoorvogel. 2013. Extracellular vesicles: Exosomes, microvesicles, and friends. *J. Cell Biol.* 200:373–383. http://dx.doi.org/10.1083/jcb.201211138

Ravi Ram, K., S. Ji, and M.F. Wolfner. 2005. Fates and targets of male accessory gland proteins in mated female *Drosophila melanogaster. Insect Biochem. Mol. Biol.* 35:1059–1071. http://dx.doi.org/10.1016/j.ibmb.2005.05.001

Record, M., K. Carayon, M. Poirot, and S. Silvente-Poirot. 2014. Exosomes as new vesicular lipid transporters involved in cell-cell communication and various pathophysiologies. *Biochim. Biophys. Acta*. 1841:108–120. http://dx.doi.org/10.1016/j.bbalip.2013.10.004

Rideout, E.J., A.J. Dornan, M.C. Neville, S. Eadie, and S.F. Goodwin. 2010. Control of sexual differentiation and behavior by the doublesex gene in *Drosophila melanogaster. Nat. Neurosci.* 13:458–466. http://dx.doi.org/10.1038/nn.2515

Rodríguez-Martínez, H., U. Kvist, J. Ernerudh, L. Sanz, and J.J. Calvete. 2011. Seminal plasma proteins: what role do they play? *Am. J. Reprod. Immunol.* 66(Suppl. 1):11–22. http://dx.doi.org/10.1111/j.1600-0897.2011.01033.x

Ronquist, G. 2012. Prostasomes are mediators of intercellular communication: from basic research to clinical implications. *J. Intern. Med.* 271:400–413. http://dx.doi.org/10.1111/j.1365-2796.2011.02487.x

Ronquist, K.G., G. Ronquist, A. Larsson, and L. Carlsson. 2010. Proteomic analysis of prostate cancer metastasis-derived prostasomes. *Anticancer Res.* 30:285–290.

Rylett, C.M., M.J. Walker, G.J. Howell, A.D. Shirras, and R.E. Isaac. 2007. Male accessory glands of *Drosophila melanogaster* make a secreted angiotensin I-converting enzyme (ANCE), suggesting a role for the peptide-processing enzyme in seminal fluid. *J. Exp. Biol.* 210:3601–3606. http://dx.doi.org/10.1242/jeb.009035

Sahlén, G., A. Ahlander, A. Frost, G. Ronquist, B.J. Norlén, and B.O. Nilsson. 2004. Prostasomes are secreted from poorly differentiated cells of prostate cancer metastases. *Prostate*. 61:291–297. http://dx.doi.org/10.1002/pros.20090

Santel, A., T. Winhauer, N. Blümer, and R. Renkawitz-Pohl. 1997. The *Drosophila* don juan (dj) gene encodes a novel sperm specific protein component characterized by an unusual domain of a repetitive amino acid motif. *Mech. Dev.* 64:19–30. http://dx.doi.org/10.1016/S0925-4773(97)00031-2

Savina, A., M. Vidal, and M.I. Colombo. 2002. The exosome pathway in K562 cells is regulated by Rab11. *J. Cell Sci.* 115:2505–2515.

Savina, A., C.M. Fader, M.T. Damiani, and M.I. Colombo. 2005. Rab11 promotes docking and fusion of multivesicular bodies in a calcium-dependent manner. *Traffic*. 6:131–143. http://dx.doi.org/10.1111/j.1600-0854.2004.00257.x

Schroeder, B., S. Srivatsan, A. Shaw, D. Billadeau, and M.A. McNiven. 2012. CIN85 phosphorylation is essential for EGFR ubiquitination and sorting into multivesicular bodies. *Mol. Biol. Cell*. 23:3602–3611. http://dx.doi.org/10.1091/mbc.E11-08-0666

Sirot, L.K., M.C. Hardstone, M.E.H. Helinski, J.M.C. Ribeiro, M. Kimura, P. Deewatthanawong, M.F. Wolfner, and L.C. Harrington. 2011. Towards a semen proteome of the dengue vector mosquito: protein identification and potential functions. *PLoS Negl. Trop. Dis.* 5:e989. http://dx.doi.org/10.1371/journal.pntd.0000989

Soekmadji, C., P.J. Russell, and C.C. Nelson. 2013. Exosomes in prostate cancer: putting together the pieces of a puzzle. *Cancers (Basel)*. 5:1522–1544. http://dx.doi.org/10.3390/cancers5041522

Stenmark, H. 2009. Rab GTPases as coordinators of vesicle traffic. *Nat. Rev. Mol. Cell Biol.* 10:513–525. http://dx.doi.org/10.1038/nrm2728

Stenmark, H., R.G. Parton, O. Steele-Mortimer, A. Lütcke, J. Gruenberg, and M. Zerial. 1994. Inhibition of rab5 GTPase activity stimulates membrane fusion in endocytosis. *EMBO J.* 13:1287–1296.

Sullivan, R., and F. Saez. 2013. Epididymosomes, prostasomes, and liposomes: their roles in mammalian male reproductive physiology. *Reproduction*. 146:R21–R35. http://dx.doi.org/10.1530/REP-13-0058

Sweeney, S.T., and G.W. Davis. 2002. Unrestricted synaptic growth in spinster-a late endosomal protein implicated in TGF-beta-mediated synaptic growth regulation. *Neuron*. 36:403–416. http://dx.doi.org/10.1016/S0896-6273(02)01014-0

Tamai, K., N. Tanaka, T. Nakano, E. Kakazu, Y. Kondo, J. Inoue, M. Shiina, K. Fukushima, T. Hoshino, K. Sano, et al. 2010. Exosome secretion of dendritic cells is regulated by Hrs, an ESCRT-0 protein. *Biochem. Biophys. Res. Commun.* 399:384–390. http://dx.doi.org/10.1016/j.bbrc.2010.07.083

Tanaka, T., and A. Nakamura. 2008. The endocytic pathway acts downstream of Oskar in *Drosophila* germ plasm assembly. *Development*. 135:1107–1117. http://dx.doi.org/10.1242/dev.017293

Downloaded from jcb.rupress.org on October 5, 2014

Published August 25, 2014

Tavoosidana, G., G. Ronquist, S. Darmanis, J. Yan, L. Carlsson, D. Wu, T. Conze, P. Ek, A. Semjonow, E. Eltze, et al. 2011. Multiple recognition assay reveals prostasomes as promising plasma biomarkers for prostate cancer. *Proc. Natl. Acad. Sci. USA*. 108:8809–8814. http://dx.doi.org/10.1073/pnas.1019330108

Théry, C., M. Ostrowski, and E. Segura. 2009. Membrane vesicles as conveyors of immune responses. *Nat. Rev. Immunol.* 9:581–593. http://dx.doi.org/10.1038/nri2567

Trajkovic, K., C. Hsu, S. Chiantia, L. Rajendran, D. Wenzel, F. Wieland, P. Schwille, B. Brügger, and M. Simons. 2008. Ceramide triggers budding of exosome vesicles into multivesicular endosomes. *Science*. 319:1244–1247. http://dx.doi.org/10.1126/science.1153124

Tsuneizumi, K., T. Nakayama, Y. Kamoshida, T.B. Kornberg, J.L. Christian, and T. Tabata. 1997. Daughters against dpp modulates dpp organizing activity in *Drosophila* wing development. *Nature*. 389:627–631. http://dx.doi.org/10.1038/39362

Vlassov, A.V., S. Magdaleno, R. Setterquist, and R. Conrad. 2012. Exosomes: current knowledge of their composition, biological functions, and diagnostic and therapeutic potentials. *Biochim. Biophys. Acta*. 1820:940–948. http://dx.doi.org/10.1016/j.bbagen.2012.03.017

Walker, M.J., C.M. Rylett, J.N. Keen, N. Audsley, M. Sajid, A.D. Shirras, and R.E. Isaac. 2006. Proteomic identification of *Drosophila melanogaster* male accessory gland proteins, including a pro-cathepsin and a soluble gamma-glutamyl transpeptidase. *Proteome Sci.* 4:9. http://dx.doi.org/10.1186/1477-5956-4-9

Wegner, C.S., L. Malerød, N.M. Pedersen, C. Progida, O. Bakke, H. Stenmark, and A. Brech. 2010. Ultrastructural characterization of giant endosomes induced by GTPase-deficient Rab5. *Histochem. Cell Biol.* 133:41–55. http://dx.doi.org/10.1007/s00418-009-0643-8

Wolfner, M.F. 1997. Tokens of love: functions and regulation of *Drosophila* male accessory gland products. *Insect Biochem. Mol. Biol.* 27:179–192. http://dx.doi.org/10.1016/S0965-1748(96)00084-7

Zhang, J., K.L. Schulze, P.R. Hiesinger, K. Suyama, S. Wang, M. Fish, M. Acar, R.A. Hoskins, H.J. Bellen, and M.P. Scott. 2007. Thirty-one flavors of *Drosophila* rab proteins. *Genetics*. 176:1307–1322. http://dx.doi.org/10.1534/genetics.106.066761

Downloaded from jcb.rupress.org on October 5, 2014

Corrigan et al, http://www.jcb.org/cgi/content/full/jcb.201401072/DC1

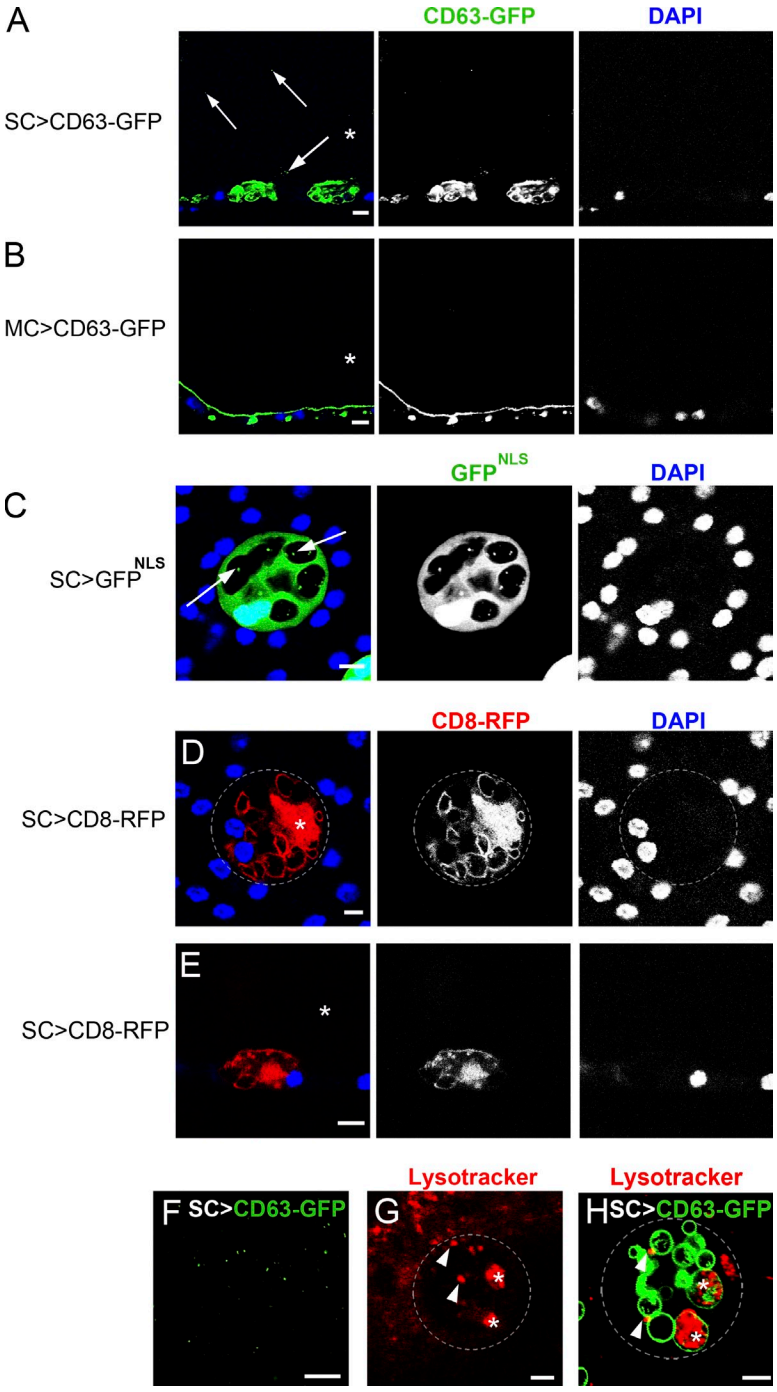


Figure S1. **SCs and not MCs secrete CD63-positive puncta.** (A and B) Transverse sections of AG (in an equivalent focal plane to Fig. 1 C) showing that CD63-GFP is secreted in puncta (arrows; see F for higher magnification image at higher gain setting) into the AG lumen (asterisks) when expressed by SCs (A) but not MCs, imaged here in the middle of the gland where no SCs are present (B). (C) Puncta containing cytoplasmic GFP can also occasionally be seen inside SC vacuoles (arrows) in the surface section. (D and E) CD8-RFP localizes either within (asterisk in D) or at the limiting membrane of large vacuoles (surface section in D) but is not secreted into the AG lumen (asterisk, transverse section in E). (F) Many CD63-GFP–positive puncta secreted by SCs into the AG lumen are detected when the sensitivity and resolution of confocal imaging is increased. (G and H) The w^{1118} (non-GFP marked) control SC (G), imaged live, contains two large (>2 µm, asterisks) and several small (<2 µm, arrowheads) acidic compartments, which stain strongly with LysoTracker red, similar to CD63-GFP–expressing SCs (H). Accurately counting these compartments is not possible because their limiting membranes are not marked. All images show SCs from 3-d-old males incubated at 28.5°C after eclosion. Fixed cell nuclei are stained with DAPI. Approximate outline of cell is marked in D, G, and H. Bars: (A, B, and F) 10 µm; (C–E, G, and H) 5 µm.

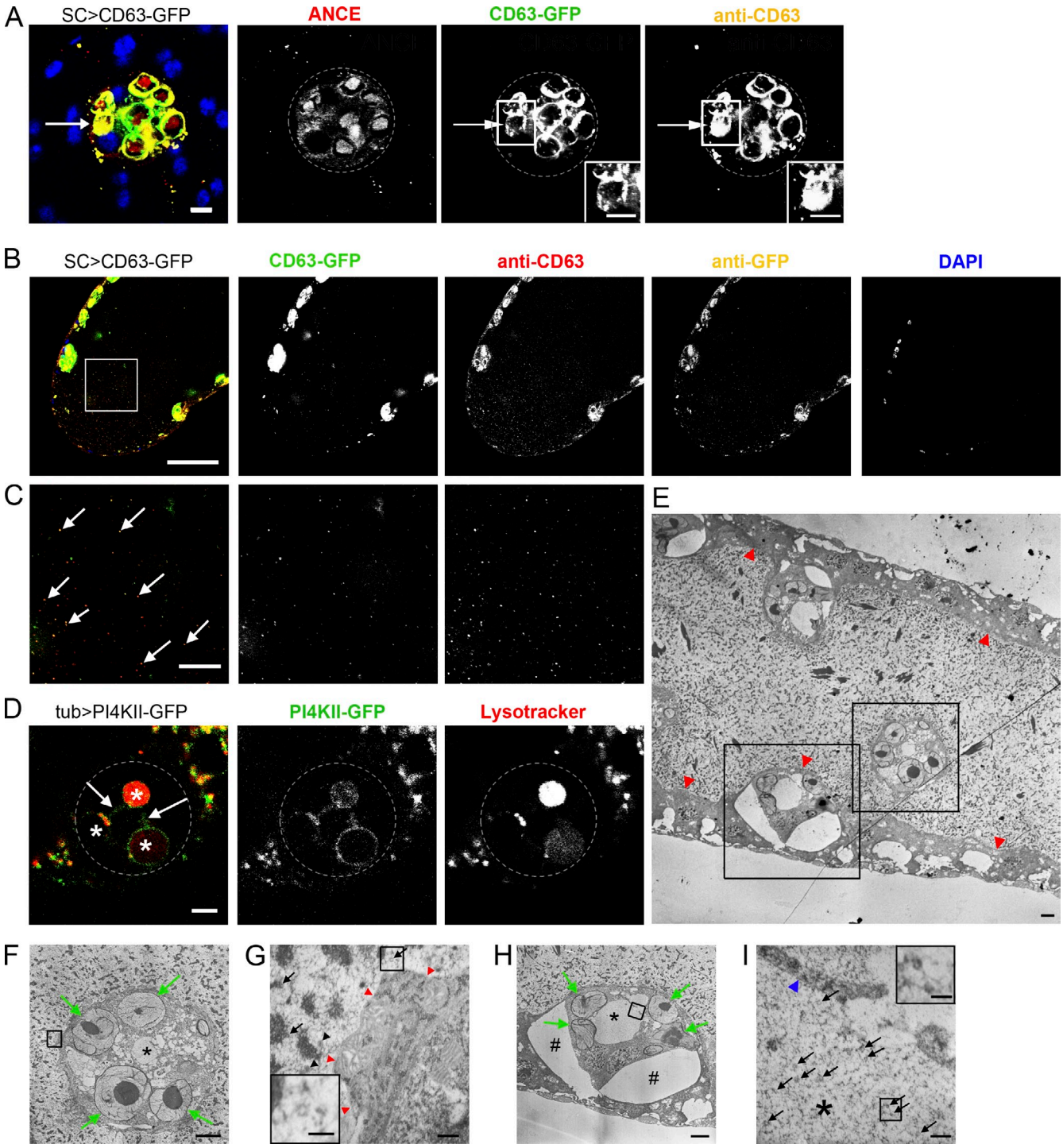


Figure S2. **SCs have large acidic compartments containing internalized CD63-GFP.** (A) A CD63-GFP–expressing SC stained with anti-ANCE and anti-CD63 antibodies reveals one compartment that is filled with CD63 but has low GFP fluorescence (arrows; insets show higher magnification images of boxed regions that include this compartment). This compartment does not contain a dense ANCE core (arrows). (B and C) Transverse section through the lumen of an AG containing CD63-GFP–expressing SCs stained with anti-CD63 and anti-GFP antibodies. Many CD63-GFP fluorescent puncta in the AG lumen colocalize with the anti-CD63 antibody (e.g., arrows in C). C is a higher magnification image of the square outlined in B. (D) Live image of an SC from a *tub-PI4KII-GFP* fly stained with LysoTracker. The late endosome and lysosome marker PI4KII localizes to the limiting membrane of large acidic compartments (asterisks) as well as tubulations extending between them (arrows), which have been observed previously in *Drosophila* salivary gland cells (Burgess et al., 2012). (E–I) Electron micrographs of virgin w^{1118} male AGs. MCs (apical membranes marked with red arrowheads in E) make up the majority of the monolayered epithelium; SCs (boxed in E) are dispersed between MCs, bulge into the lumen, and can be seen in transverse (e.g., cell in H) or surface (e.g., cell protruding into lumen in F) section. SCs contain SVs, comprising an electron-dense core and fibrillar material (F and H, green arrows) and one or two large and less electron-dense, non-SV compartments (F and H, asterisks; H shown at high magnification in I), which by a process of elimination, must represent the large acidic compartments seen in live confocal imaging. The AG lumen contains a range of secreted structures (E), including putative membrane-bound vesicles (G, closed arrows and arrowheads; red arrowheads mark apical surface of epithelium), some of which (G, closed arrows; boxed area enlarged in inset) resemble the ~40-nm vesicles (I, arrows; enlarged in inset) observed inside the large multivesicular compartments in SCs (I, asterisk). These compartments therefore appear to be the counterparts of much smaller mammalian MVBs. F and H are higher magnification images of the boxed regions in E; G and I show higher magnification images of the regions boxed in F and H, respectively. All images show SCs from 3-d-old males incubated at 28.5°C after eclosion. Note that despite attempting several fixation protocols, we were unable to prevent spaces forming at high frequency between SC and MC plasma membranes in the epithelium (# in H). Preservation of compartment membranes was also not optimal (e.g., blue arrowhead in I). Approximate outline of cell is marked in A and D. Bars: (A [main images and insets] and D) 5 µm; (B) 50 µm; (C) 10 µm; (E, F, and H) 2 µm; (G and I, main images) 200 nm; (G and I, insets) 100 nm.

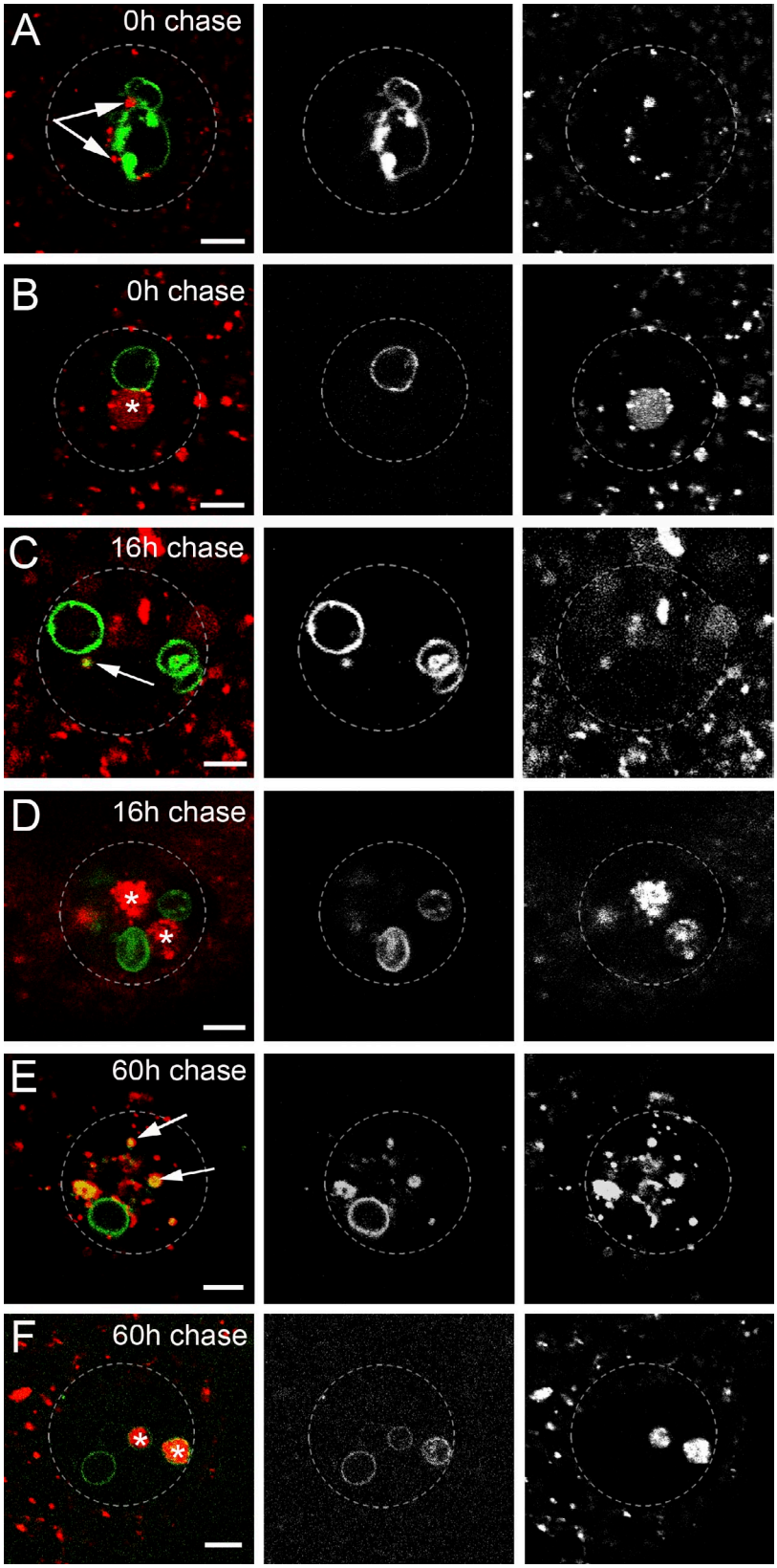


Figure S3. **Analysis of CD63-GFP trafficking and internalization in mMVBLs.** Images from Fig. 3 showing individual color channels: an 8-h pulse of CD63-GFP (induced by inhibition of GAL80^{ts} at 28.5°C) was chased at 18°C for 0–60 h, and proportions of cells with one or more LysoTracker red–positive iLEs (arrows in A, C, and E) and mMVBLs (asterisks in B, D, and F), which were CD63-GFP positive, were determined. The rate of CD63 traffic into endolysosomes is not identical in all cells (Fig. 3 G). Note that when the temperature is shifted down at the end of the pulse, transcripts encoding CD63-GFP are not immediately degraded, so new protein will continue to be made, potentially explaining the persistence of GFP fluorescence in SVs and iLEs. Approximate outline of cell is marked. Bars, 5 µm.

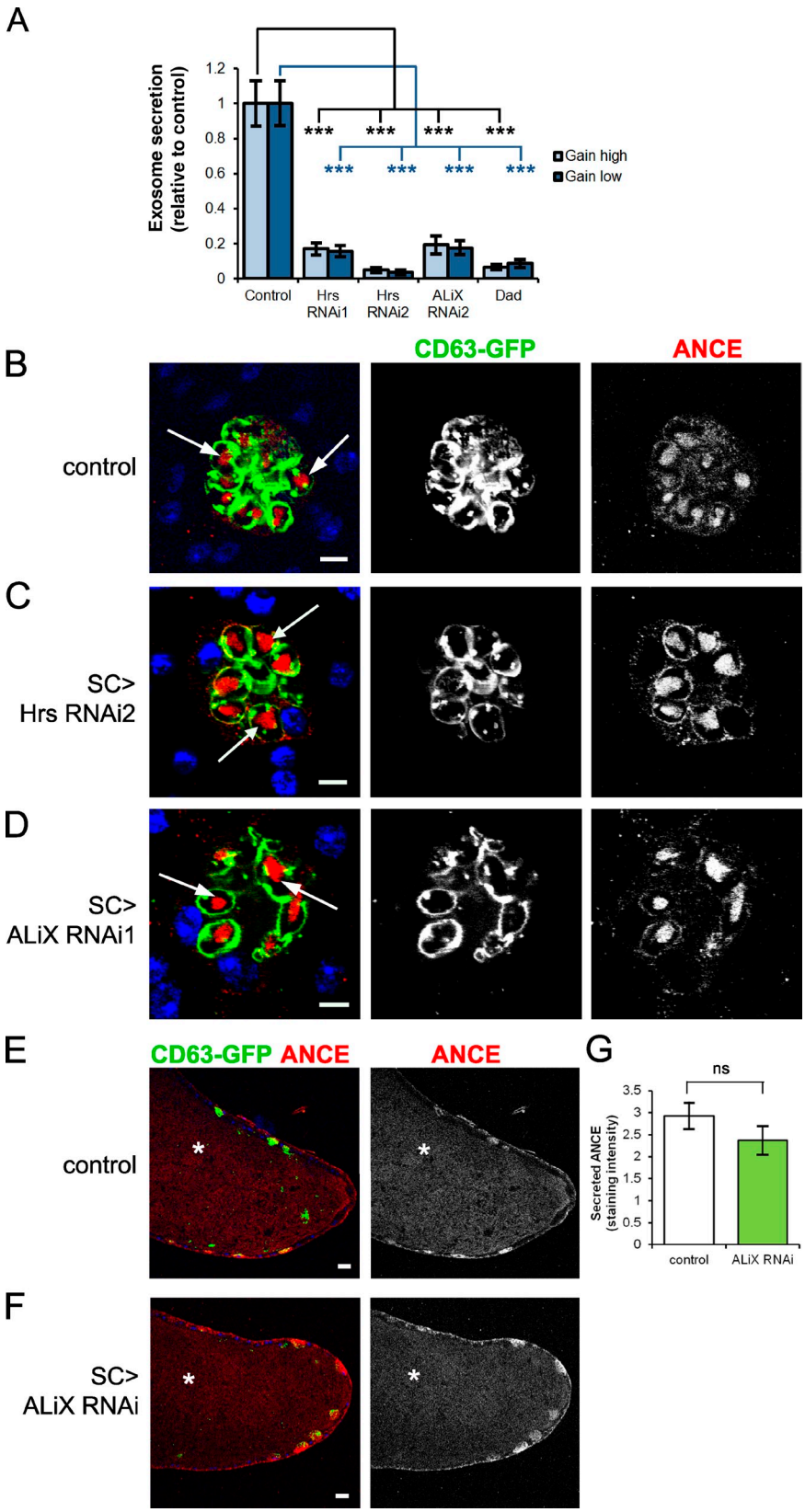


Figure S4. **Blocking ESCRT function in SCs does not affect ANCE secretion.** (A) Relative numbers of SC-expressed CD63-GFP–positive puncta in the AG lumen were quantified for *SC>Hrs-RNAi*, *SC>ALiX-RNAi*, and *SC>Dad* males compared with control males at two confocal gain settings that altered absolute counts by approximately twofold. No effect on relative levels was observed. (B–E) ANCE, which normally localizes to the dense core of control SC SVs (B, arrows) and is secreted into the gland lumen (E, asterisks) but is not detectably expressed in MCs, does not show altered subcellular localization in *Hrs-RNAi*– or *ALiX-RNAi*–expressing SCs (C and D, respectively, arrows). DAPI stains nuclei (blue). (E–G) There is no significant difference in the level of diffuse staining for ANCE in the AG lumen (E and F, asterisks) when *ALiX* is knocked down in SCs (F and G), as measured by calculating the mean signal intensities of three stacked confocal images from the AG lumen taken at 5-µm intervals. Control and *SC>ALiX-RNAi* males were subjected to the same mating protocol as in A, whereas B–D were obtained from virgin males. Data in A and G were analyzed using an unpaired two-tailed Student's *t* test (***, $P < 0.001$, $n > 11$) after the Shapiro–Wilk test to confirm normality. Error bars indicate ±SE. Bars: (B–D) 5 µm; (E and F) 20 µm.

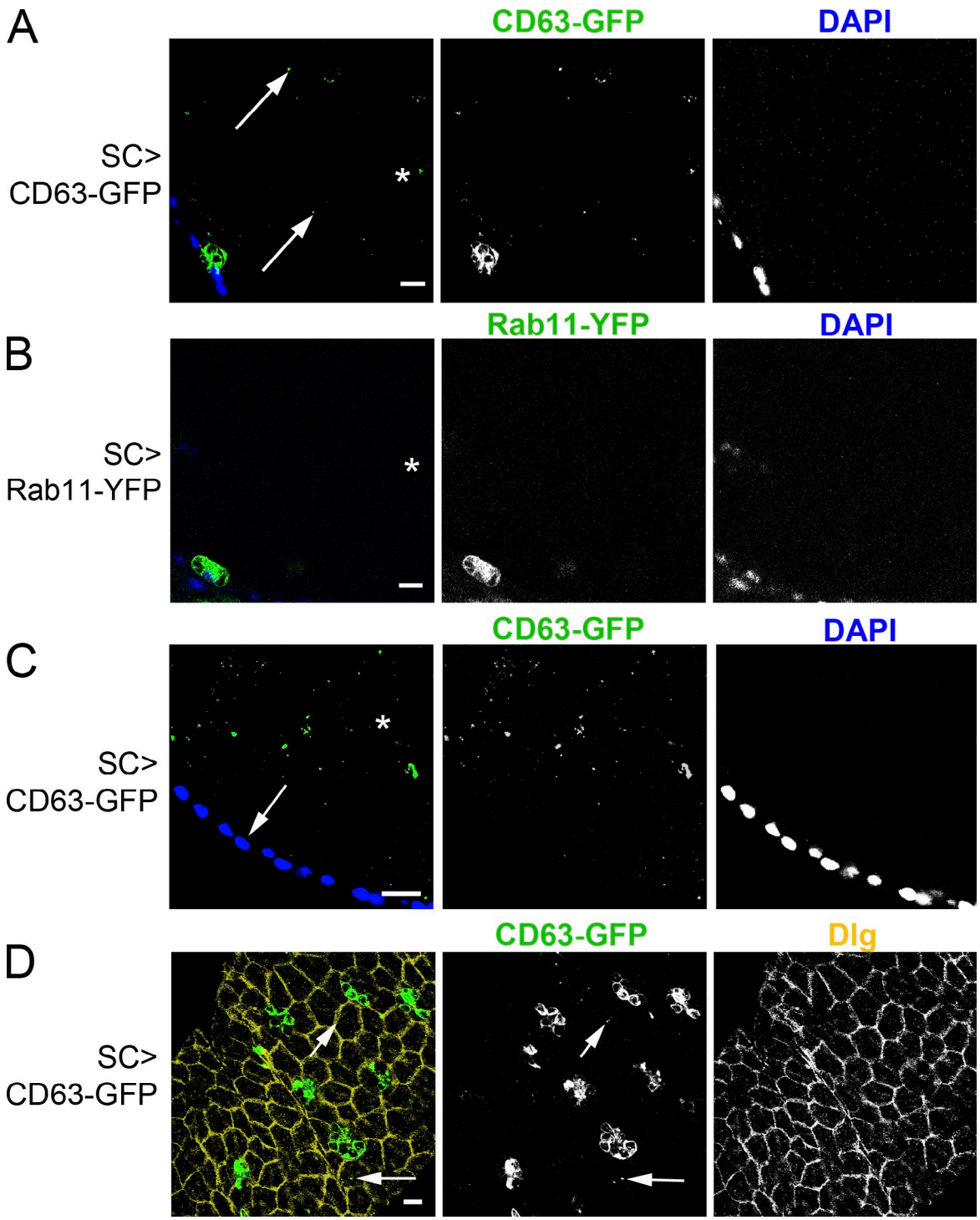
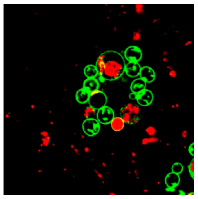
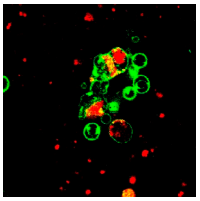


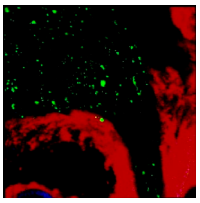
Figure S5. **SC-specific CD63-GFP is transferred to neighboring MCs, but Rab11-YFP is not secreted.** (A and B) Analysis of Rab11-YFP and CD63-GFP secretion when expressed in SCs. Unlike CD63-GFP (A, arrows), YFP-tagged Rab11 is not secreted by SCs, even when highly overexpressed under GAL4 control (B). Images show transverse sections including the lumen (A and B, asterisks) and SCs from 3-d-old males. (C) Transverse section showing no obvious interaction can be seen between CD63-GFP–positive exosomes and the apical surface of MCs (arrow; the asterisk marks the lumen) in most of the AG at 3 d. (D) However, GFP is internalized by the MCs surrounding SCs (arrows). discs large (Dlg) marks apically positioned lateral septate junctions between MCs (junctions between MCs and larger SCs are more apical). DAPI stains nuclei. Bars, 10 µm.



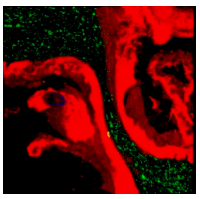
Video 1. **Acidic mMVBLs fuse to nonacidic SVs in SCs.** SC from a 2-d-old male expressing CD63-GFP (green) and stained with LysoTracker red was imaged by time-lapse confocal microscopy using a laser-scanning confocal microscope (LSM 510; Carl Zeiss). Frames were taken every 13.6 s. Stills from this video are shown in Fig. 4 A. Video was produced over a 5-min period. Note how CD63-GFP appears to be transferred to the limiting membrane of the mMVBL at the moment of fusion.



Video 2. **mMVBLs contain CD63-GFP–positive invaginations and acidic microdomains inside mMVBLs.** SC from a 2-d-old male expressing CD63-GFP (green) and stained with LysoTracker red was imaged by time-lapse confocal microscopy using a laser-scanning confocal microscope (LSM 510; Carl Zeiss). Frames were taken every 16.3 s. Stills from this video are shown in Fig. 4 B. Note one CD63-GFP–positive invagination appears to form an ILV-like punctum. A line of peripheral acidic microdomains appears after this event either de novo or through imaging a slightly different plane of the section in the mMVBL. The video was produced over a 5-min period.



Video 3. **CD63-GFP exosomes may fuse with unmarked sperm tails in females.** Rotating 3D projection of a confocal z stack including the image shown in Fig. 6 D. A z series was collected using a laser-scanning confocal microscope (LSM 510; Carl Zeiss) and the rotating 3D projection movie was recorded using ImageJ 3D Viewer. Note the presence of extended strands of GFP fluorescence and some parallel pairs of short GFP-positive lines that presumably surround sperm tails to which exosomes have recently fused (marked in Fig. 6 D). The female reproductive tract epithelium is marked with CD8-RFP.



Video 4. **Accumulation of CD63-GFP exosomes along the surface of the female reproductive tract epithelium.** Rotating 3D projection of a confocal z stack including the image shown in Fig. 7 B, highlighting a single GFP-positive interaction site at the epithelial surface that is marked in this figure. A z series was collected using a laser-scanning confocal microscope (LSM 510; Carl Zeiss), and the rotating 3D projection video was recorded using ImageJ 3D Viewer. The female reproductive tract epithelium is marked with CD8-RFP.

Reference

Burgess, J., L.M. Del Bel, C.-I.J. Ma, B. Barylko, G. Polevoy, J. Rollins, J.P. Albanesi, H. Krämer, and J.A. Brill. 2012. Type II phosphatidylinositol 4-kinase regulates trafficking of secretory granule proteins in *Drosophila*. *Development*. 139:3040–3050. http://dx.doi.org/10.1242/dev.077644